GENETIC ANALYSIS OF SYNAPTIC GROWTH AND NEUROTOXIC EFFECTS OF RADIATION EXPOSURE DURING DEVELOPOMENT IN *DROSOPHILA MELANOGASTER*

By

Lisa Sudmeier

A dissertation submitted in partial fulfillment of the requirements for the degree of

Doctor of Philosophy

(Neuroscience)

at the

University of Wisconsin-Madison

2015

Date of final oral examination: 5/19/2015

This dissertation is approved by the following members of the Final Oral Committee:

Grace Boekhoff-Falk, Associate Professor, Cell and Regenerative Biology
Erik Dent, Associate Professor, Neuroscience
Barry Ganetzky, Professor, Genetics and Medical Genetics
Anna Huttenlocher, Professor, Medical Microbiology and Immunology and Pediatrics
Donata Oertel, Professor, Neuroscience

DEDICATION

I would first like to express my gratitude to my advisor, Barry Ganetzky. I was thrilled when he decided to let me join his lab, and I've benefitted greatly from his dedication to teaching and enthusiasm for science. Under Barry's mentorship I received the support I needed to develop as a scientist and the freedom to explore the biological questions that excited me most.

The Ganetzky lab provided the ideal research environment for me to grow as a scientist. I would like to acknowledge the current post-doctoral fellows in the lab, Daniel Babcock, Stanislava Chtarbanova, Richard Daniels and Carin Loewen. They were a constant source of support throughout my graduate training and have always been willing to discuss scientific questions, troubleshoot problems, analyze confusing results and suggest new experiments. I cannot thank them enough for their contributions to my development as a scientist.

I was fortunate to train with three other graduate students, Xu Chen, Megan Campbell and Yang Cao. They were all strong examples of successful, productive graduate students. I would like to express deepest gratitude to Yang, with whom I collaborated on the NMJ project presented in this dissertation. I would like to thank Robert Kreber and Ling Ling Ho, the Ganetzky lab managers. Bob irradiated all of the larvae for the experiments in Part 2 of this dissertation. Finally, I would like to thank the two undergraduates who worked with me, Brian Robichaud and Suma Samudrala. They were incredibly helpful and it was a pleasure to have them in the lab.

The project described in Part 2 of this dissertation was motivated by a clinical rotation I did with Steve Howard in radiation oncology. I am grateful to Steve for the support, advice, and clinical expertise he has provided throughout this project.

I would also like to thank David Wassarman for his contributions to our weekly lab meetings, my committee members, Grace Boekhoff-Falk, Erik Dent, Anna Huttlocher and Donata Oertel, and the MSTP and NTP directors and staff for their support.

I would be remiss to not thank my past scientific advisors for their mentorship and encouragement: Ross Cagan, Jill Fink, Marcos Vidal, Pascal Meier, Francois Leulier and Craig Micchelli. They nurtured my excitement for science and motivated me to pursue a career in biomedical research. I would especially like to thank Craig, who trusted me with independent projects, challenged me, and taught me the value of rigorous science and critical analysis.

I would also like to thank my friends. From growing up, to Washington University, to Madison I have been fortunate to have a strong network of love and support. Finally I would like to acknowledge and express my deepest gratitude to my family – my siblings, Todd, Jennifer, Sally and Katie, my parents Dave and Jo, and my boyfriend Jesse.

TABLE OF CONTENTS

ABSTRACT

The laboratory fruit fly *Drosophila melanogaster* has been used for decades to identify and analyze molecular pathways underlying processes such as development and the innate immune response and for modeling complex diseases. The genetic tools available in Drosophila have facilitated the discovery of signal transduction pathways that have later been found to be essential for human development and disease pathogenesis. Drosophila has been especially useful for studying development and diseases of the nervous system. Insights gained from work in Drosophila on synaptic growth, circuit formation, synaptic plasticity and maintenance, and neuroprotection have informed our understanding of neurodevelopmental disorders and neurodegeneration. In this thesis, I describe the use of Drosophila in two different projects. The first is characterization of a novel signaling pathway regulating growth of the larval neuromuscular junction. The second is the development of an experimental model to investigate neurotoxic effects of radiation exposure during development.

Using the larval neuromuscular junction as a model synapse we have identified the lipocalin GLaz, the ortholog of human Apolipoprotein D (hApoD) as a novel regulator of synaptic growth. In *GLaz* mutants we observe NMJ overgrowth as measured by an increase in bouton number at the presynaptic terminal. We have shown that postsynaptic insulin signaling promotes growth of the presynaptic terminal and that insulin signaling is increased in *GLaz* mutants. Overexpression of GLaz in glia causes NMJ undergrowth. Overexpression of hApoD in glia also results in NMJ undergrowth, indicating conservation of function between GLaz and ApoD. NMJ undergrowth associated with glial overexpression of GLaz is suppressed by simultaneously increasing insulin signaling in muscle. These studies uncover a novel role for lipocalins in regulation of synaptic

growth and support a model in which GLaz is secreted from glia and antagonizes postsynaptic insulin signaling to restrict NMJ growth.

We have also used Drosophila to model the neurotoxic side effects of radiation exposure during development. Cranial radiation therapy (CRT) is an effective treatment for pediatric central nervous system malignancies but survivors often suffer from neurological and neurocognitive side effects that persist many years after radiation exposure. Although the highest doses of radiation are targeted to the anatomical location of the tumor, damage to healthy tissue is a side effect of therapy. We have shown that many of the side effects observed in human patients treated with CRT during development can be modeled in Drosophila. Adult flies exposed to radiation during larval development display reduced survival to adulthood, early death, impaired locomotor behavior, and neurodegeneration. These phenotypes are consistent with premature aging, which is commonly observed in adults who received CRT early in life. One hallmark of this premature aging is chronic inflammation. Similarly, we find persistent activation of the innate immune system in adult flies that were exposed to radiation during larval development. Expression of NF-κB target genes is increased systemically in adult flies following radiation exposure during development, notably in the brain. Although chronic inflammation may be contributing to premature aging, we further demonstrate that the innate immune response is protective acutely following radiation. Together these data demonstrate that the innate immune pathway is a potential therapeutic target for reducing the side-effects of CRT. The use of this experimental model in genetic screens should facilitate identification of additional radioprotective or radiosensitizing pathways, which may be of further therapeutic value.

PART 1: GENETIC ANALYSIS OF SYNAPTIC GROWTH IN *DROSOPHILA MELANOGASTER*

CHAPTER 1

Introduction to Synaptic Development and Insulin Signaling

Clinical importance of studying synapse development

Synapses are the basic functional units in the nervous system, the sites where electrical information is processed, integrated and transmitted, the sites of plastic changes in structure and function that underlie learning and memory, and the sites of pathology in many neurodevelopmental and neurodegenerative conditions (Penzes et al., 2011). Understanding the mechanisms responsible for synaptic pathology is important for developing therapeutic strategies to improve treatment of these conditions. A direct way to uncover the cellular pathways that are perturbed in pathological conditions is to identify and study the pathways that control normal synaptic development because these pathways are the ones most likely to be disrupted by disease. Although a number of signal transduction pathways have been implicated in synaptic development, we still lack comprehensive understanding of the mechanisms that govern synaptic complexity and architecture, and additional pathways remain to be identified (Collins and DiAntonio, 2007).

Changes in synaptic growth and morphology, including altered size, shape or number of dendritic spines is a hallmark of many neurodevelopmental and neurodegenerative conditions, including epilepsy, Autism Spectrum Disorder (ASD), and Alzheimer's disease (AD) (Penzes et al., 2011). In AD, synaptic pathology, particularly at cholinergic and glutamateric synapses, correlates with early stages of the disease when memory deficits are subtle (Selkoe, 2002). Loss of presynaptic terminals is observed in the amyloid-precursor-protein (APP) mouse before plaque deposition even begins (Selkoe, 2002), and synapse loss is correlated with the severity of cognitive decline (DeKosky and Scheff, 1990). The importance of tightly regulated synaptic growth and pruning, on the other hand, is evident in disorders such as ASD in which excessive

synaptic growth in the first three years of life may contribute to the development of the disorder (Bourgeron, 2009).

Pathways regulating synaptic growth are potential therapeutic targets for the design of treatments to prevent synaptic loss in neurodegenerative conditions such as in AD, or to promote the natural pruning process in conditions of synaptic overgrowth, such as in ASD. The fruit fly *Drosophila melanogaster* is an ideal model system for elucidating the mechanisms controlling synaptic development because of the powerful molecular and genetic tools that can be used to manipulate and track cellular processes in a temporally and spatially restricted manner. The Drosophila larval neuromuscular junction (NMJ) is an especially useful system for studying synaptic development because of its size, accessibility, and stereotypic morphology, which facilitate imaging and quantifying NMJ size by counting the number of boutons and synaptic branches (Collins and DiAntonio, 2007). Furthermore, the Drosophila NMJ is a glutamatergic synapse, a feature shared with the excitatory synapses of the vertebrate central nervous system (CNS).

It is especially intriguing to study the role of the insulin signaling in synaptic development because the nervous system has historically been thought of as an insulin-insensitive tissue. Only in recent years has evidence emerged demonstrating a role for insulin signaling in synaptic plasticity and circuit function (Chiu et al., 2008). Diabetic animal models have been used to study the pathogenesis of diabetic neuropathy resulting in the identification of causative mechanisms, including activation of proinflammatory pathways, protein kinase C activation, and a reduction in neurotrophic factors (Obrosova, 2009; Yasuda et al., 2003), but the possibility that insulin signaling plays a more direct role in regulating synaptic growth and function has only recently been appreciated. Finally, population-based studies have shown a modest, but reproducible link between Diabetes Mellitus and the development of Alzheimer's Disease

(Arvanitakis et al., 2004; Luchsinger et al., 2001) emphasizing the importance of further studies to elucidate the molecular mechanisms that may link the pathophysiological sequelae of these two diseases.

Insulin Signaling in Drosophila

Drosophila insulin receptor is a tyrosine kinase dimer. Activation of this receptor triggers a lipid kinase cascade involving familiar players such as PI3 kinase (PI3K), PTEN, and Akt (Brazil and Hemmings, 2001; Bohni et al., 1999). These kinases regulate the activity of metabolic programs, largely through the forkhead transcription factor FOXO (Barthel et al., 2005; Wang et al., 2011) and the target of rapamycin (TOR). The Drosophila insulin receptor (InR) is essential for development, and loss of function mutations are embryonic lethal (Fernandez et al., 1995). The alpha subunit of InR is ligand-binding, and the beta subunit has tyrosine kinase activity. Two isoforms of the InR are generated from the Drosophila *InR* gene (Fernandez et al., 1995). The alpha subunit is invariant, but there are two forms of the beta subunit (Fernandez et al., 1995). Upon InR activation, the beta subunits undergo tyrosine phosphorylation. The phosphorylated form of one of the two beta isoforms directly activates PI3K (Fernandez et al., 1995). The other InR isoform acts through Chico, the Drosophila homolog of the mammalian insulin receptor substrate (Bohni et al., 1999). Signaling through the two InR isoforms appears to converge at PI3K because phosphorylated Chico activates PI3K (Bohni et al., 1999).

There are seven insulin-like peptide genes (*dilp1-7*) in Drosophila (Brogiolo et al., 2001; Rulifson et al., 2002). *Dilp1-5* have significant homology to mammalian insulins, while *dilp6* and *-7* are less similar (Rulifson et al., 2002). Neurosecretory cells in the pars intercerebralis

region of the Drosophila brain are responsible for the majority of expression of *dilp1,-2, -3,* and -*5* (Brogiolo et al., 2001; Rulifson et al., 2002). These cells, (insulin-producing cells or IPCs) secrete DILPs into the hemolymph, supplying most of the insulin signal during larval growth. Ablating these IPCs results in growth retardation (smaller at all stages of development and as adults) and developmental delay (pupariation normally occurs 5-6 days after egg lay, but in flies lacking IPCs it occurs at 12 days) (Rulifson et al., 2003). The metabotropic $GABA_B$ receptor is expressed on IPCs. Activation of this receptor functions to inhibit DILP synthesis and release (Enell et al., 2010). *Dilp4* and -*6* are expressed in the Drosophila gut, and *dilp7* is expressed in the ventral nerve cord (Brogiolo et al., 2001).

The best characterized role of insulin signaling in Drosophila is regulating metabolic homeostasis. It has been shown that the Drosophila fat body acts as a nutrient sensor and relays information to the IPCs in the Drosophila brain (Rajan et al., 2012). In the fed state, the fat body secretes Unpaired 2 (Upd2) which activates JAK/STAT signaling in the GABAergic neurons that synapse with the IPCs to regulate release of DILPs (Rajan et al., 2012). JAK/STAT activation in these neurons decreases their inhibitory output on IPCs resulting in increased DILP release from the IPCs (Rajan et al., 2012).

Insulin signaling mutants demonstrate its importance in regulation of growth and nutrient status. Flies homozygous for a loss of function mutation in *chico* are almost half the size of wild type flies (Bohni et al., 1999). In mosaic flies, *chico* mutant cells display slower growth, smaller size, and form smaller organs (Bohni et al., 1999). Interestingly, *chico* flies, despite their small size, have lipid levels almost two times greater than wild type controls (Bohni et al., 1999). Inhibition of InR activity specifically in body wall muscles of Drosophila results in smaller muscle size and a surprising reduction in the size of other organs (Demontis and Perrimon, 2009). It has been

shown that InR acts through FOXO to regulate *dmyc* expression, which controls progression through the cell cycle (Demontis and Perrimon, 2009). The homeostatic role of insulin signaling also intersects with the immune response. Insulin signaling in the fat body and elsewhere is specifically inhibited by Toll signaling within the fat body (DiAngelo et al., 2009). Through its regulation of insulin signaling, Toll signaling in the fat body decreases nutrient storage and growth and causes developmental delay (DiAngelo et al., 2009).

Insulin signaling also has a well characterized role in regulating lifespan. In files with *InR* hypomorphic heteroallelic combinations, dwarf females have an 85% extension of lifespan (Tatar et al., 2001). Dwarf males specifically show reduced mortality at later ages (Tatar et al., 2001). Flies homozygous for *chico* null mutations display a 48% increase in lifespan (Clancy et al., 2001). Heterozygous *chico* flies (*chico*$^{+/-}$) display a 36% increase in lifespan (Clancy et al., 2001). Since heterozygous *chico* flies are normal sized, the lifespan extension associated with *chico* is not entirely due to its effect on body size (Clancy et al., 2001).

Insulin signaling in synaptic development

An important study from Vivan Budnik's lab in 1993 localized the insulin receptor to neuronal tissue. This work showed that the insulin receptor is present at the Drosophila NMJ, specifically on the muscle cells at the site of motor neuron branching, surrounded by boutons (Gorczyca et al., 1993). Insulin receptors were first detected at the NMJ during the early 2nd instar stage, which is after synaptic contacts have been made (Gorczyca et al., 1993). This suggests that insulin signaling at the NMJ is not required for synaptogenesis, but may play a role in synaptic maturation (Gorczyca et al., 1993).

The signaling machinery downstream of insulin receptor activation (including PI3K, FOXO, and TOR) has been shown to play important roles in plasticity at the synapse. PI3K has been shown to be involved in regulating neuronal excitability (Howlett et al., 2008). Metabotropic glutamate receptors (mGluRs) located on the terminals of presynaptic motor neuron axons at the NMJ act to decrease neuronal excitability when activated (Howlett et al., 2008). Recent evidence suggests that this process involves activation of PI3 kinase (PI3K) and downstream inhibition of the transcription factor FOXO (Howlett et al., 2008). FOXO has been shown to negatively regulate the stability of microtubules in the motor neuron at the NMJ (Nechipurenko and Broihier, 2012). There is also evidence supporting the idea that TOR-regulated translation is involved in synaptic plasticity at the Drosophila Neuromuscular Junction (Penney et al., 2012). One study suggests that postsynaptic TOR acts to enhance neurotransmitter release when there is a reduction in postsynaptic glutamate receptor activity at the NMJ (Penney et al., 2012).

A role for insulin signaling in synaptic plasticity has also been identified. Experiments performed in HEK293 cells and in cultured mouse hippocampal neurons showed that insulin promotes translocation of the $GABA_A$ receptor from an intracellular compartment to the cell membrane (Wan et al., 1997). Treatment of rat hippocampal slices with insulin also significantly increases functional postsynaptic $GABA_A$ receptor density (Wan et al., 1997). A role for insulin signaling in synaptic plasticity *in vivo* has been identified in *Xenopus* tectal neurons (Chiu et al., 2008). *Xenopus* tectal neurons expressing a dominant-negative insulin receptor (DN-InR) display smaller light-evoked responses (Chiu et al., 2008). DN-InR neurons are also characterized by lower synapse density, decreased frequency of AMPA mini EPSCs, and aberrant structural plasticity of the dendritic arbor (Chiu et al., 2008). Insulin signaling has also been shown to be important in olfactory associative learning (Naganos et al., 2012).

Finally, Insulin signaling in the post-embryonic Drosophila brain has been shown to be important in the process of gliogenesis (Avet-Rochex, et al., 2012). Specifically, the insulin receptor is required for post-embryonic perineural and cortex glia proliferation (Avet-Rochex et al., 2012). Most of gliogenesis occurs during the second and third larval instars. In situ hybridization analysis demonstrated that *dilp6* is extensively expressed in the CNS at the beginning of the 3rd instar stage and diminishes by the end of the 3rd instar (Avet-Rochex et al., 2012). *Dilp6* loss of function mutants or a reduction in PI3K or TOR signaling in glia all lead to a reduction in the number of glial cells (Avet-Rochex et al., 2012).

References

Arvanitakis, Z., Wilson, R. S., Bienias, J. L., Evans, D. A. and Bennett, D. A. (2004). Diabetes mellitus and risk of Alzheimer disease and decline in cognitive function. *Arch Neurol* **61**, 661-6.

Avet-Rochex, A., Kaul, A. K., Gatt, A. P., McNeill, H. and Bateman, J. M. (2012). Concerted control of gliogenesis by InR/TOR and FGF signalling in the Drosophila post-embryonic brain. *Development* **139**, 2763-72.

Barthel, A., Schmoll, D. and Unterman, T. G. (2005). FoxO proteins in insulin action and metabolism. *Trends Endocrinol Metab* **16**, 183-9.

Böhni, R., Riesgo-Escovar, J., Oldham, S., Brogiolo, W., Stocker, H., Andruss, B. F., Beckingham, K. and Hafen, E. (1999). Autonomous control of cell and organ size by CHICO, a Drosophila homolog of vertebrate IRS1-4. *Cell* **97**, 865-75.

Bourgeron, T. (2009). A synaptic trek to autism. *Curr Opin Neurobiol* **19**, 231-4.

Brazil, D. P. and Hemmings, B. A. (2001). Ten years of protein kinase B signalling: a hard Akt to follow. *Trends Biochem Sci* **26**, 657-64.

Brogiolo, W., Stocker, H., Ikeya, T., Rintelen, F., Fernandez, R. and Hafen, E. (2001). An evolutionarily conserved function of the Drosophila insulin receptor and insulin-like peptides in

growth control. *Curr Biol* **11**, 213-21.

Chiu, S. L., Chen, C. M. and Cline, H. T. (2008). Insulin receptor signaling regulates synapse number, dendritic plasticity, and circuit function in vivo. *Neuron* **58**, 708-19.

Clancy, D. J., Gems, D., Harshman, L. G., Oldham, S., Stocker, H., Hafen, E., Leevers, S. J. and Partridge, L. (2001). Extension of life-span by loss of CHICO, a Drosophila insulin receptor substrate protein. *Science* **292**, 104-6.

Collins, C. A. and DiAntonio, A. (2007). Synaptic development: insights from Drosophila. *Curr Opin Neurobiol* **17**, 35-42.

DeKosky, S. T. and Scheff, S. W. (1990). Synapse loss in frontal cortex biopsies in Alzheimer's disease: correlation with cognitive severity. *Ann Neurol* **27**, 457-64.

Demontis, F. and Perrimon, N. (2009). Integration of Insulin receptor/Foxo signaling and dMyc activity during muscle growth regulates body size in Drosophila. *Development* **136**, 983-93.

DiAngelo, J. R., Bland, M. L., Bambina, S., Cherry, S. and Birnbaum, M. J. (2009). The immune response attenuates growth and nutrient storage in Drosophila by reducing insulin signaling. *Proc Natl Acad Sci U S A* **106**, 20853-8.

Enell, L. E., Kapan, N., Söderberg, J. A., Kahsai, L. and Nässel, D. R. (2010). Insulin signaling, lifespan and stress resistance are modulated by metabotropic GABA receptors on insulin producing cells in the brain of Drosophila. *PLoS One* **5**, e15780.

Fernandez, R., Tabarini, D., Azpiazu, N., Frasch, M. and Schlessinger, J. (1995). The Drosophila insulin receptor homolog: a gene essential for embryonic development encodes two receptor isoforms with different signaling potential. *EMBO J* **14**, 3373-84.

Gorczyca, M., Augart, C. and Budnik, V. (1993). Insulin-like receptor and insulin-like peptide are localized at neuromuscular junctions in Drosophila. *J Neurosci* **13**, 3692-704.

Howlett, E., Lin, C. C., Lavery, W. and Stern, M. (2008). A PI3-kinase-mediated negative feedback regulates neuronal excitability. *PLoS Genet* **4**, e1000277.

Luchsinger, J. A., Tang, M. X., Stern, Y., Shea, S. and Mayeux, R. (2001). Diabetes mellitus and risk of Alzheimer's disease and dementia with stroke in a multiethnic cohort. *Am J Epidemiol* **154**, 635-41.

Naganos, S., Horiuchi, J. and Saitoe, M. (2012). Mutations in the Drosophila insulin receptor substrate, CHICO, impair olfactory associative learning. *Neurosci Res* **73**, 49-55.

Nechipurenko, I. V. and Broihier, H. T. (2012). FoxO limits microtubule stability and is itself negatively regulated by microtubule disruption. *J Cell Biol* **196**, 345-62.

Obrosova, I. G. (2009). Diabetic painful and insensate neuropathy: pathogenesis and potential treatments. *Neurotherapeutics* **6**, 638-47.

Penney, J., Tsurudome, K., Liao, E. H., Elazzouzi, F., Livingstone, M., Gonzalez, M., Sonenberg, N. and Haghighi, A. P. (2012). TOR is required for the retrograde regulation of synaptic homeostasis at the Drosophila neuromuscular junction. *Neuron* **74**, 166-78.

Penzes, P., Cahill, M. E., Jones, K. A., VanLeeuwen, J. E. and Woolfrey, K. M. (2011). Dendritic spine pathology in neuropsychiatric disorders. *Nat Neurosci* **14**, 285-93.

Rajan, A. and Perrimon, N. (2012). Drosophila cytokine unpaired 2 regulates physiological homeostasis by remotely controlling insulin secretion. *Cell* **151**, 123-37.

Rulifson, E. J., Kim, S. K. and Nusse, R. (2002). Ablation of insulin-producing neurons in flies: growth and diabetic phenotypes. *Science* **296**, 1118-20.

Selkoe, D. J. (2002). Alzheimer's disease is a synaptic failure. *Science* **298**, 789-91.

Tatar, M., Kopelman, A., Epstein, D., Tu, M. P., Yin, C. M. and Garofalo, R. S. (2001). A mutant Drosophila insulin receptor homolog that extends life-span and impairs neuroendocrine function. *Science* **292**, 107-10.

Wan, Q., Xiong, Z. G., Man, H. Y., Ackerley, C. A., Braunton, J., Lu, W. Y., Becker, L. E.,

MacDonald, J. F. and Wang, Y. T. (1997). Recruitment of functional GABA(A) receptors to postsynaptic domains by insulin. *Nature* **388**, 686-90.

Wang, B., Moya, N., Niessen, S., Hoover, H., Mihaylova, M. M., Shaw, R. J., Yates, J. R., Fischer, W. H., Thomas, J. B. and Montminy, M. (2011). A hormone-dependent module regulating energy balance. *Cell* **145**, 596-606.

Yasuda, H., Terada, M., Maeda, K., Kogawa, S., Sanada, M., Haneda, M., Kashiwagi, A. and Kikkawa, R. (2003). Diabetic neuropathy and nerve regeneration. *Prog Neurobiol* **69**, 229-85.

CHAPTER 2

GLaz regulates neuromuscular junction growth by antagonizing postsynaptic insulin signaling in Drosophila

This work was carried out in collaboration with Yang Cao, PhD. The data in Figures 1,2,3 and 6 and images in Figure 5 were generated by Dr. Cao. The candidate edited these figures in preparing this chapter. The data in Supplementary Figure 5 was generated by Dr. Richard Daniels. The candidate generated the data in the remaining figures, made the figures and wrote this chapter.

Abstract

The Drosophila lipocalin GLaz is best characterized for its role in aging and the stress response. Although *GLaz* is expressed in the developing nervous system, a role for GLaz in regulating synaptic development has not been investigated. Here, we demonstrate that GLaz, the ortholog of human Apolipoprotein D (hApoD), negatively regulates growth of the Drosophila larval neuromuscular junction (NMJ). In *GLaz* mutants we observe NMJ overgrowth as measured by an increase in bouton number at the presynaptic terminal. We have shown that postsynaptic insulin signaling promotes growth of the presynaptic terminal and that insulin signaling is increased in *GLaz* mutants. Overexpression of GLaz in glia causes NMJ undergrowth. Overexpression of hApoD in glia also results in NMJ undergrowth, indicating conservation of function between GLaz and ApoD. NMJ undergrowth associated with glial overexpression of GLaz is suppressed by simultaneously increasing insulin signaling in muscle. These studies uncover a novel role for lipocalins in regulation of synaptic growth and support a model in which GLaz is secreted from glia and antagonizes postsynaptic insulin signaling to restrict NMJ growth.

Introduction

Proper formation of neural circuits requires accurate and precise development of synapses. Synapses are the basic functional units of the nervous system, the sites of information transfer, processing and integration. Impaired formation of synapses underlies many neurodevelopomental disorders including autism and fragile X syndrome (He and Portera-Cailliau, 2013; Berkel et al., 2010; Shinoda et al., 2013). Although much effort has been invested in identifying the genetic and molecular pathways regulating synapse development, we still lack a complete understanding of this complex process. The Drosophila larval neuromuscular junction (NMJ) has long proven to be an ideal model for studying synapse development and plasticity (Collins and DiAntonio, 2007). Larval NMJs are large glutamatergic synapses with stereotyped morphologies. Many of the regulators of NMJ growth that have already been identified are conserved with vertebrates (Featherstone and Broadie, 2000; Keshishian et al., 1996; Collins and DiAntonio, 2007).

A number of pathways that regulate NMJ development act via secretion of neurotrophic factors that function at the NMJ to regulate presynaptic terminal growth. Wingless signaling promotes NMJ growth through secretion of the Wingless ligand from presynaptic terminals, which activates both pre- and postsynaptic Frizzled2 receptors (Packard et al., 2002; Salinas, 2005). The TGF-β-BMP ligand Glass bottom boat (Gbb) is secreted from muscle and promotes NMJ growth by signaling through receptors expressed on the presynaptic membrane (McCabe et al., 2003; Aberle et al., 2002; Marqués et al., 2002). Release of Gbb is further regulated by the TGF-β ligand Maverick, which is secreted from NMJ glia and activates the Punt receptor in muscle (Fuentes-Medel et al., 2012).

Here, we show that the lipocalin family member glial lazarillo (GLaz), the Drosophila ortholog of human apolipoprotein D (hApoD) is a negative regulator of NMJ growth. Lipocalins are small, secreted proteins that can bind hydrophobic ligands (Flower, 1996). Lipocalins have been widely studied and are involved in numerous biological processes from regulation of metabolism, to stress response, to aging (Hull-Thompson et al., 2009; Walker et al., 2006; Sanchez et al., 2006). There are three Drosophila lipocalins - GLaz, NLaz and karl. NLaz functions to regulate metabolic homeostasis, and is induced by stress (Hull-Thompson et al., 2009). Karl expression is also increased under stress, but unlike NLaz it does not prevent starvation (Hull-Thompson et al., 2009).

Human ApoD (hApoD) is a highly conserved protein that is expressed in many different human tissues, (Provost et al., 1990; Dassati et al., 2014), however rodent ApoD expression is mainly in the central nervous system (Rassart et al., 2000). ApoD expression is increased in a number of conditions including Alzheimer's Disease, schizophrenia, bipolar disorder and normal aging (Terrisse et al., 1998; Navarro et al., 2003; Kalman et al., 2000; Sutcliffe and Thomas, 2002; Lee et al., 2000). In a meta-analysis of genes upregulated with age in humans, rats and mice, ApoD was the most significantly overexpressed gene with age (de Magalhaes et al., 2009). In the mouse brain, ApoD protects against oxidative damage and lipid peroxidation (Ganfornina et al., 2008) and is thought to be important for combating stress in the aging brain (Dassati et al., 2014). Nerve crush experiments in rats also demonstrated increased ApoD in the regenerating nerve (Boyles et al., 1990). In mice, ApoD overexpression results in metabolic defects including insulin resistance (Do Carmo et al., 2009) and loss of ApoD causes dyslipidemia (Jimenez-Palomares et al., 2011), suggesting a role for ApoD in metabolic regulation. Although there has been a lack of studies investigating roles of hApoD during development, gene expression

analyses in human prefrontal cortex demonstrated that *ApoD* expression increases throughout life. *ApoD* expression is low in the neonatal stage and continues to increase throughout development as the human brain is maturing, suggesting that it may play an important role in development (Kim et al., 2009).

In adult flies, the Drosophila ortholog of hApoD, GLaz, promotes longevity and resistance to oxidative stress (Sanchez et al., 2006; Walker et al., 2006). Loss of GLaz results in a shortened lifespan, impaired motor behavior and increased sensitivity to paraquat treatment (Sanchez et al., 2006). Overexpression of GLaz causes lifespan extension and enhanced resistance to hyperoxia and starvation (Walker et al., 2006). Overexpression of hApoD in adult Drosophila results in phenotypes similar to *GLaz* expression, including lifespan extension and stress resistance, demonstrating functional conservation of GLaz and hApoD (Muffat et al., 2008). Like *hApoD*, *GLaz* expression is also induced by stress in adult flies (Muffat et al., 2008).

Despite the roles GLaz plays in the adult, to date no studies have investigated potential roles for GLaz in development. A number of pathways that are involved in the stress response in adult flies, including autophagy and Toll-like signaling, are also important in regulation of synapse development (Shen and Ganetzky, 2009; Ballard et al., 2014). The characterized function of GLaz in the Drosophila stress response and the association of hApoD expression with neurological disorders as well as the expression of *hApoD* and *GLaz* in the developing nervous system (Sanchez et al., 2000) led us to investigate whether GLaz plays a role in synaptic development. Here we demonstrate that glial expression of *GLaz* negatively regulates NMJ development. Our data suggest that post-synaptic insulin signaling promotes NMJ growth and that GLaz inhibits insulin signaling in muscle to restrict NMJ growth. These results demonstrate

that in addition to its roles promoting longevity and stress resistance in adult flies, GLaz also regulates the growth and development of the larval NMJ.

Results

GLaz is a negative regulator of NMJ growth

To determine whether GLaz has a role in regulating NMJ growth, we examined NMJ morphology in *GLaz* mutant larvae. We found that mutations in *GLaz* cause an increase in mean bouton number at NMJ4 (Fig. 1). The number of boutons in *GLaz* mutants is increased by 40% compared with wild-type or heterozygous (GLaz/+) controls. We also confirmed that NMJ overgrowth is observed in larvae with heteroallelic combinations of *GLaz* mutations, including a deficiency spanning the *GLaz* locus on chromosome 2R. The NMJ overgrowth observed in *GLaz* mutants suggests that GLaz negatively regulates NMJ growth.

GLaz expression in glia regulates NMJ growth

When GLaz was first characterized in Drosophila it was named glial Lazarillo because the embryonic cells expressing GLaz stained positively for the glial marker Repo (Sanchez et al., 2000). mRNA expression data demonstrates that *GLaz* is expressed in the larval CNS, but not the larval carcass (FlyAtlas), suggesting that of the cells that make up the NMJ, including neurons, glia and muscle, GLaz is likely secreted from glia to regulate NMJ growth. To test whether GLaz expression in glia is required to regulate NMJ growth, we reduced GLaz expression using the glial-specific *Repo-Gal4* driver and RNAi directed against GLaz transcripts. We observed a mild increase in bouton number in *Repo>UAS-GLaz-RNAi* larvae compared with wild-type controls (Fig. 2), supporting a model in which GLaz is secreted from glia to restrict NMJ growth. To test

whether GLaz expression in other larval tissues may be contributing to the secreted pool of GLaz that regulates NMJ growth, we also tested whether ubiquitous expression of *GLaz-RNAi* using the *Tubulin-Gal4* driver results in NMJ overgrowth. We observed greater NMJ overgrowth in *Tubulin>UAS-GLaz-RNAi* larvae compared to controls and *Repo>UAS-GLaz-RNAi* larvae (Fig. 2). Together, these data suggest that glial-derived Glaz restricts NMJ growth. However, there may be other sources of GLaz in addition to glia.

Consistent with a model in which GLaz is secreted from glia to restrict NMJ growth, glial expression of GLaz in an otherwise wild-type larva (*Repo-Gal4>UAS-GLaz*) results in a significant decrease in bouton number compared with control larvae (Fig. 3). Furthermore, *Repo>>GLaz* expression in *GLaz* mutants leads to full rescue of bouton number to wild-type levels. Together, these data suggest that GLaz expression in glia is sufficient to restrict NMJ growth.

Previous work in flies studying the role of Glaz in the adult stress response demonstrated that overexpressing human apolipoprotein D (hApoD) in flies resulted in similar lifespan extension and stress resistance as overexpressing GLaz (Walker et al., 2006; Sanchez et al., 2006; Muffat et al., 2008). This evidence for evolutionarily conserved function led us to test whether overexpressing hApoD in glia would result in similar effects on NMJ development as overexpressing GLaz. Consistent with previous reports of conserved functionality, we observe NMJ undergrowth, as measured by a reduction in bouton number in *Repo-Gal4>UAS-hApoD* larvae similar to that observed in *Repo>>GLaz* larvae (Fig. 3). Moreover, glial expression of hApoD in a *GLaz* mutant background fully rescues NMJ overgrowth and results in a reduction in bouton number to wild-type levels (Fig. 3). To our knowledge, there are no data demonstrating a role for hApoD in development of the mammalian nervous system, although it is known that

expression of *hApoD* increases in the prefrontal cortex throughout development (Kim et al., 2009). Our data suggest that the biochemical functions of GLaz and hApoD may be evolutionarily conserved.

GLaz restricts insulin signaling

Lipocalins are known to be involved in diverse biological processes including regulation of metabolism. ApoD overexpression was shown to cause metabolic defects including insulin resistance in mice (Do Carmo et al., 2009). Work in Drosophila has demonstrated that NLaz is a negative regulator of insulin signaling in larvae (Hull-Thompson et al., 2009) and that fat body physiology is impaired in adult *GLaz* mutants (Sanchez et al., 2006). Based on these studies, we hypothesized that GLaz also negatively regulates insulin signaling. To test this, we used a pleckstrin homology domain-green fluorescent protein (GFP-PH) reporter under the control of a β-tubulin promoter (tGPH) to assess PI3K activity in fat bodies of *GLaz* mutant larvae as a measure of insulin signaling (Hull-Thompson et al., 2009; Britton et al., 2002). Similar to observations in *NLaz* mutant larvae (Hull-Thompson et al., 2009), we observed an increase in membrane localization of the PH-GFP reporter in the fat bodies of *GLaz* larvae indicating an increase in insulin signaling (Fig. 4). These data suggest that GLaz restricts insulin signaling.

Post-synaptic insulin signaling promotes NMJ growth and is epistatic to GLaz

Because GLaz negatively regulates insulin signaling, and insulin signaling is a growth-promoting pathway, we hypothesized that GLaz may function through insulin signaling to restrict NMJ growth. To explore this possibility, we first asked whether insulin signaling in glia, neurons or muscle, the three types of cells at the NMJ, regulates NMJ growth. To test this, we decreased insulin signaling by expressing a dominant-negative form of the insulin receptor (*UAS-InR*^{DN})

using the glial driver *Repo-Gal4*, the neuronal driver *c155-Gal4*, or the muscle driver *24B-Gal4*. In contrast to our results expressing GLaz in glia, decreasing insulin signaling in glia does not lead to a detectable change in NMJ morphology (Fig. 5). The number of boutons in *Repo>UAS-InR^{DN}* NMJs are similar to controls. Similarly, we observed no difference in NMJ size in *c155>UAS-InR^{DN}* larvae compared with controls, suggesting that insulin signaling is not required in the presynaptic terminal for NMJ growth (Fig. 5). Conversely, NMJs in *24B>UAS-InR^{DN}* larvae have fewer boutons compared with controls indicating that postsynaptic insulin signaling promotes NMJ growth (Fig. 5). This finding is also consistent with early reports that the insulin receptor is localized postsynaptically at the NMJ (Gorczyca et al., 1993).

Insulin signaling is also known to affect larval body wall muscle size (Demontis and Perrimon, 2009). We do see a reduction in body wall muscle size in *24B>UAS-InR^{DN}* larvae (Supplementary Fig. 1), and we acknowledge that reduced muscle size itself is associated with fewer boutons in the presynaptic terminal since boutons are added as the muscle grows (Zito et al., 1999). Consistent with this, we see that bouton number tracks muscle size throughout development when insulin signaling is manipulated in muscle (Supplementary Fig. 2). However, we cannot separate the effect of reduced muscle size from reduced insulin signaling itself on the number of boutons in the presynaptic terminal. Therefore, we present the data here as they are, that reduced insulin signaling in muscle results in both a decrease in bouton number and a smaller body wall muscle area, and aim to avoid overinterpretation of these data.

Our results thus far indicate that GLaz negatively regulates NMJ growth and insulin signaling, and that postsynaptic insulin signaling positively regulates NMJ growth. If GLaz restricts NMJ growth by antagonizing postsynaptic insulin signaling, the NMJ overgrowth observed in GLaz mutants should be caused by increased postsynaptic insulin signaling. If this is true, impaired

insulin signaling should prevent NMJ overgrowth in *GLaz* larvae. To test this, we reduced postsynaptic insulin signaling using *UAS-InR^{DN}* and the muscle driver *24B-Gal4* in *GLaz* mutants. We observe NMJ undergrowth in *GLaz $^{-/-}$;24B>UAS-InR^{DN}* larvae, characterized by bouton numbers similar to that observed in *24B>UAS-InR^{DN}* larvae (Figure 6). These data indicate that postsynaptic insulin signaling is epistatic to GLaz in regulation of NMJ growth and suggests that GLaz antagonizes postsynaptic insulin signaling to restrict NMJ growth.

To further test this we used both the LexA/LexAop and Gal4/UAS systems to overexpress GLaz in glia and increase insulin signaling in muscle in the same larva. We predicted that if GLaz negatively regulates insulin signaling to restrict NMJ growth, the NMJ undergrowth observed when GLaz is overexpressed in glia should be prevented by increasing insulin signaling in muscle. Glial overexpression of GLaz using the LexA system results in similar NMJ undergrowth to glial overexpression of GLaz using the Gal4 system (Fig 6). Conversely, when insulin signaling is increased in muscle by expressing an activated form of the insulin receptor (*UAS-InR^{Act}*) using *24B-Gal4*, we observe an increase in bouton number, similar to *GLaz* mutants (Fig. 6J and K). In *Repo-LexA>LexAop-GLaz;24B-Gal4>UAS-InR^{Act}* larvae we observe presynaptic terminal overgrowth, similar to the presynaptic terminal overgrowth seen in *24B>UAS-InR^{Act}* larvae (Fig. 6). Together these data indicate that postsynaptic insulin signaling is antagonized by glial-derived GLaz to restrict presynaptic terminal growth.

To further test the functional conservation of GLaz and hApoD we also overexpressed hApoD in glia and tested whether insulin signaling in muscle prevents NMJ undergrowth. As with GLaz, in *Repo-LexA>LexAop-hApoD;24B-Gal4>UAS-InR^{Act}* larvae we observe NMJ overgrowth characterized by bouton numbers similar to *24B>UAS-InR^{Act}* larvae (Fig. 6). These data provide additional support for the functional conservation of GLaz and hApoD.

Discussion

Using a candidate-gene approach, we discovered that the Drosophila lipocalin GLaz negatively regulates growth of the larval NMJ by antagonizing insulin signaling in postsynaptic muscle. In addition, we demonstrate that overexpression of the human ortholog of GLaz, hApoD, in glia results in phenotypes similar to overexpression of GLaz. This work demonstrates a new role for GLaz in the regulation of synaptic development in Drosophila. Additionally, our findings suggest that there may be a mechanistic link between pathways regulating synaptic growth and those regulating stress response and metabolic homeostasis.

Our findings indicate that GLaz antagonizes insulin signaling to regulate NMJ growth. The literature on insulin signaling in the nervous system is expansive. Insulin receptors have long been known to be present in the human CNS and are thought to be involved in numerous processes from learning and memory to neurodegeneration and development (Song et al., 2003; Craft et al., 1999; Wickelgren, 1998; Zaia and Piantanelli, 2000; Zhao et al., 1999). Model systems have been extensively used to elucidate the roles of insulin signaling in the nervous system. In Drosophila development, insulin signaling in photoreceptor cells functions to guide axons from the retina to the brain (Song et al., 2003). Insulin signaling in flies is also important for peripheral nervous system development, specifically sensory organ precursor formation (Dutriaux et al., 2013). Insulin signaling also promotes growth of Drosophila peptidigergic neurons during metamorphosis (Gu et al., 2014). Conversely, inhibition of insulin signaling in dendrite arborization neurons is required for normal pruning during metamorphosis (Wong et al., 2013). Specific insulin-like peptides in C. elegans have been shown to regulate olfactory learning (Chen et al., 2013). Consistent with our results indicating that insulin signaling functions non-autonomously to regulate growth of the NMJ presynaptic terminal, other studies

have demonstrated non-autonomous roles for insulin signaling in the developing nervous system. For example, in C. elegans, insulin signaling in the hypodermis regulates neuronal migration (Kennedy et al., 2013).

Together with the studies mentioned above, we believe our data provide additional support for the importance of the insulin signaling pathway in development of the nervous system. Neural development is a carefully regulated process that requires substantial energy expenditure. It is consistent with evolutionary logic that the metabolic state of a developing organism and development of the individual organ systems be closely coupled to allow coordinated growth. Nonetheless, different cell types likely have unique mechanisms for mediating cross-talk between metabolic state sensors and pro-growth pathways. Moreover, fine-tuning of pathways like the insulin signaling pathway allow it to be used both for metabolically-regulated growth and for more subtle control of discrete developmental events. For example, GLaz restricts insulin signaling postsynaptically to regulate presynaptic terminal growth without obvious effects on overall development and size of the whole larva.

Our data demonstrate that postsynaptic insulin signaling promotes NMJ growth. This suggests that when energy sources are restricted and there is less insulin signaling in the organism, reduced insulin signaling in muscle will lead to a reduction in boutons at the presynaptic terminal. This, however, is an oversimplified interpretation. Insulin signaling has different effects in different cell types, and while decreased insulin signaling in only muscle cells leads to NMJ undergrowth, global reduction in insulin signaling will have additional non-autonomous effects on presynaptic terminal growth. For example, a global reduction in insulin signaling causes smaller body size, developmental delay and extended lifespan (Böhni et al., 1999; Brogiolo et al., 2001; Clancy et al., 2001; Oldham et al., 2002; Rulifson et al., 2002). When we

looked at NMJs in *chico* mutants, which have reduced global insulin signaling, we observed mild NMJ overgrowth, even though postsynaptic insulin signaling had also been reduced through loss of chico (Supplementary Fig. 3). This mild overgrowth could be due to a number of different causes, all of which we could not explore here, including slower progression through the developmental stages during which boutons are added allowing more time to generate new boutons (Zito et al., 1999; Rulifson et al., 2002; Miller et al., 2012). Another non-autonomous effect of insulin signaling on NMJ growth can be seen by manipulating insulin signaling only in the prothoracic gland using the driver *Phm-Gal4*. In contrast to reduced insulin signaling in muscle, *Phm>UAS-InR-DN* or *Phm>UAS-InR-RNAi* larvae have overgrown NMJs (Supplementary Fig. 3). This NMJ overgrowth is likely due to both the delayed development of these larvae (due to reduced ecdysone release), which stay in the larval stages days longer than controls and the large body size of these larvae (Miller et al, 2012; Mirth et al., 2005; Caldwell et al., 2005).

These data demonstrate the challenges of trying to isolate the role in NMJ development of such a globally important pathway as insulin signaling, which despite its main role in growth and metabolism has unique and important functions in many different cell types. Moreover, the effect of manipulating insulin signaling in muscle on muscle size itself leads to an even greater challenge in dissecting the downstream mechanisms that allow insulin signaling in muscle to be translated to a pro-growth signal in the presynaptic terminal. We have investigated the effects on NMJ growth of reduced activity of individual components of the canonical insulin signaling pathway in muscle (Supplementary Fig. 4). Although we see NMJ undergrowth with each manipulation, there are also significant effects on muscle and larval size that cannot be isolated from the effects on NMJ growth (Supplementary Figs. 1 and 4). Together these results indicate

that insulin signaling in muscle non-autonomously promotes presynaptic terminal growth. At this point, we do not know the degree to which that regulation is due to trans-synaptic communication on muscle size or additional signaling components, and it would be difficult and non-physiologic to try to separate the two.

Our data demonstrate that GLaz negatively regulates NMJ growth by antagonizing insulin signaling in muscle. Thus, the mild NMJ overgrowth observed in GLaz mutants is likely due to a fine-tuned increase in postsynaptic insulin signaling. Smaller-scale regulation of insulin signaling allows for precise control of presynaptic terminal morphology without drastic effects on cell and body size. Moreover, the NMJ overgrowth in *GLaz* mutants and undergrowth in *Repo>>GLaz* and *Repo>>hApoD* larvae are not associated with changes in synaptic function (Supplementary Fig 5). Thus, the physiological implications of NMJ growth regulation by GLaz are not clear at this point.

It will be of interest to learn the mechanisms regulating GLaz secretion. For example, GLaz expression in adult flies is increased following paraquat treatment, heat shock or hyperoxia (Muffat et al., 2008), suggesting that stress may also be a trigger for GLaz expression in the developing larva. Transcription of the two other Drosophila lipocalins, *NLaz* and *Karl*, but not *GLaz* is induced by JNK activation to promote metabolic homeostasis (Hull-Thompson et al., 2009). Other pathways may specifically promote GLaz expression. Overexpression of GLaz promotes stress resistance in flies, and loss of GLaz results in increased sensitivity to stress (Walker et al., 2006; Sanchez et al., 2006). Previous studies of the Drosophila NMJ demonstrated that compensatory mechanisms promote maintenance of synaptic strength in NMJs with fewer boutons (Stewart et al., 1996). One possibility is that increased GLaz expression under stress could restrict bouton addition at the NMJ, and allow for the formation of a normally-

functioning synapse without the additional energy expenditure required to form normal numbers of boutons. Thus, the role of GLaz in NMJ development could be to protect synapses from stress.

In summary, we have demonstrated that the lipocalin GLaz is secreted from glia and restricts NMJ growth by antagonizing postsynaptic insulin signaling. This study provides new information about the mechanisms regulating growth of the Drosophila NMJ and identifies a novel role for lipocalins in synaptic development. A careful characterization of the biological contexts in which GLaz expression is induced and secretion is highest during development will be necessary to fully understand the significance of the role GLaz plays in regulation of NMJ growth.

Materials and Methods

Fly Stocks

Stocks used: *Repo-Gal4*, *24B-Gal4*, *c155-Gal4*, *Dmef2-Gal4, Tubulin-Gal4, CantonS* (wild type control), $chico^{KG00032}$, $GLaz^{MB01748}$, $GLaz^{MI02243}$, *Df(2R)Exel8057, UAS-PI3K-RNAi, UAS-Akt-RNAi, UAS-*TOR^{DN}, *UAS-*InR^{DN}, and *UAS-*InR^{Act} (Bloomington Stock Center). $GLaz^{1}$ (Dr. Maria D. Ganfornina ,Universidad de Valladolid-CSIC, Valladolid, Spain). *UAS-GLaz* and *UAS-hApoD* (Dr. David Walker, University of California-Los Angeles, Los Angeles, California). *UAS-FOX-WT* (Marc Tatar, Brown University). $chico^{1}$and $chico^{2}$ (Ernst Hafen, ETH Zurich). *UAS-GLazRNAi* flies (#107433) were obtained from the Vienna *Drosophila* RNAi Center. All crosses were performed on cornmeal/molasses fly medium and maintained at 25°C.

Immunohistochemistry

Wandering third instar larvae were dissected in cold Ca2+-free saline and fixed for 20 minutes in 4% formaldehyde in phosphate-buffered saline (PBS) then washed with PBST (PBS with 0.1% Triton). Dissected samples were incubated in FITC-conjugated anti-HRP (Jackson ImmunoResearch) at 1:200 overnight at 4°C. Samples were washed with PBST and mounted on glass slides in Vectashield mounting medium (Vector Laboratories).

Imaging and quantification

NMJ's were imaged with a Ziess 510 confocal microscope (63x objective). Boutons were counted at NMJ4 in abdominal segments A2-A4 under an epifluorescencce microscope (40x objective). Muscle 4 area was measured from bright field images (10x objective) using ImageJ software.

Quantification of GFP-PH Membrane Intensity

Wandering 3rd instar larval fat bodies were dissected in 1X PBS and fixed at room temperature for 30 minutes in 4% formaldehyde in phosphate buffer (4% formaldehyde, 0.1M phosphate buffer (pH 7.2), 0.2% TritonX-100). Samples were then washed with 1X PBS and placed in blocking buffer (PBS, 0.2% TritonX-100, 0.1% normal goat serum) for at 4°C overnight. Fat bodies were incubated in primary antibody diluted with blocking buffer at 4°C overnight then washed 2X with PBST (PBS + 0.1% TritonX-100) and incubated in secondary antibody diluted with blocking buffer for 4 hours at room temperature, then washed 2X again with PBST. Samples were mounted on glass slides in Vectashield mounting medium (Vector Laboratories). Antibodies used: Chicken anti-GFP (1:500, Life Technologies) and Goat anti-Mouse Alexa Fluor-488 (1:200, Life Technologies). Confocal images were taken from two location s in fat bodies from 10-12 larvae per genotype (40x objective). All imaging parameters (gain, number of

slides and slice thickness, laser power) were identical for all samples. ImageJ was used to outline cell membranes and nuclei and measure MEAN fluorescence intensity of each outlined area on a SINGLE SLICE from each image. On average, two cells were measured per image. For each cell, mean membrane fluorescence was divided by mean nuclear fluorescence. These values were averaged to obtain the values represented graphically in figure 4.

Electrophysiology

Larvae were dissected in HL-3 containing 0.5 mM Ca2+, first by cutting along the dorsal midline, pinning out the sides and removing the internal organs. The segmental nerves were cut and brain removed. Muscle 6 of segments A3 and A4 of female wandering 3rd instar larvae were targeted for recording using glass microelectrodes with access resistances of 16-30 megaohms when filled with 3M KCl. Data was analyzed if the muscle input resistance was greater than or equal to 5 megaohms and resting potential less than or equal to -60 mV. Spontaneous miniature event amplitude and frequency were analyzed using the first 70 events in the MiniAnalysis program (Synaptosoft) and EJPs were quantified by averaging 100 evoked events using pClamp software (Molecular Devices). EJPs were evoked using a 0.5 msec stimulus delivered to the cut end of the appropriate segmental nerve in a suction electrode. Stimulus voltage was set to just above the threshold required to stimulate both Ib and Is motoneurons.

Western Blotting

Wandering 3rd instar larvae were sliced open dorsally and eviscerated in PBS then immediately transferred to microcentrifuge tubes on dry ice. 5 larvae were dissected per genotype per trial. Fifteen microliters of sample buffer containing SDS and 2-mercaptoethanol was added to the samples, which were then squished, heated for 5minutes at 100°C and spun 10 minutes at

1400RPM. Ten microliters of this lysate was loaded to individual lanes of the gel and run for separation. Protein was transferred to PVDF membranes overnight at 4°C. Antibodies used: Rabbit anti-Akt (Cell Signaling Technologies #9272, 1:500), Rabbit anti-S505-phosphorylated Drosophila Akt (Cell Signaling Technologies #4054, 1:500), Goat anti-Actin (Santa Cruz Biotechnology #1616, 1:1500), Donkey anti Rabbit IR dye 800 (1:15000), Donkey anti Goat IR dye 650 (1:15000). All staining was done in LI-COR TBS blocking buffer. After staining for p-Akt and actin, membranes were stripped using the LI-COR stripping buffer and protocol and restained for Akt. Images were obtained using a LI-COR Odyssey Infrared Imaging machine and quantified using the LI-COR Image Studio software.

qRT-PCR: Wandering 3rd instar larvae were either first dissected as described for Western Blotting or whole larvae were transferred to microcentrifuge tubes and frozen at -80°C. RNA was extracted from frozen samples using TRI Reagent RT (Molecular Research Center, Cincinnati, OH). The iScript cDNA Synthesis Kit (Bio-Rad, Hercules, CA) was used to generate cDNA. Quantitative real-time PCR was performed using SYBR Green Supermix (Bio-Rad, Hercules, CA). *Rp49* was used as the reference gene. PCR was performed with a Bio-Rad iCycler and the following program: 35 cycles: step1: 95°C for 10 seconds, step 2: 60°C for 30 seconds, step 3: 72°C for 40 seconds each cycle.

References

Aberle, H., Haghighi, A. P., Fetter, R. D., McCabe, B. D., Magalhães, T. R. and Goodman, C. S. (2002). wishful thinking encodes a BMP type II receptor that regulates synaptic growth in Drosophila. *Neuron* **33**, 545-58.

Ballard, S. L., Miller, D. L. and Ganetzky, B. (2014). Retrograde neurotrophin signaling through Tollo regulates synaptic growth in Drosophila. *J Cell Biol* **204**, 1157-72.

Berkel, S., Marshall, C. R., Weiss, B., Howe, J., Roeth, R., Moog, U., Endris, V., Roberts, W., Szatmari, P., Pinto, D. et al. (2010). Mutations in the SHANK2 synaptic scaffolding gene in autism spectrum disorder and mental retardation. *Nat Genet* **42**, 489-91.

Böhni, R., Riesgo-Escovar, J., Oldham, S., Brogiolo, W., Stocker, H., Andruss, B. F., Beckingham, K. and Hafen, E. (1999). Autonomous control of cell and organ size by CHICO, a Drosophila homolog of vertebrate IRS1-4. *Cell* **97**, 865-75.

Boyles, J. K., Notterpek, L. M. and Anderson, L. J. (1990). Accumulation of apolipoproteins in the regenerating and remyelinating mammalian peripheral nerve. Identification of apolipoprotein D, apolipoprotein A-IV, apolipoprotein E, and apolipoprotein A-I. *J Biol Chem* **265**, 17805-15.

Britton, J. S., Lockwood, W. K., Li, L., Cohen, S. M. and Edgar, B. A. (2002). Drosophila's insulin/PI3-kinase pathway coordinates cellular metabolism with nutritional conditions. *Dev Cell* **2**, 239-49.

Brogiolo, W., Stocker, H., Ikeya, T., Rintelen, F., Fernandez, R. and Hafen, E. (2001). An

evolutionarily conserved function of the Drosophila insulin receptor and insulin-like peptides in growth control. *Curr Biol* **11**, 213-21.

Caldwell, P. E., Walkiewicz, M. and Stern, M. (2005). Ras activity in the Drosophila prothoracic gland regulates body size and developmental rate via ecdysone release. *Curr Biol* **15**, 1785-95.

Chen, Z., Hendricks, M., Cornils, A., Maier, W., Alcedo, J. and Zhang, Y. (2013). Two insulin-like peptides antagonistically regulate aversive olfactory learning in C. elegans. *Neuron* **77**, 572-85.

Clancy, D. J., Gems, D., Harshman, L. G., Oldham, S., Stocker, H., Hafen, E., Leevers, S. J. and Partridge, L. (2001). Extension of life-span by loss of CHICO, a Drosophila insulin receptor substrate protein. *Science* **292**, 104-6.

Collins, C. A. and DiAntonio, A. (2007). Synaptic development: insights from Drosophila. *Curr Opin Neurobiol* **17**, 35-42.

Craft, S., Asthana, S., Newcomer, J. W., Wilkinson, C. W., Matos, I. T., Baker, L. D., Cherrier, M., Lofgreen, C., Latendresse, S., Petrova, A. et al. (1999). Enhancement of memory in Alzheimer disease with insulin and somatostatin, but not glucose. *Arch Gen Psychiatry* **56**, 1135-40.

Dassati, S., Waldner, A. and Schweigreiter, R. (2014). Apolipoprotein D takes center stage in the stress response of the aging and degenerative brain. *Neurobiol Aging* **35**, 1632-42.

de Magalhães, J. P., Curado, J. and Church, G. M. (2009). Meta-analysis of age-related gene

expression profiles identifies common signatures of aging. *Bioinformatics* **25**, 875-81.

Demontis, F. and Perrimon, N. (2009). Integration of Insulin receptor/Foxo signaling and dMyc activity during muscle growth regulates body size in Drosophila. *Development* **136**, 983-93.

Do Carmo, S., Fournier, D., Mounier, C. and Rassart, E. (2009). Human apolipoprotein D overexpression in transgenic mice induces insulin resistance and alters lipid metabolism. *Am J Physiol Endocrinol Metab* **296**, E802-11.

Dutriaux, A., Godart, A., Brachet, A. and Silber, J. (2013). The insulin receptor is required for the development of the Drosophila peripheral nervous system. *PLoS One* **8**, e71857.

Featherstone, D. E. and Broadie, K. (2000). Surprises from Drosophila: genetic mechanisms of synaptic development and plasticity. *Brain Res Bull* **53**, 501-11.

Flower, D. R. (1996). The lipocalin protein family: structure and function. *Biochem J* **318 (Pt 1)**, 1-14.

Fuentes-Medel, Y., Ashley, J., Barria, R., Maloney, R., Freeman, M. and Budnik, V. (2012). Integration of a retrograde signal during synapse formation by glia-secreted TGF-β ligand. *Curr Biol* **22**, 1831-8.

Ganfornina, M. D., Do Carmo, S., Lora, J. M., Torres-Schumann, S., Vogel, M., Allhorn, M., González, C., Bastiani, M. J., Rassart, E. and Sanchez, D. (2008). Apolipoprotein D is involved in the mechanisms regulating protection from oxidative stress. *Aging Cell* **7**, 506-15.

Gorczyca, M., Augart, C. and Budnik, V. (1993). Insulin-like receptor and insulin-like peptide

are localized at neuromuscular junctions in Drosophila. *J Neurosci* **13**, 3692-704.

Gu, T., Zhao, T. and Hewes, R. S. (2014). Insulin signaling regulates neurite growth during metamorphic neuronal remodeling. *Biol Open* **3**, 81-93.

He, C. X. and Portera-Cailliau, C. (2013). The trouble with spines in fragile X syndrome: density, maturity and plasticity. *Neuroscience* **251**, 120-8.

Hull-Thompson, J., Muffat, J., Sanchez, D., Walker, D. W., Benzer, S., Ganfornina, M. D. and Jasper, H. (2009). Control of Metabolic Homeostasis by Stress Signaling Is Mediated by the Lipocalin NLaz. *PLoS Genet* **5**, e1000460.

Jiménez-Palomares, M., Cózar-Castellano, I., Ganfornina, M. D., Sánchez, D. and Perdomo, G. (2011). Genetic deficiency of apolipoprotein D in the mouse is associated with nonfasting hypertriglyceridemia and hyperinsulinemia. *Metabolism* **60**, 1767-74.

Kalman, J., McConathy, W., Araoz, C., Kasa, P. and Lacko, A. G. (2000). Apolipoprotein D in the aging brain and in Alzheimer's dementia. *Neurol Res* **22**, 330-6.

Kennedy, L. M., Pham, S. C. and Grishok, A. (2013). Nonautonomous regulation of neuronal migration by insulin signaling, DAF-16/FOXO, and PAK-1. *Cell Rep* **4**, 996-1009.

Keshishian, H., Broadie, K., Chiba, A. and Bate, M. (1996). The drosophila neuromuscular junction: a model system for studying synaptic development and function. *Annu Rev Neurosci* **19**, 545-75.

Kim, W. S., Wong, J., Weickert, C. S., Webster, M. J., Bahn, S. and Garner, B. (2009). Apolipoprotein-D expression is increased during development and maturation of the human

prefrontal cortex. *J Neurochem* **109**, 1053-66.

Lee, C. K., Weindruch, R. and Prolla, T. A. (2000). Gene-expression profile of the ageing brain in mice. *Nat Genet* **25**, 294-7.

Marqués, G., Bao, H., Haerry, T. E., Shimell, M. J., Duchek, P., Zhang, B. and O'Connor, M. B. (2002). The Drosophila BMP type II receptor Wishful Thinking regulates neuromuscular synapse morphology and function. *Neuron* **33**, 529-43.

McCabe, B. D., Marqués, G., Haghighi, A. P., Fetter, R. D., Crotty, M. L., Haerry, T. E., Goodman, C. S. and O'Connor, M. B. (2003). The BMP homolog Gbb provides a retrograde signal that regulates synaptic growth at the Drosophila neuromuscular junction. *Neuron* **39**, 241-54.

Miller, D. L., Ballard, S. L. and Ganetzky, B. (2012). Analysis of synaptic growth and function in Drosophila with an extended larval stage. *J Neurosci* **32**, 13776-86.

Mirth, C., Truman, J. W. and Riddiford, L. M. (2005). The role of the prothoracic gland in determining critical weight for metamorphosis in Drosophila melanogaster. *Curr Biol* **15**, 1796-807.

Muffat, J., Walker, D. W. and Benzer, S. (2008). Human ApoD, an apolipoprotein up-regulated in neurodegenerative diseases, extends lifespan and increases stress resistance in Drosophila. *Proc Natl Acad Sci U S A* **105**, 7088-93.

Navarro, A., Del Valle, E., Astudillo, A., González del Rey, C. and Tolivia, J. (2003). Immunohistochemical study of distribution of apolipoproteins E and D in human cerebral beta

amyloid deposits. *Exp Neurol* **184**, 697-704.

Oldham, S., Stocker, H., Laffargue, M., Wittwer, F., Wymann, M. and Hafen, E. (2002). The Drosophila insulin/IGF receptor controls growth and size by modulating PtdInsP(3) levels. *Development* **129**, 4103-9.

Packard, M., Koo, E. S., Gorczyca, M., Sharpe, J., Cumberledge, S. and Budnik, V. (2002). The Drosophila Wnt, wingless, provides an essential signal for pre- and postsynaptic differentiation. *Cell* **111**, 319-30.

Provost, P. R., Weech, P. K., Tremblay, N. M., Marcel, Y. L. and Rassart, E. (1990). Molecular characterization and differential mRNA tissue distribution of rabbit apolipoprotein D. *J Lipid Res* **31**, 2057-65.

Rassart, E., Bedirian, A., Do Carmo, S., Guinard, O., Sirois, J., Terrisse, L. and Milne, R. (2000). Apolipoprotein D. *Biochim Biophys Acta* **1482**, 185-98.

Rulifson, E. J., Kim, S. K. and Nusse, R. (2002). Ablation of insulin-producing neurons in flies: growth and diabetic phenotypes. *Science* **296**, 1118-20.

Salinas, P. C. (2005). Retrograde signalling at the synapse: a role for Wnt proteins. *Biochem Soc Trans* **33**, 1295-8.

Sánchez, D., Ganfornina, M. D., Torres-Schumann, S., Speese, S. D., Lora, J. M. and Bastiani, M. J. (2000). Characterization of two novel lipocalins expressed in the Drosophila embryonic nervous system. *Int J Dev Biol* **44**, 349-59.

Sanchez, D., López-Arias, B., Torroja, L., Canal, I., Wang, X., Bastiani, M. J. and

Ganfornina, M. D. (2006). Loss of glial lazarillo, a homolog of apolipoprotein D, reduces lifespan and stress resistance in Drosophila. *Curr Biol* **16**, 680-6.

Shen, W. and Ganetzky, B. (2009). Autophagy promotes synapse development in Drosophila. *J Cell Biol* **187**, 71-9.

Shinoda, Y., Sadakata, T. and Furuichi, T. (2013). Animal models of autism spectrum disorder (ASD): a synaptic-level approach to autistic-like behavior in mice. *Exp Anim* **62**, 71-8.

Song, J., Wu, L., Chen, Z., Kohanski, R. A. and Pick, L. (2003). Axons guided by insulin receptor in Drosophila visual system. *Science* **300**, 502-5.

Stewart, B. A., Schuster, C. M., Goodman, C. S. and Atwood, H. L. (1996). Homeostasis of synaptic transmission in Drosophila with genetically altered nerve terminal morphology. *J Neurosci* **16**, 3877-86.

Sutcliffe, J. G. and Thomas, E. A. (2002). The neurobiology of apolipoproteins in psychiatric disorders. *Mol Neurobiol* **26**, 369-88.

Terrisse, L., Poirier, J., Bertrand, P., Merched, A., Visvikis, S., Siest, G., Milne, R. and Rassart, E. (1998). Increased levels of apolipoprotein D in cerebrospinal fluid and hippocampus of Alzheimer's patients. *J Neurochem* **71**, 1643-50.

Walker, D. W., Muffat, J., Rundel, C. and Benzer, S. (2006). Overexpression of a Drosophila homolog of apolipoprotein D leads to increased stress resistance and extended lifespan. *Curr Biol* **16**, 674-9.

Wickelgren, I. (1998). Tracking insulin to the mind. *Science* **280**, 517-9.

Wong, J. J., Li, S., Lim, E. K., Wang, Y., Wang, C., Zhang, H., Kirilly, D., Wu, C., Liou, Y. C., Wang, H. et al. (2013). A Cullin1-based SCF E3 ubiquitin ligase targets the InR/PI3K/TOR pathway to regulate neuronal pruning. *PLoS Biol* **11**, e1001657.

Zaia, A. and Piantanelli, L. (2000). Insulin receptors in the brain cortex of aging mice. *Mech Ageing Dev* **113**, 227-32.

Zhao, W., Chen, H., Xu, H., Moore, E., Meiri, N., Quon, M. J. and Alkon, D. L. (1999). Brain insulin receptors and spatial memory. Correlated changes in gene expression, tyrosine phosphorylation, and signaling molecules in the hippocampus of water maze trained rats. *J Biol Chem* **274**, 34893-902.

Zito, K., Parnas, D., Fetter, R. D., Isacoff, E. Y. and Goodman, C. S. (1999). Watching a synapse grow: noninvasive confocal imaging of synaptic growth in Drosophila. *Neuron* **22**, 719-29.

Figure 1

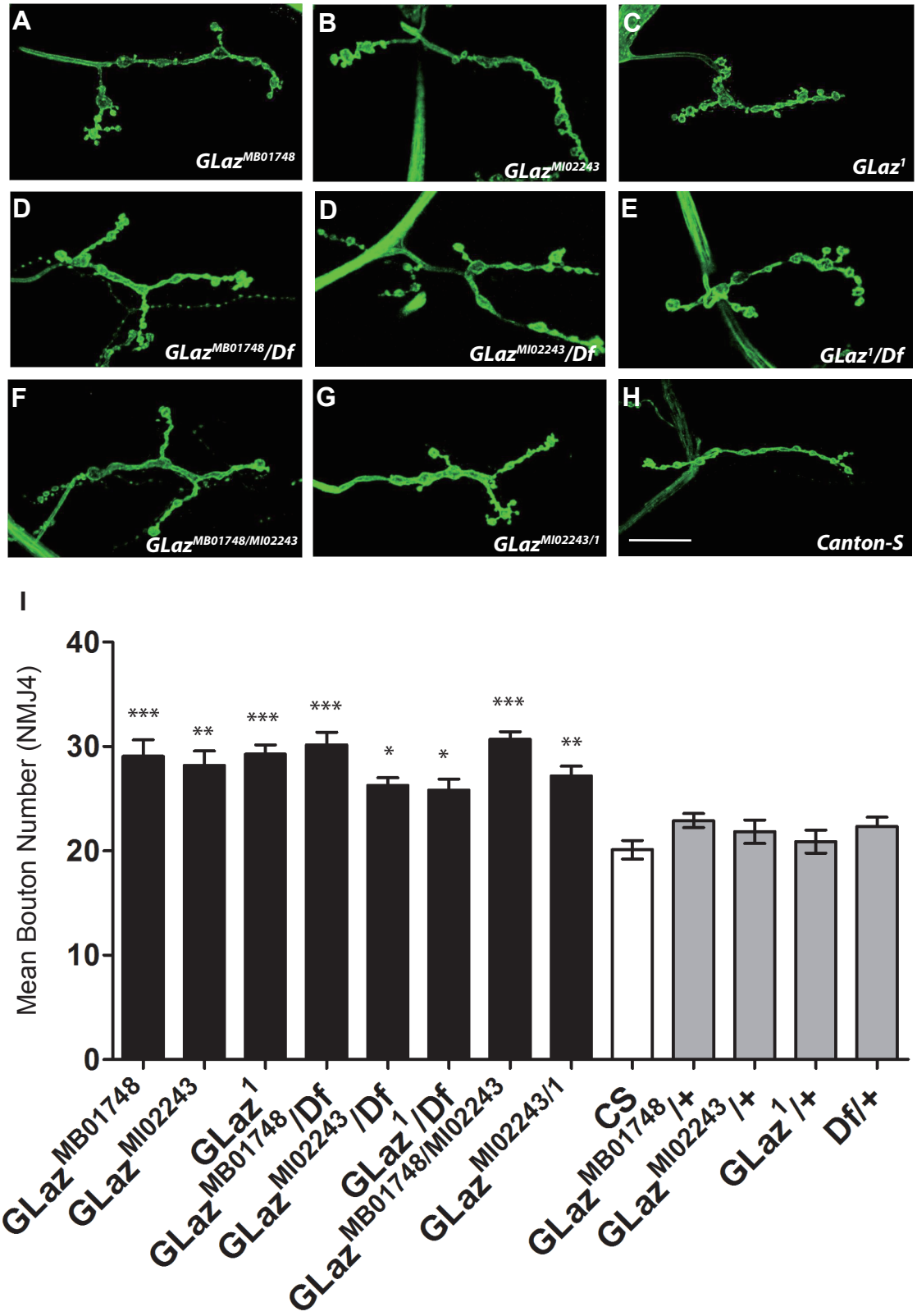
A
GLaz MB01748
B
GLaz MI02243
C
GLaz 1
D
GLaz MB01748/Df
D
GLaz MI02243/Df
E
GLaz 1/Df
F
GLaz MB01748/MI02243
G
GLaz MI02243/1
H
Canton-S
I
Mean Bouton Number (NMJ4)
40
30
20
10
0
***
**
***
***
*
*
***
**
GLaz MB01748
GLaz MI02243
GLaz 1
GLaz MB01748 /Df
GLaz MI02243 /Df
GLaz 1 /Df
GLaz MB01748/MI02243
GLaz MI02243/1
CS
GLaz MB01748 /+
GLaz MI02243 /+
GLaz 1 /+
Df/+

Figure 1. **GLaz restricts NMJ growth.** (A-H) Representative confocal images of NMJ4 immunostained with FITC-anti-HRP from larvae of indicated genotypes. (I) Quantification of boutons at NMJ4 in larvae of indicated genotypes. *GLaz* mutant larvae (A-G) display a significant increase in bouton number compared with *Canton-S* control larvae (H). Error bars indicate SEM. ***$p<0.001$, **$p<0.01$, *$p<0.05$. $n \geq 17$. Scale bar = 20 μm.

Figure 2

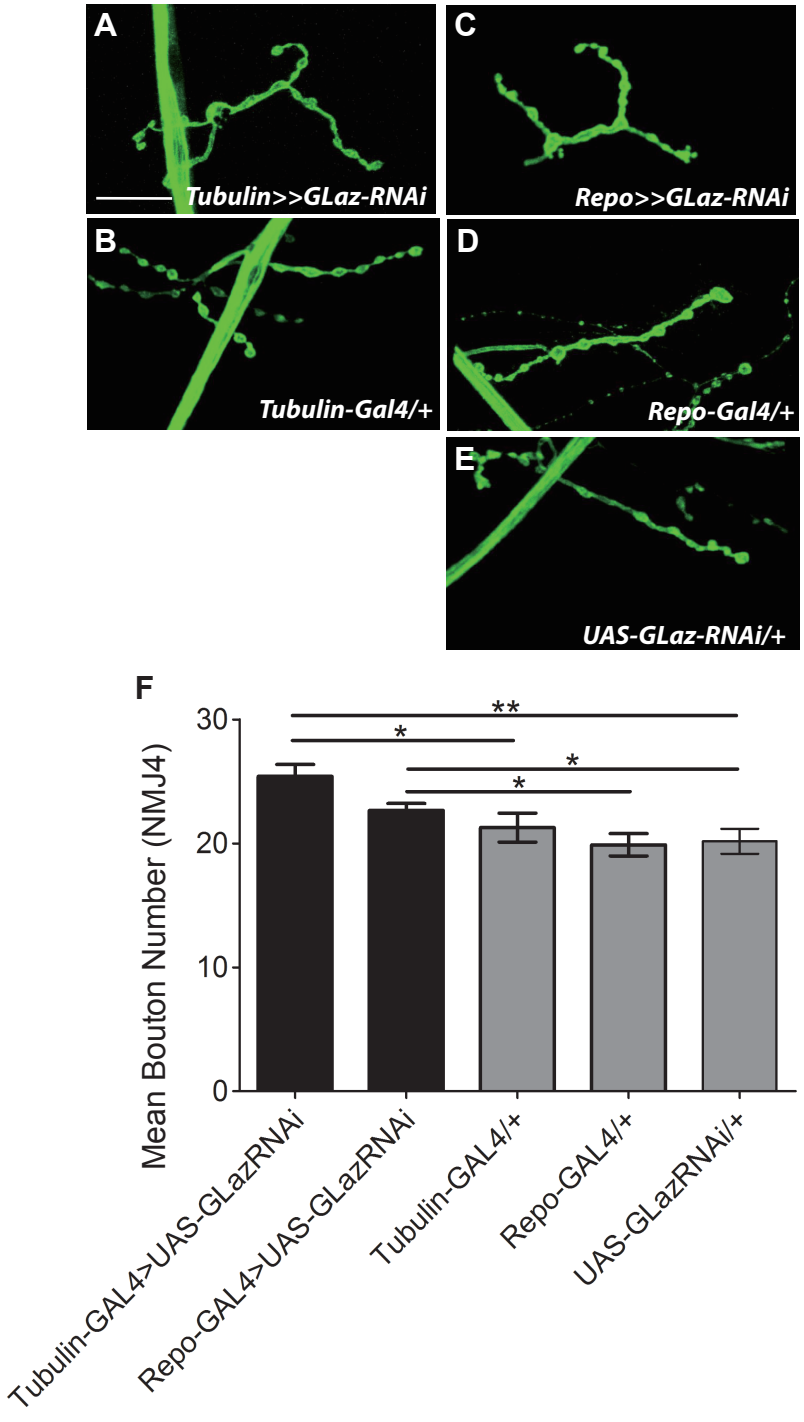
A
Tubulin>>GLaz-RNAi
C
Repo>>GLaz-RNAi
B
Tubulin-Gal4/+
D
Repo-Gal4/+
E
UAS-GLaz-RNAi/+
F
Mean Bouton Number (NMJ4)
30
20
10
0
**
*
*
*
Tubulin-GAL4>UAS-GLazRNAi
Repo-GAL4>UAS-GLazRNAi
Tubulin-GAL4/+
Repo-GAL4/+
UAS-GLazRNAi/+

Figure 2. **Glial expression of GLaz restricts NMJ growth.** (A-E) Representative confocal images of NMJ4 immunostained with FITC-anti-HRP from *Tubulin-Gal4>UAS-GLaz-RNAi* (A) and *Repo-Gal4>UAS-GLaz-RNAi* (C) larvae and controls: *Tubulin-Gal4/+* (B), *Repo-Gal4/+* (D), and *UAS-GLaz/+* (E). (F) Quantification of boutons at NMJ4 in larvae of indicated genotypes. *Repo-Gal4>UAS-GLaz-RNAi* larvae display a mild increase in mean bouton number(C, F) suggesting that at least some of the NMJ overgrowth observed in GLaz mutant larvae is due to loss of glial-derived GLaz. *Tubulin-Gal4>UAS-GLaz-RNAi* larvae also display mild NMJ overgrowth (A, F), but this phenotype is stronger than that observed in *Repo-Gal4>UAS-GLaz-RNAi* larvae suggesting that additional sources contribute to the pool of GLaz restricting NMJ growth. Error bars indicate SEM. **$p<0.01$, *$p<0.05$. Scale bar = 20µm.

Figure 3

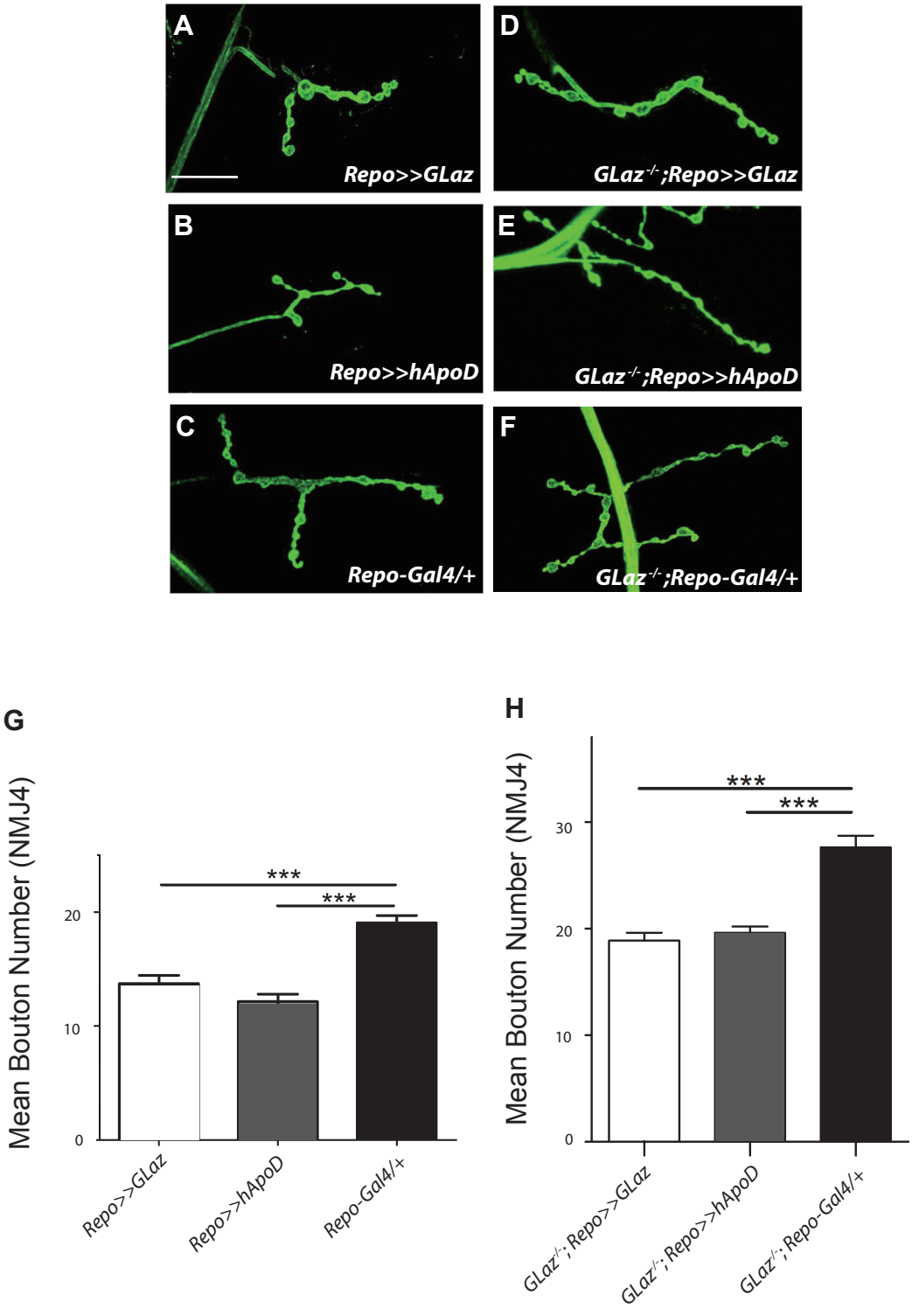
A
Repo>>GLaz
D
GLaz-/-;Repo>>GLaz
B
Repo>>hApoD
E
GLaz-/-;Repo>>hApoD
C
Repo-Gal4/+
F
GLaz-/-;Repo-Gal4/+
G
Mean Bouton Number (NMJ4)
0
10
20
***
***
Repo>>GLaz
Repo>>hApoD
Repo-Gal4/+
H
Mean Bouton Number (NMJ4)
0
10
20
30
***
***
GLaz-/-;Repo>>GLaz
GLaz-/-;Repo>>hApoD
GLaz-/-;Repo-Gal4/+

Figure 3. **Glial expression of GLaz or hApoD rescues NMJ overgrowth in *GLaz* mutants.** (A-F) Representative confocal images of NMJ4 immunostained with FITC-anti-HRP from larvae of indicated genotypes. (G, H) Quantification of boutons at NMJ4 in larvae of genotypes shown. Glial expression of GLaz in wild-type larvae (*Repo-Gal4>UAS-GLaz*) leads to a decrease in bouton number (A, G) compared with control larvae (C, G). Glial expression of the mammalian ortholog of GLaz, hApoD in wild-type larvae (*Repo-Gal4>UAS-hApoD*) also leads to a decrease in bouton number (B, G) compared with control larvae (C, G). Bouton number is restored to wild-type levels in *GLaz* mutant larvae (D, E and H) by glial expression of GLaz or hApoD (*$GLaz^{MB01748}$/$GLaz^{MI02243}$;Repo-Gal4>UAS-GLaz* and *$GLaz^{MB01748}$/$GLaz^{MI02243}$;Repo-Gal4>UAS-hApoD*). Error bars indicate SEM. ***$p<0.001$, $n\geq16$, Scale Bar = 20μm.

Figure 4

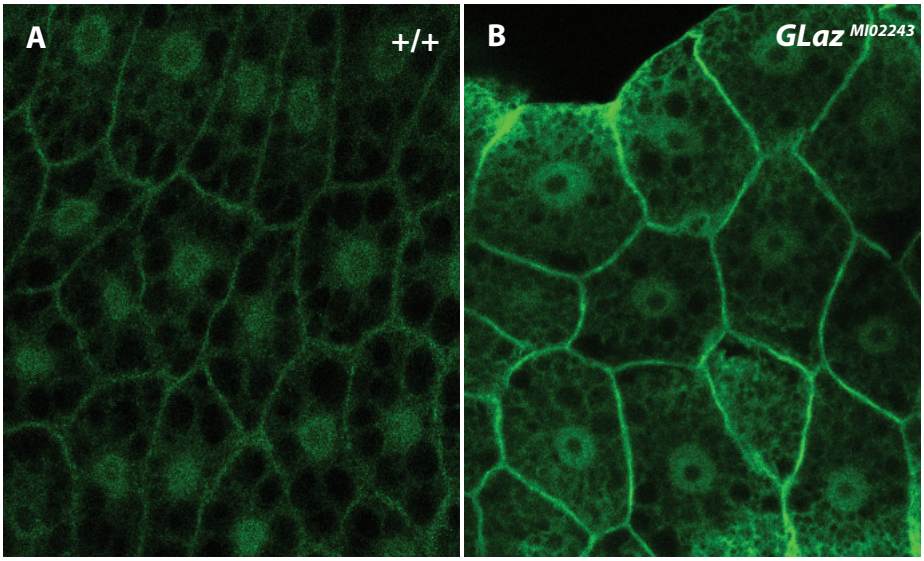
A
+/+
B
GLaz MI02243

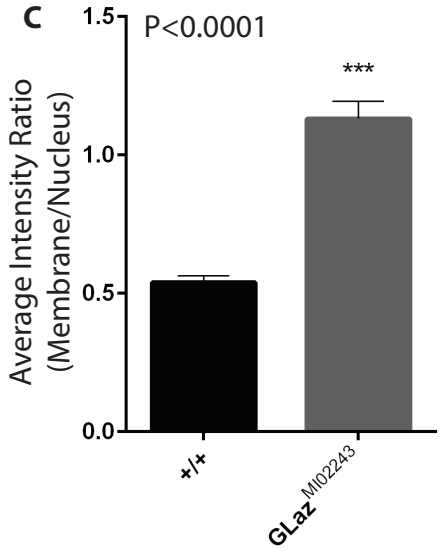
C
P<0.0001
***
Average Intensity Ratio
(Membrane/Nucleus)
1.5
1.0
0.5
0.0
+/+
GLaz MI02243

Figure 4. **Membrane localization of tGPH, a measure of PI3K activity, is increased in *GLaz* mutants.** (A,B) Single slice confocal images of control (A) and *GLaz*^{MI02243} (B) fat bodies. Average fluorescence intensity of individual cell membranes and nuclei was measured using NIH ImageJ on single slice images. (C) Ratios of membrane/nuclear fluorescence for wild-type and *GLaz*^{MI02243} fat bodies. At least 3 cells were measured per larva. n=6 larvae for *wild-type*, n=8 larvae for *GLaz* ^{MI02243}. P value calculated from Student's t-test.

Figure 5

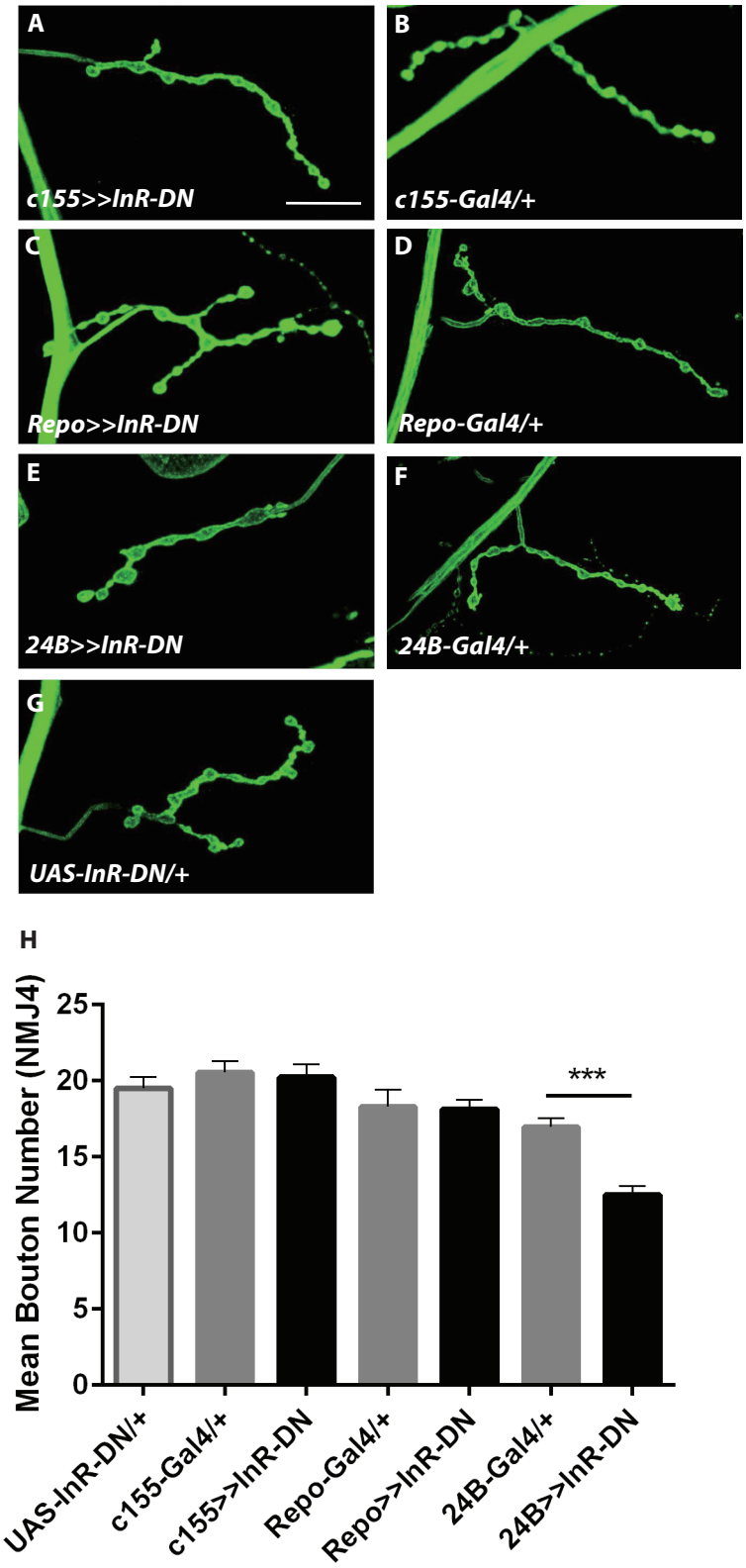
A
c155>>InR-DN
B
c155-Gal4/+
C
Repo>>InR-DN
D
Repo-Gal4/+
E
24B>>InR-DN
F
24B-Gal4/+
G
UAS-InR-DN/+
H
Mean Bouton Number (NMJ4)
25
20
15
10
5
0
***
UAS-InR-DN/+
c155-Gal4/+
c155>>InR-DN
Repo-Gal4/+
Repo>>InR-DN
24B-Gal4/+
24B>>InR-DN

Figure 5. **Insulin signaling in muscle promotes presynaptic terminal growth.** (A-G) Representative confocal images of NMJ4 immunostained with FITC-anti-HRP from larvae of indicated genotypes. (H) Quantification of boutons at NMJ4 in larvae of genotypes shown. Expression of a dominant negative insulin receptor (*UAS-InR*^{K1409A}) in neurons or glia (*c155-Gal4>UAS-InR-DN* and *Repo-Gal4>UAS-InR-DN*) does not affect presynaptic terminal growth (A, C and H). Expression of *InR-DN* in muscle (*24B-Gal4>UAS-InR-DN*) leads to a decrease in bouton number compared with control larvae (E-H). Error bars indicate SEM. ***$p<0.001$. $n\geq17$, Scale Bar = 20μm.

Figure 6

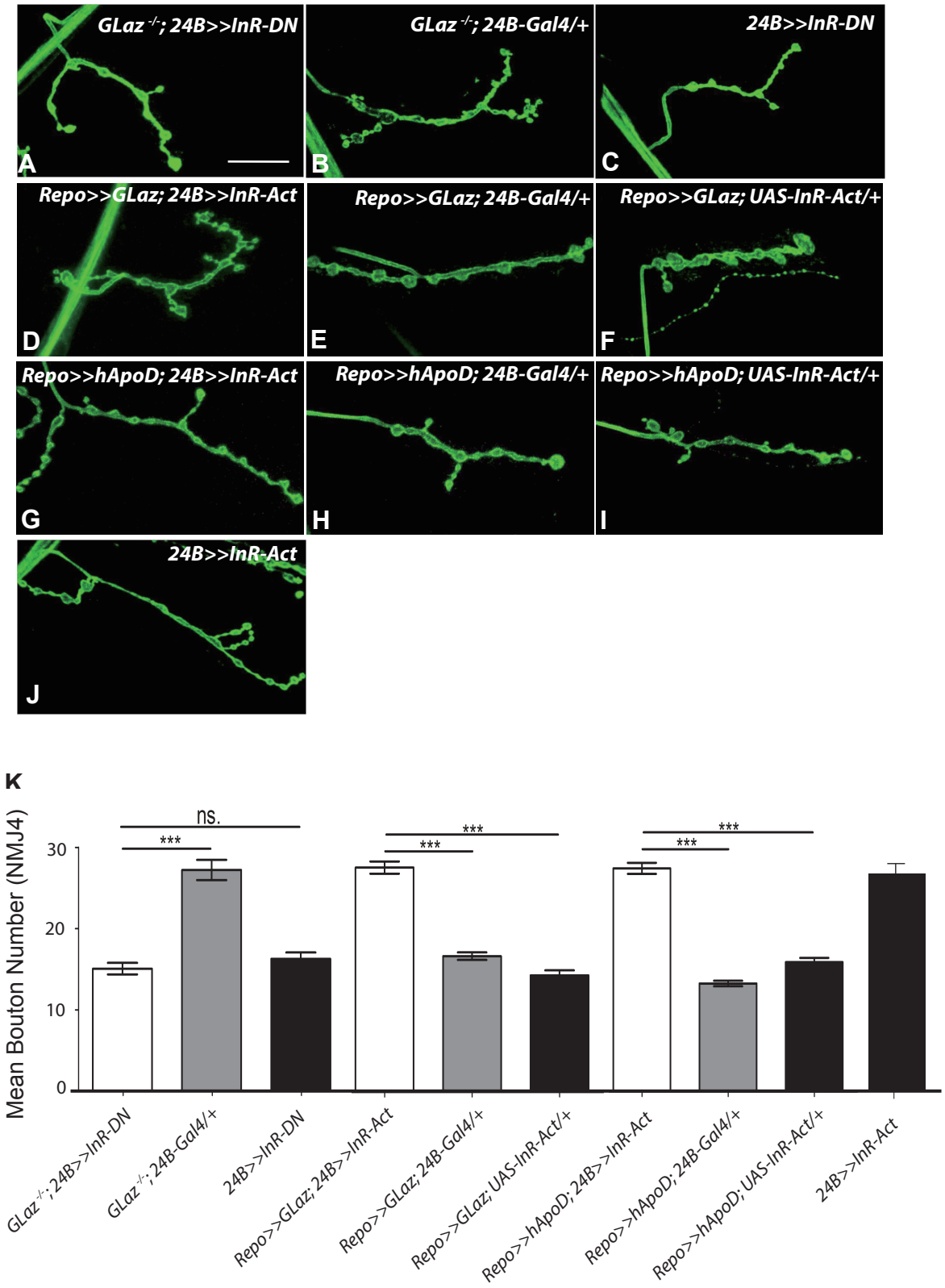
GLaz -/-; 24B>>InR-DN
GLaz -/-; 24B-Gal4/+
24B>>InR-DN
A
B
C
Repo>>GLaz; 24B>>InR-Act
Repo>>GLaz; 24B-Gal4/+
Repo>>GLaz; UAS-InR-Act/+
D
E
F
Repo>>hApoD; 24B>>InR-Act
Repo>>hApoD; 24B-Gal4/+
Repo>>hApoD; UAS-InR-Act/+
G
H
I
24B>>InR-Act
J
K
Mean Bouton Number (NMJ4)
30
20
10
0
ns.
***
***
***
***
***
***
GLaz-/-;24B>>InR-DN
GLaz-/-;24B-Gal4/+
24B>>InR-DN
Repo>>GLaz;24B>>InR-Act
Repo>>GLaz;24B-Gal4/+
Repo>>GLaz;UAS-InR-Act/+
Repo>>hApoD;24B>>InR-Act
Repo>>hApoD;24B-Gal4/+
Repo>>hApoD;UAS-InR-Act/+
24B>>InR-Act

Figure 6. **Postsynaptic insulin signaling is epistatic to GLaz in regulation of NMJ growth.** (A-J) Representative confocal images of NMJ4 immunostained with FITC-anti-HRP from larvae of indicated genotypes. (K) Quantification of boutons at NMJ4 in larvae of genotypes shown. Reduced insulin signaling in muscle in *GLaz* mutant larvae (*GLaz*^{MI02243}/*GLaz*^{1}*; 24B-Gal4>UAS-InR-DN*) results in NMJ undergrowth similar to that observed when insulin signaling is reduced in muscle in wild-type larvae (*24B-Gal4>UAS-InR-DN*) (A-C, K). Muscle expression of an activated allele (*UAS-InR*^{A1325D}) of the insulin receptor (*24B-Gal4>UAS-InR-Act*) leads to an increase in bouton number (J, K). Overexpression of GLaz or hApoD in glia in wild-type larvae (*Repo-LexA>LexAop-GLaz* and *Repo-LexA>LexAop-hApoD*) leads to a decrease in bouton number (E, F, H, I, K). Expression of InR-Act in muscle in larvae overexpressing GLaz or or hApoD in glia (*Repo-LexA>LexAop-GLaz; 24B-Gal4>UAS-InR-Act* and *Repo-LexA>LexAop-hApoD; 24B-Gal4>UAS-InR-Act*) leads to NMJ overgrowth similar to that observed in *24B-Gal4>UAS-InR*^{A1325D} larvae indicating that insulin signaling in muscle is epistatic to GLaz at the NMJ (D, G, J and K).

Supplementary Figure 1

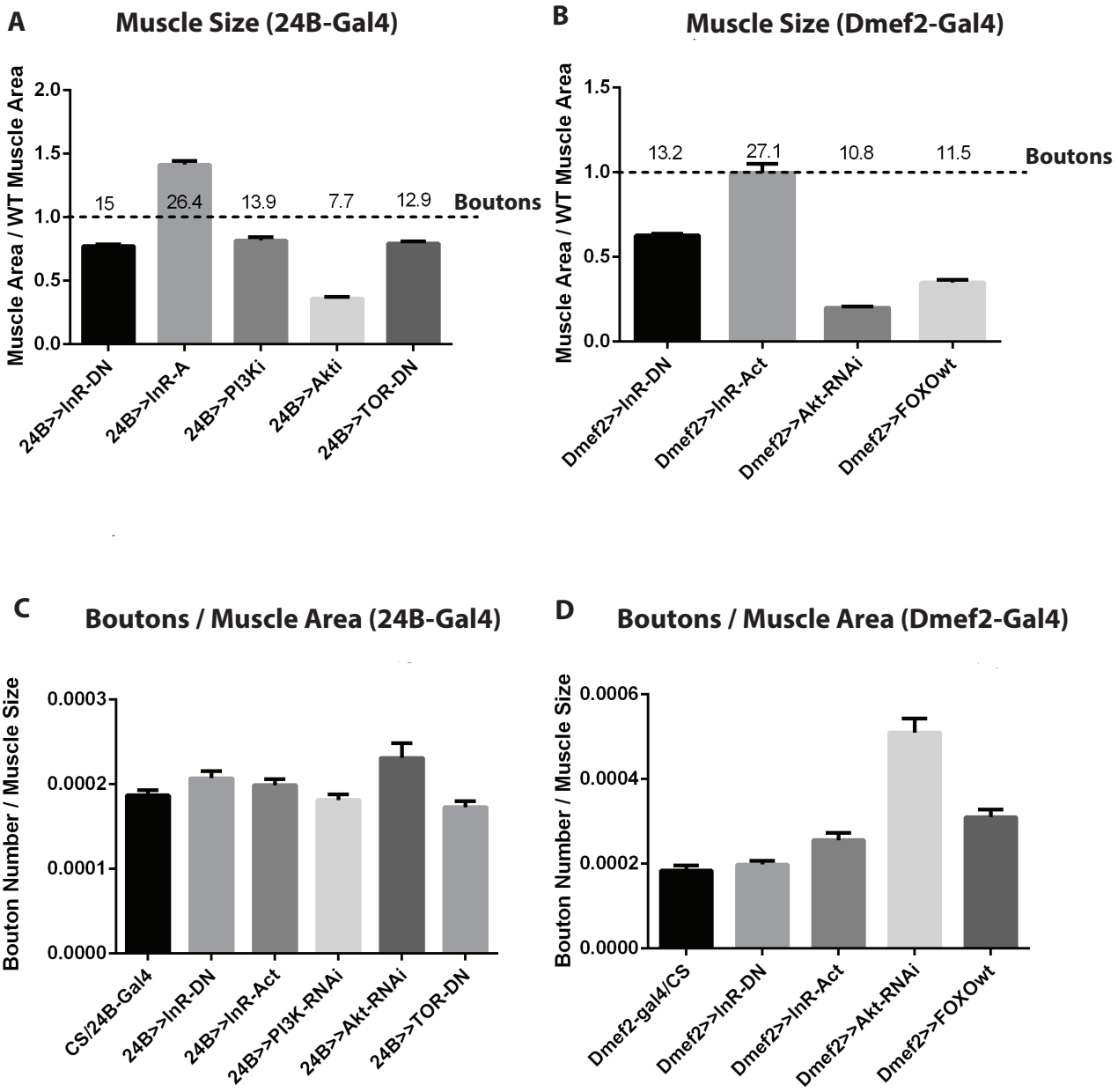

Figure S1. **Insulin signaling promotes growth of larval body wall muscles**. The area of muscle 4 was measured in dissected wandering 3rd instar larvae with muscle-specific reduced or increased activation of the insulin signaling pathway. Two different muscle drivers were tested: *24B-Gal4* and *Dmef2-Gal4*. (A, B) Muscle 4 area normalized to muscle 4 area of *24B-Gal4/CS* or *Dmef2-Gal4/CS* larvae. The dotted line indicates muscle size of the control. Numbers above the dotted line are average number of boutons at NMJ4 in these larvae. (C, D) Bouton counts normalized to muscle area. At least 6 larvae were dissected and analyzed for each genotype. Error bars represent SEM. n≥16.

Supplementary Figure 2

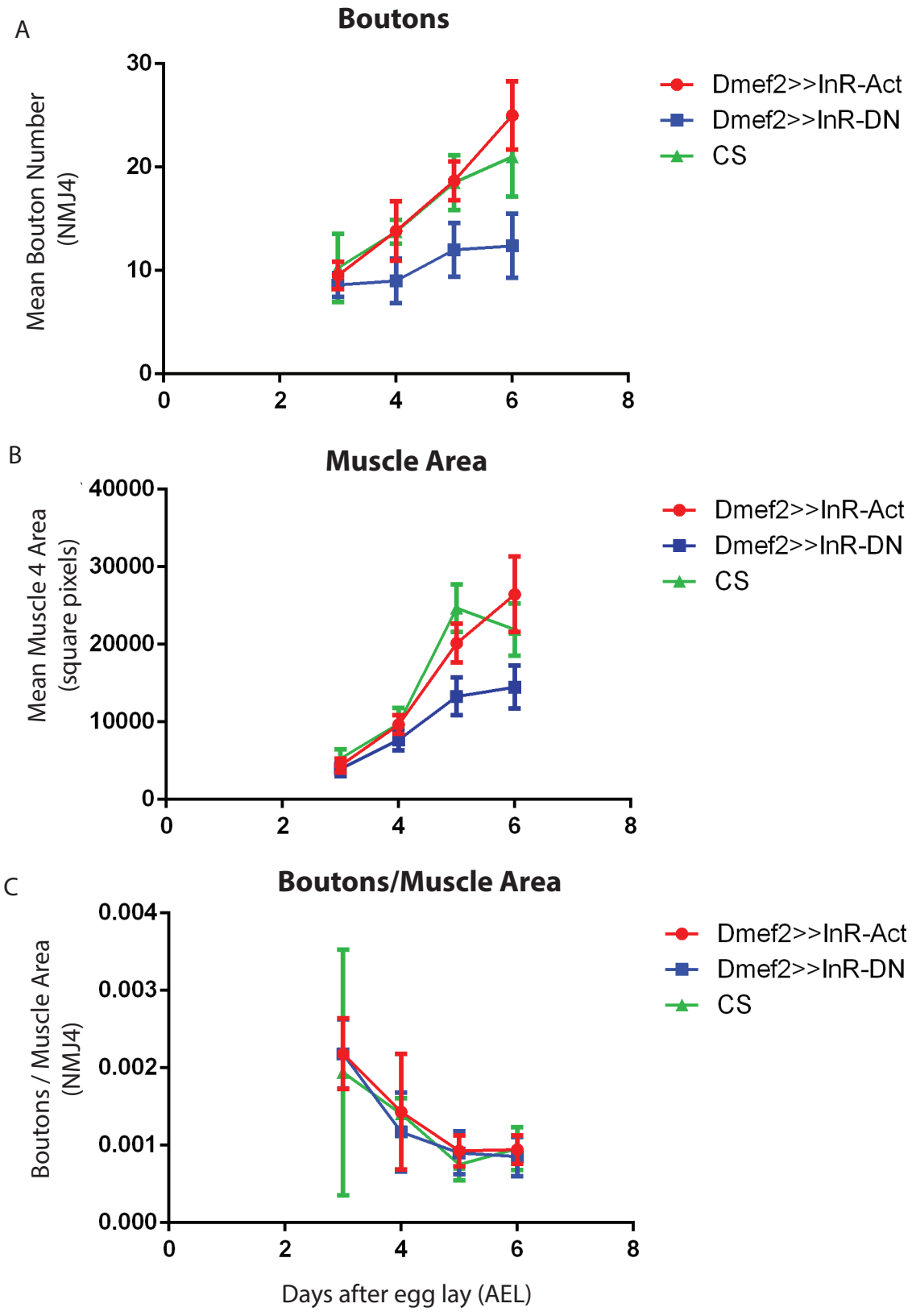

Figure S2. **Boutons are added as muscle area increases during larval development**. Bouton number and muscle size were measured in larvae 3, 4, 5 and 6 days after egg lay (AEL) to track the coupling between bouton number and muscle size in genotypes with NMJ overgrowth (*Dmef2>>InR-Act*), NMJ undergrowth (*Dmef2>>InR-DN*) and controls (*Canton-S*). (A) Bouton number increases throughout larval development. *Dmef2>>InR-DN* larvae already have undergrown NMJs at 4 days AEL. The overgrowth in *Dmef2>>InR-Act* larvae occurs between 5 and 6 days AEL. (B) Muscle increases area throughout larval development. *Dmef2>>InR-DN* larvae have smaller muscle size compared to *CS* and *Dmef2>>InR-Act* larvae at 5 days AEL. *CS* muscle growth levels off between 5 and 6 days AEL. By 6 days AEL, muscle area is greatest in *Dmef2>>InR-Act* larvae. (C) Bouton counts normalized to muscle area at each day AEL. Bouton number and muscle size appear to be closely coupled in each genotype tested. $n \geq 6$ for each genotype at each stage (except *CS* at 3 days AEL n=3). Error bars represent SEM.

Supplementary Figure 3

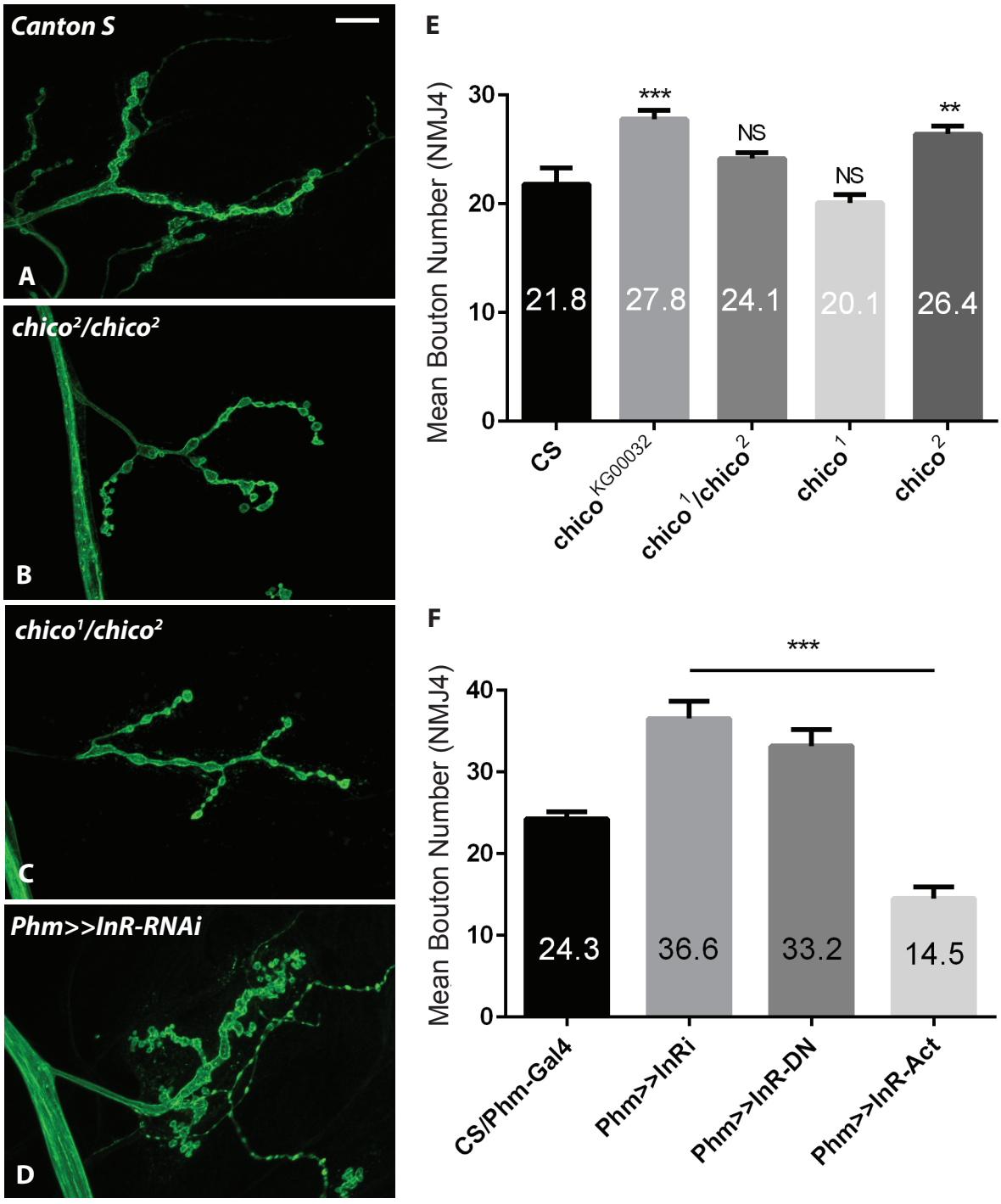

Figure S3. **Insulin signaling in non-NMJ cells affects NMJ size**. (A-D) Representative confocal images of NMJ4 immunostained with FITC-anti-HRP from larvae of indicated genotypes. (E, F) Quantification of boutons at NMJ4 in larvae of indicated genotypes. Some *chico* mutants (B, C, E) display NMJ overgrowth compared to controls (A, E). Specifically reducing insulin signaling in the prothoracic gland using the driver *Phm-Gal4* (*Phm>>InR-RNAi* or *Phm>>InR-DN*) results in extension of larval stage and NMJ overgrowth, shown in (D) and quantified in (F). Increasing insulin signaling in the prothoracic gland (*Phm>>InR-Act*) results in NMJ undergrowth, quantified in (F). Error bars indicate SEM. ***$p<0.001$, **$p<0.01$. $n \geq 8$. Scale bar = 20 µm.

Supplementary Figure 4

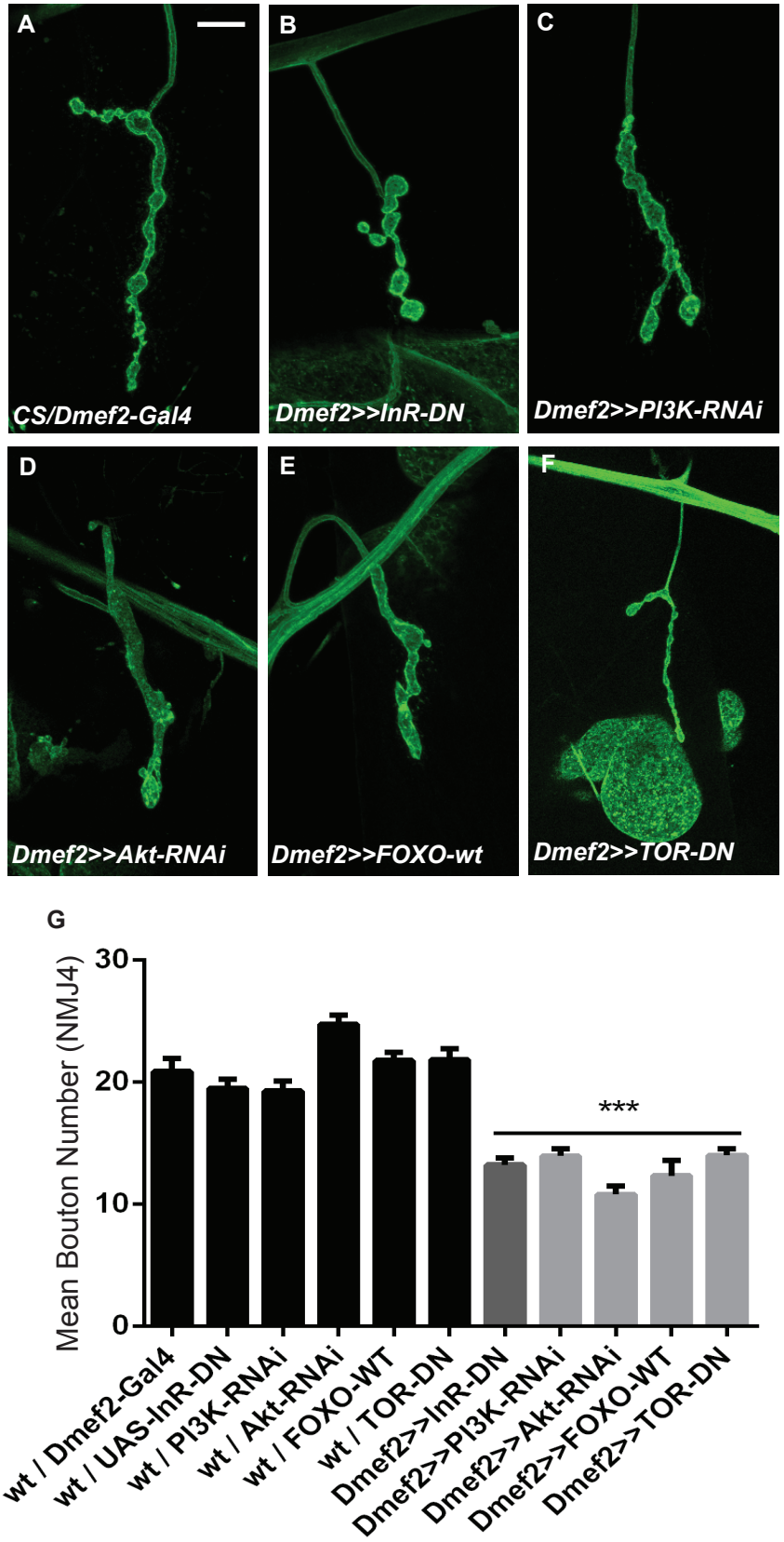

Figure S4. **The canonical insulin signaling pathway in muscle promotes presynaptic terminal growth**. Inhibition of downstream components of the canonical insulin signaling pathway or overexpression of *FOXO* in muscle results in NMJ undergrowth similar to expression of a dominant negative insulin receptor in muscle. (A-F) Representative confocal images of NMJ4 immunostained with FITC-anti-HRP from larvae of indicated genotypes. Control larvae (A), and larvae with muscle-specific expression of *InR-DN* (B), *PI3K-RNAi* (C), *Akt-RNAi* (D), *FOXO-wt* (E) and *TOR-DN* (F). (G) Quantification of bouton number. Each bar represents mean bouton number at NMJ4. Error bars are SEM. ***$P<0.001$, $n\geq16$.

Supplementary Figure 5

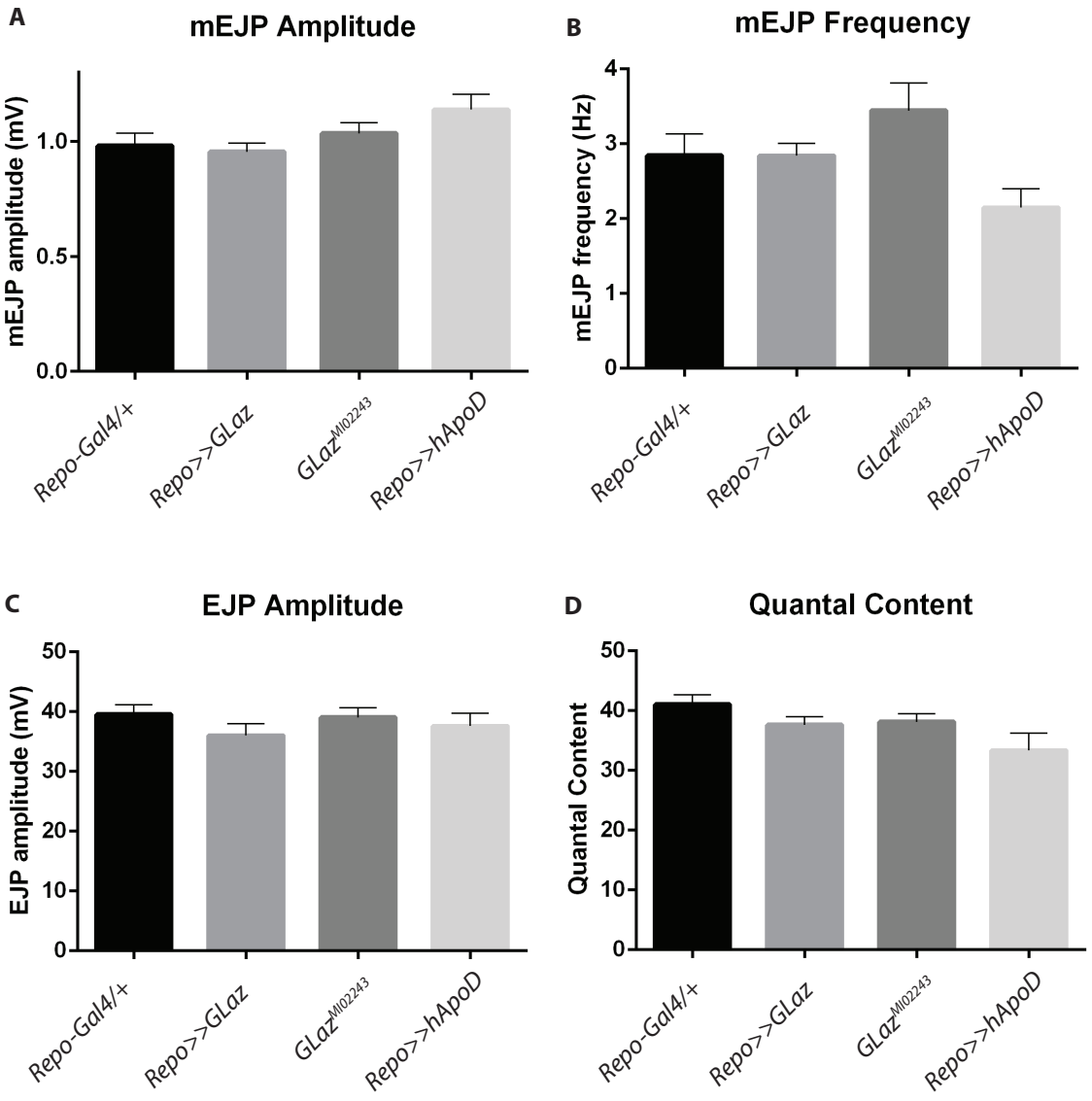

Figure S5. **Synaptic function is not altered in *GLaz* mutant larvae**. (A, B) Quantification of the mean mini Excitatory Junction Potential (mEJP) amplitude (A) and frequency (B) from muscle 4 in third instar larvae of indicated genotypes. (C) Quantification of the mean EJP amplitude from muscle 4 in third instar larvae of indicated genotypes. Neither mean mEJP amplitude, mEJP frequency or EJP amplitude are affected in *GLaz* mutants or with *GLaz* or *hApoD* overexpression in glia. (D) Quantal content is unaffected in *GLaz* mutant, *Repo>>GLaz* and *Repo>>hApoD* larvae compared with controls. $n \geq 11$ Error bars indicate SEM.

Supplementary Figure 6

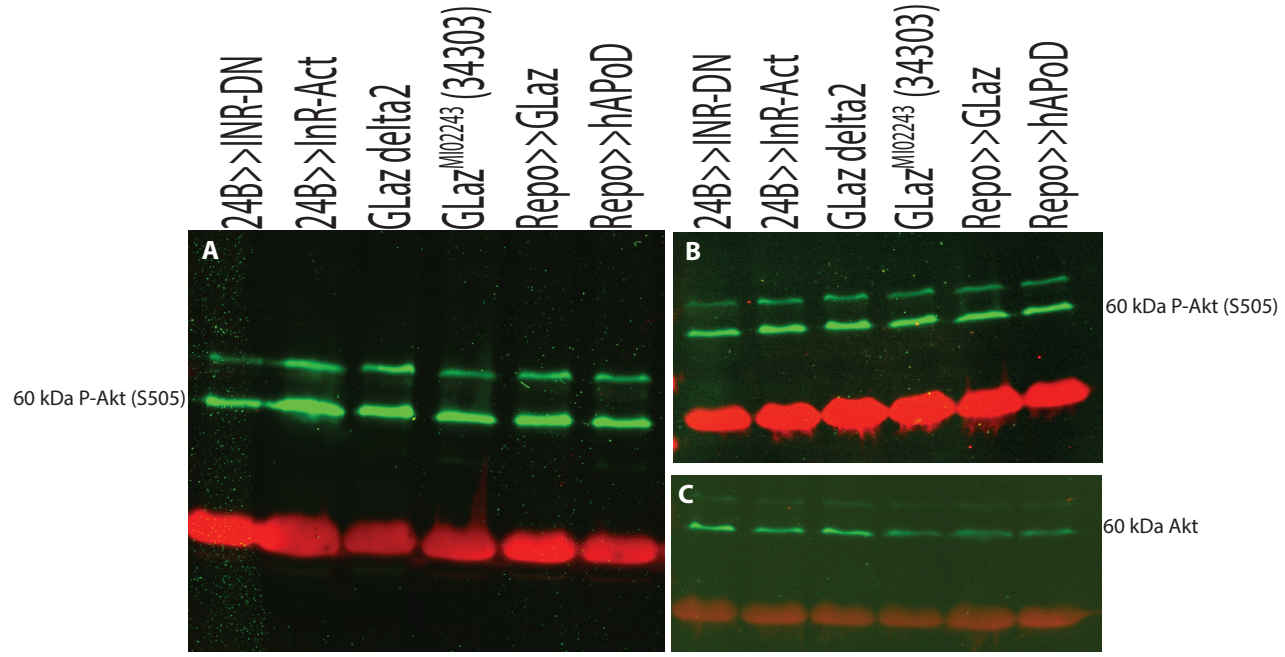

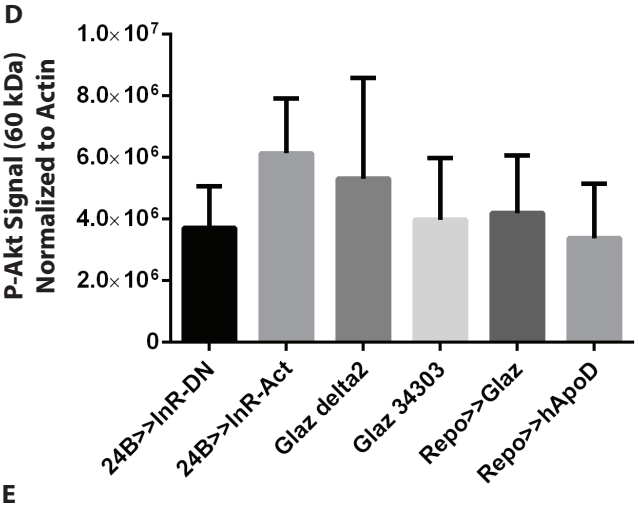

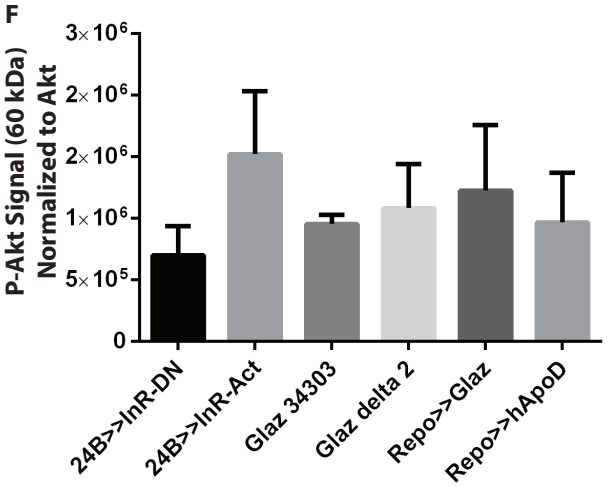

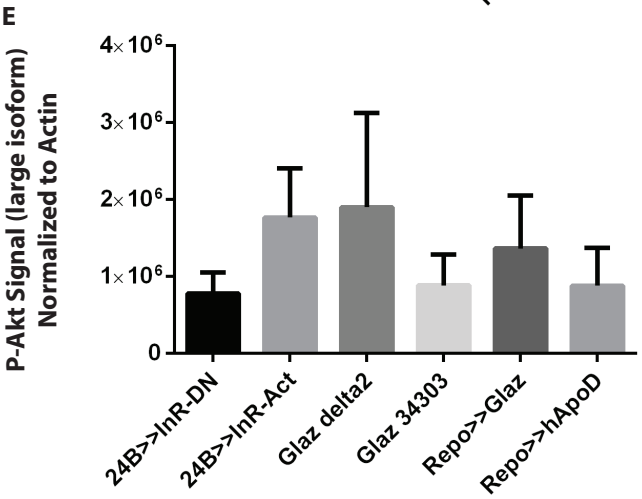

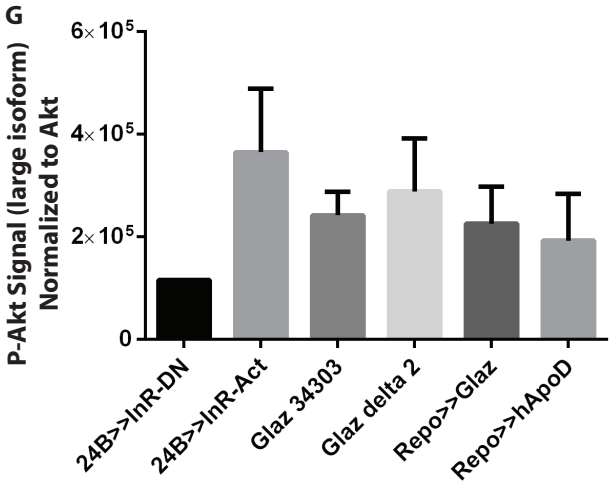

Figure S6. **Akt activity is not increased in *GLaz* mutants**. Levels of serine-505-phosphorylated Akt protein in body wall muscles of wandering 3rd instar larvae were quantified by western blot. Insulin signaling increases activity of Drosophila Akt, which is activated by phosphorylation of serine 505. Therefore, we predicted that there would be elevated P-Akt levels in body wall muscles with increased insulin signaling (*24B>>InR-Act* and *Glaz* mutants), and decreased P-Akt levels in body wall muscles with reduced insulin signaling (*24B>>InR-DN* and *GLaz* overexpression) However, we observe no statistically significant difference in P-Akt levels among the genotypes tested when P-Akt is normalized to actin (A, D &E) or total Akt (B, C, F & G). 4 trials for P-Akt normalized to actin. Two trials for P-Akt normalized to total Akt. Error bars are SEM.

Supplementary Figure 7

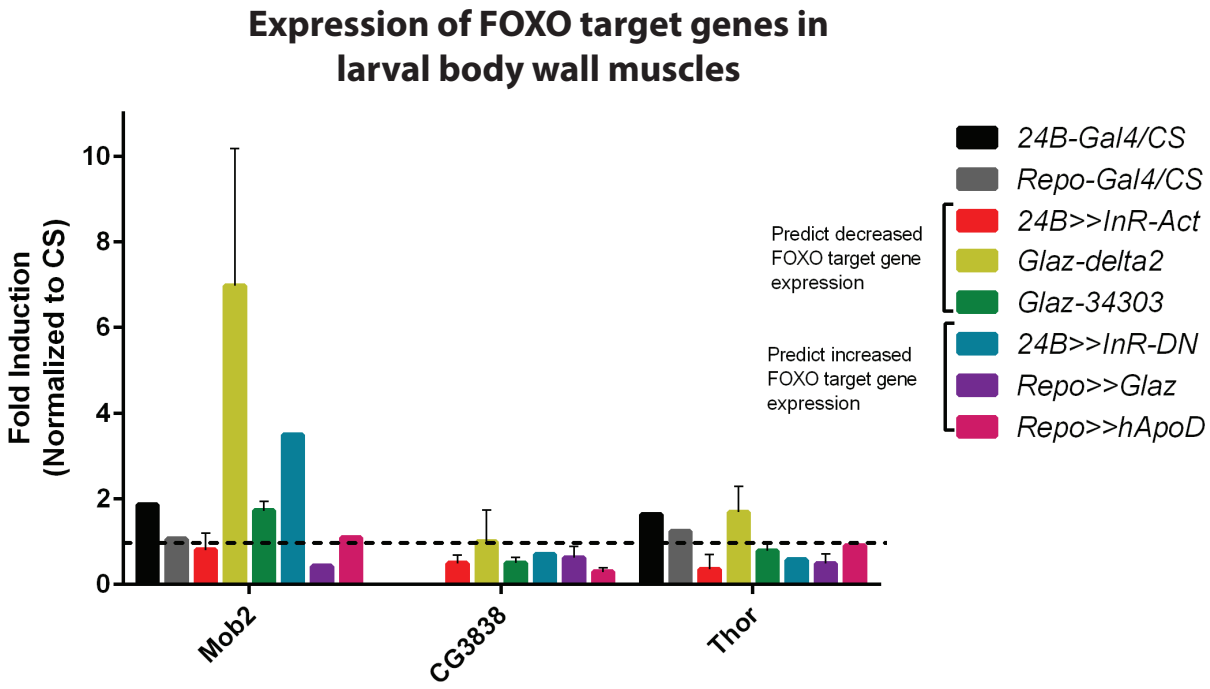

Figure S7 . **FOXO activity is not decreased body wall muscles in GLaz mutants**. Quantitative RT-PCR was used to measure transcript levels of FOXO target genes in body wall muscles of wandering 3rd instar larvae of indicated genotypes. When the insulin signaling pathway is activated, FOXO is sequestered in the cytoplasm. FOXO translocates to the nucleus and induces transcription of target genes in the absence of insulin signaling. Therefore, we predicted an increase in FOXO target gene expression when insulin signaling is decreased and a decrease in FOXO target gene expression when insulin signaling in increased. Each of the FOXO target genes tested here was induced greater than 18 fold in cultured S2 cells expressing a constitutively nuclear FOXO (Gershman et al., 2007). The results shown here demonstrate that there is no correlation between FOXO target gene expression and insulin signaling in body wall muscles. Error bars (SEM) are absent where genotypes were only tested once. Genotypes with error bars have two biological replicates. *CG3838* expression was not tested in *24B-Gal4/CS* or *Repo-Gal4/CS* larvae. *Rp49* was used as the reference gene.

Supplementary Figure 8

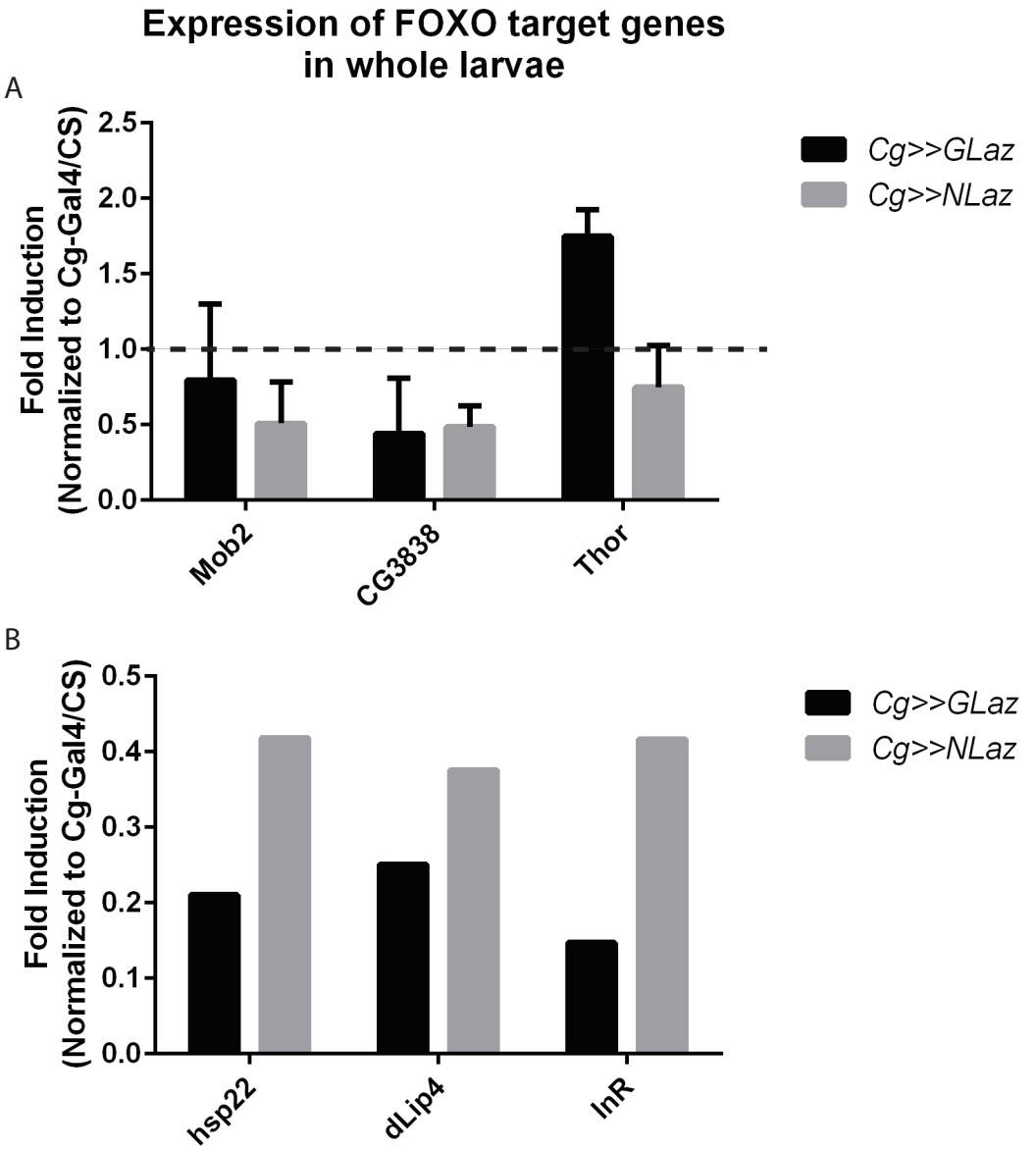

Figure S8. **Global FOXO activity is not increased when GLaz is overexpressed in fat body.** Quantitative RT-PCR was also used to measure transcript levels of FOXO target genes in whole wandering 3rd instar larvae with increased *GLaz* or *NLaz* expression in fat body (using *Cg-Gal4*). In (A), mRNA transcripts that were analyzed with qRT-PCR in body wall muscles (Figure S7) were measured. Only transcript levels of *Thor* in *Cg>>GLaz* larvae are consistent with decreased insulin signaling and increased FOXO activity. With a different fat body-specific Gal4 (*ppl-Gal4*) driving *NLaz* expression, previous reports have demonstrated an increase in expression of the FOXO target genes *InR, dLip4* and *hsp22* in whole larvae (Hull-Thompson et al., 2009). (B) When *GLaz* or *NLaz* are overexpressed in fat body using the *Cg-Gal4* driver, there is no observed increase in expression of *InR, dLip4* or *hsp22* in whole larvae. The graph in (A) shows mean transcript level normalized to *Cg-Gal4/CS* for two trials. Error bars are SEM. The graph in (B) shows the transcript level normalized to *Cg-Gal4/CS* for one trial.

PART 2: ANALYSIS OF THE NEUROTOXIC EFFECTS OF RADIATION EXPOSURE DURING DEVELOPMENT IN DROSOPHILA MELANOGASTER

CHAPTER 3

Radiation biology: Investigations in radiation resistance

Radiation resistance in extremophiles

Radiation therapy is an integral component of treatment regimens for malignancy. Two of the goals of studying radiation biology are to increase the efficacy radiation-induced tumor cell death and to protect healthy cells from radiation-induced damage. Radioresistant organisms have been studied for decades to determine biological mechanisms conferring protection from radiation. Early studies on the cellular effects of radiation focused on DNA damage (Hutchinson, 1966), and it was originally thought that differences in radiation resistance were due to varying efficiencies of DNA repair mechanisms (Daly, 2009). In-tact DNA repair mechanisms are critical for recovering from radiation-induced damage. This is evident clinically in individuals with Ataxia telangiectasia (A-T), which is caused by mutations in the ATM kinase, an important mediator of the DNA damage response. One of the main phenotypes in individuals with A-T is increased radiosensitivity (McKinnon, 2012). Moreover, mechanisms associated with efficient repair have been identified in radiation resistant species. For example, the highly efficient DNA repair machinery of the bacteria *Deinococus radiodurans* can reassemble a shattered genome following a 7,000 Gy dose of radiation (Zahradka, et al., 2006; Slade et al., 2009) and loss of genes involved in DNA repair result in radiosensitivity (Gutman et al., 1993). However, DNA damage and repair mechanisms are only part of the story. The genome sequences of *Deinococcus radiodurans* and *Deinococcus geothermalis*, two extremophiles that are very resistant to radiation, do not seem to contain novel DNA repair mechanisms (White et al., 1999; and Makarova et al., 2001; Makarova et al., 2007). Furthermore, radiation sensitivity in *D. radiodurans DNA polymerase* mutants can be rescued by the *Escherichia coli DNA polymerase I* gene (Gutman et al., 1994), suggesting that the *D. radiodurans* enzymes are not functionally unique.

The fact that DNA damage alone is not the sole predictor of survival following radiation is best illustrated by varying radiation resistance among species with genomes of similar sizes. The number of double-strand breaks (DSBs) induced per dose of absorbed radiation within a given length of DNA is relatively constant across organisms (Daly, 2009). Therefore, organisms with smaller genomes accumulate fewer DSBs. If radiation resistance were largely determined by DNA damage, radiation resistance would decrease as genome size increases. Although the most radioresistant organisms that have been discovered are bacteria, which have substantially smaller genomes than mammals, genome size is not directly related to radiation resistance. For example, 200 Gy is a lethal dose for most bacteria, but invertebrates such as adult Drosophila are resistant to doses over 500 Gy, and other invertebrates such as *Caenorhabditis elegans* can survive doses of 3,000-5,000 Gy (Daly 2009). Increased genome ploidy could be predicted to promote radiation resistance as it facilitates more efficient DSB repair, but there is also no association between ploidy and radioresistance (Daly 2009).

The radioresistance of some extremophile bacteria may be due to less protein oxidation by reactive oxygen species (ROS) following irradiation (Daly et al., 2007). Radiolysis of water molecules produces ROS, which cause damage by oxidizing macromolecules such as proteins, lipids and DNA (Daly, 2009). This damage can be mitigated by reducing the generation of ROS or increasing their elimination. Radioresistant bacteria such as *D. radiodurans* accumulate more manganese and less iron (increased Mn:Fe ratio) compared to radiosensitive bacteria. Mn^{2+} accumulation protects proteins by preventing ROS generation from iron redox cycling (Daly, 2009). Resistance to radiation-induced protein oxidation is correlated with Mn:Fe ratios in different species of bacteria supporting the hypothesis that bacteria with high levels of Mn^{2+} have reduced levels of ROS (Daly et al., 2004; Daly et al., 2009). The number of DNA DSBs induced

by radiation does not appear to be affected by Mn^{2+} levels, consistent with the idea that DNA damage is due to direct effects of radiation on the macromolecule itself, but protein oxidation is an indirect effect of radiation-generated ROS (Daly et al., 2007). Because there is less protein oxidation in bacteria with high Mn^{2+}, the integrity of cellular enzymes is maintained allowing them to efficiently repair radiation-induced damage, such as DNA DSBs. In contrast, increased oxidation in less radioresistant species compromises the function of enzymes including those involved in DNA repair leading to error-prone repair and mutagenesis. Other radiation resistant organisms may have different antioxidants that function similarly to manganese complexes such as melanin or trehalose (Daly, 2009). Preventing Mn^{2+} accumulation in *D. radiodurans* results in radiation sensitivity (Daly et al., 2004), demonstrating the importance of manganese in the extreme radiation resistance of these bacteria. Later work expanded on ROS scavenging in *D. radiodurans* and showed that loss of an enzyme involved in carotenoid synthesis also resulted in increased radiosensitvity (Tian et al., 2007). These results suggest that targeting manganese accumulation or pathways involved in ROS scavenging and prevention of protein oxidation may be an effective strategy for reducing cellular damage from radiation.

Radiation resistance is likely attributable to multiple factors. Efficient DNA damage repair and ROS scavenging appear to be critical, but these mechanisms vary, and the ideal pathways likely depend on the cell and environment. A better understanding of the diversity in ROS scavenging pathways, how these pathways evolved, the species specificity of these mechanisms, and most important how they are regulated in response to radiation will be crucial. Recently, a *D. radiodurans* transposon mutant library was generated and screened to identify radioresistance genes (Dulermo et al., 2015). This work demonstrated that the extreme radioresistance of this organism is due to complex interactions among multiple pathways including signal transduction,

membrane transport and metabolic pathways in addition to the predicted roles of DNA damage repair and stress response pathways (Dulermo et al, 2015). The results of this study indicate that there is much to be learned about the cellular response to radiation beyond the classical response pathways studied thus far.

Future directions for radiation resistance research

The effect of radiation on tissues is not simply due to the sum of the effect on individual cells. The radiation response also involves cell-cell and cell-environment communication that alters signaling pathways and transcription leading to coordinated tissue responses (Barcellos-Hoff et al, 2005). Therefore, although much has been learned from studies on radioresistant bacteria, future work should also focus on the effects of radiation in multicellular organisms. Although critical knowledge about the molecular responses within cells to radiation can be gained through work on single-celled extremophiles, the translation of this information to medically useful therapeutics requires an understanding of how whole tissues respond to radiation damage. Identification of genes that confer radiation sensitivity or resistance in multicellular organisms will aid in efforts to harness the therapeutic toxicity of radiation to more effectively kill tumor cells and reduce damage to healthy cells. For example, genetic variants in a tumor that are associated with altered radiation sensitivity can be identified through sequencing of the tumor genome and inform radiation treatment planning. Moreover, through tumor-targeted drug delivery (Gao et al., 2013; Eriste et al., 2013), compounds that antagonize radioprotective genes or promote the activity of radiosensitive genes can be used to increase the susceptibility of the tumor to radiation-induced cell death.

An additional benefit of studying the radiation response in multicellular organisms is the ability to dissect the effect of radiation on different types of tissue and the long-term effects of radiation on developing tissue (Emami et al., 1991; Kempf et al., 2014). For example, studies in mammals have demonstrated that there are tissue-specific changes in gene expression following radiation exposure (Chang et al., 2011). Moreover, clinical studies have shown long-term neurocognitive deficits in patients that received cranial radiation therapy during development (Edelstein et al., 2011; Ellenberg et al., 2009; Mulhern et al., 2005). These studies demonstrate the need for therapeutic strategies to protect developing tissues, especially the nervous system, from radiation-induced damage.

Drosophila offers the genetic tools to dissect radioresistance mechanisms in specific tissues both in adults and during development. Most important, Drosophila can be used to perform unbiased genetic screens to identify novel biological pathways underlying the response to radiation. Identification of the genes and molecular mechanisms in Drosophila that confer radioresistance or radiosensitivity will aid in efforts to develop therapeutic strategies that promote radiosensitivity of malignant cells and protect healthy tissues from radiation damage.

References

Barcellos-Hoff, M. H., Park, C. and Wright, E. G. (2005). Radiation and the microenvironment - tumorigenesis and therapy. *Nat Rev Cancer* **5**, 867-75.

Chang, C. T., Lin, H., Ho, T. Y., Li, C. C., Lo, H. Y., Wu, S. L., Huang, Y. F., Liang, J. A. and Hsiang, C. Y. (2011). Comprehensive assessment of host responses to ionizing radiation by nuclear factor-κB bioluminescence imaging-guided transcriptomic analysis. *PLoS One* **6**, e23682.

Daly, M. J. (2009). A new perspective on radiation resistance based on Deinococcus radiodurans. *Nat Rev Microbiol* **7**, 237-45.

Daly, M. J., Gaidamakova, E. K., Matrosova, V. Y., Vasilenko, A., Zhai, M., Leapman, R. D., Lai, B., Ravel, B., Li, S. M., Kemner, K. M. et al. (2007). Protein oxidation implicated as the primary determinant of bacterial radioresistance. *PLoS Biol* **5**, e92.

Daly, M. J., Gaidamakova, E. K., Matrosova, V. Y., Vasilenko, A., Zhai, M., Venkateswaran, A., Hess, M., Omelchenko, M. V., Kostandarithes, H. M., Makarova, K. S. et al. (2004). Accumulation of Mn(II) in Deinococcus radiodurans facilitates gamma-radiation resistance. *Science* **306**, 1025-8.

Dulermo, R., Onodera, T., Coste, G., Passot, F., Dutertre, M., Porteron, M., Confalonieri, F., Sommer, S. and Pasternak, C. (2015). Identification of New Genes Contributing to the Extreme Radioresistance of Deinococcus radiodurans Using a Tn5-Based Transposon Mutant Library. *PLoS One* **10**, e0124358.

Edelstein, K., Spiegler, B. J., Fung, S., Panzarella, T., Mabbott, D. J., Jewitt, N., D'Agostino, N. M., Mason, W. P., Bouffet, E., Tabori, U. et al. (2011). Early aging in adult survivors of childhood medulloblastoma: long-term neurocognitive, functional, and physical outcomes. *Neuro-Oncology*. 13, 536-45.

Ellenberg, L., Liu, Q., Gioia, G., Yasui, Y., Packer, R. J., Mertens, A., Donaldson, S. S., Stovall, M., Kadan-Lottick, N., Armstrong, G. et al. (2009). Neurocognitive status in long-term survivors of childhood CNS malignancies: a report from the Childhood Cancer Survivor Study. *Neuropsychology*. 23, 705-717.

Emami, B., Lyman, J., Brown, A., Coia, L., Goitein, M., Munzenrider, J. E., Shank, B., Solin, L. J. and Wesson, M. (1991). Tolerance of normal tissue to therapeutic irradiation. *Int J Radiat Oncol Biol Phys* **21**, 109-22.

Eriste, E., Kurrikoff, K., Suhorutšenko, J., Oskolkov, N., Copolovici, D. M., Jones, S., Laakkonen, P., Howl, J. and Langel, Ü. (2013). Peptide-based glioma-targeted drug delivery vector gHoPe2. *Bioconjug Chem* **24**, 305-13.

Gao, H., Yang, Z., Zhang, S., Cao, S., Pang, Z., Yang, X. and Jiang, X. (2013). Glioma-homing peptide with a cell-penetrating effect for targeting delivery with enhanced glioma localization, penetration and suppression of glioma growth. *J Control Release* **172**, 921-8.

Gutman, P. D., Fuchs, P. and Minton, K. W. (1994). Restoration of the DNA damage resistance of Deinococcus radiodurans DNA polymerase mutants by Escherichia coli DNA polymerase I and Klenow fragment. *Mutat Res* **314**, 87-97.

Gutman, P. D., Fuchs, P., Ouyang, L. and Minton, K. W. (1993). Identification, sequencing,

and targeted mutagenesis of a DNA polymerase gene required for the extreme radioresistance of Deinococcus radiodurans. *J Bacteriol* **175**, 3581-90.

Hutchinson, F. (1966). The molecular basis for radiation effects on cells. *Cancer Res* **26**, 2045-52.

Kempf, S. J., Casciati, A., Buratovic, S., Janik, D., von Toerne, C., Ueffing, M., Neff, F., Moertl, S., Stenerlöw, B., Saran, A., Atkinson, M. J., Eriksson, P., Pazzaglia, S. and Tapio, S. (2014). The cognitive defects of neonatally irradiated mice are accompanied by changed synaptic plasticity, adult neurogenesis and neuroinflammation. *Molecular Neurodegeneration.* 9, 1-17.

Makarova, K. S., Aravind, L., Wolf, Y. I., Tatusov, R. L., Minton, K. W., Koonin, E. V. and Daly, M. J. (2001). Genome of the extremely radiation-resistant bacterium Deinococcus radiodurans viewed from the perspective of comparative genomics. *Microbiol Mol Biol Rev* **65**, 44-79.

Makarova, K. S., Omelchenko, M. V., Gaidamakova, E. K., Matrosova, V. Y., Vasilenko, A., Zhai, M., Lapidus, A., Copeland, A., Kim, E., Land, M. et al. (2007). Deinococcus geothermalis: the pool of extreme radiation resistance genes shrinks. *PLoS One* **2**, e955.

McKinnon, P. J. (2012). ATM and the molecular pathogenesis of ataxia telangiectasia. *Annu Rev Pathol* **7**, 303-21.

Mulhern, R. K., Palmer, S. L., Merchant, T. E., Wallace, D., Kocak, M., Brouwers, P., Krull, K., Chintagumpala, M., Stargatt, R., Ashley, D. M., et al. (2005). Neurocognitive

consequences of risk-adapted therapy for childhood medulloblastoma. *Journal of Clinical Oncology*. 23, 5511-5519.

Slade, D., Lindner, A. B., Paul, G. and Radman, M. (2009). Recombination and replication in DNA repair of heavily irradiated Deinococcus radiodurans. *Cell* **136**, 1044-55.

Tian, B., Xu, Z., Sun, Z., Lin, J. and Hua, Y. (2007). Evaluation of the antioxidant effects of carotenoids from Deinococcus radiodurans through targeted mutagenesis, chemiluminescence, and DNA damage analyses. *Biochim Biophys Acta* **1770**, 902-11.

White, O., Eisen, J. A., Heidelberg, J. F., Hickey, E. K., Peterson, J. D., Dodson, R. J., Haft, D. H., Gwinn, M. L., Nelson, W. C., Richardson, D. L. et al. (1999). Genome sequence of the radioresistant bacterium Deinococcus radiodurans R1. *Science* **286**, 1571-7.

Zahradka, K., Slade, D., Bailone, A., Sommer, S., Averbeck, D., Petranovic, M., Lindner, A. B. and Radman, M. (2006). Reassembly of shattered chromosomes in Deinococcus radiodurans. *Nature* **443**, 569-73.

CHAPTER 4

A *Drosophila* model to investigate the neurotoxic side effects of radiation exposure

This paper is being published in *Disease Models and Mechanisms* (2015, in press) by Lisa J. Sudmeier, Steven P. Howard, and Barry Ganetzky

Abstract

Children undergoing cranial radiation therapy (CRT) for pediatric central nervous system malignancies are at increased risk for neurological deficits later in life. We developed a model of neurotoxic damage in adult *Drosophila* following irradiation during juvenile development with the goal of elucidating underlying neuropathological mechanisms and ultimately identifying potential therapeutic targets. Wild-type third instar larvae were irradiated with single doses of gamma radiation and the percentage that survived to adulthood was determined. Motor function of surviving adults was examined with a climbing assay and longevity was assessed by measuring lifespan. Neuronal cell death was assayed by immunohistochemistry in adult brains. We also tested developmental stage sensitivity by irradiating larvae at various time points in development. Irradiating late third instar larvae at a dose of 20 Gy or higher impairs motor activity of surviving adults. A dose of 40 Gy or higher results in a precipitous reduction in the percentage of larvae that survive to adulthood. A dose-dependent decrease in adult longevity is paralleled by a dose-dependent increase in activated Death caspase-1 (Dcp1) in adult brains. Survival to adulthood and adult lifespan are more severely impaired with decreasing larval age at time of irradiation. Our initial survey of the *Drosophila* Genome Reference Panel demonstrates that differences in genotype can confer phenotypic differences in radio-sensitivity for developmental survival and motor function. This work demonstrates the usefulness of *Drosophila* to model the toxic effects of radiation during development with the potential to unravel underlying mechanisms and to discover novel therapeutic interventions.

Introduction

Cranial radiation therapy (CRT) is a mainstay of treatment for brain tumors, along with surgery and chemotherapy. CRT preferentially kills malignant cells by inducing DNA damage that results in cell cycle arrest and death of dividing cells. Therapy is often designed to target the tumor resection bed and a margin; lower doses of radiation are sometimes delivered to the rest of the brain to target micrometastases. Prophylactic CRT may also be administered to high-risk patients to reduce or prolong the time to development of brain metastases. CRT has consistently prolonged survival in pediatric brain tumor patients, and as therapies have improved, the rate of cure and length of disease free survival has also increased, especially in pediatric brain tumor patients (Armstrong, 2010). As therapy has become more effective and patients live longer, the long-term sequelae of this treatment, particularly in pediatric patients, have received increasing attention. Individuals who undergo CRT before the age of 18 have a particularly increased incidence of many neurological and cognitive side effects, including impairments of memory, attention, visuo-spatial processing, learning ability, and motor control and dexterity in addition to increased prevalence of seizure disorders (Armstrong et al., 2009; Edelstein et al., 2011b; Ellenberg et al., 2009; Mulhern et al., 2005; Packer et al., 2003; Redmond et al., 2013). Pathological analysis has demonstrated CRT-associated changes in the brain during development including disrupted neurogenesis, demyelination, cortical atrophy, and damage to the microvasculature (Ball et al., 1992; Jain et al., 2005; Monje et al., 2002; Schuitema et al., 2013). As increasingly effective therapy results in more pediatric brain tumor survivors, there is increasing need for radioprotective strategies to reduce the damage to healthy tissue during treatment.

For decades, thiol compounds have been studied for their radioprotective properties mediated through DNA binding and scavenging of reactive oxygen species (Hosseinimehr, 2007). These compounds effectively confer radioprotection in preclinical animal models but have limited clinical usefulness because they are difficult to administer and have a number of toxic side effects (Hosseinimehr, 2007; McAleer et al., 2005; Srinivasan et al., 2002). Thus, there is considerable interest in developing related but less toxic compounds that still provide radioprotection.

Identification of novel therapeutic targets offers another approach for developing improved radioprotective agents with reduced toxicity. These targets may differ among tissues and may offer a more specific and effective strategy for protecting healthy cells from high doses of therapeutic radiation. To identify potential targets for drug development, it is necessary to have a more complete and detailed understanding of the key biochemical pathways and molecular mechanisms that underlie the immediate and long-term neurotoxic effects of radiation exposure. Unbiased forward genetic screens in *Drosophila* have been crucial to the molecular dissection of other complex biological mechanisms including autophagy, programmed cell death, the cell cycle, and embryonic patterning (Mulakkal et al., 2014; Jenkins et al., 2013; Hérranz and Milán, 2008; Nüsslein-Volhard and Wieschaus; 1980). Using the appropriate experimental model, this approach should be equally valuable in deciphering the mechanism(s) of the acute and long-term sequelae of radiation during development. Previous radiation studies in *Drosophila* have identified lethal doses for larvae and examined effects of irradiating adults (Balock et al., 1963; Ogaki and Nakashima-Tanaka, 1966; Parsons et al., 1969; Pyo et al., 2014; Vaisnav et al., 2014; Westerman and Parsons, 1973), but the long-term effects on adults of radiation exposure during

larval development have not been examined. Here we show that many of the important neurotoxic side effects resulting from radiation therapy during development in humans can be reasonably mimicked in *Drosophila.* Moreover, we demonstrate that genetic background substantially affects radiosensitivity. These results demonstrate that *Drosophila* can serve as a useful experimental model for studying the neurotoxic consequence of radiation exposure and ultimately for identifying specific genes and proteins involved in the molecular mechanism of radiation-induced damage.

Results

Radiation during development reduces survival to adulthood

Drosophila develop from embryos to adults in approximately 10 days at 25°C. Upon hatching, first instar larvae feed, grow, and undergo two successive molts to become third instar larvae over the next two days. After another 2.5-3 days, metamorphosis begins with the onset of pupariation. Five days later, mature adults emerge from pupal cases. The majority of neurons in the adult central nervous system are derived from neural precursors originating in a post-embryonic wave of neurogenesis that peaks in mid-third instar larvae (Ito and Hotta, 1992; Siegrist et al., 2010; Truman and Bate, 1988). To investigate how radiation exposure during development affects adult outcomes, we irradiated larvae in the late ("wandering") third larval instar stage. Varying doses of gamma radiation were delivered in a single fraction from a Cesium-137 source. Following irradiation, larvae were allowed to complete development, and the percent of surviving adults was quantified. Consistent with previous studies (Balock et al., 1963), we found that doses of radiation up to 30 Gy had little effect on subsequent survival (Fig. 1A). At higher doses, survival to adulthood was reduced; exposure to 40-50 Gy reduced the

percent of adult survivors by 50%. Like other insects, *Drosophila* are remarkably resistant to radiation compared with mammals, but like mammals, they are more sensitive to radiation during development than in adulthood (Balock et al., 1963; Grahn, 1958; Ogaki and Nakashima-Tanaka, 1966; Parsons et al., 1969; Vaisnav et al., 2014; Westerman and Parsons, 1973).

Radiation during development reduces adult lifespan

To determine whether radiation exposure during larval development had long-term effects on flies that were able to complete development, we measured the lifespan of surviving adults. At 50 Gy, the highest dose of radiation tested, we observed substantial adult mortality (>40% for *CS* and *OR-R*) within 48 hours of eclosion (Fig. 1B). Because this very early adult mortality is likely to be the result of residual developmental defects caused by radiation exposure, we excluded flies that died within 48 hours of eclosion from subsequent lifespan measurement. Survival curves for the remaining *Canton-S* adults demonstrated that lifespan decreased as radiation dose increased (Fig. 2). These results also indicate that lifespan of surviving adults is more sensitive to the effects of radiation during larval development than survival of irradiated larvae to adulthood. For example, irradiation of *Canton-S* larvae at 30 Gy and 40 Gy, reduces median lifespan of the surviving adults by more than 50% compared with non-irradiated controls even though these doses have only a modest effect on viability of the irradiated larvae (93% and 84% survival to the adult stage, respectively). This more sensitive dose-dependent effect of radiation on survival highlights a parallel with humans in that as time since radiation treatment increases, side effects worsen (Edelstein et al., 2011a).

Radiation sensitivity increases with decreasing age of exposure

In pediatric CRT, there is an inverse correlation between age of patient at treatment and severity of the long-term neurocognitive side effects from radiation (Edelstein et al., 2011b; Mulhern et al., 2005). To determine whether a similar relationship occurs in *Drosophila*, we examined the effect of radiation exposure at different stages of larval development on adult eclosion. We irradiated larvae at various developmental stages from 1-5 days AEL (after egg lay) and quantified survival to adulthood as well as lifespan of survivors. We chose a dose of 30 Gy because it has little effect on survival to eclosion when larvae are irradiated at 5 days AEL but has strong effects on lifespan of surviving adults (Figs 1,2). Consistent with the observations in human patients, we found that as the age of larvae at time of exposure decreased, the sensitivity to radiation increased (Fig. 3). For example, the fraction of larvae surviving to adulthood exceeded 85% when larvae were irradiated at 3-5 days AEL. In contrast, irradiation at 2 days AEL decreased adult survival to less than 20% and there was complete absence of survivors at 1 day AEL (Fig. 3A).

Although the percent of adult survivors was similar when larvae between 3-5 days AEL were irradiated at 30 Gy, lifespan of the surviving adults differed depending on larval age at time of exposure. In particular, adult survivors of larvae irradiated at 3 day AEL have significantly shorter lifespans than adult survivors of larvae irradiated at 4 or 5 days AEL (Fig. 3B). Once again, these results parallel results in human patients following CRT with side effects of radiation exposure becoming more severe as the time interval since treatment increases (Edelstein et al., 2011a).

Radiation during development causes behavioral deficits in adults

A particularly unfortunate consequence of pediatric CRT is neurocognitive, motor, and behavioral disorders later in life. To determine whether irradiation of *Drosophila* larvae during development also causes neurological deficits at a later stage in life, we assayed locomotor ability of adult flies as a convenient behavioral readout (Fig. 4). Wild-type flies are negatively geotactic, and after being tapped gently to the bottom of a culture vial the flies will quickly climb towards the top. To quantify climbing ability, we determined the fraction of flies that climbed past a line marking a vertical distance of 5 cm from the bottom of the vial within 10 seconds. This assay provides a good assessment of overall neurological function because proper performance requires sensory input, central processing, and motor output. We observed that larval irradiation results in behavioral impairment of adult survivors, with increasing impairment at higher doses (Fig. 4). Like adult lifespan, climbing behavior is a more radiosensitive phenotype than survival to adulthood following larval irradiation. Thus, although irradiating late third instar larvae at 20 Gy has only a minimal effect on survival to adulthood, the climbing pass rate of surviving adults is reduced by more than 25% compared with non-irradiated controls. We did not determine a climbing pass rate for adults that survived larval irradiation at 40 or 50 Gy because their locomotor behavior is so severely impaired that these flies hardly climb at all.

Radiation during development causes cell death in adult brains

Our studies on lifespan and behavior on adult flies following larval irradiation demonstrate that in *Drosophila,* as in humans, radiation exposure can have persistent, long-term effects resulting in neurological impairment as well as reduced lifespan. We hypothesized that at least some of the damaging effects of radiation on the nervous system would be observable at the cellular level. To test this hypothesis, we irradiated late third instar larvae, dissected brains from the resultant

adults after aging them for three days, and stained them for activated Dcp-1 (Death caspase-1), a *Drosophila* effector caspase (Hay and Guo, 2006), which along with Drice (Death related ICE-like caspase) is a commonly used marker for cells undergoing apoptosis in *Drosophila* (Hay and Guo, 2006; Florentin and Arama, 2012). We observed a dose-dependent increase in the number of activated Dcp-1-labeled cells compared with non-irradiated controls indicating that there is an increase in number of cells undergoing apoptosis in adult brains following larval irradiation (Fig. 5). We observed a similar dose-dependent increase in Dcp-1-positive cells in brains of 12-day old adults (e. g. approximately 2.5 weeks after irradiation) (Fig. 5). Although there are fewer Dcp-1-labeled cells in brains of 12-day old flies compared with 3-day old flies, their level is still elevated compared with controls, demonstrating that an early exposure to radiation has ongoing deleterious consequences much later in life. Co-labeling cells with antibodies against Repo and Elav to mark glia and neurons, respectively (Halter et al., 1995; O'Neill et al., 1994), revealed that most of this Dcp-1 activation is occurring in neurons (Fig. 5E-H). The cumulative effect of continuous apoptosis in adult brains over several weeks is very likely to be a major factor in the neurological impairment we observe in these flies following larval irradiation that may become more severe with time since irradiation.

Sensitivity to radiation depends on genetic background

An important goal in developing a *Drosophila* model of radiation-induced neurotoxicity is to identify and unravel the key molecular mechanisms that underlie the observed effects of radiation on viability and neurological function. In particular, because of the genetic tools available in *Drosophila*, we can easily ask whether there are genetic differences in sensitivity to the effects of radiation and, if so, identify variants in specific genes that confer radioresistance or

radiosensitivity to discover the proteins and pathways that play major roles in mediating the observed effects of radiation. One way to discover such variants is by conducting a screen following chemical mutagenesis for new mutants that are more sensitive or resistant to radiation than wild-type flies. Another approach is to take advantage of existing variation in natural populations to screen for the phenotypes of interest. This latter approach is facilitated by the *Drosophila* Genetic Reference Panel (DGRP), a collection of over 200 sequenced highly inbred lines, each generated from single females captured from a natural population (Huang et al., 2014; Mackay et al., 2012). Thus, each line represents the genetic variants present in the genome of a single fly. Because the genome for each line has been fully sequenced, these lines are an extremely valuable resource for association mapping in which a phenotype of interest can be correlated with variants in a specific gene. Investigators have previously used these lines to identify candidate genes involved in a variety of biological mechanisms including sleep, longevity, and olfactory behavior (Durham et al., 2014; Harbison et al., 2013; Swarup et al., 2013).

We performed an initial survey of the DGRP lines to determine whether this collection harbors genetic variants that affect survival to eclosion following larval irradiation. For this analysis we determined an “eclosion index” (see Materials and Methods) for 52 DGRP lines following a 20Gy dose of radiation during the late third larval instar. We observed significant variation in the effect of radiation on survival to eclosion among the DGRP lines tested (Fig. 6). To expand our analysis of the effect of genetic background on radiation sensitivity, we also examined a subset of the DGRP collection for adult climbing behavior after irradiating late third instar larvae at 20 Gy. Single-trial data suggest that the effect of radiation on adult climbing behavior, measured by

calculating a “climbing index” (see Materials and Methods) also varies over a wide range among the DGRP lines tested (data not shown). An unexpected finding was that the eclosion index or climbing index for some DGRP lines had a negative value, indicating that survival to adulthood or locomotor activity improved following irradiation compared with the unirradiated controls. At this point, we remain uncertain about the significance of this result. Although there are plausible biological mechanisms by which moderate doses of radiation could confer some benefit to particular genetic variants, we cannot rule out the possibility of experimental artifact. In addition, in at least several instances, negative indices were associated with DGRP lines whose survival to eclosion or locomotor ability was poor even without irradiation. The observed results could thus be more indicative of a poor starting phenotype than real benefits of irradiation. Further experiments will be necessary to resolve these possibilities. Examination of the eclosion index results shown in Figure 6 and our preliminary climbing index data (not shown) also indicates that although some lines appear to be more resistant to radiation than our standard wild-type strain both for eclosion and climbing ability, overall there does not appear to be a strong correlation between these two indices in the various lines tested. These results suggest that while variants in some genes may confer overall radiation resistance, it is more common for radiosensitivity of survival to eclosion to be affected by a different set of genetic variants from those affecting radiosensitivity of locomotor activity. Thus, it is likely that the deleterious effects of radiation on these two phenotypes are mediated by distinct cellular mechanisms.

Overall, these results demonstrate that survival to adulthood following larval irradiation is a quantitative trait that is dependent on genetic background. Moreover, genetic variants affecting this trait appear to be well represented in the DGRP lines suggesting that additional screening

will be useful for identifying specific genes affecting the long-lasting damage induced by radiation exposure during development.

Discussion

The goal of this work was to establish a *Drosophila* model for investigating the neurotoxic side effects of radiation therapy during development. Exposing late third instar larvae to radiation results in a dose-dependent decrease in survival to eclosion, shortened adult lifespan, impaired locomotion, and increased cell death in the adult brain. The effects of radiation on eclosion and adult lifespan are more severe when larvae are irradiated at progressively earlier stages in development. These findings parallel those in humans, where neurological side effects worsen with increasing radiation dose (Redmond et al., 2013) and younger age at time of radiation treatment (Edelstein et al., 2011b; Mulhern et al., 2005). Thus, many of the most important deleterious effects of CRT in humans are paralleled in *Drosophila*, suggesting that the *Drosophila* model can be useful in elucidating key genetic mechanisms responsible for the neurotoxic effects of radiation that are likely to be conserved between flies and humans.

Despite the experimental advantages of using *Drosophila* as an experimental model, it is important to recognize that there are significant biological and technical differences between our radiation exposure model in flies and CRT in humans that must be considered when trying to extrapolate from flies to humans. One important difference is that unlike CRT, where radiation is targeted to particular regions of the brain, we can only expose entire larvae to irradiation because of their small size. Thus, although we are particularly interested in the deleterious effects of radiation on the nervous system and focus on phenotypes such as climbing behavior and

neuronal cell death in the brain, we cannot be certain that these phenotypes and others such as successful eclosion do not involve effects of irradiation on other tissues. Nonetheless, all the phenotypes we focus on are known to have a significant dependence on the nervous system, and it is a reasonable working hypothesis to assume that these phenotypes are at least providing some measure of neural function following radiation exposure. Ultimately, by identifying specific genetic variants that confer different radiosensitive phenotypes, we can test the validity of our hypothesis by manipulating expression of these genes in a tissue specific manner.

It has been proposed that many of the neurological side effects of CRT are due to a decline in neurogenesis following radiation (Monje et al., 2002; Kempf et al., 2014; Son et al., 2015). Although there is considerable neurogenesis in the adult mammalian brain (Aimone et al., 2014), the adult fly brain is largely, although not entirely, post-mitotic (Siegrist et al., 2010; von Trotha et al., 2009). Consequently, it would be difficult to detect a decrease in neurogenesis in the *Drosophila* brain following radiation exposure. On the other hand, in the transition from the larval nervous system to the adult nervous system that takes place during pupariation and metamorphosis in *Drosophila*, there is continued neurogenesis for about three days (Siegrist et al., 2010), which could be impacted by radiation exposure during the larval stage. Thus, although a *Drosophila* model may not be able to precisely replicate every feature of CRT in humans, this is also true in the majority of instances where *Drosophila* has been used to model human biological and disease mechanisms including embryonic pattern formation, sleep, circadian rhythm, cancer, epilepsy, retinal degeneration etc. (Nusslein-Volhard and Wieschaus, 1980; Potdar and Sheeba, 2013; Hardin, 2011; Rudrapatna et al., 2012; Cunliffe et al., 2015; Xiong and Bellen, 2013). With awareness of the limits of the model and appropriate caution in data

interpretation, a Drosophila model, although imperfect, can nonetheless provide powerful new insights and starting points for unraveling normal and pathological biological mechanisms in humans.

Another important difference in our experimental model is that we delivered radiation exposure in a single, unfractionated dose to late third instar larvae whereas CRT generally utilizes fractionated exposure delivered in smaller doses over many days to achieve a final total dose to reduce toxicity to normal tissue while effectively killing malignant cells (Ahmed et al., 2014). Because the third larval instar in *Drosophila* only lasts for 2-3 days, there is a very narrow time window over which radiation exposure could be fractionated. Moreover, because *Drosophila* are inherently more radioresistant than humans and can readily tolerate much higher doses of radiation, there is no particular reason to fractionate the doses of radiation used in our experiments. Whether this difference in radiation delivery between our fly model and CRT is of sufficient mechanistic significance that there would be no overlap between the genes and signaling pathways in flies and humans that confer radioresistance remains to be determined. Nonetheless, it seems reasonable to assume that fundamental biological consequences of radiation on the nervous system will be conserved between flies and humans regardless of fractionation. Therefore, we believe it is likely that identification of radioresistant genes in *Drosophila* will ultimately still be valuable in unraveling key pathways responsible for long-term sequelae of CRT in humans.

One important area where a Drosophila model of CRT can play a particularly important role is in discovery and development new radioprotective agents with potential for clinical application.

Although radioprotective thiols have been studied for decades, their clinical application has been limited owing to their toxic side effects and their ineffectiveness when administered orally (Hosseinimehr, 2007). One of the most important strengths of a *Drosophila* model is that it can be used for unbiased genetic screens to identify key molecular players underlying radiation-induced damage. Our initial screen of the DGRP lines indicates that *Drosophila* can be used to identify genetic variants that confer large differences in radiation sensitivity. Because of the genetic tools available in *Drosophila*, once candidate genes for these differences in radiosensitivity are identified, the relevant molecular pathways can be readily studied. Understanding these pathways and their molecular components provides a rational strategy for identification of novel therapeutic targets. Moreover, with the growing emphasis on genome sequence-driven personalized medicine, knowledge of which genetic variants confer greater or lesser sensitivity to the deleterious side effects of radiation should enable the development of CRT regimens specifically tailored to individual patients.

In addition to the expected immediate deleterious effects of CRT, a much more puzzling consequence is the ongoing long-term effects, which are still evident years or decades after treatment. For example, magnetic resonance spectroscopic analysis of pediatric CRT patients demonstrated metabolic changes associated with brain tissue damage up to 18 months after completion of therapy (Blamek et al., 2010). Magnetic resonance diffusion tensor imaging of adults 25 years after CRT revealed loss of white matter integrity compared with healthy controls (Schuitema et al., 2013). The cellular targets and the cascade of events triggered by irradiation that are responsible for these persistent long-term toxic effects remain very poorly understood. It is therefore of interest that we observe comparable long-term effects in our *Drosophila* model.

Notably, when we examined adult brains following irradiation of third instar larvae, we found a dose-dependent elevation of activated-caspase staining compared with unirradiated controls not only in 3-day old adults but also in 12-day old adults, e. g. 17 days after irradiation, suggesting an increase in cell death. With a mean lifespan for control flies in our experiments of approximately 45 days, a timespan of 17 days would be roughly equivalent to decades in humans. *A priori*, one might have expected that cell death would be sharply elevated immediately after irradiation and that the process would be completed a short time thereafter. Although the number of cells with activated Dcp-1 is markedly lower in the brains of 12-day old adults compared with 3-day old adults following larval irradiation, it is still significantly higher than unirradiated controls. These results strongly suggest that larval irradiation not only has immediate effects resulting in cell death, but also triggers some kind of persistent dyshomeostasis in cells that survive the acute effects of irradiation resulting in their eventual death at a much later time.

The long-term neurotoxic side effects of CRT are one of the most difficult issues to confront in treating pediatric cancer patients. However, if we can gain a better understanding of the cellular and molecular basis of these delayed effects, it might also open a large window for therapeutic intervention to reduce side effects of CRT in pediatric patients. For example, our observation that brain cells continue to undergo programmed cell death in adult flies 17 days after irradiation suggests that after the desired tumor-killing benefits of CRT have been achieved in pediatric patients, there might be an opportunity to initiate appropriate therapy that would limit subsequent ongoing damage to healthy cells and thereby mitigate toxic side effects. To achieve such a favorable outcome, it will be necessary to have a much more detailed understanding of the

persistent toxic cascade triggered by irradiation and the genes and protein products responsible for orchestrating this long-lasting toxicity. As in the search for new radioprotective compounds, we believe that the genetic and molecular tools available in *Drosophila* offer a powerful and systematic approach that can help provide the missing information.

Translational Impact

Clinical issue: Children who undergo cranial radiation therapy (CRT) to treat central nervous system (CNS) malignancies are at increased risk for neurocognitive deficits, impaired coordination and motor control, and seizure disorder. The severity of these side effects often worsens as age at treatment decreases. For decades, thiol compounds have been studied for their radioprotective properties, but they have limited clinical usefulness because they are difficult to administer and have a number of toxic side effects. Thus, there is considerable interest in trying to develop less toxic strategies. One approach is to characterize the molecular pathways underlying radiation-induced neurotoxicity to identify novel therapeutic targets for enhancing radioprotection in healthy tissue. *Drosophila* is an ideal model for the molecular dissection of such complex biological mechanisms.

Results: This article demonstrates that *Drosophila* may be used to model radiation-induced neurotoxicity. Irradiating *Drosophila* during the larval stage produces measurable phenotypes in adults that parallel those seen in survivors of pediatric CNS malignancies who received CRT. Irradiating late third instar larvae at a dose of 40 Gy or higher results in a precipitous reduction in the percentage of larvae that survive and develop into adults. A dose of 20 Gy or higher impairs motor activity of surviving adults. A dose-dependent decrease in adult longevity is paralleled by

a dose-dependent increase in activated caspase in adult brains. Survival to adulthood and adult lifespan are more severely impaired with decreasing larval age at time of irradiation. Genetic background of the irradiated larvae affects survival to adulthood and adult motor ability, demonstrating that there is a genetic component to radiation sensitivity.

Implications and future directions: This work demonstrates the usefulness of *Drosophila* to model the toxic effects of radiation during development with the potential to unravel underlying mechanisms and to discover novel therapeutic interventions. Screening the *Drosophila* Genome Reference Panel (DGRP) will allow for quantitative trait locus (QTL) mapping of genetic variants that alter developmental survival and motor function following irradiation. From this screen candidate genes will be identified and tested for their ability to alter these radiation-sensitive phenotypes. Once genes of interest are confirmed, molecular pathways underlying radiation-induced neurotoxicity can be dissected to identify therapeutic targets for reducing damage to healthy tissue during radiation therapy.

Materials and Methods

***Drosophila* strains and culture**: Flies were maintained on standard cornmeal-molasses medium at 25°C, except for lifespan assays, which were performed at 29°C. Two standard wild-type lines (*Canton-S* and *Oregon-R*) and one common white-eyed background strain (w^{1118}) were used as controls. The *Drosophila* Genetic Reference Panel (DGRP) (Mackay et al., 2012) was used for experiments in Figure 6. For all experiments involving irradiation of late third instar larvae, adults were allowed to mate and lay eggs in culture bottles on standard medium and cleared from the bottles after 4-5 days to prevent larval crowding. Wandering third instar larvae were collected when they emerged from food. Known numbers of larvae were placed in culture vials

with an absorbent tissue at the bottom to reduce excess moisture and prevent newly eclosed flies from getting stuck.

Irradiation of late third instar larvae: Vials containing 30-50 late third instar larvae were placed on a rotating plate and exposed to a single dose of gamma radiation (10, 20, 30, 40 or 50 Gy) using a Cesium-137 irradiator (J. L. Sheppard & Associates San Francisco, California USA; Mark I unit, Model 30, Serial Number 668) with an average dose rate of 6.5 Gy/min. Control larvae were handled identically but without radiation exposure. Irradiated and control larvae were then allowed to complete development at 25°C and all adults that subsequently emerged were collected and counted.

Irradiation of larvae at earlier developmental stages: Cultures of *Canton-S* adults were allowed to lay eggs on small petri dishes containing apple juice-agar medium. Approximately 24 hours later (1 day after egg lay, AEL), newly hatched first instar larvae were collected and transferred to fresh apple juice plates covered in standard cornmeal-molasses medium and allowed to develop at 25°C until the specified time of irradiation. For irradiation of first instar larvae, they were transferred directly after hatching to fresh vials containing standard medium. For irradiation of larvae at later stages, they were collected, counted, and transferred to vials containing approximately 6mL of standard medium softened by the addition of 1-2 mL of water. In all cases, control vials were handled identically without irradiation.

Lifespan Analysis: Newly eclosed adults were collected, sorted by sex, and transferred to fresh vials (10 males or females per vial) containing standard medium and aged at 29°C. Flies were

transferred to fresh food every other day at which time the number of surviving flies was recorded. Adult flies that died within 48 hours of eclosion were counted but excluded from lifespan analysis. Males and females both demonstrate dose-dependent radiation sensitivity in all of our assays. However, as many studies on lifespan in *Drosophila* show, there are a number of biological differences between males and females that affect survival for reasons unrelated to the investigation at hand. In particular, because so much of the physiology of females is dedicated to egg production, we wanted to eliminate this source of variability and for the studies presented here concentrated primarily on analyzing males (Bonduriansky et al., 2008).

Climbing Assay: Newly-eclosed adults were collected and aged in vials of standard medium at 25°C (≤11 flies of the same sex per vial) for 5-6 days before testing. For the behavioral test, flies ($N \leq 11$) of the same sex were transferred to the climbing apparatus consisting of two empty plastic culture vials taped together at the open end (vial diameter: 2.3 cm, height: 9.3 cm). After a 1-minute recovery, flies were gently tapped to the bottom, and the number that climbed vertically beyond a 5-cm mark within 10 seconds was recorded. The test was repeated 5 times for each cohort of flies with 1-minute rest periods between each test (adapted from Ali et al., 2011).

Immunohistochemistry: Adult brains were dissected in 1X PBS and fixed at room temperature for 25-30 minutes in 4% formaldehyde in phosphate buffer (4% formaldehyde, 0.1M phosphate buffer (pH 7.2), 0.2% TritonX-100). Samples were then washed with 1X PBS and placed in blocking buffer (PBS, 0.2% TritonX-100, 0.1% normal goat serum) for 2 hours at room temperature or 4°C overnight. Brains were incubated in primary antibodies diluted with blocking

buffer at 4°C overnight then washed 2X with PBST (PBS + 0.1% TritonX-100) and incubated in secondary antibodies diluted with blocking buffer for 4 hours at room temperature, then washed 2X again with PBST. DAPI was added in the final wash for 30 minutes at room temperature. Brains were mounted on slides in Vectashield (Vector Laboratories, Burlingame, California USA). The antibodies used are as follows: Rabbit anti-cleaved Dcp-1 (Cell Signaling Technology, Danvers, Massachusetts USA; #9578, 1:100), Mouse anti-Repo (Developmental Studies Hybridoma Bank, University of Iowa, Iowa City, Iowa USA; 8D12, 1:50), Rat anti-Elav (Developmental Studies Hybridoma Bank, University of Iowa, Iowa City, Iowa USA; 7E8A10, 1:250), DAPI (Sigma-Aldrich, St. Louis, Missouri, USA; 1mg/L), Goat anti-Mouse Alexa Fluor-488 (Life Technologies, Carlsbad, California USA; 1:200), Goat anti-Rabbit Alexa Fluor-568 (Life Technologies, Carlsbad, California USA; 1:200), Goat anti-Rat Alexa Fluor-633 (Invitrogen, Carlsbad, California USA; 1:200).

Microscopy: Adult brains were imaged using a Zeiss 510 Confocal Laser Scanning Microscope (Carl Zeiss Microscopy, Jena, Thuringia Germany). ImageJ Software (National Institutes of Health, Bethesda, Maryland USA) and Adobe Photoshop CC (Adobe Systems, San Jose, California USA) were used for adjusting image brightness and contrast.

Calculation of Indices for DGRP Lines: Eclosion index = percent eclosion [non-irradiated] - percent eclosion [20 Gy]. **Climbing index** = climbing pass rate [non-irradiated] - climbing pass rate [20 Gy].

Statistical Analyses: GraphPad Prism (GraphPad Software San Diego, California USA) was used for Student's T-Test analyses of eclosion, climbing, and DCP-1-positive cells and for one-way ANOVA of the DGRP eclosion indices. The DLife software package (Scott Pletcher University of Michigan, Ann Arbor, Michigan USA) was used for Log-Rank tests on survival curves.

Acknowledgements

We are grateful to Brian Robichaud and Sai-Suma Samudrala for their help with the preliminary screen presented in Figure 6. We thank Zach Harvanek and Michael Waterson for performing the Log-Rank Analysis on our lifespan data using the DLife software (Scott Pletcher, University of Michigan). We also thank members of the Ganetzky Laboratory for comments on the manuscript and helpful discussions, especially Robert Kreber for irradiating all of the larvae used in these experiments.

References

Ahmed, K. A., Correa, C. R., Dilling, T. J., Rao, N. G., Shridhar, R., Trotti, A. M., Wilder, R. B. and Caudell, J. J. (2014). Altered fractionation schedules in radiation treatment: a review. *Seminars in Oncology.* 41, 730-50.

Aimone, J. B., Li, Y., Lee, S. W., Clemenson, G. D., Deng, W. and Gage, F. H. (2014). Regulation and function of adult neurogenesis: from genes to cognition. *Physiological Reviews.* 94, 991-1026.

Ali, Y. O., Escala, W., Ruan, K.. and Zhai, R. G. (2011). Assaying locomotor, learning, and memory deficits in Drosophila models of neurodegeneration. *Journal of Visualized Experiments*. (49), e2504.

Armstrong, G. T., Liu, Q., Yasui, Y., Huang, S., Ness, K. K., Leisenring, W., Hudson, M. M., Donaldson, S. S., King, A. A., Stoval, M., et al. (2009). Long-term outcomes among adult survivors of childhood central nervous system malignancies in the Childhood Cancer Survivor Study. *Journal of the National Cancer Institute*. 101, 946-958.

Armstrong, G. T. (2010). Long-term survivors of childhood central nervous system malignancies: The experience of the Childhood Cancer Survivor Study. *European Journal of Paediatric Neurology*. 14, 298-303.

Ball, W. S., Prenger, E. C. and Ballard, E. T. (1992). Neurotoxicity of radio/chemotherapy in children: pathologic and MR correlation. *American Journal of Neuroradiology*. 13, 761-776.

Balock, J. W., Burditt, A. K. and Christenson, L. D. (1963). Effects of gamma radiation on various stages of three fruit fly species. *Journal of Economic Entomology.* 56, 42-46.

Blamek, S., Larysz, D., Ficek, K., Sokol, M., Miszczyk, L. and Tarnawski, R. (2010). MR Spectroscopic evaluation of brain tissue damage after treatment for pediatric brain tumors. *Acta Neurochirurgica Supplementum*. 106, 183-186.

Bonduriansky, R., Maklakov, A., Zajitschek, F. and Brooks, R. (2008). Sexual selection, sexual conflict and the evolution of ageing and life span. *Functional Ecology.* 22, 443-453.

Cunliffe, V. T., Baines, R. A., Giachello, C. N. G., Lin, W., Morgan, A., Reuber, M., Russell, C., Walker, M. C. and Williams, R. S. B. (2015). Epilepsy research methods update: understanding the causes of epileptic seizures and identifying new treatments using non-mammalian model organisms. *Seizure.* 24, 44-51.

Durham, M. F., Magwire, M. M., Stone, E. A. and Leips, J. (2014). Genome-wide analysis in Drosophila reveals age-specific effects of SNPs on fitness traits. *Nature Communications*. 5, 4338.

Edelstein, K., Spiegler, B. J., Fung, S., Panzarella, T., Mabbott, D. J., Jewitt, N., D'Agostino, N. M., Mason, W. P., Bouffet, E., Tabori, U. et al. (2011a). Early aging in adult survivors of childhood medulloblastoma: long-term neurocognitive, functional, and physical outcomes. *Neuro-Oncology*. 13, 536-45.

Edelstein, K., D'Agostino, N., Bernstein, L. J., Nathan, P. C., Greenberg, M. L., Hodgson, D. C., Millar, B. A., Laperriere, N. and Spiegler, B. J. (2011b). Long-term neurocognitive outcomes in young adult survivors of childhood acute lymphoblastic leukemia. *Journal of Pediatric Hematology/Oncology*. 33, 450-8.

Ellenberg, L., Liu, Q., Gioia, G., Yasui, Y., Packer, R. J., Mertens, A., Donaldson, S. S., Stovall, M., Kadan-Lottick, N., Armstrong, G. et al. (2009). Neurocognitive status in long-term survivors of childhood CNS malignancies: a report from the Childhood Cancer Survivor Study. *Neuropsychology*. 23, 705-717.

Florentin, A. and Arama, E. (2012). Caspase levels and execution efficiencies determine the apoptotic potential of the cell. *The Journal of Cell Biology*. 196, 513-527.

Grahn, D. (1958). Acute radiation response of mice from a cross between radiosensitive and radioresistant strains. *Genetics*. 43, 835-43.

Halter, D. A., Urban, J., Rickert, C., Ner, S. S., Ito, K., Travers, A. A. and Technau, G. M. (1995). The homeobox gene repo is required for the differentiation and maintenance of glia function in the embryonic nervous system of Drosophila melanogaster. 121, 317-332.

Harbison, S. T., McCoy, L. J. and Mackay, T. F. (2013). Genome-wide association study of sleep in Drosophila melanogaster. *BMC Genomics*. 14, 281-98.

Hardin, P. E. (2011). Molecular genetic analysis of circadian timekeeping in Drosophila. *Advances in Genetics.* 74, 141-73.

Hay, B. A. and Guo, M. (2006). Caspase-dependent cell death in Drosophila. *Annual Review of Cell and Developmental Biology*. 22, 623-650.

Hérranz, H. and Milán, M. (2014). Signalling molecules, growth regulators and cell cycle control in Drosophila. *Cell Cycle*. 7, 3335-3337.

Hosseinimehr, S. J. (2007). Trends in the development of radioprotective agents. *Drug Discovery Today*. 12, 794-805.

Huang, W., Massouras, A., Inoue, Y., Peiffer, J., Ramia, M., Tarone, A. M., Turlapati, L., Zichner, T., Zhu, D., Lyman, R. F., et al. (2014). Natural variation in genome architecture among 205 Drosophila melanogaster Genetic Reference Panel lines. *Genome Research*. 24, 1193-1208.

Ito, K. and Hotta, Y. (1992). Proliferation pattern of postembryonic neuroblasts in the brain of Drosophila melanogaster. *Developmental Biology*. 149, 134-48.

Jain, R., Robertson, P. L., Gandhi, D., Gujar, S. K., Muraszko, K. M. and Gebarski, S. (2005). Radiation-induced cavernomas of the brain. *American Journal of Neuroradiology*. 26, 1158-62.

Jenkins, V. K., Timmons, A. K. and McCall, K. (2013). Diversity of cell death pathways: insight from the fly ovary. *Trends in Cell Biology*. 23, 567-574.

Kempf, S. J., Casciati, A., Buratovic, S., Janik, D., von Toerne, C., Ueffing, M., Neff, F., Moertl, S., Stenerlöw, B., Saran, A., Atkinson, M. J., Eriksson, P., Pazzaglia, S. and Tapio, S. (2014). The cognitive defects of neonatally irradiated mice are accompanied by changed synaptic plasticity, adult neurogenesis and neuroinflammation. *Molecular Neurodegeneration*. 9, 1-17.

Mackay, T. F. C., Richards, S., Stone, E. A., Barbadilla, A., Ayroles, J. F., Zhu, D., Casillas, S., Han, Y., Magwire, M. M., Cridland, J. M., et al. (2012). The Drosophila melanogaster Genetic Reference Panel. *Nature*. 482, 173-178.

McAleer, M. F., Davidson, C., Davidson, W. R., Yentzer, B., Farber, S. A., Rodeck, U. and Dicker, A. P. (2005). Novel use of zebrafish as a vertebrate model to screen radiation protectors and sensitizers. *International Journal of Radiation Oncology Biology Physics*. 61, 10-13.

Monje, M. L., Mizumatsu, S., Fike, J. R. and Palmer, T. D. (2002). Irradiation induces neural precursor-cell dysfunction. *Nature Medicine*. 8, 955-962.

Mulakkal, N. M., Nagy, P., Szabolcs, T., Tusco, R., Juhasz, G. and Nexis, I. (2014). Autophagy in Drosophila: From historical studies to current knowledge. *BioMed Research International.* 2014, 1-24.

Mulhern, R. K., Palmer, S. L., Merchant, T. E., Wallace, D., Kocak, M., Brouwers, P., Krull, K., Chintagumpala, M., Stargatt, R., Ashley, D. M., et al. (2005). Neurocognitive consequences of risk-adapted therapy for childhood medulloblastoma. *Journal of Clinical Oncology*. 23, 5511-5519.

Nüsslein-Volhard, C. and Wieschaus, E. (1980). Mutations affecting segment number and polarity in Drosophila. *Nature.* 287, 795-801.

Ogaki, M. and Nakashima-Tanaka, E. (1966). Inheritance of radioresistance in Drosophila. I. *Mutation Research*. 3, 438-43.

O'Neill, E. M., Rebay, I., Tjian, R. and Rubin, G. M. (1994). The activities of two Ets-related transcription factors required for Drosophila eye development are modulated by the Ras/MAPK pathway. *Cell.* 78, 137-147.

Packer, R. J., Gurney, J. G., Punyko, J. A., Donaldson, S. S., Inskip, P. D., Stovall, M., Yasui, Y., Mertens, A. C., Sklar, C. A., Nicholson, H. S., et al. (2003). Long-term neurologic

and neurosensory sequelae in Adult survivors of a childhood brain tumor: Childhood Cancer Survivor Study. *Journal of Clinical Oncology*. 21, 3255-3261.

Parsons, P. A., MacBean, I. T. and Lee, B. T. O. (1969). Polymorphism in natural populations for genes controlling radioresistance in Drosophila. *Genetics*. 61, 211-218.

Potdar, S. and Sheeba, V. (2013). Lessons from sleeping flies: insights from Drosophila melanogaster on the neuronal circuitry and importance of sleep. *Journal of Neurogenetics.* 27, 23-42.

Pyo, J., Park, J., Na, H., Jeon, H., Lee, S., Kim, J., Park, S., Jin, Y., Kim, Y. and Yoo, M. (2014). Functional modification of intestinal stem cells by ionizing radiation. *Radiation Research*. 181, 376-386.

Redmond, K. J., Mahone, E. M., Terezakis, S., Ishaq, O., Ford, E., McNutt, T., Kleinberg, L., Cohen, K. J., Wharam, M. and Horska, A. (2013). Association between radiation dose to neuronal progenitor cell niches and temporal lobes and performance on neuropsychological testing in children: a prospective study. *Neuro-Oncology*. 15, 360-9.

Rudrapatna, V. A., Cagan, R. L. and Das, T. K. (2012). Drosophila cancer models. *Developmental Dynamics.* 241, 107-118.

Schuitema, I., Deprez, S., Van Hecke, W., Daams, M., Uyttebroeck, A., Sunaert, S., Barkhof, F., van Dulmen-den Broeder, E., van der Pal, H. J., van den Bos, C., et al. (2013). Accelerated aging, decreased white matter integrity, and associated neuropsychological dysfunction 25 years after pediatric lymphoid malignancies. *Journal of Clinical Oncology*. 31, 3378-3388.

Siegrist, S. E., Haque, N. S., Chen, C., Hay, B. A. and Hariharan, I. K. (2010). Inactivation of both foxo and reaper promotes long-term adult neurogenesis in Drosophila. *Current Biology*. 20, 643-648.

Son, Y., Yang, M., Wang, H. and Moon, C. (2015). Hippocampal dysfunctions caused by cranial irradiation: a review of the experimental evidence. *Brain, behavior, and immunity*. 45, 287-96.

Srinivasan, V., Pendergrass, J. A. Jr., Kumar, K. S., Landauer, M. R. and Seed, T. M. (2002). Radioprotection, pharmacokinetic and behavioural studies in mouse implanted with biodegradable drug (amifostine) pellets. *International Journal of Radiation Biology*. 78, 535-43.

Swarup, S., Huang, W., Mackay, T. F. and Anholt, R. R. H. (2013). Analysis of natural variation reveals neurogenetic networks for Drosophila olfactory behavior. *Proceedings of the National Academy of Sciences*. 110, 1017-1022.

Truman, J. W. and Bate, M. (1988). Spatial and temporal patterns of neurogenesis in the central nervous system of Drosophila melanogaster. *Developmental Biology*. 125, 145-57

Vaisnav, M., Xing, C., Ku, H., Hwang, D., Stojadinovic, S., Pertsemlidis, A. and Abrams, J. M. (2014). Genome-wide association analysis of radiation resistance in Drosophila melanogaster. Palsson A, ed. *PLoS ONE*. 9, e104858.

von Trotha, J. W., Egger, B. and Brand, A. H. (2009). Cell proliferation in the Drosophila adult brain revealed by clonal analysis and bromodeoxyuridine labelling. *Neural Development*. 4, 1-8

Westerman, J. M. and Parsons, P. A. (1973). Variations in genetic architecture at different doses of gamma-radiation as measured by longevity in Drosophila melanogaster. *Canadian Journal of Genetics and Cytology.* 15, 289-98.

Xiong, B. and Bellen, H. J. (2013). Rhodopsin homeostasis and retinal degeneration: lessons from the fly. *Trends in Neurosciences.* 36, 652-60.

Figure 1

A

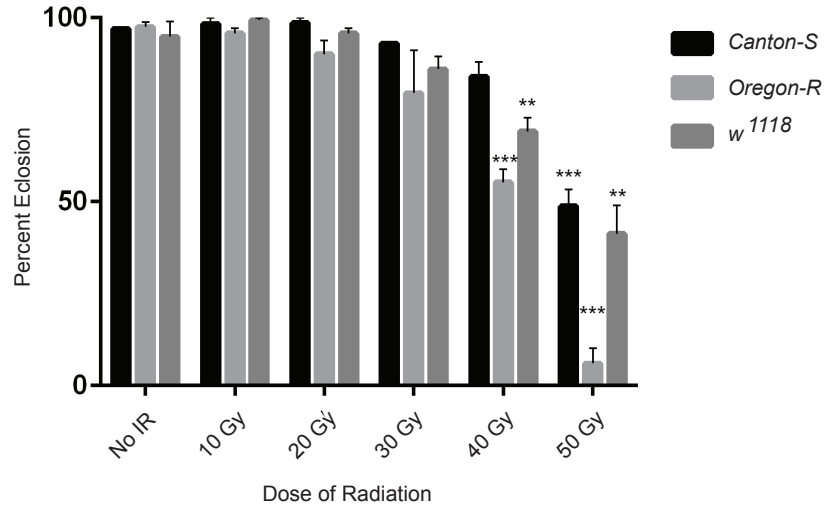

B

Percent of Adults that Die within 48 hours of Eclosion			
Dose	***CS***	***OR-R***	***w 1118***
No IR	0.9 ± 0.9	1.4 ± 0.7	2.6 ± 2.6
10 Gy	0	0	0
20 Gy	0.8 ± 0.8	1.1 ± 1.1	0
30 Gy	1.4 ± 1.4	5.5 ± 3.1	0
40 Gy	* 9.6 ± 2.0	2.3 ± 1.1	2.0 ± 2.0
50 Gy	* 53.5 ± 15.0	40.5 ± 21.2	11.9 ± 6.0

Fig. 1. Irradiation during late third larval instar reduces survival to adulthood. (A) For each dose of radiation, the percentage of irradiated late third-instar larvae (5 days AEL) that complete development and eclose as adults is shown for three different laboratory strains. Values shown are mean ± SEM for three independent trials of 30-50 larvae per dose per trial. *P<0.05, **p<0.01, ***p<0.001 based on Student's t test comparing 40 Gy and 50 Gy to No IR. (B) The percentage of adult survivors from panel A. that died within 48 hours following eclosion. Values shown are mean ± SEM. *p<0.05 based on Student's t test comparing *CS* 40 Gy and 50 Gy to No IR.

Figure 2

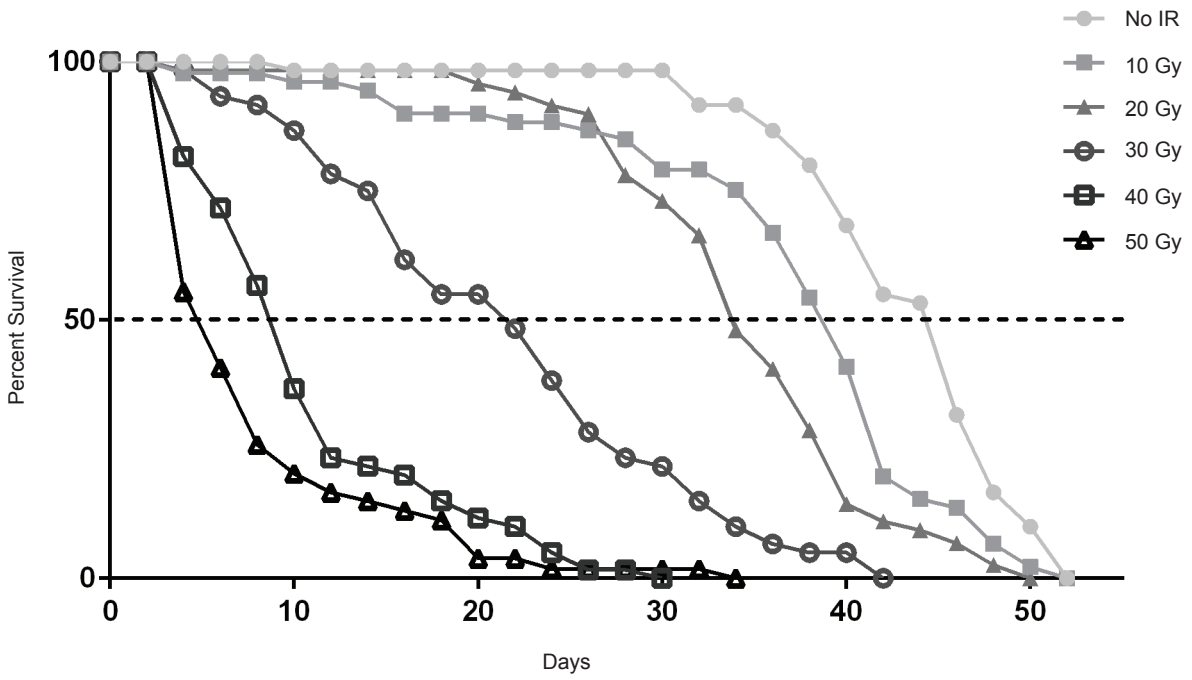
No IR
10 Gy
20 Gy
30 Gy
40 Gy
50 Gy
100
50
0
Percent Survival
0
10
20
30
40
50
Days

Fig. 2. Irradiation during larval development reduces lifespan of surviving adults. Percent survival at 29°C vs. adult age (days after eclosion) is graphed for each dose of radiation administered during the late third larval instar (5 days AEL). Only flies surviving the first 48 hours of adulthood are included in this analysis. Median lifespan is marked with the dashed line. Median survival is 5, 9, 21, 34, 39 and 44 days for 50 Gy, 40 Gy, 30 Gy, 20 Gy, 10 Gy and No IR, respectively. Each survival curve is based on three independent trials of 10-20 male *Canton-S* flies each. Data points on the graph represent mean percent survival. P values from Log-Rank test on each independent trial comparing No IR v. 30 Gy are: 5.68e-11, 1.9e-8, and 7.8e-7.

Figure 3

A

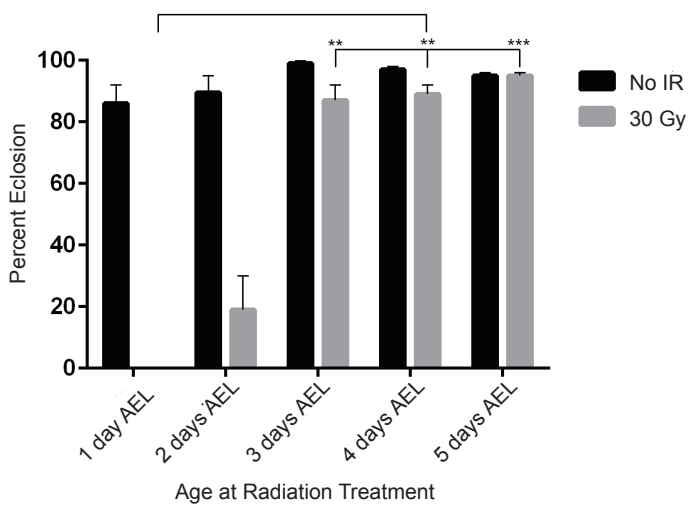
100
80
60
40
20
0
Percent Eclosion
**
**
***
No IR
30 Gy
1 day AEL
2 days AEL
3 days AEL
4 days AEL
5 days AEL
Age at Radiation Treatment

B

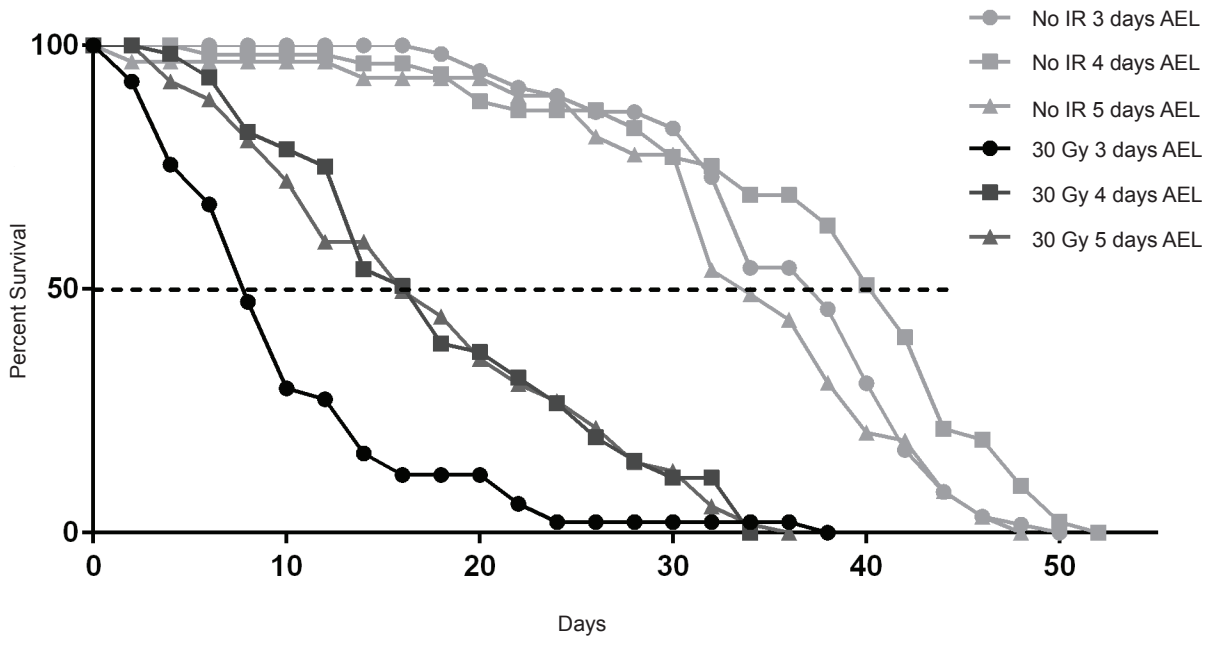
100
50
0
Percent Survival
0
10
20
30
40
50
Days
No IR 3 days AEL
No IR 4 days AEL
No IR 5 days AEL
30 Gy 3 days AEL
30 Gy 4 days AEL
30 Gy 5 days AEL

Fig. 3. Radiation sensitivity depends on developmental stage. (A) Percentage of larvae irradiated (30 Gy) at the indicated time points that complete development and eclose as adults. Values shown are mean ± SEM for two independent trials of 30-50 *Canton-S* larvae each. **p<0.01, ***p<0.001 based on Student's t test comparing 3d after egg lay (AEL), 4d AEL and 5d AEL to 1d AEL (30 Gy). (B) Percent survival at 29°C vs. adult age (days after eclosion) is graphed for survivors of radiation (30 Gy) administered at the indicated time points along with unirradiated controls. Only flies that survived the first 48 hours of adulthood are included in this analysis. Median lifespan is marked with the dashed line. Median survival is 7, 16 and 16 days for 30 Gy 3d AEL, 4d AEL and 5d AEL, respectively. Each survival curve is based on three independent trials of 10-20 male *Canton-S* flies each. Data points on the graph represent mean percent survival. P values from Log-Rank test on each independent trial comparing 30Gy 3d AEL and 30 Gy 5d AEL are: 0.0187, 0.00412, and 0.00693.

Figure 4

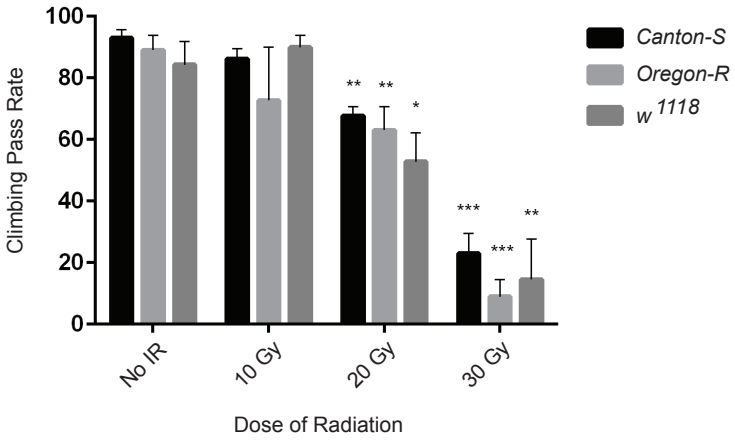
100
80
60
40
20
0
Climbing Pass Rate
**
**
*
***
***
**
No IR
10 Gy
20 Gy
30 Gy
Dose of Radiation
Canton-S
Oregon-R
w 1118

Fig. 4. Irradiation during larval development results in a dose-dependent decrease in locomotor ability in adults. Climbing pass rate was assayed for adult males from three laboratory strains following irradiation of late third instar larvae (5 days AEL). Each group ($N \leq 11$) of 5-6 day old adults was tested 5 times with 1-minute recovery periods between tests. Three independent trials were performed for each strain at each dose. The histogram shows the percent of flies that climb above 5 cm in 10 seconds for each strain. Values shown are mean ± SEM. *p<0.05, **p<0.01, ***p<0.001 based on Student's t test comparing 20 Gy and 30 Gy to No IR.

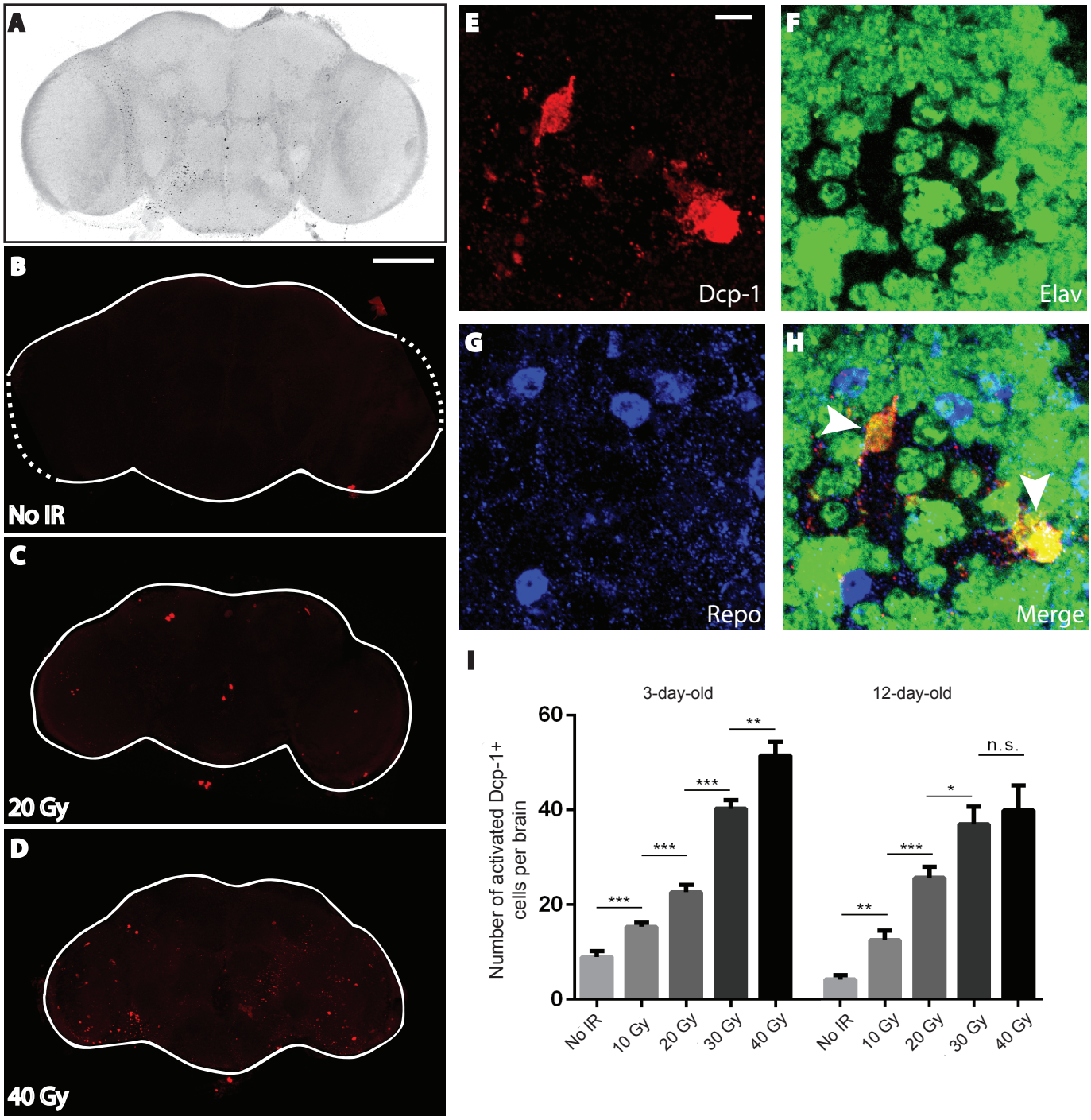
A
B
No IR
C
20 Gy
D
40 Gy
E
Dcp-1
F
Elav
G
Repo
H
Merge
I
3-day-old
12-day-old
Number of activated Dcp-1+ cells per brain
60
40
20
0
**
***
***
***
***
*
n.s.
No IR
10 Gy
20 Gy
30 Gy
40 Gy
No IR
10 Gy
20 Gy
30 Gy
40 Gy

Fig. 5. Irradiation during larval development increases frequency of cells expressing a cell death marker in adult brains. Following exposure of late third instar (5 day AEL) *Canton-S* larvae to the indicated doses of radiation, surviving adults were aged for 3 days after eclosion before brains were dissected for confocal microscopy. (A-D) Confocal stacks of whole brains immunostained for activated-Dcp-1. (A) Grayscale image of a non-irradiated brain with enhanced contrast to show anatomy (B-D) RGB images showing activated Dcp-1-positive cells (red). (E-H) Cells with activated Dcp-1 in adult brains following larval irradiation are predominantly neurons not glia. Higher magnification confocal stacks of 3-day-old adult *Canton-S* brains following irradiation of late third instar larvae at 40 Gy stained for activated Dcp-1 (E), the neuronal nuclear marker Elav (F), and the glial nuclear marker Repo (G). Dcp-1 shows colocalization with Elav but not Repo (arrowheads) (H). (I) Quantification of the number of Dcp-1- positive brain cells in 3-day-old and 12-day-old adult *Canton-S* flies following irradiation of third instar larvae at the indicated dose. Two independent assays of 5-8 brains per dose were performed. Values shown are mean ± SEM. *$p<0.05$, **$p<0.01$, ***$p<0.001$ based on Student's t test comparing the number of activated Dcp-1+ cells at a given dose of radiation with the corresponding number at the previous lower dose. Scale bars: 100µm (B-D), 5µm (E-H).

Figure 6

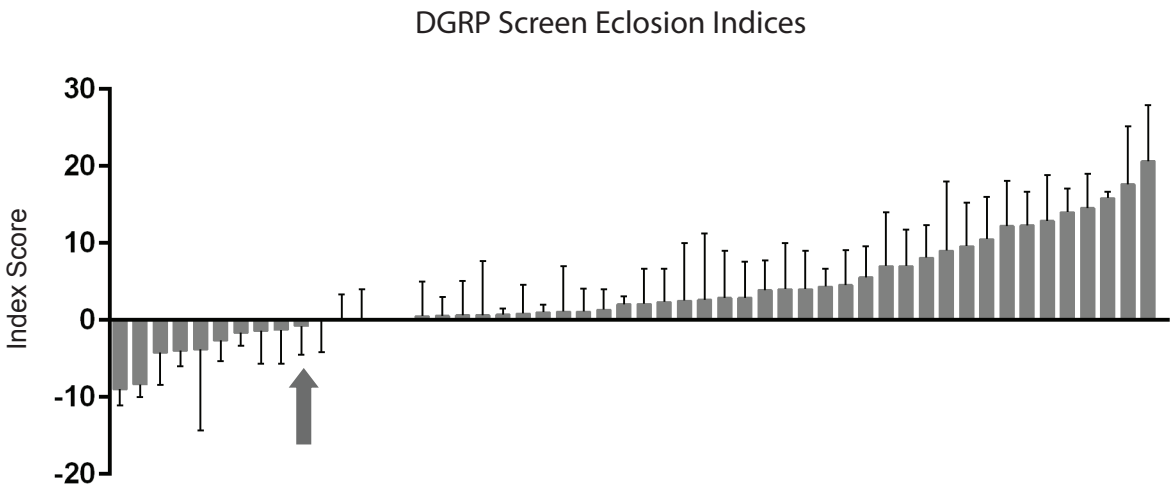

Fig. 6. Genetic background affects radiosensitivity. Bar graph showing the eclosion index for each of the 52 DGRP lines that were assayed for sensitivity to radiation organized from lowest to highest index. Values shown are mean ± SEM for two-four independent trials of 20-30 larvae each. P=0.0056 based on a one-way ANOVA. Arrow indicates where the *Canton-S* eclosion index falls.

CHAPTER 5

Genome wide association study of radiosensitivity

Introduction

The *Drosophila melanogaster* Genetic Reference Panel (DGRP) is a collection of over 200 fully sequenced Drosophila lines, each generated from a single mated female (Mackay et al., 2012; Huang et al., 2014). This collection can be used for genome wide association studies (GWAS) in which phenotypes of interest are correlated with specific genetic variants. These lines have been used to identify candidate genes involved in biological processes including longevity, sleep, olfactory behavior and radiation resistance in adult flies (Harbison et al., 2013; Swarup et al., 2013; Durham et al., 2014; Vaisnav et al., 2014). We have used this collection to perform a GWAS of sensitivity to radiation during development.

Results

We screened over 100 of the Drosophila lines in the DGRP for sensitivity to radiation as measured by survival to eclosion following radiation exposure during larval development. Using the eclosion assay described in Chapter 4, we calculated an eclosion index for each DGRP line tested (% eclosion of unirradiated v. % eclosion following 20 Gy dose of radiation). We used the DGRP2 webtool (dgrp2.gnets.ncsu.edu) to analyze three eclosion phenotype data sets. For one subset of the DGRP lines we also analyzed locomotor behavior in adults following radiation exposure during larval development, as described in Chapter 4, (climbing in unirradiated flies v. climbing in flies exposed to 20 Gy during larval development). We also used the DGRP2 webtool to analyze this locomotor phenotype data set. Each DGRP analysis identified genetic variants associated with radiosensitivity.

Trial 1:

We screened 60 of the DGRP lines for sensitivity to radiation as measured by eclosion following radiation exposure (20 Gy) during the late third instar larval stage. Each of these lines was only tested once. Locomotor behavior in adults following radiation exposure during larval development was tested, using the climbing assay described in Chapter 4, in 57 of these lines. Male and female locomotor behavior was tested separately, and each line was tested once (one set of males and one set of females per line). There were 27 genomic variants were associated with the radiosensitivity of eclosion, all with $p \leq 10^{-05}$. There were 105 genomic variants associated with the sensitivity of adult climbing behavior to radiation exposure during development. Some of these genomic variants were associated with the overall sensitivity of motor behavior in adults to radiation exposure during development and others were associated with the male- or female-specific sensitivity of adult locomotor behavior to radiation exposure during development. (Tables 1-5)

Trial 2:

We screened 51 DGRP lines for sensitivity to radiation as measured by eclosion following radiation exposure (20 Gy) during the late third instar larval stage. Each of these lines was tested 2-4 times. The average eclosion index from all trials for each line was used for the GWAS. There were 19 genomic variants associated with the radiosensitivity of eclosion ($p \leq 10^{-05}$). (Tables 6 & 7)

Trial 3:

We screend 114 DGRP lines for sensitivity to radiation as measured by eclosion following radiation exposure (20 Gy) during the late third instar stage. Each of these lines was only tested

once to generate the eclosion index used for the GWAS. There were 51 genomic variants associated with the radiosensitivity of eclosion ($p \leq 10^{-05}$). (Tables 8 & 9)

Discussion

We performed three separate GWAS to identify genetic variants associated with radiosensitivity as measured by survival to eclosion following radiation exposure during larval development. We also performed one GWAS to identify genetic variants associated with radiosensitivity as measured by adult locomotor behavior following radiation exposure during development. The more lines we tested, the more genomic variants that were significantly associated with radiosensitivity. Analyzing more lines also resulted in more genomic variants with smaller p values. However, to increase the likelihood that statistically significant variants are truly affecting radiosensitivity each line should be tested multiple times to determine the average phenotype.

We have begun the process of testing loss of function mutations in genes that were identified as having variants associated with radiosensitivity in these GWAS. Some of these genes, including a cationic amino acid transporter and a centrosome-associated protein appear to be radioprotective genes. Further experiments will be necessary to confirm these phenotypes and test additional genes identified in the GWAS.

References

Durham, M. F., Magwire, M. M., Stone, E. A. and Leips, J. (2014). Genome-wide analysis in Drosophila reveals age-specific effects of SNPs on fitness traits. *Nat Commun* **5**, 4338.

Harbison, S. T., McCoy, L. J. and Mackay, T. F. (2013). Genome-wide association study of sleep in Drosophila melanogaster. *BMC Genomics* **14**, 281.

Huang, W., Massouras, A., Inoue, Y., Peiffer, J., Ràmia, M., Tarone, A. M., Turlapati, L., Zichner, T., Zhu, D., Lyman, R. F. et al. (2014). Natural variation in genome architecture among 205 Drosophila melanogaster Genetic Reference Panel lines. *Genome Res* **24**, 1193-208.

Mackay, T. F., Richards, S., Stone, E. A., Barbadilla, A., Ayroles, J. F., Zhu, D., Casillas, S., Han, Y., Magwire, M. M., Cridland, J. M. et al. (2012). The Drosophila melanogaster Genetic Reference Panel. *Nature* **482**, 173-8.

Swarup, S., Huang, W., Mackay, T. F. and Anholt, R. R. (2013). Analysis of natural variation reveals neurogenetic networks for Drosophila olfactory behavior. *Proc Natl Acad Sci U S A* **110**, 1017-22.

Vaisnav, M., Xing, C., Ku, H. C., Hwang, D., Stojadinovic, S., Pertsemlidis, A. and Abrams, J. M. (2014). Genome-wide association analysis of radiation resistance in Drosophila melanogaster. *PLoS One* **9**, e104858.

TABLE 1: Trial 1 - Alleles and P values (Eclosion)									
ID	MinorAllele	MajorAllele	RefAllele	MAF	MinorAlleleCount	MajorAlleleCount	SingleEff	SinglePval	SingleMixedPval
3L_13818269_SNP	T	C	T	0.2105	12	45	-8.793	2.12E-07	1.38E-07
3L_13183936_SNP	G	A	A	0.1207	7	51	-10.15	2.75E-06	1.45E-06
2R_14966473_SNP	T	C	C	0.0678	4	55	-12.92	3.70E-06	1.92E-06
2L_17566620_SNP	T	A	A	0.1579	9	48	-9.041	4.43E-06	2.06E-06
3L_13565325_SNP	T	C	C	0.2069	12	46	-8.051	4.02E-06	2.19E-06
3L_3561643_SNP	C	A	A	0.1	6	54	-10.57	4.80E-06	3.00E-06
X_10444486_SNP	G	T	G	0.283	15	38	-7.452	1.11E-05	3.42E-06
X_5180901_SNP	C	A	A	0.1207	7	51	-9.843	6.91E-06	3.49E-06
3L_13633902_SNP	G	A	A	0.2642	14	39	-7.606	2.27E-06	3.52E-06
3L_13635725_SNP	C	G	G	0.2143	12	44	-7.908	3.39E-06	4.06E-06
3L_13818237_SNP	G	A	G	0.2241	13	45	-7.64	7.39E-06	4.14E-06
2R_8714680_DEL	A	ATACACT…	ATACACT…	0.2545	14	41	-7.499	1.07E-05	4.32E-06
3L_13565367_SNP	A	T	T	0.2241	13	45	-7.606	8.29E-06	4.67E-06
3L_4002219_SNP	G	A	A	0.07018	4	53	-12.48	1.14E-05	5.08E-06
3L_13818252_SNP	A	C	A	0.25	13	39	-7.704	5.21E-06	5.20E-06
3L_4081777_SNP	A	G	A	0.0678	4	55	-12.4	1.05E-05	5.87E-06
X_6487489_SNP	T	C	T	0.4068	24	35	6.327	7.83E-06	6.31E-06
3L_3797403_SNP	G	A	A	0.1034	6	52	-10.28	9.84E-06	6.47E-06
3L_15483250_SNP	C	G	G	0.08772	5	52	-11.16	1.20E-05	6.59E-06
2L_7012663_SNP	G	A	A	0.4821	27	29	-6.353	1.47E-05	7.15E-06
3L_13596972_INS	AGCCAAGGA	A	A	0.1429	8	48	-9.037	6.92E-06	7.89E-06
2R_19519512_SNP	G	A	A	0.2982	17	40	-6.848	1.82E-05	7.97E-06
X_16614922_SNP	T	G	G	0.1379	8	50	-8.998	1.56E-05	8.17E-06
3L_15247204_SNP	A	G	G	0.08333	5	55	-11.02	1.30E-05	8.45E-06
3L_3913367_SNP	C	T	T	0.2321	13	43	-7.463	1.19E-05	8.62E-06
2L_2047853_DEL	T	TTTGCCA…	TTTGCCA…	0.1071	6	50	-10.17	1.32E-05	8.93E-06
X_15510610_SNP	G	C	C	0.1579	9	48	-8.549	1.69E-05	9.02E-06

TABLE 2: Trial 1 - Location of genetic variants (Eclosion)

ID	GeneAnnotation
3L_13818269_SNP	SiteClass[||||],TranscriptAnnot[INTERGENIC(MODIFIER|||||||||)]
3L_13183936_SNP	SiteClass[||||],TranscriptAnnot[INTERGENIC(MODIFIER|||||||||)]
2R_14966473_SNP	SiteClass[FBgn0004168|5-HT1A|INTRON|0],TranscriptAnnot[INTRON(MODIFIER|||834|5-HT1A|protein_coding|CODING|FBtr0086577|1)]
2L_17566620_SNP	SiteClass[FBgn0262398|mir-124|DOWNSTREAM|151],TranscriptAnnot[DOWNSTREAM(MODIFIER||||mir-124|miRNA|NON_CODING|FBtr0304299|);DOWNSTREAM(MODIFIER||||m
3L_13565325_SNP	SiteClass[FBgn0264001|bru-3|INTRON|0],TranscriptAnnot[INTRON(MODIFIER|||331|bru-3|protein_coding|CODING|FBtr0330348|4);INTRON(MODIFIER|||337|bru-3|protein_codin
3L_3561643_SNP	SiteClass[FBgn0005640|Eip63E|INTRON|0],TranscriptAnnot[INTRON(MODIFIER|||501|Eip63E|protein_coding|CODING|FBtr0110922|2);INTRON(MODIFIER|||509|Eip63E|protein_c
X_10444486_SNP	SiteClass[FBgn0085443|spri|INTRON|0],TranscriptAnnot[INTRON(MODIFIER|||1541|spri|protein_coding|CODING|FBtr0310438|1);INTRON(MODIFIER|||1541|spri|protein_coding|
X_5180901_SNP	SiteClass[||||],TranscriptAnnot[INTERGENIC(MODIFIER|||||||||)]
3L_13633902_SNP	SiteClass[FBgn0264001|bru-3|INTRON|0],TranscriptAnnot[INTRON(MODIFIER|||331|bru-3|protein_coding|CODING|FBtr0330348|2);INTRON(MODIFIER|||337|bru-3|protein_codin
3L_13635725_SNP	SiteClass[FBgn0264001|bru-3|INTRON|0],TranscriptAnnot[INTRON(MODIFIER|||331|bru-3|protein_coding|CODING|FBtr0330348|2);INTRON(MODIFIER|||337|bru-3|protein_codin
3L_13818237_SNP	SiteClass[||||],TranscriptAnnot[INTERGENIC(MODIFIER|||||||||)]
2R_8714680_DEL	SiteClass[||||],TranscriptAnnot[INTERGENIC(MODIFIER|||||||||)]
3L_13565367_SNP	SiteClass[FBgn0264001|bru-3|INTRON|0],TranscriptAnnot[INTRON(MODIFIER|||331|bru-3|protein_coding|CODING|FBtr0330348|4);INTRON(MODIFIER|||337|bru-3|protein_codin
3L_4002219_SNP	SiteClass[||||],TranscriptAnnot[INTERGENIC(MODIFIER|||||||||)]
3L_13818252_SNP	SiteClass[||||],TranscriptAnnot[INTERGENIC(MODIFIER|||||||||)]
3L_4081777_SNP	SiteClass[FBgn0004516|Gad1|INTRON|0],TranscriptAnnot[INTRON(MODIFIER|||510|Gad1|protein_coding|CODING|FBtr0073275|3);INTRON(MODIFIER|||510|Gad1|protein_codin
X_6487489_SNP	SiteClass[FBgn0029878|Pat1|SYNONYMOUS_CODING|0;FBgn0264380|CR43832|UPSTREAM|387],TranscriptAnnot[SYNONYMOUS_CODING(LOW|SILENT|agT/agC|S92|685|Pat1|prote
3L_3797403_SNP	SiteClass[FBgn0052264|CG32264|INTRON|0],TranscriptAnnot[INTRON(MODIFIER|||822|CG32264|protein_coding|CODING|FBtr0308639|2);INTRON(MODIFIER|||927|CG32264|pr
3L_15483250_SNP	SiteClass[||||],TranscriptAnnot[INTERGENIC(MODIFIER|||||||||)]
2L_7012663_SNP	SiteClass[FBgn0263026|CG43321|UTR_3_PRIME|0;FBgn0263027|CG43322|UPSTREAM|733],TranscriptAnnot[UPSTREAM(MODIFIER|||359|CG43322|protein_coding|CODING|FBtr03
3L_13596972_INS	SiteClass[FBgn0264001|bru-3|INTRON|0],TranscriptAnnot[INTRON(MODIFIER|||331|bru-3|protein_coding|CODING|FBtr0330348|3);INTRON(MODIFIER|||337|bru-3|protein_codin
2R_19519512_SNP	SiteClass[FBgn0004795|retn|UPSTREAM|623],TranscriptAnnot[INTERGENIC(MODIFIER|||||||||);UPSTREAM(MODIFIER|||906|retn|protein_coding|CODING|FBtr0072072|);UPSTREA
X_16614922_SNP	SiteClass[FBgn0085354|CG34325|INTRON|0;FBgn0052572|CG32572|UPSTREAM|294],TranscriptAnnot[INTRON(MODIFIER|||179|CG34325|protein_coding|CODING|FBtr0112527|1)
3L_15247204_SNP	SiteClass[||||],TranscriptAnnot[INTERGENIC(MODIFIER|||||||||)]
3L_3913367_SNP	SiteClass[FBgn0004910|Eip63F-1|INTRON|0],TranscriptAnnot[INTRON(MODIFIER|||161|Eip63F-1|protein_coding|CODING|FBtr0303420|4);INTRON(MODIFIER|||166|Eip63F-1|prot
2L_2047853_DEL	SiteClass[FBgn0028952|Kebab|UTR_3_PRIME|0],TranscriptAnnot[UTR_3_PRIME(MODIFIER|||547|Kebab|protein_coding|CODING|FBtr0077825|5);UTR_3_PRIME(MODIFIER|||548
X_15510610_SNP	SiteClass[FBgn0003463|sog|INTRON|0],TranscriptAnnot[INTRON(MODIFIER|||1038|sog|protein_coding|CODING|FBtr0074063|1);INTRON(MODIFIER|||1038|sog|protein_coding|C

TABLE 3: Trial 1 - Alleles and P values (Climbing Behavior)									
ID	MinorAllele	MajorAllele	RefAllele	MAF	MinorAlleleCount	MajorAlleleCount	AvgEff	AvgPval	AvgMixedPval
3R_25904206_SNP	C	G	G	0.07273	4	51	-19.63	6.33E-07	2.29E-07
2R_13585501_SNP	G	A	A	0.07143	4	52	-19.56	5.68E-07	2.56E-07
X_16874742_SNP	C	T	T	0.1404	8	49	-14.19	7.06E-07	3.95E-07
X_16874648_SNP	T	G	G	0.1154	6	46	-16.28	4.80E-07	3.00E-07
2R_13586361_SNP	C	T	T	0.09804	5	46	-16.64	3.43E-06	1.98E-06
2R_11968893_SNP	A	G	G	0.1731	9	43	11.53	7.53E-05	3.49E-05
2R_11787259_SNP	A	G	G	0.07143	4	52	-18.5	3.07E-06	1.54E-06
2L_5380930_SNP	G	A	A	0.08929	5	51	-16.53	4.22E-06	2.08E-06
3L_3096877_SNP	C	T	T	0.08	4	46	9.733	0.02822	1.94E-02
2L_12224867_SNP	G	A	A	0.07273	4	51	-17.64	1.28E-05	5.86E-06
3L_9011102_SNP	C	T	T	0.1154	6	46	2.523	0.5	4.76E-01
2L_12224769_SNP	T	C	C	0.07143	4	52	-17.6	1.10E-05	6.09E-06
3R_25904255_SNP	C	G	G	0.09259	5	49	-16.28	8.57E-06	3.36E-06
2R_9847609_SNP	C	T	T	0.125	7	49	-14.53	2.45E-06	1.19E-06
3R_15334723_SNP	A	G	G	0.07143	4	52	-17.64	1.08E-05	5.70E-06
X_21150049_SNP	C	G	C	0.2456	14	43	-10.66	5.66E-06	3.47E-06
2L_12224810_SNP	T	C	C	0.08163	4	45	-17.45	2.88E-05	8.71E-06
2L_2620117_SNP	G	C	C	0.07018	4	53	-18.56	2.30E-06	1.36E-06
2R_19510830_SNP	T	A	A	0.07018	4	53	-18.56	2.30E-06	1.36E-06
X_5302467_SNP	C	T	C	0.3273	18	37	-9.477	2.24E-05	1.22E-05
3L_3097162_SNP	A	G	G	0.07143	4	52	9.116	0.02861	2.83E-02
3L_14120731_SNP	T	A	A	0.1154	6	46	5.032	0.1491	1.53E-01
3L_14120733_SNP	A	C	C	0.1154	6	46	5.032	0.1491	1.53E-01
X_7816116_SNP	A	G	G	0.1053	6	51	4.986	0.1635	1.54E-01
2R_9847602_SNP	C	T	T	0.125	7	49	-13.92	6.81E-06	4.07E-06
2R_9847745_SNP	T	G	G	0.1429	8	48	-13.4	4.57E-06	2.42E-06
3R_9901916_SNP	C	A	A	0.1887	10	43	-12.1	1.28E-05	3.99E-06
2R_9845266_SNP	T	C	C	0.1429	8	48	-13.37	5.14E-06	2.61E-06
2R_18478905_SNP	A	C	C	0.1071	6	50	8.829	0.01086	1.01E-02
2L_5385350_DEL	T	TT	TT	0.1071	6	50	-14.67	1.13E-05	5.89E-06
3L_10728936_SNP	G	A	A	0.125	6	42	7.009	0.05794	4.58E-02
2R_9844244_SNP	T	G	G	0.1404	8	49	-13.27	5.03E-06	3.07E-06

ID	MinorAllele	MajorAllele	RefAllele	MAF	MinorAlleleCount	MajorAlleleCount	AvgEff	AvgPval	AvgMixedPval
2R_9844257_SNP	C	T	T	0.1404	8	49	-13.27	5.03E-06	3.07E-06
2R_9847417_SNP	C	G	G	0.1404	8	49	-13.27	5.03E-06	3.07E-06
2R_20270560_SNP	T	C	C	0.07273	4	51	8.483	0.0494	4.20E-02
3R_26732538_SNP	C	T	T	0.07143	4	52	-17.97	5.35E-06	3.50E-06
X_20330162_SNP	T	C	C	0.1273	7	48	-13.98	8.56E-06	3.74E-06
3R_27472609_SNP	T	C	C	0.1053	6	51	-14.31	1.67E-05	1.07E-05
3R_23498694_SNP	T	C	C	0.2105	12	45	-10.31	4.39E-05	2.94E-05
2R_9846441_SNP	A	G	G	0.1091	6	49	-14.88	6.63E-06	4.18E-06
3R_12730125_SNP	T	C	C	0.07273	4	51	-17.63	1.14E-05	5.93E-06
3R_27472682_SNP	A	T	T	0.1071	6	50	-14.24	2.12E-05	1.24E-05
3L_14121120_SNP	G	A	A	0.1455	8	47	6.045	0.05893	4.94E-02
3L_12534904_SNP	T	G	G	0.1111	6	48	-13.04	0.0001627	8.33E-05
3L_18118527_SNP	A	T	A	0.07273	4	51	-15.44	3.28E-05	1.05E-04
2L_3525076_SNP	A	G	G	0.1071	6	50	-14.8	8.75E-06	4.70E-06
3L_5045493_SNP	T	A	A	0.08929	5	51	5.612	0.1481	1.39E-01
2R_11972610_SNP	T	G	G	0.1429	8	48	3.967	0.2141	2.01E-01
2R_11972617_SNP	T	G	G	0.1429	8	48	3.967	0.2141	2.01E-01
2R_11972618_SNP	T	A	A	0.1429	8	48	3.967	0.2141	2.01E-01
2R_11919047_SNP	T	A	A	0.1404	8	49	-12.99	8.78E-06	5.49E-06
2L_12448459_SNP	T	A	A	0.1053	6	51	-13.69	4.39E-05	2.94E-05
3R_18753968_SNP	T	C	C	0.07692	4	48	-17.04	2.65E-05	1.44E-05
3R_12733078_SNP	A	T	T	0.07407	4	50	-17.6	1.41E-05	6.33E-06
2R_3801754_SNP	C	T	T	0.1731	9	43	3.379	0.282	2.57E-01
2L_3524813_SNP	C	T	T	0.1091	6	49	-14.76	1.12E-05	5.18E-06
3R_12730124_SNP	T	C	C	0.08889	4	41	-17.5	3.99E-05	8.88E-06
3R_13940909_SNP	C	T	T	0.1296	7	47	-13.8	6.64E-06	5.41E-06
3R_6180778_SNP	T	C	C	0.1887	10	43	-11.2	7.05E-06	2.61E-05
3L_9870455_SNP	A	T	T	0.09434	5	48	5.744	0.1535	1.31E-01
X_13736636_SNP	A	T	T	0.1071	6	50	-14.7	5.48E-06	5.64E-06
2R_18481060_SNP	C	T	T	0.1667	9	45	5.782	0.05331	4.90E-02
3R_25512112_SNP	A	C	C	0.09091	5	50	-15.66	1.19E-05	9.02E-06
2R_19322816_SNP	C	G	G	0.1053	6	51	8.97	0.01048	8.86E-03
2R_19322844_SNP	T	C	C	0.1053	6	51	8.97	0.01048	8.86E-03

ID	MinorAllele	MajorAllele	RefAllele	MAF	MinorAlleleCount	MajorAlleleCount	AvgEff	AvgPval	AvgMixedPval
2R_19322847_SNP	T	C	C	0.1053	6	51	8.97	0.01048	8.86E-03
2L_11944516_SNP	A	C	C	0.08511	4	43	-16.41	8.76E-05	3.67E-05
3L_2774293_SNP	A	C	C	0.07273	4	51	-15	0.0002895	1.76E-04
2R_15049013_SNP	T	C	C	0.07018	4	53	7.56	0.07709	7.06E-02
2L_968134_DEL	T	TGGCAGGCGAT	TGGCAGGCGA	0.07273	4	51	11.83	0.005335	3.89E-03
2R_19016671_SNP	C	G	G	0.4909	27	28	9.146	1.14E-05	6.13E-06
2L_8677115_SNP	T	C	C	0.07547	4	49	7.477	0.09199	7.47E-02
2R_15317440_SNP	C	T	C	0.3273	18	37	-9.729	1.12E-05	6.38E-06
3L_10298614_SNP	C	T	T	0.09091	5	50	7.848	0.04521	3.71E-02
2L_3796856_SNP	T	A	A	0.07407	4	50	7.873	0.07141	6.00E-02
2L_19623111_SNP	T	G	G	0.07843	4	47	-16.67	2.43E-05	2.43E-05
X_5487419_SNP	T	A	A	0.125	7	49	-13.51	1.66E-05	8.81E-06
2L_19623108_SNP	T	A	A	0.07407	4	50	-16.64	1.84E-05	2.40E-05
2R_19511025_SNP	A	G	G	0.09091	5	50	-15.82	1.53E-05	7.05E-06
2R_19511060_SNP	T	C	C	0.09091	5	50	-15.82	1.53E-05	7.05E-06
3L_18051860_SNP	C	T	T	0.07843	4	47	-17.55	1.62E-05	7.18E-06
3L_11389640_SNP	C	T	T	0.1455	8	47	-11.91	8.42E-05	4.35E-05
X_5681700_SNP	C	T	T	0.1429	8	48	-11.67	0.0001038	6.29E-05
X_8902132_SNP	T	G	G	0.193	11	46	-11.3	1.17E-05	7.43E-06
3L_11934093_SNP	A	T	T	0.09434	5	48	-15.21	3.90E-05	1.88E-05
2L_12224850_SNP	C	T	T	0.1837	9	40	-11.37	0.0001208	5.31E-05
X_16874757_SNP	C	T	T	0.1754	10	47	-11.69	1.24E-05	7.86E-06
3R_15373339_SNP	T	C	C	0.09804	5	46	-13.23	0.0006831	2.78E-04
3L_15298262_SNP	A	G	G	0.09259	5	49	7.084	0.06617	6.11E-02
3L_5987846_DEL	A	AGA	AGA	0.07407	4	50	-17.24	1.62E-05	1.06E-05
2L_19622968_SNP	G	T	T	0.07547	4	49	-16.54	2.16E-05	2.78E-05
2R_19500928_SNP	T	G	T	0.09091	5	50	-15.47	2.45E-05	1.22E-05
3R_10901804_SNP	A	T	T	0.1509	8	45	-11.01	0.0004412	1.98E-04
2R_17652665_SNP	G	C	C	0.07143	4	52	-15.17	0.0002188	1.43E-04
2L_10458705_SNP	T	A	A	0.09434	5	48	6.862	0.08613	7.02E-02
2R_13589140_SNP	C	T	T	0.1132	6	47	-14.1	4.38E-05	1.68E-05
2L_22308859_SNP	A	G	A	0.1489	7	40	9.837	0.003106	2.24E-03
3L_11934457_SNP	T	A	A	0.08929	5	51	-15.15	3.14E-05	1.93E-05

ID	MinorAllele	MajorAllele	RefAllele	MAF	MinorAlleleCount	MajorAlleleCount	AvgEff	AvgPval	AvgMixedPval
2R_14549280_SNP	A	C	C	0.07407	4	50	-16.63	4.82E-05	2.43E-05
X_13736629_SNP	A	T	T	0.1053	6	51	-14.39	1.48E-05	9.43E-06
2L_12153562_SNP	A	G	G	0.3818	21	34	8.796	5.14E-05	3.00E-05
2R_19116550_INS	TACCAAAAAAAAA	T	T	0.07407	4	50	-17.31	2.28E-05	9.57E-06
3L_16408661_SNP	A	T	T	0.1481	8	46	-10.9	9.15E-05	2.25E-04
2R_3188182_SNP	T	C	C	0.1321	7	46	4.988	0.1352	1.29E-01
X_9161929_INS	CC	C	C	0.08163	4	45	7.839	0.05833	6.22E-02

TABLE 4: Trial 1 - P values by sex (Climbing Behavior)									
ID	FemaleEff	FemalePval	FemaleMixe	MaleEff	MaleEffPval	MaleMixedI	DiffEff	DiffPval	DiffMixedPval
3R_25904206_SNP	-25.59	1.93E-07	6.17E-08	-13.67	0.0001249	7.03E-05	-11.92	0.0004701	2.86E-04
2R_13585501_SNP	-25.48	1.76E-07	7.11E-08	-13.63	0.0001133	7.38E-05	-11.85	0.000455	3.08E-04
X_16874742_SNP	-18.27	3.31E-07	1.79E-07	-10.11	8.89E-05	6.14E-05	-8.161	0.001034	7.93E-04
X_16874648_SNP	-20.02	1.73E-07	6.53E-07	-12.55	3.27E-05	9.26E-06	-7.48	0.001796	7.97E-03
2R_13586361_SNP	-22.04	6.75E-07	4.04E-07	-11.24	0.0005101	3.74E-04	-10.8	0.0003116	2.90E-04
2R_11968893_SNP	11.31	0.003096	1.76E-03	11.75	7.76E-07	4.79E-07	-0.4384	0.8649	8.58E-01
2R_11787259_SNP	-24.14	1.07E-06	4.94E-07	-12.85	0.0003185	2.09E-04	-11.29	0.000929	6.32E-04
2L_5380930_SNP	-21.58	1.47E-06	6.91E-07	-11.49	0.0003844	2.48E-04	-10.09	0.001034	7.29E-04
3L_3096877_SNP	17.53	0.001386	5.91E-04	1.94	0.6188	5.99E-01	15.59	5.57E-06	7.29E-07
2L_12224867_SNP	-23.75	2.22E-06	8.53E-07	-11.52	0.001545	1.04E-03	-12.24	0.0003292	1.87E-04
3L_9011102_SNP	8.975	0.04953	4.08E-02	-3.93	0.2268	1.98E-01	12.91	8.18E-07	8.71E-07
2L_12224769_SNP	-23.7	1.88E-06	8.99E-07	-11.5	0.00141	1.06E-03	-12.2	0.0003005	1.94E-04
3R_25904255_SNP	-21.34	3.17E-06	1.04E-06	-11.22	0.0005934	3.67E-04	-10.12	0.001226	7.22E-04
2R_9847609_SNP	-17.05	1.53E-05	8.22E-06	-12.02	8.58E-06	4.48E-06	-5.03	0.06728	5.90E-02
3R_15334723_SNP	-19.16	0.000214	1.35E-04	-16.13	2.61E-06	1.27E-06	-3.027	0.397	3.82E-01
X_21150049_SNP	-13.88	2.22E-06	1.31E-06	-7.439	0.0004197	3.10E-04	-6.444	0.001359	1.05E-03
2L_12224810_SNP	-23.51	8.14E-06	1.35E-06	-11.38	0.001802	1.29E-03	-12.13	0.000631	2.32E-04
2L_2620117_SNP	-21.64	1.67E-05	1.07E-05	-15.49	6.45E-06	3.98E-06	-6.152	0.07886	7.23E-02
2R_19510830_SNP	-21.64	1.67E-05	1.07E-05	-15.49	6.45E-06	3.98E-06	-6.152	0.07886	7.23E-02
X_5302467_SNP	-12.91	3.30E-06	1.50E-06	-6.049	0.002625	1.97E-03	-6.857	0.0002538	1.50E-04
3L_3097162_SNP	16.64	0.0007513	1.11E-03	1.587	0.6751	6.66E-01	15.06	1.06E-07	1.81E-06
3L_14120731_SNP	11.31	0.009445	9.14E-03	-1.248	0.6814	6.85E-01	12.56	6.29E-06	1.97E-06
3L_14120733_SNP	11.31	0.009445	9.14E-03	-1.248	0.6814	6.85E-01	12.56	6.29E-06	1.97E-06
X_7816116_SNP	11.22	0.01102	9.34E-03	-1.245	0.6904	6.84E-01	12.46	3.48E-06	2.09E-06
2R_9847602_SNP	-15.51	8.17E-05	6.60E-05	-12.33	4.51E-06	2.21E-06	-3.18	0.2334	2.37E-01
2R_9847745_SNP	-15.68	2.82E-05	1.58E-05	-11.13	1.25E-05	7.52E-06	-4.546	0.08033	7.14E-02
3R_9901916_SNP	-15.47	8.73E-06	2.58E-06	-8.728	0.0004317	1.97E-04	-6.747	0.004905	2.86E-03
2R_9845266_SNP	-15.68	2.78E-05	1.57E-05	-11.05	1.67E-05	9.01E-06	-4.634	0.07454	6.59E-02
2R_18478905_SNP	15	0.0004698	3.68E-04	2.654	0.3845	3.85E-01	12.35	5.56E-06	2.79E-06
2L_5385350_DEL	-18.98	5.55E-06	2.82E-06	-10.36	0.0005312	3.49E-04	-8.617	0.002562	1.90E-03
3L_10728936_SNP	13.24	0.00368	2.16E-03	0.782	0.8085	8.00E-01	12.45	6.87E-06	2.93E-06
2R_9844244_SNP	-15.56	2.77E-05	1.82E-05	-10.98	1.58E-05	1.01E-05	-4.578	0.07528	6.89E-02

ID	FemaleEff	FemalePval	FemaleMixe	MaleEff	MaleEffPval	MaleMixedI	DiffEff	DiffPval	DiffMixedPval
2R_9844257_SNP	-15.56	2.77E-05	1.82E-05	-10.98	1.58E-05	1.01E-05	-4.578	0.07528	6.89E-02
2R_9847417_SNP	-15.56	2.77E-05	1.82E-05	-10.98	1.58E-05	1.01E-05	-4.578	0.07528	6.89E-02
2R_20270560_SNP	15.87	0.002736	1.98E-03	1.099	0.7732	7.65E-01	14.77	5.83E-06	3.20E-06
3R_26732538_SNP	-22.38	7.75E-06	4.63E-06	-13.56	0.000105	8.18E-05	-8.829	0.0112	8.85E-03
X_20330162_SNP	-16.95	2.07E-05	9.75E-06	-11.01	7.21E-05	3.65E-05	-5.944	0.03094	2.49E-02
3R_27472609_SNP	-18.77	6.11E-06	3.76E-06	-9.852	0.0009372	7.16E-04	-8.913	0.001606	1.26E-03
3R_23498694_SNP	-14.11	6.32E-06	3.89E-06	-6.503	0.004153	3.38E-03	-7.604	0.0002873	2.09E-04
2R_9846441_SNP	-17.65	3.03E-05	1.81E-05	-12.11	2.77E-05	1.95E-05	-5.538	0.06197	5.19E-02
3R_12730125_SNP	-22.48	8.13E-06	4.22E-06	-12.78	0.0003632	2.33E-04	-9.699	0.004905	3.82E-03
3R_27472682_SNP	-18.66	7.87E-06	4.46E-06	-9.81	0.001093	7.69E-04	-8.854	0.001873	1.38E-03
3L_14121120_SNP	11.42	0.003797	2.57E-03	0.6751	0.8102	8.03E-01	10.74	1.01E-05	4.51E-06
3L_12534904_SNP	-13.23	0.003189	1.99E-03	-12.86	9.30E-06	4.63E-06	-0.3657	0.904	9.00E-01
3L_18118527_SNP	-22.4	2.00E-06	4.65E-06	-8.489	0.01037	1.81E-02	-13.91	3.09E-05	1.47E-05
2L_3525076_SNP	-18.49	1.09E-05	5.71E-06	-11.11	0.0001617	1.10E-04	-7.382	0.01063	8.56E-03
3L_5045493_SNP	12.18	0.01118	9.37E-03	-0.9515	0.7789	7.74E-01	13.13	9.33E-06	4.83E-06
2R_11972610_SNP	9.315	0.0184	1.51E-02	-1.382	0.6186	6.09E-01	10.7	9.20E-06	4.83E-06
2R_11972617_SNP	9.315	0.0184	1.51E-02	-1.382	0.6186	6.09E-01	10.7	9.20E-06	4.83E-06
2R_11972618_SNP	9.315	0.0184	1.51E-02	-1.382	0.6186	6.09E-01	10.7	9.20E-06	4.83E-06
2R_11919047_SNP	-16.41	7.96E-06	4.95E-06	-9.562	0.0002366	1.70E-04	-6.846	0.00671	5.57E-03
2L_12448459_SNP	-18.56	8.10E-06	5.04E-06	-8.822	0.003367	2.71E-03	-9.737	0.0005027	3.74E-04
3R_18753968_SNP	-18.68	0.0004572	2.18E-04	-15.41	4.14E-06	5.04E-06	-3.277	0.3695	3.45E-01
3R_12733078_SNP	-22.33	1.39E-05	5.11E-06	-12.86	0.0002658	2.12E-04	-9.471	0.006317	4.84E-03
2R_3801754_SNP	8.501	0.02877	2.12E-02	-1.743	0.5178	5.01E-01	10.24	7.81E-06	5.13E-06
2L_3524813_SNP	-18.42	1.40E-05	6.47E-06	-11.1	0.0001902	1.13E-04	-7.318	0.01198	9.26E-03
3R_12730124_SNP	-22.48	3.91E-05	5.29E-06	-12.52	0.0007603	3.69E-04	-9.962	0.009593	3.19E-03
3R_13940909_SNP	-15.77	3.58E-05	4.99E-05	-11.84	1.19E-05	7.04E-06	-3.93	0.1122	1.44E-01
3R_6180778_SNP	-15.05	3.40E-06	5.46E-06	-7.347	0.0006518	2.10E-03	-7.704	0.0009491	5.62E-04
3L_9870455_SNP	12.29	0.0135	8.88E-03	-0.8013	0.8194	8.10E-01	13.09	1.76E-05	5.58E-06
X_13736636_SNP	-18.47	4.52E-06	5.84E-06	-10.92	0.000197	1.49E-04	-7.552	0.006954	7.06E-03
2R_18481060_SNP	10.86	0.003311	2.66E-03	0.6989	0.7897	7.87E-01	10.17	9.57E-06	5.66E-06
3R_25512112_SNP	-20.07	9.98E-06	5.74E-06	-11.25	0.0003461	3.48E-04	-8.815	0.005056	3.59E-03
2R_19322816_SNP	14.97	0.0005021	3.73E-04	2.966	0.341	3.30E-01	12.01	9.22E-06	5.77E-06
2R_19322844_SNP	14.97	0.0005021	3.73E-04	2.966	0.341	3.30E-01	12.01	9.22E-06	5.77E-06

ID	FemaleEff	FemalePval	FemaleMixe	MaleEff	MaleEffPval	MaleMixedI	DiffEff	DiffPval	DiffMixedPval
2R_19322847_SNP	14.97	0.0005021	3.73E-04	2.966	0.341	3.30E-01	12.01	9.22E-06	5.77E-06
2L_11944516_SNP	-17.43	0.001233	6.65E-04	-15.39	1.37E-05	5.78E-06	-2.033	0.5755	5.61E-01
3L_2774293_SNP	-14.73	0.006006	4.32E-03	-15.27	1.07E-05	5.97E-06	0.5424	0.8807	8.76E-01
2R_15049013_SNP	14.76	0.00508	4.17E-03	0.3569	0.9244	9.23E-01	14.41	9.54E-06	5.98E-06
2L_968134_DEL	19.03	0.0002548	1.53E-04	4.622	0.2233	2.06E-01	14.41	1.31E-05	6.13E-06
2R_19016671_SNP	10.86	3.76E-05	2.44E-05	7.429	5.52E-05	2.81E-05	3.433	0.05824	5.33E-02
2L_8677115_SNP	14.68	0.006812	4.51E-03	0.271	0.9444	9.41E-01	14.41	6.70E-06	6.36E-06
2R_15317440_SNP	-12.01	1.99E-05	1.03E-05	-7.445	0.0001299	9.56E-05	-4.569	0.01905	1.48E-02
3L_10298614_SNP	14.34	0.002928	1.96E-03	1.352	0.696	6.84E-01	12.99	1.45E-05	6.45E-06
2L_3796856_SNP	15.07	0.005322	3.47E-03	0.6784	0.8576	8.54E-01	14.39	1.11E-05	6.51E-06
2L_19623111_SNP	-18.1	0.0002386	3.65E-04	-15.24	1.25E-05	6.85E-06	-2.86	0.375	4.11E-01
X_5487419_SNP	-17.17	1.32E-05	6.90E-06	-9.845	0.0004215	2.74E-04	-7.32	0.006686	5.13E-03
2L_19623108_SNP	-18.08	0.0002267	3.56E-04	-15.19	7.17E-06	6.97E-06	-2.894	0.3744	4.04E-01
2R_19511025_SNP	-18.46	7.07E-05	3.97E-05	-13.17	3.64E-05	1.83E-05	-5.29	0.0932	8.80E-02
2R_19511060_SNP	-18.46	7.07E-05	3.97E-05	-13.17	3.64E-05	1.83E-05	-5.29	0.0932	8.80E-02
3L_18051860_SNP	-22	7.35E-06	7.95E-06	-13.1	0.000451	1.62E-04	-8.901	0.004474	8.54E-03
3L_11389640_SNP	-16.21	1.61E-05	7.35E-06	-7.607	0.005116	3.60E-03	-8.599	0.0006492	3.93E-04
X_5681700_SNP	-12.21	0.00162	1.16E-03	-11.14	1.39E-05	7.37E-06	-1.068	0.6853	6.76E-01
X_8902132_SNP	-13.97	1.77E-05	1.14E-05	-8.618	0.0001589	1.12E-04	-5.354	0.0168	1.45E-02
3L_11934093_SNP	-19.9	1.73E-05	7.52E-06	-10.53	0.001254	9.17E-04	-9.365	0.00235	1.92E-03
2L_12224850_SNP	-15.6	2.69E-05	7.81E-06	-7.152	0.00577	4.63E-03	-8.444	0.0005928	2.99E-04
X_16874757_SNP	-14.59	1.53E-05	9.77E-06	-8.798	0.0002094	1.50E-04	-5.791	0.01248	1.06E-02
3R_15373339_SNP	-12.79	0.01125	6.45E-03	-13.67	1.89E-05	8.35E-06	0.8779	0.7882	7.81E-01
3L_15298262_SNP	13.52	0.004907	3.73E-03	0.6515	0.8457	8.45E-01	12.86	2.02E-05	8.47E-06
3L_5987846_DEL	-21.88	1.29E-05	8.57E-06	-12.59	0.000442	2.99E-04	-9.294	0.007514	5.77E-03
2L_19622968_SNP	-18.01	0.0002646	3.84E-04	-15.07	7.99E-06	8.66E-06	-2.937	0.372	3.98E-01
2R_19500928_SNP	-19.74	1.86E-05	8.69E-06	-11.19	0.0005851	3.79E-04	-8.551	0.006759	4.83E-03
3R_10901804_SNP	-16.14	2.71E-05	8.82E-06	-5.871	0.03743	2.75E-02	-10.27	4.47E-05	1.49E-05
2R_17652665_SNP	-15.32	0.003844	2.88E-03	-15.02	1.47E-05	8.92E-06	-0.3024	0.9327	9.31E-01
2L_10458705_SNP	13.28	0.007229	4.46E-03	0.4401	0.8991	8.95E-01	12.84	1.92E-05	9.03E-06
2R_13589140_SNP	-18.21	2.76E-05	9.21E-06	-10	0.001071	6.20E-04	-8.205	0.005549	3.35E-03
2L_22308859_SNP	15.43	0.0002267	9.43E-05	4.244	0.1461	1.40E-01	11.19	6.61E-05	9.29E-06
3L_11934457_SNP	-19.67	1.73E-05	9.29E-06	-10.63	0.0008851	7.76E-04	-9.039	0.003203	2.75E-03

ID	FemaleEff	FemalePval	FemaleMixe	MaleEff	MaleEffPval	MaleMixedI	DiffEff	DiffPval	DiffMixedPval
2R_14549280_SNP	-21.8	2.19E-05	9.42E-06	-11.45	0.001658	1.13E-03	-10.35	0.003212	1.94E-03
X_13736629_SNP	-18.03	1.63E-05	1.04E-05	-10.74	0.0002677	1.94E-04	-7.29	0.01108	9.39E-03
2L_12153562_SNP	11.64	1.57E-05	9.48E-06	5.95	0.002265	1.59E-03	5.691	0.001629	1.37E-03
2R_19116550_INS	-21.23	4.18E-05	1.76E-05	-13.38	0.0002001	1.06E-04	-7.85	0.02806	2.09E-02
3L_16408661_SNP	-15.99	6.36E-06	1.07E-05	-5.82	0.01794	2.86E-02	-10.17	4.23E-05	1.82E-05
2R_3188182_SNP	10.42	0.008937	1.03E-02	-0.4418	0.882	8.78E-01	10.86	7.46E-07	1.49E-05
X_9161929_INS	14.47	0.003797	5.35E-03	1.213	0.7427	7.43E-01	13.25	6.42E-06	4.65E-05

TABLE 5: Trial 1 - Location of genetic variants (Climbing Behavior)	
ID	**GeneAnnotation**
3R_25904206_SNP	SiteClass[FBgn0015542|sima|INTRON|0],TranscriptAnnot[INTRON(MODIFIER||||1507|sima|protein_coding|CODING|FBtr0085565|6);INTRON(MODIFIER||||426|sima|protein_
2R_13585501_SNP	SiteClass[FBgn0027872|rdgBbeta|SYNONYMOUS_CODING|0],TranscriptAnnot[SYNONYMOUS_CODING(LOW|SILENT|atT/atC|I63|273|rdgBbeta|protein_coding|CODING|FBtr00
X_16874742_SNP	SiteClass[FBgn0030810|CG9059|INTRON|0],TranscriptAnnot[INTRON(MODIFIER||||1082|CG9059|protein_coding|CODING|FBtr0330412|2);INTRON(MODIFIER||||1098|CG905
X_16874648_SNP	SiteClass[FBgn0030810|CG9059|INTRON|0],TranscriptAnnot[INTRON(MODIFIER||||1082|CG9059|protein_coding|CODING|FBtr0330412|2);INTRON(MODIFIER||||1098|CG905
2R_13586361_SNP	SiteClass[FBgn0045800|Uhg1|UPSTREAM|241;FBgn0063381|snoRNA:Me28S-G3081a|UPSTREAM|352;FBgn0027872|rdgBbeta|UPSTREAM|495;FBgn0063385|snoRNA:Me28S-A
2R_11968893_SNP	SiteClass[FBgn0034072|Dg|DOWNSTREAM|279],TranscriptAnnot[DOWNSTREAM(MODIFIER||||1179|Dg|protein_coding|CODING|FBtr0087258|);DOWNSTREAM(MODIFIER|||
2R_11787259_SNP	SiteClass[FBgn0264089|sli|INTRON|0],TranscriptAnnot[INTRON(MODIFIER||||1469|sli|protein_coding|CODING|FBtr0330730|2);INTRON(MODIFIER||||1480|sli|protein_coding
2L_5380930_SNP	SiteClass[FBgn0262097|CG42850|SYNONYMOUS_CODING|0],TranscriptAnnot[SYNONYMOUS_CODING(LOW|SILENT|Ttg/Ctg|L13|274|CG42850|protein_coding|CODING|FBtr03
3L_3096877_SNP	SiteClass[FBgn0035398|Cht7|INTRON|0;FBgn0052272|tRNA:CR32272|DOWNSTREAM|14;FBgn0052285|tRNA:CR32285|DOWNSTREAM|201;FBgn0052287|tRNA:CR32287|DOW
2L_12224867_SNP	SiteClass[FBgn0000114|aret|INTRON|0],TranscriptAnnot[INTRON(MODIFIER||||573|aret|protein_coding|CODING|FBtr0331646|1);INTRON(MODIFIER||||573|aret|protein_co
3L_9011102_SNP	SiteClass[FBgn0035956|Doc2|NON_SYNONYMOUS_CODING|0],TranscriptAnnot[NON_SYNONYMOUS_CODING(MODERATE|MISSENSE|Acc/Gcc|T59A|469|Doc2|protein_coding
2L_12224769_SNP	SiteClass[FBgn0000114|aret|INTRON|0],TranscriptAnnot[INTRON(MODIFIER||||573|aret|protein_coding|CODING|FBtr0331646|1);INTRON(MODIFIER||||573|aret|protein_co
3R_25904255_SNP	SiteClass[FBgn0015542|sima|INTRON|0],TranscriptAnnot[INTRON(MODIFIER||||1507|sima|protein_coding|CODING|FBtr0085565|6);INTRON(MODIFIER||||426|sima|protein_
2R_9847609_SNP	SiteClass[FBgn0033886|CG13349|START_GAINED|0;FBgn0013770|Cp1|UPSTREAM|555],TranscriptAnnot[START_GAINED(LOW||||389|CG13349|protein_coding|CODING|FBtr0
3R_15334723_SNP	SiteClass[FBgn0260003|Dys|INTRON|0],TranscriptAnnot[INTRON(MODIFIER||||1323|Dys|protein_coding|CODING|FBtr0334565|10);INTRON(MODIFIER||||1669|Dys|protein_
X_21150049_SNP	SiteClass[FBgn0052521|CG32521|INTRON|0],TranscriptAnnot[INTRON(MODIFIER||||230|CG32521|protein_coding|CODING|FBtr0331813|2);INTRON(MODIFIER||||233|CG325
2L_12224810_SNP	SiteClass[FBgn0000114|aret|INTRON|0],TranscriptAnnot[INTRON(MODIFIER||||573|aret|protein_coding|CODING|FBtr0331646|1);INTRON(MODIFIER||||573|aret|protein_co
2L_2620117_SNP	SiteClass[FBgn0263322|CG43403|UPSTREAM|70],TranscriptAnnot[INTERGENIC(MODIFIER|||||||||);UPSTREAM(MODIFIER||||42|CG43403|protein_coding|CODING|FBtr03087
2R_19510830_SNP	SiteClass[||||],TranscriptAnnot[INTERGENIC(MODIFIER|||||||||)]
X_5302467_SNP	SiteClass[FBgn0029762|NAAT1|INTRON|0],TranscriptAnnot[INTRON(MODIFIER||||641|NAAT1|protein_coding|CODING|FBtr0070797|1)]
3L_3097162_SNP	SiteClass[FBgn0035398|Cht7|INTRON|0;FBgn0052272|tRNA:CR32272|UPSTREAM|199;FBgn0052286|tRNA:CR32286|UPSTREAM|357;FBgn0052285|tRNA:CR32285|DOWNSTRE
3L_14120731_SNP	SiteClass[FBgn0042630|Sox21b|INTRON|0],TranscriptAnnot[INTRON(MODIFIER||||571|Sox21b|protein_coding|CODING|FBtr0075747|1);INTRON(MODIFIER||||571|Sox21b|p
3L_14120733_SNP	SiteClass[FBgn0042630|Sox21b|INTRON|0],TranscriptAnnot[INTRON(MODIFIER||||571|Sox21b|protein_coding|CODING|FBtr0075747|1);INTRON(MODIFIER||||571|Sox21b|p
X_7816116_SNP	SiteClass[FBgn0029979|CG10777|DOWNSTREAM|75;FBgn0260858|Ykt6|DOWNSTREAM|117],TranscriptAnnot[DOWNSTREAM(MODIFIER||||199|Ykt6|protein_coding|CODING
2R_9847602_SNP	SiteClass[FBgn0033886|CG13349|UTR_5_PRIME|0;FBgn0013770|Cp1|UPSTREAM|562],TranscriptAnnot[UPSTREAM(MODIFIER||||341|Cp1|protein_coding|CODING|FBtr00875
2R_9847745_SNP	SiteClass[FBgn0033886|CG13349|INTRON|0;FBgn0013770|Cp1|UPSTREAM|419],TranscriptAnnot[INTRON(MODIFIER||||389|CG13349|protein_coding|CODING|FBtr0087610|1
3R_9901916_SNP	SiteClass[FBgn0038197|foxo|INTRON|0],TranscriptAnnot[INTRON(MODIFIER||||613|foxo|protein_coding|CODING|FBtr0082886|4);INTRON(MODIFIER||||613|foxo|protein_co
2R_9845266_SNP	SiteClass[FBgn0262739|AGO1|INTRON|0;FBgn0033886|CG13349|DOWNSTREAM|767],TranscriptAnnot[DOWNSTREAM(MODIFIER||||389|CG13349|protein_coding|CODING|F
2R_18478905_SNP	SiteClass[FBgn0260866|dnr1|INTRON|0],TranscriptAnnot[INTRON(MODIFIER||||676|dnr1|protein_coding|CODING|FBtr0071837|1);INTRON(MODIFIER||||696|dnr1|protein_c
2L_5385350_DEL	SiteClass[||||],TranscriptAnnot[INTERGENIC(MODIFIER|||||||||)]
3L_10728936_SNP	SiteClass[||||],TranscriptAnnot[INTERGENIC(MODIFIER|||||||||)]
2R_9844244_SNP	SiteClass[FBgn0262739|AGO1|INTRON|0],TranscriptAnnot[INTRON(MODIFIER||||984|AGO1|protein_coding|CODING|FBtr0087612|2);INTRON(MODIFIER||||984|AGO1|protei

ID	GeneAnnotation
2R_9844257_SNP	SiteClass[FBgn0262739|AGO1|INTRON|0],TranscriptAnnot[INTRON(MODIFIER|||984|AGO1|protein_coding|CODING|FBtr0087612|2);INTRON(MODIFIER|||984|AGO1|prote
2R_9847417_SNP	SiteClass[FBgn0033886|CG13349|SYNONYMOUS_CODING|0;FBgn0013770|Cp1|UPSTREAM|747],TranscriptAnnot[SYNONYMOUS_CODING(LOW|SILENT|acC/acG|T59|389|CG1
2R_20270560_SNP	SiteClass[FBgn0000037|mAcR-60C|INTRON|0],TranscriptAnnot[INTRON(MODIFIER|||788|mAcR-60C|protein_coding|CODING|FBtr0072367|4);INTRON(MODIFIER|||805|mA
3R_26732538_SNP	SiteClass[|||],TranscriptAnnot[INTERGENIC(MODIFIER||||||||)]
X_20330162_SNP	SiteClass[FBgn0052506|CG32506|INTRON|0],TranscriptAnnot[INTRON(MODIFIER|||1155|CG32506|protein_coding|CODING|FBtr0307539|1)]
3R_27472609_SNP	SiteClass[FBgn0039862|kek6|INTRON|0],TranscriptAnnot[INTRON(MODIFIER|||836|kek6|protein_coding|CODING|FBtr0085821|2);INTRON(MODIFIER|||843|kek6|protein_c
3R_23498694_SNP	SiteClass[FBgn0039536|CG18437|SYNONYMOUS_CODING|0],TranscriptAnnot[SYNONYMOUS_CODING(LOW|SILENT|ttC/ttT|F2183|3284|CG18437|protein_coding|CODING|FBt
2R_9846441_SNP	SiteClass[FBgn0033886|CG13349|SYNONYMOUS_CODING|0;FBgn0262739|AGO1|UPSTREAM|847],TranscriptAnnot[SYNONYMOUS_CODING(LOW|SILENT|tcC/tcT|S293|389|CG
3R_12730125_SNP	SiteClass[FBgn0264857|iab-8|INTRON|0],TranscriptAnnot[INTRON(MODIFIER||||iab-8|ncRNA|NON_CODING|FBtr0306340|1);INTRON(MODIFIER||||iab-8|ncRNA|NON_COD
3R_27472682_SNP	SiteClass[FBgn0039862|kek6|INTRON|0],TranscriptAnnot[INTRON(MODIFIER|||836|kek6|protein_coding|CODING|FBtr0085821|2);INTRON(MODIFIER|||843|kek6|protein_c
3L_14121120_SNP	SiteClass[FBgn0042630|Sox21b|INTRON|0],TranscriptAnnot[INTRON(MODIFIER|||571|Sox21b|protein_coding|CODING|FBtr0075747|1);INTRON(MODIFIER|||571|Sox21b|p
3L_12534904_SNP	SiteClass[FBgn0263587|CR43612|EXON|0;FBgn0036302|sowah|INTRON|0],TranscriptAnnot[EXON(MODIFIER||||CR43612|ncRNA|NON_CODING|FBtr0309823|1);INTRON(MO
3L_18118527_SNP	SiteClass[|||],TranscriptAnnot[INTERGENIC(MODIFIER||||||||)]
2L_3525076_SNP	SiteClass[FBgn0031548|CG8852|UPSTREAM|55],TranscriptAnnot[INTERGENIC(MODIFIER||||||||);UPSTREAM(MODIFIER|||663|CG8852|protein_coding|CODING|FBtr00899
3L_5045493_SNP	SiteClass[FBgn0005775|Con|INTRON|0],TranscriptAnnot[INTRON(MODIFIER|||691|Con|protein_coding|CODING|FBtr0309972|2)]
2R_11972610_SNP	SiteClass[FBgn0034072|Dg|INTRON|0],TranscriptAnnot[INTRON(MODIFIER|||1179|Dg|protein_coding|CODING|FBtr0087258|10);INTRON(MODIFIER|||1262|Dg|protein_coc
2R_11972617_SNP	SiteClass[FBgn0034072|Dg|INTRON|0],TranscriptAnnot[INTRON(MODIFIER|||1179|Dg|protein_coding|CODING|FBtr0087258|10);INTRON(MODIFIER|||1262|Dg|protein_coc
2R_11972618_SNP	SiteClass[FBgn0034072|Dg|INTRON|0],TranscriptAnnot[INTRON(MODIFIER|||1179|Dg|protein_coding|CODING|FBtr0087258|10);INTRON(MODIFIER|||1262|Dg|protein_coc
2R_11919047_SNP	SiteClass[FBgn0034070|SP2353|UPSTREAM|418],TranscriptAnnot[INTERGENIC(MODIFIER||||||||);UPSTREAM(MODIFIER|||1361|SP2353|protein_coding|CODING|FBtr0087
2L_12448459_SNP	SiteClass[FBgn0032435|Oatp33Eb|UPSTREAM|25;FBgn0032434|CG5421|UPSTREAM|327],TranscriptAnnot[INTERGENIC(MODIFIER||||||||);UPSTREAM(MODIFIER|||426|CG
3R_18753968_SNP	SiteClass[FBgn0017590|klg|INTRON|0],TranscriptAnnot[INTRON(MODIFIER|||545|klg|protein_coding|CODING|FBtr0084337|2)]
3R_12733078_SNP	SiteClass[FBgn0264857|iab-8|INTRON|0],TranscriptAnnot[INTRON(MODIFIER||||iab-8|ncRNA|NON_CODING|FBtr0306340|1);INTRON(MODIFIER||||iab-8|ncRNA|NON_COD
2R_3801754_SNP	SiteClass[FBgn0050377|CG30377|INTRON|0;FBgn0033232|CG12159|DOWNSTREAM|778],TranscriptAnnot[DOWNSTREAM(MODIFIER|||197|CG12159|protein_coding|CODIN
2L_3524813_SNP	SiteClass[FBgn0031548|CG8852|UPSTREAM|318;FBgn0031547|Sr-CIV|UPSTREAM|757],TranscriptAnnot[INTERGENIC(MODIFIER||||||||);UPSTREAM(MODIFIER|||406|Sr-CIV
3R_12730124_SNP	SiteClass[FBgn0264857|iab-8|INTRON|0],TranscriptAnnot[INTRON(MODIFIER||||iab-8|ncRNA|NON_CODING|FBtr0306340|1);INTRON(MODIFIER||||iab-8|ncRNA|NON_COD
3R_13940909_SNP	SiteClass[FBgn0003499|sr|INTRON|0],TranscriptAnnot[INTRON(MODIFIER|||1186|sr|protein_coding|CODING|FBtr0083542|3);INTRON(MODIFIER|||1271|sr|protein_coding
3R_6180778_SNP	SiteClass[FBgn0015396|jumu|INTRON|0],TranscriptAnnot[INTRON(MODIFIER|||719|jumu|protein_coding|CODING|FBtr0082237|1)]
3L_9870455_SNP	SiteClass[|||],TranscriptAnnot[INTERGENIC(MODIFIER||||||||)]
X_13736636_SNP	SiteClass[FBgn0052626|CG32626|INTRON|0],TranscriptAnnot[INTRON(MODIFIER|||258|CG32626|protein_coding|CODING|FBtr0309245|1);INTRON(MODIFIER|||771|CG326
2R_18481060_SNP	SiteClass[FBgn0260866|dnr1|UPSTREAM|587],TranscriptAnnot[INTERGENIC(MODIFIER||||||||);UPSTREAM(MODIFIER|||676|dnr1|protein_coding|CODING|FBtr0071837|);U
3R_25512112_SNP	SiteClass[FBgn0039682|Obp99c|INTRON|0;FBgn0013972|Gycalpha99B|DOWNSTREAM|632],TranscriptAnnot[DOWNSTREAM(MODIFIER|||676|Gycalpha99B|protein_coding|C
2R_19322816_SNP	SiteClass[|||],TranscriptAnnot[INTERGENIC(MODIFIER||||||||)]
2R_19322844_SNP	SiteClass[|||],TranscriptAnnot[INTERGENIC(MODIFIER||||||||)]

ID	GeneAnnotation
2R_19322847_SNP	SiteClass[||||],TranscriptAnnot[INTERGENIC(MODIFIER|||||||||)]
2L_11944516_SNP	SiteClass[FBgn0005664|Cry|INTRON|0],TranscriptAnnot[INTRON(MODIFIER||||477|Cry|protein_coding|CODING|FBtr0080281|1)]
3L_2774293_SNP	SiteClass[FBgn0044452|Atg2|UPSTREAM|45;FBgn0035372|CG12093|UPSTREAM|286],TranscriptAnnot[INTERGENIC(MODIFIER|||||||||);UPSTREAM(MODIFIER|||1906|Atg2|
2R_15049013_SNP	SiteClass[FBgn0000578|ena|SYNONYMOUS_CODING|0],TranscriptAnnot[SYNONYMOUS_CODING(LOW|SILENT|tcC/tcT|S647|684|ena|protein_coding|CODING|FBtr0086582|);S
2L_968134_DEL	SiteClass[||||],TranscriptAnnot[INTERGENIC(MODIFIER|||||||||)]
2R_19016671_SNP	SiteClass[FBgn0034825|CG3215|SYNONYMOUS_CODING|0],TranscriptAnnot[SYNONYMOUS_CODING(LOW|SILENT|tcC/tcG|S255|358|CG3215|protein_coding|CODING|FBtr007
2L_8677115_SNP	SiteClass[FBgn0032057|CG9287|SYNONYMOUS_CODING|0;FBgn0001114|Glt|DOWNSTREAM|311],TranscriptAnnot[DOWNSTREAM(MODIFIER||||1026|Glt|protein_coding|COI
2R_15317440_SNP	SiteClass[FBgn0020440|Fak|DOWNSTREAM|724;FBgn0012051|CalpA|DOWNSTREAM|885],TranscriptAnnot[DOWNSTREAM(MODIFIER||||1198|Fak|protein_coding|CODING|F
3L_10298614_SNP	SiteClass[||||],TranscriptAnnot[INTERGENIC(MODIFIER|||||||||)]
2L_3796856_SNP	SiteClass[FBgn0031571|CG3921|SYNONYMOUS_CODING|0],TranscriptAnnot[SYNONYMOUS_CODING(LOW|SILENT|acA/acT|T1562|3115|CG3921|protein_coding|CODING|FBtr
2L_19623111_SNP	SiteClass[FBgn0000464|Lar|INTRON|0],TranscriptAnnot[INTRON(MODIFIER||||1912|Lar|protein_coding|CODING|FBtr0305950|1);INTRON(MODIFIER|||1927|Lar|protein_coo
X_5487419_SNP	SiteClass[FBgn0263511|Vsx1|UPSTREAM|887],TranscriptAnnot[INTERGENIC(MODIFIER|||||||||);UPSTREAM(MODIFIER||||837|Vsx1|protein_coding|CODING|FBtr0070781|)]
2L_19623108_SNP	SiteClass[FBgn0000464|Lar|INTRON|0],TranscriptAnnot[INTRON(MODIFIER||||1912|Lar|protein_coding|CODING|FBtr0305950|1);INTRON(MODIFIER|||1927|Lar|protein_coo
2R_19511025_SNP	SiteClass[||||],TranscriptAnnot[INTERGENIC(MODIFIER|||||||||)]
2R_19511060_SNP	SiteClass[||||],TranscriptAnnot[INTERGENIC(MODIFIER|||||||||)]
3L_18051860_SNP	SiteClass[FBgn0000568|Eip75B|SYNONYMOUS_CODING|0],TranscriptAnnot[SYNONYMOUS_CODING(LOW|SILENT|ccA/ccG|P275|1412|Eip75B|protein_coding|CODING|FBtr007
3L_11389640_SNP	SiteClass[FBgn0036156|CG11726|DOWNSTREAM|867],TranscriptAnnot[DOWNSTREAM(MODIFIER||||291|CG11726|protein_coding|CODING|FBtr0076172|);INTERGENIC(MOD
X_5681700_SNP	SiteClass[FBgn0261610|CG42699|SYNONYMOUS_CODING|0],TranscriptAnnot[SYNONYMOUS_CODING(LOW|SILENT|gcT/gcC|A750|897|CG42699|protein_coding|CODING|FBtr
X_8902132_SNP	SiteClass[FBgn0264384|CR43836|INTRON|0;FBgn0261549|rdgA|INTRON|0],TranscriptAnnot[INTRON(MODIFIER||||1009|rdgA|protein_coding|CODING|FBtr0302663|3);INTRO
3L_11934093_SNP	SiteClass[||||],TranscriptAnnot[INTERGENIC(MODIFIER|||||||||)]
2L_12224850_SNP	SiteClass[FBgn0000114|aret|INTRON|0],TranscriptAnnot[INTRON(MODIFIER|||573|aret|protein_coding|CODING|FBtr0331646|1);INTRON(MODIFIER|||573|aret|protein_co
X_16874757_SNP	SiteClass[FBgn0030810|CG9059|INTRON|0],TranscriptAnnot[INTRON(MODIFIER|||1082|CG9059|protein_coding|CODING|FBtr0330412|2);INTRON(MODIFIER|||1098|CG905
3R_15373339_SNP	SiteClass[FBgn0260003|Dys|INTRON|0],TranscriptAnnot[INTRON(MODIFIER|||1323|Dys|protein_coding|CODING|FBtr0334565|10);INTRON(MODIFIER|||1669|Dys|protein_
3L_15298262_SNP	SiteClass[FBgn0036493|CG7255|INTRON|0],TranscriptAnnot[INTRON(MODIFIER|||1063|CG7255|protein_coding|CODING|FBtr0100360|1);INTRON(MODIFIER|||607|CG7255
3L_5987846_DEL	SiteClass[||||],TranscriptAnnot[INTERGENIC(MODIFIER|||||||||)]
2L_19622968_SNP	SiteClass[FBgn0000464|Lar|INTRON|0],TranscriptAnnot[INTRON(MODIFIER||||1912|Lar|protein_coding|CODING|FBtr0305950|1);INTRON(MODIFIER|||1927|Lar|protein_coo
2R_19500928_SNP	SiteClass[FBgn0034885|CG4019|INTRON|0;FBgn0034883|CG17664|INTRON|0],TranscriptAnnot[INTRON(MODIFIER||||249|CG4019|protein_coding|CODING|FBtr0072102|1);I
3R_10901804_SNP	SiteClass[FBgn0038282|dpr9|INTRON|0],TranscriptAnnot[INTRON(MODIFIER|||602|dpr9|protein_coding|CODING|FBtr0089376|2)]
2R_17652665_SNP	SiteClass[FBgn0264716|CR43984|EXON|0;FBgn0050395|CG30395|UPSTREAM|329;FBgn0264714|CG43982|DOWNSTREAM|465],TranscriptAnnot[DOWNSTREAM(MODIFIER|||
2L_10458705_SNP	SiteClass[FBgn0027611|LM408|SYNONYMOUS_CODING|0],TranscriptAnnot[SYNONYMOUS_CODING(LOW|SILENT|gtA/gtT|V123|1080|LM408|protein_coding|CODING|FBtr008
2R_13589140_SNP	SiteClass[FBgn0045800|Uhg1|EXON|0;FBgn0063374|snoRNA:snR38:54Eb|UPSTREAM|54;FBgn0063375|snoRNA:Me28S-G3277a|DOWNSTREAM|112;FBgn0063380|snoRNA:U3
2L_22308859_SNP	SiteClass[FBgn0039972|CG17018|INTRON|0],TranscriptAnnot[INTRON(MODIFIER|||1272|CG17018|protein_coding|CODING|FBtr0306235|1)]
3L_11934457_SNP	SiteClass[FBgn0036224|Rpt4R|UPSTREAM|666],TranscriptAnnot[INTERGENIC(MODIFIER|||||||||);UPSTREAM(MODIFIER||||398|Rpt4R|protein_coding|CODING|FBtr0076040

ID	GeneAnnotation
2R_14549280_SNP	SiteClass[FBgn0259202|CG42306|UPSTREAM|227;FBgn0034372|Gint3|UPSTREAM|227],TranscriptAnnot[INTERGENIC(MODIFIER||||||||);UPSTREAM(MODIFIER||||121|CG42
X_13736629_SNP	SiteClass[FBgn0052626|CG32626|INTRON|0],TranscriptAnnot[INTRON(MODIFIER|||258|CG32626|protein_coding|CODING|FBtr0309245|1);INTRON(MODIFIER|||771|CG326
2L_12153562_SNP	SiteClass[FBgn0051760|CG31760|NON_SYNONYMOUS_CODING|0],TranscriptAnnot[NON_SYNONYMOUS_CODING(MODERATE|MISSENSE|aGg/aAg|R12K|1093|CG31760|prote
2R_19116550_INS	SiteClass[||||],TranscriptAnnot[INTERGENIC(MODIFIER|||||||||)]
3L_16408661_SNP	SiteClass[FBgn0036629|CG4573|NON_SYNONYMOUS_CODING|0;FBgn0028399|TMS1|DOWNSTREAM|175],TranscriptAnnot[DOWNSTREAM(MODIFIER||||456|TMS1|protein_c
2R_3188182_SNP	SiteClass[FBgn0003174|pwn|UTR_3_PRIME|0],TranscriptAnnot[UTR_3_PRIME(MODIFIER||||1343|pwn|protein_coding|CODING|FBtr0332462|11);UTR_3_PRIME(MODIFIER|||
X_9161929_INS	SiteClass[FBgn0052703|Erk7|UPSTREAM|199;FBgn0030120|CG17440|DOWNSTREAM|541],TranscriptAnnot[DOWNSTREAM(MODIFIER||||366|CG17440|protein_coding|CODIN

TABLE 6: Trial 2 - Alleles and P values (Eclosion)									
ID	MinorAllele	MajorAllele	RefAllele	MAF	MinorAlleleCount	MajorAlleleCount	SingleEff	SinglePval	SingleMixedPval
2L_12053257_SNP	G	C	C	0.07843	4	47	-6.269	1.52E-06	8.21E-07
2L_12053266_SNP	A	T	T	0.07843	4	47	-6.269	1.52E-06	8.21E-07
3L_14340149_SNP	T	C	C	0.1837	9	40	-4.221	6.83E-06	3.75E-06
3L_1482470_SNP	G	A	A	0.2	10	40	-3.991	9.45E-06	5.43E-06
X_14799722_SNP	G	A	A	0.1224	6	43	-4.912	1.21E-05	5.64E-06
2L_9398110_SNP	G	C	G	0.1333	6	39	-4.932	1.63E-05	5.95E-06
X_10069295_SNP	G	T	T	0.16	8	42	-4.337	1.19E-05	6.00E-06
2L_19648347_SNP	C	A	A	0.08333	4	44	-5.854	1.65E-05	6.52E-06
3L_3383767_SNP	T	C	C	0.1176	6	45	-4.868	1.11E-05	6.64E-06
X_14258152_SNP	A	T	T	0.3469	17	32	-3.359	1.34E-05	6.79E-06
2L_5752523_SNP	A	G	G	0.44	22	28	3.175	1.31E-05	7.56E-06
3L_15739434_SNP	A	C	C	0.2708	13	35	-3.618	1.65E-05	7.68E-06
2L_15929838_SNP	T	G	G	0.2292	11	37	-3.823	2.26E-05	7.76E-06
3R_3047908_SNP	A	G	A	0.1064	5	42	-5.259	1.89E-05	8.06E-06
3L_7865995_SNP	A	G	G	0.2	10	40	-3.928	1.63E-05	8.18E-06
X_14258114_SNP	T	A	A	0.3542	17	31	-3.348	1.91E-05	8.52E-06
X_5521084_SNP	T	A	A	0.1	5	45	-5.212	1.06E-05	9.24E-06
X_14332970_DEL	C	CC	CC	0.1	5	45	-5.21	1.32E-05	9.36E-06
3L_18214345_SNP	T	G	G	0.102	5	44	-5.081	4.02E-06	1.76E-05

TABLE 7: Trial 2 - Location of genetic variants (Eclosion)					
ID	**GeneAnnotation**				
2L_12053257_SNP	SiteClass[FBgn0028425|JhI-21|INTRON|0],TranscriptAnnot[INTRON(MODIFIER|||500|JhI-21|protein_coding|CODING|FBtr0089655|				
2L_12053266_SNP	SiteClass[FBgn0028425|JhI-21|INTRON|0],TranscriptAnnot[INTRON(MODIFIER|||500|JhI-21|protein_coding|CODING|FBtr0089655|				
3L_14340149_SNP	SiteClass[FBgn0001085|fz|INTRON|0],TranscriptAnnot[INTRON(MODIFIER|||581|fz|protein_coding|CODING|FBtr0075743|4);INTR(				
3L_1482470_SNP	SiteClass[FBgn0020248|stet|INTRON|0],TranscriptAnnot[INTRON(MODIFIER|||485|stet|protein_coding|CODING|FBtr0072712|5)]				
X_14799722_SNP	SiteClass[FBgn0264078|Flo-2|INTRON|0;FBgn0030593|CG9512|UPSTREAM|148;FBgn0030594|CG9509|DOWNSTREAM|645],Transcr				
2L_9398110_SNP	SiteClass[FBgn0085395|Shawl|INTRON|0;FBgn0032115|CG4438|UPSTREAM|122],TranscriptAnnot[INTRON(MODIFIER|||835|Shawl				
X_10069295_SNP	SiteClass[FBgn0264503|CG43902|INTRON|0],TranscriptAnnot[INTRON(MODIFIER|||1220|CG43902|protein_coding|CODING|FBtr03				
2L_19648347_SNP	SiteClass[FBgn0000464|Lar|INTRON|0],TranscriptAnnot[INTRON(MODIFIER|||1912|Lar|protein_coding|CODING|FBtr0305950|4);IN				
3L_3383767_SNP	SiteClass[|||],TranscriptAnnot[INTERGENIC(MODIFIER|||||||||)]				
X_14258152_SNP	SiteClass[FBgn0052600|dpr8|INTRON|0],TranscriptAnnot[INTRON(MODIFIER|||344|dpr8|protein_coding|CODING|FBtr0073913|3)				
2L_5752523_SNP	SiteClass[FBgn0031736|CG11030|INTRON|0],TranscriptAnnot[INTRON(MODIFIER|||332|CG11030|protein_coding|CODING|FBtr007				
3L_15739434_SNP	SiteClass[|||],TranscriptAnnot[INTERGENIC(MODIFIER|||||||||)]				
2L_15929838_SNP	SiteClass[FBgn0028645|beat-Ib|INTRON|0],TranscriptAnnot[INTRON(MODIFIER|||327|beat-Ib|protein_coding|CODING|FBtr00808(				
3R_3047908_SNP	SiteClass[|||],TranscriptAnnot[INTERGENIC(MODIFIER|||||||||)]				
3L_7865995_SNP	SiteClass[FBgn0052365|CG32365|INTRON|0],TranscriptAnnot[INTRON(MODIFIER|||628|CG32365|protein_coding|CODING|FBtr007				
X_14258114_SNP	SiteClass[FBgn0052600|dpr8|INTRON|0],TranscriptAnnot[INTRON(MODIFIER|||344|dpr8|protein_coding|CODING|FBtr0073913|3)				
X_5521084_SNP	SiteClass[FBgn0259994|CG42492|DOWNSTREAM|618],TranscriptAnnot[DOWNSTREAM(MODIFIER|||916|CG42492|protein_coding|				
X_14332970_DEL	SiteClass[FBgn0052600|dpr8|INTRON|0],TranscriptAnnot[INTRON(MODIFIER|||344|dpr8|protein_coding|CODING|FBtr0073913|6)				
3L_18214345_SNP	SiteClass[|||],TranscriptAnnot[INTERGENIC(MODIFIER|||||||||)]				

TABLE 8: Trial 3 - Alleles and P values (Eclosion)									
ID	MinorAllele	MajorAllele	RefAllele	MAF	MinorAlleleCount	MajorAlleleCount	SingleEff	SinglePval	SingleMixedPval
3R_9896811_SNP	G	T	T	0.08654	9	95	-12.92	2.38E-07	1.08E-07
2R_17797291_SNP	T	A	A	0.05607	6	101	-15.29	3.64E-07	1.96E-07
X_4243970_SNP	T	C	C	0.07619	8	97	-13.1	5.57E-07	3.83E-07
3R_23238151_DEL	T	TC	TC	0.09174	10	99	-11.74	6.44E-07	4.64E-07
X_11846986_SNP	G	C	C	0.05051	5	94	-15.95	1.47E-06	7.67E-07
3R_10953680_SNP	T	G	T	0.05607	6	101	-14.53	1.24E-06	8.89E-07
3L_4775891_SNP	T	C	C	0.1273	14	96	-9.839	1.46E-06	1.03E-06
2R_14554814_SNP	A	T	T	0.07619	8	97	-12.44	3.41E-06	1.63E-06
2R_13532533_SNP	A	C	C	0.05714	6	99	-14.21	3.52E-06	1.66E-06
2R_13532534_DEL	T	TTAATAACTAC	TTAATAACTA	0.05714	6	99	-14.21	3.52E-06	1.66E-06
3L_20389146_SNP	T	A	A	0.09346	10	97	-11.11	3.47E-06	2.19E-06
2R_17796799_SNP	A	T	T	0.181	19	86	-8.451	3.57E-06	2.37E-06
2R_13532562_SNP	T	G	G	0.05505	6	103	-14	3.35E-06	2.38E-06
X_18724627_SNP	T	C	C	0.05455	6	104	-13.96	3.48E-06	2.53E-06
3R_25789056_SNP	C	A	A	0.0566	6	100	-13.94	2.22E-06	2.73E-06
2R_20049365_SNP	T	C	C	0.08491	9	97	-11.54	5.32E-06	2.78E-06
3L_4776515_SNP	G	T	T	0.09091	10	100	-10.98	3.45E-06	2.84E-06
2R_17386417_SNP	T	G	G	0.05505	6	103	-13.9	3.98E-06	2.88E-06
3R_26494063_SNP	T	A	A	0.06422	7	102	-12.91	4.46E-06	2.96E-06
2R_17386388_SNP	C	A	A	0.05556	6	102	-13.87	4.55E-06	3.04E-06
3L_9479050_SNP	A	G	G	0.08333	9	99	-11.48	4.67E-06	3.12E-06
2R_5917838_INS	T	TGTT	T	0.09091	9	90	-11.51	9.73E-06	3.25E-06
3L_4776426_SNP	T	C	C	0.09091	10	100	-10.9	4.89E-06	3.43E-06
3L_8772164_INS	AA	A	A	0.06383	6	88	-13.84	3.71E-06	3.56E-06
2R_16788992_INS	TAT	T	T	0.07407	8	100	-12.01	5.15E-06	3.92E-06
3R_10963525_SNP	T	C	C	0.06731	7	97	-12.71	8.67E-06	4.57E-06
X_11838138_SNP	A	G	G	0.06364	7	103	-12.66	5.87E-06	4.75E-06
3L_15583921_SNP	A	G	G	0.07273	8	102	-11.86	6.90E-06	5.14E-06
3L_4776433_SNP	A	G	G	0.06481	7	101	-12.63	4.86E-06	5.17E-06
3L_13906905_SNP	A	G	G	0.1321	14	92	-9.217	1.08E-05	5.89E-06
3R_5663391_SNP	G	A	A	0.134	13	84	-9.564	7.11E-06	6.06E-06
2R_14888113_SNP	T	A	A	0.05405	6	105	-13.47	7.75E-06	6.09E-06

X_11330584_SNP	T	A	A	0.211	23	86	-7.513	8.16E-06	6.44E-06
2R_20691898_SNP	A	T	T	0.08182	9	101	-11.12	8.58E-06	6.63E-06
X_10056762_SNP	T	A	A	0.08491	9	97	-11.11	1.12E-05	7.07E-06
3R_10953662_SNP	A	T	A	0.06481	7	101	-12.45	1.03E-05	7.13E-06
X_7211134_SNP	C	T	T	0.1389	15	93	-8.858	1.09E-05	7.30E-06
X_18724741_SNP	A	C	C	0.0566	6	100	-13.36	1.06E-05	7.57E-06
2R_16730005_SNP	A	G	G	0.05455	6	104	-13.33	1.08E-05	7.77E-06
X_3245352_SNP	G	A	A	0.05505	6	103	-13.3	1.15E-05	8.17E-06
3R_10953647_SNP	C	A	C	0.06604	7	99	-12.39	1.31E-05	8.22E-06
3R_11336828_SNP	G	T	T	0.2404	25	79	-7.254	1.02E-05	8.57E-06
3L_11660449_SNP	G	A	A	0.233	24	79	-7.36	1.50E-05	8.79E-06
2L_22307250_SNP	T	G	T	0.1176	12	90	-9.699	1.82E-06	8.89E-06
3R_5663390_SNP	A	G	G	0.1368	13	82	-9.414	1.00E-05	9.05E-06
3R_11334948_SNP	G	C	C	0.2056	22	85	-7.538	1.34E-05	9.19E-06
3L_9476212_SNP	T	C	C	0.09091	10	100	-10.45	1.14E-05	9.30E-06
2L_19240665_SNP	T	A	A	0.1887	20	86	-7.804	8.61E-06	9.73E-06
3L_20338572_SNP	G	A	A	0.08791	8	83	-11.63	2.44E-05	9.89E-06
2R_2536487_SNP	A	G	G	0.05825	6	97	-12.68	8.69E-06	2.38E-05
2L_9433058_SNP	G	C	C	0.05714	6	99	-12.58	8.82E-06	2.79E-05

TABLE 9: Trial 3 - Location of genetic variants (Eclosion)	
ID	**GeneAnnotation**
3R_9896811_SNP	SiteClass[FBgn0038197|foxo|INTRON|0],TranscriptAnnot[INTRON(MODIFIER||||613|foxo|protein_coding|CODING|FBtr0082886|4);IN
2R_17797291_SNP	SiteClass[FBgn0085397|Fili|INTRON|0],TranscriptAnnot[INTRON(MODIFIER||||738|Fili|protein_coding|CODING|FBtr0112593|1);INTRC
X_4243970_SNP	SiteClass[FBgn0262738|norpA|INTRON|0],TranscriptAnnot[INTRON(MODIFIER||||1095|norpA|protein_coding|CODING|FBtr0070650|4
3R_23238151_DEL	SiteClass[FBgn0016061|side|INTRON|0],TranscriptAnnot[INTRON(MODIFIER||||929|side|protein_coding|CODING|FBtr0289998|2);INT
X_11846986_SNP	SiteClass[FBgn0263111|cac|INTRON|0],TranscriptAnnot[INTRON(MODIFIER||||1783|cac|protein_coding|CODING|FBtr0307324|22);IN
3R_10953680_SNP	SiteClass[FBgn0261859|CG42788|INTRON|0],TranscriptAnnot[INTRON(MODIFIER||||1559|CG42788|protein_coding|CODING|FBtr0303
3L_4775891_SNP	SiteClass[FBgn0035574|Gef64C|INTRON|0],TranscriptAnnot[INTRON(MODIFIER||||1984|Gef64C|protein_coding|CODING|FBtr007334
2R_14554814_SNP	SiteClass[FBgn0023214|edl|DOWNSTREAM|212],TranscriptAnnot[DOWNSTREAM(MODIFIER||||177|edl|protein_coding|CODING|FBtr
2R_13532533_SNP	SiteClass[||||],TranscriptAnnot[INTERGENIC(MODIFIER|||||||||)]
2R_13532534_DEL	SiteClass[||||],TranscriptAnnot[INTERGENIC(MODIFIER|||||||||)]
3L_20389146_SNP	SiteClass[FBgn0028978|trbl|DOWNSTREAM|242],TranscriptAnnot[DOWNSTREAM(MODIFIER||||484|trbl|protein_coding|CODING|FBtr
2R_17796799_SNP	SiteClass[FBgn0085397|Fili|INTRON|0],TranscriptAnnot[INTRON(MODIFIER||||738|Fili|protein_coding|CODING|FBtr0112593|1);INTRC
2R_13532562_SNP	SiteClass[||||],TranscriptAnnot[INTERGENIC(MODIFIER|||||||||)]
X_18724627_SNP	SiteClass[FBgn0030963|CG7101|UTR_5_PRIME|0;FBgn0259927|CG42450|DOWNSTREAM|330],TranscriptAnnot[DOWNSTREAM(MODIF
3R_25789056_SNP	SiteClass[FBgn0004622|Takr99D|INTRON|0],TranscriptAnnot[INTRON(MODIFIER||||517|Takr99D|protein_coding|CODING|FBtr030165
2R_20049365_SNP	SiteClass[FBgn0015544|spag|DOWNSTREAM|344;FBgn0034985|CG3328|UPSTREAM|648],TranscriptAnnot[DOWNSTREAM(MODIFIER||
3L_4776515_SNP	SiteClass[FBgn0035574|Gef64C|INTRON|0],TranscriptAnnot[INTRON(MODIFIER||||1984|Gef64C|protein_coding|CODING|FBtr007334
2R_17386417_SNP	SiteClass[FBgn0034631|CG10496|UTR_3_PRIME|0;FBgn0010470|Fkbp13|UPSTREAM|986],TranscriptAnnot[UPSTREAM(MODIFIER|||2
3R_26494063_SNP	SiteClass[||||],TranscriptAnnot[INTERGENIC(MODIFIER|||||||||)]
2R_17386388_SNP	SiteClass[FBgn0034631|CG10496|DOWNSTREAM|20;FBgn0010470|Fkbp13|UPSTREAM|957],TranscriptAnnot[DOWNSTREAM(MODIFIEF
3L_9479050_SNP	SiteClass[FBgn0036004|Jarid2|UTR_3_PRIME|0;FBgn0036005|pall|DOWNSTREAM|498],TranscriptAnnot[DOWNSTREAM(MODIFIER|||
2R_5917838_INS	SiteClass[FBgn0033473|CG12128|UTR_3_PRIME|0;FBgn0033474|CG1407|INTRON|0],TranscriptAnnot[INTRON(MODIFIER|||227|CG14
3L_4776426_SNP	SiteClass[FBgn0035574|Gef64C|INTRON|0],TranscriptAnnot[INTRON(MODIFIER||||1984|Gef64C|protein_coding|CODING|FBtr007334
3L_8772164_INS	SiteClass[FBgn0261259|Fhos|INTRON|0],TranscriptAnnot[INTRON(MODIFIER||||1152|Fhos|protein_coding|CODING|FBtr0306631|2);I
2R_16788992_INS	SiteClass[FBgn0015524|otp|INTRON|0],TranscriptAnnot[INTRON(MODIFIER||||409|otp|protein_coding|CODING|FBtr0290289|2)]
3R_10963525_SNP	SiteClass[FBgn0038291|CG3984|SYNONYMOUS_CODING|0;FBgn0038290|CG6912|UPSTREAM|823],TranscriptAnnot[SYNONYMOUS_CO
X_11838138_SNP	SiteClass[FBgn0263111|cac|INTRON|0],TranscriptAnnot[INTRON(MODIFIER||||1783|cac|protein_coding|CODING|FBtr0307324|26);IN
3L_15583921_SNP	SiteClass[FBgn0036518|RhoGAP71E|INTRON|0],TranscriptAnnot[INTRON(MODIFIER||||301|RhoGAP71E|protein_coding|CODING|FBtr
3L_4776433_SNP	SiteClass[FBgn0035574|Gef64C|INTRON|0],TranscriptAnnot[INTRON(MODIFIER||||1984|Gef64C|protein_coding|CODING|FBtr007334
3L_13906905_SNP	SiteClass[FBgn0026376|Rgl|INTRON|0],TranscriptAnnot[INTRON(MODIFIER||||774|Rgl|protein_coding|CODING|FBtr0075794|2);INTR
3R_5663391_SNP	SiteClass[FBgn0037766|Teh1|INTRON|0],TranscriptAnnot[INTRON(MODIFIER||||279|Teh1|protein_coding|CODING|FBtr0082151|2);IN

2R_14888113_SNP	SiteClass[FBgn0265356|tn|INTRON|0],TranscriptAnnot[INTRON(MODIFIER||||1353|tn|protein_coding|CODING|FBtr0086572|6);INTRO
X_11330584_SNP	SiteClass[FBgn0262740|Evi5|INTRON|0],TranscriptAnnot[INTRON(MODIFIER||||773|Evi5|protein_coding|CODING|FBtr0300732|4);INT
2R_20691898_SNP	SiteClass[||||],TranscriptAnnot[INTERGENIC(MODIFIER|||||||||)]
X_10056762_SNP	SiteClass[FBgn0264503|CG43902|INTRON|0],TranscriptAnnot[INTRON(MODIFIER||||1220|CG43902|protein_coding|CODING|FBtr0332
3R_10953662_SNP	SiteClass[FBgn0261859|CG42788|INTRON|0],TranscriptAnnot[INTRON(MODIFIER||||1559|CG42788|protein_coding|CODING|FBtr0303
X_7211134_SNP	SiteClass[FBgn0029941|CG1677|INTRON|0;FBgn0029943|Atg5|INTRON|0],TranscriptAnnot[INTRON(MODIFIER||||1000|CG1677|prote
X_18724741_SNP	SiteClass[FBgn0030963|CG7101|NON_SYNONYMOUS_CODING|0;FBgn0259927|CG42450|DOWNSTREAM|444],TranscriptAnnot[DOWNS
2R_16730005_SNP	SiteClass[||||],TranscriptAnnot[INTERGENIC(MODIFIER|||||||||)]
X_3245352_SNP	SiteClass[||||],TranscriptAnnot[INTERGENIC(MODIFIER|||||||||)]
3R_10953647_SNP	SiteClass[FBgn0261859|CG42788|INTRON|0],TranscriptAnnot[INTRON(MODIFIER||||1559|CG42788|protein_coding|CODING|FBtr0303
3R_11336828_SNP	SiteClass[||||],TranscriptAnnot[INTERGENIC(MODIFIER|||||||||)]
3L_11660449_SNP	SiteClass[FBgn0052085|CG32085|INTRON|0],TranscriptAnnot[INTRON(MODIFIER||||666|CG32085|protein_coding|CODING|FBtr00761
2L_22307250_SNP	SiteClass[||||],TranscriptAnnot[INTERGENIC(MODIFIER|||||||||)]
3R_5663390_SNP	SiteClass[FBgn0037766|Teh1|INTRON|0],TranscriptAnnot[INTRON(MODIFIER||||279|Teh1|protein_coding|CODING|FBtr0082151|2);IN
3R_11334948_SNP	SiteClass[FBgn0264775|CG44013|NON_SYNONYMOUS_CODING|0;FBgn0264776|CG44014|UPSTREAM|340],TranscriptAnnot[NON_SYN
3L_9476212_SNP	SiteClass[FBgn0036004|Jarid2|SYNONYMOUS_CODING|0],TranscriptAnnot[SYNONYMOUS_CODING(LOW|SILENT|ggC/ggT|G1567|2351
2L_19240665_SNP	SiteClass[||||],TranscriptAnnot[INTERGENIC(MODIFIER|||||||||)]
3L_20338572_SNP	SiteClass[FBgn0036973|Rbbp5|DOWNSTREAM|264],TranscriptAnnot[DOWNSTREAM(MODIFIER||||489|Rbbp5|protein_coding|CODING
2R_2536487_SNP	SiteClass[FBgn0029131|debcl|UTR_5_PRIME|0],TranscriptAnnot[UTR_5_PRIME(MODIFIER||||300|debcl|protein_coding|CODING|FBtr
2L_9433058_SNP	SiteClass[FBgn0011232|scat|SYNONYMOUS_CODING|0],TranscriptAnnot[SYNONYMOUS_CODING(LOW|SILENT|ctC/ctG|L322|940|scat|

CHAPTER 6

Inflammation and radiation exposure

The Drosophila innate immune system

Inflammation is the biological response initiated upon tissue damage or infection that promotes pathogen clearance and repairs tissue integrity. The mammalian immune response is complex and involves adaptive and innate immunity, both of which have humoral and cellular components. Acute inflammation resolves after tissue repair is completed, while chronic inflammation persists and can have deleterious consequences on tissue function (Buckley et al., 2001).

Drosophila has been a key model organism for elucidating mechanisms of the host defense system (Lemaitre and Hoffmann, 2007). Drosophila, and all invertebrates, lack an adaptive immune system and rely on innate immunity (Bulet et al., 2004). Although there are important differences between the Drosophila and mammalian immune responses, many of the innate immunity genes in Drosophila have mammalian homologs (Hoffmann, 2003). The Drosophila innate immune response involves pathogen recognition, phagocytosis, activation of immune signaling cascades, and induction of antimicrobial peptide (AMP) gene expression (Hoffmann, 2003; Bulet et al., 2004).

AMPs mediate the humoral component of Drosophila innate immunity (Lemaitre and Hoffmann, 2007). Most AMPs are positively charged and amphipathic, allowing them to interact with and disrupt the negatively charged cell walls and membranes of infectious organisms (Bulet et al., 2004). There are seven classes of AMPs in Drosophila: Diptericin, Attacin, Drosocin and Cecropin mainly act against gram-negative bacteria. Defensin acts primarily against gram-positive bacteria. Drosomycin and Metchnikowin are both anti-fungals (Lemaitre and Hoffmann, 2007).

In 1972, Boman et al. demonstrated that a bacterial injection into the abdomen of adult male flies can act as a vaccine. This antimicrobial response is largely due to expression and secretion of AMPs from the fat body (Boman et al., 1972; Lemaitre and Hoffmann, 2007). Expression of AMPs is regulated by immune-activated transcription factors via the Toll and Imd pathways. These pathways have different temporal patterns of activation, with the Imd pathway inducing early transcription and Toll inducing a longer transcriptional response with a delayed start (Lemaitre and Hoffmann, 2007). The canonical Toll signaling pathway consists of the cytokine Spätzle, the Toll membrane receptor, the adapters MyD88 and Tube, the Pelle kinase, Cactus, which is homologous to IκB, and the transcription factors Dorsal and Dif (Belvin and Anderson, 1996; Tauszig-Delamasure et al., 2002; Valanne et al., 2011). Loss of activity of the Toll pathway results in impaired immunity with decreased Drosomycin expression and increased susceptibility to infection, especially by fungi and gram-positive bacteria (Lemaitre et al., 1996; Rutschmann et al., 2002). The Drosophila Toll pathway is similar to the signaling cascade activated by Interleukin-1 and the toll-like receptors in mammals demonstrating evolutionary conservation (Lemaitre and Hoffmann, 2007). Toll also has important roles in Drosophila development (Nüsslein-Volhard and Wieschaus, 1980).

Whereas the Toll pathway is largely responsible for defense against fungi and gram-positive bacteria, the Imd pathway regulates defense against gram-negative bacteria (De Gregorio et al., 2002; Lemaitre et al., 1995). The canonical Imd pathway consists of the transmembrane receptor PCRP-LC, TAK1 (the Mitogen-Activated Protein 3 kinase), an Inhibitor of Apoptosis protein (DIAP2), IKKβ/ird5, IKKγ/Kenny (the Drosophila form of the IKK signalosome), dFADD, the caspase Dredd, and Relish, which is an NFκB transcription factor (Myllymäki et al., 2014). The major AMP of the Imd pathway is Diptericin. The Imd pathway can also activate the JNK

pathway via TAK1 (Boutros et al., 2002). Unlike the Toll pathway, there is no known role for the Imd pathway in development. Imd expression can activate apoptosis, but Imd-dependent apoptosis does not appear to play a role in the host defense against bacterial infection. (Georgel et al., 2001).

In response to pathogens, induction of AMP expression and secretion largely occurs in the fat body, which is homologous to the mammalian liver (Hoffmann, 2003). Epithelial tissues exposed to the external environment such as the digestive and respiratory tracts can increase AMP expression to mount local immune responses (Ferrandon et al., 1998; Tzou et al., 2000). Recent evidence also demonstrates that AMP expression can be induced in the Drosophila brain (Cao et al., 2013; Petersen et al., 2012).

Inflammation and neurodegeneration

Negative feedback built into inflammatory pathways keep inflammation in check, allowing for a robust response to the offending agent that is terminated upon clearance and tissue repair (Palmai-Pallag and Bachrati, 2014). Chronic inflammation, however, is associated with sustained generation of reactive oxygen species (ROS) and inflammatory cell activation that can itself damage tissues and increase susceptibility to diseases such as cancer and neurodegenerative disorders (Palmai-Pallag and Bachrati, 2014).

Persistent inflammation in the nervous system has been associated with a number of neurological diseases. Activation of toll-like receptors (TLRs) and production of cytokines in the brain may contribute to the pathogenesis of ischemic stroke and multiple sclerosis (Okun et al., 2009). Chronic neuroinflammation is also thought to play a role in the progression of Alzheimer's Disease, although short-term early activation of the immune system may be beneficial (Hensley,

2010). Persistent inflammation following traumatic brain injury is associated with white matter degeneration (Johnson et al., 2013). In mice lacking the Toll adapter MyD88, acute brain injury lesions are smaller than in wild-type controls suggesting that activation of immune signaling promotes injury-associated pathology (Koedel at al., 2007). Taken together, these examples demonstrate that persistent inflammation can have long-term negative side effects. Although initial activation of the immune response following an insult is necessary to promote repair, ongoing activation of the response is often associated with negative outcomes.

In Drosophila, chronic activation of the Imd pathway results in age-dependent neurdegeneration (Cao et al., 2013). Specifically overexpressing AMPs in either neurons or glia is sufficient to promote neurodegeneration in Drosophila (Cao et al., 2013). Moreover, knockdown of the Drosophila ATM kinase in glial cells results in increased AMP expression in glial cells and death of both neurons and glia (Petersen et al., 2012). Together, these studies demonstrate that activation of the innate immune system in the fly brain in the absence of infection or external injury is sufficient to cause neurodegeneration.

We developed a fly model to study the long-term neurotoxic consequences of radiation exposure during development. The phenotypes we observe in adult flies that were irradiated as larvae, including early death, impaired locomotor behavior and increased neuronal cell death, are consistent with premature aging and neurodegeneration (Sudmeier et al., in press). One possibility is that these neurodegenerative phenotypes are caused by radiation-induced activation of the Drosophila innate immune system.

Radiation exposure and inflammation

Chronic inflammation is associated with radiation exposure. A dose-dependent, persistent, subclinical level of inflammation has been reported in Atomic bomb survivors more than five decades after radiation exposure (Neriishi et al., 2001; Hayashi et al., 2005). In addition to increased rates of cancer, there are also increased rates of non-cancer inflammatory diseases in A-bomb survivors including liver cirrhosis and thyroid disease (Yamada et al., 2004). Analysis of T-cell immunity in these survivors demonstrated changes similar to those observed in natural aging, further supporting a model in which chronic inflammation contributes to radiation-associated disease phenotypes (Kusunoki et al., 2010).

Genetic background is an important determinant of the biological response to radiation in humans (Brooks and Dauer, 2014) and model organisms. For example there are radioresistant and radiosensitive strains of mice, which differ in radiation-induced chromosomal instability and susceptibility to radiation-induced Acute Myeloid Leukemia (r-AML) (Watson et al., 1997; Lorimore et al., 2001). The varied radiation sensitivity of different genetic backgrounds may be due to differences in the inflammatory response to radiation. In the mouse strain with increased susceptibility to r-AML, factors secreted from irradiated cells in the bone marrow three months after radiation exposure induced chromosomal instability in hemopoietic cells, suggesting oncogenic conversion. Treatment with a nonsteriodal anti-inflammatory drug (NSAID) reduced both inflammation and chromosomal instability 100 days post-irradiation supporting a model in which activation of the immune system contributes to the radiation-induced chromosome instability (Mukherjee et al., 2012). Together, these results demonstrate that depending on genetic background, post-radiation inflammation can be beneficial as in the r-AML resistant strain, or detrimental as observed in the r-AML sensitive strain.

There is also specific evidence for a genetic effect on macrophage activation and apoptosis levels following radiation (Lorimore et al., 2001; Mothersill et al., 1999; Watson et al., 1997; Ponnaiya et al., 1997). When mice were exposed to whole-body gamma radiation, macrophages in the spleen and bone marrow were activated by increased apoptosis of irradiated cells. Phagocytic clearance of apoptotic cells appears to be a component of the early response to radiation, as measures of macrophage activation are increased within 6 hours after irradiation. Over time, however, macrophage activation and associated nitric oxide production continues to increase while apoptotic cells decrease. Together, these findings support a model in which activated macrophages play a role in the prolonged inflammatory effects of radiation (Lorimore et al., 2001; Coates et al., 2008). Phagocytic macrophages can also have anti-inflammatory effects (Savill et al., 2002). For example, cultured macrophages increase transforming growth factor-β1 (TGF-β1) production, which is an inhibitor of inflammation, upon ingestion of apoptotic cells in vitro (Fadok et al., 1998).

Studies in zebrafish demonstrated that increased inflammation following UV irradiation of embryos has a protective effect. Transcription of the pro-inflammatory cytokine *il-1β* is increased in zebrafish embryos post-UV exposure. Knockdown of *il-1β* results in increased sensitivity of zebrafish embryos to UV radiation, and overexpression of *il-1β* promotes resistance to UV radiation (Banerjee and Leptin, 2014). Together, these results demonstrate an early radioprotective role for inflammation, and specifically IL-1β, during zebrafish development.

Tissue responses to radiation

Radiation mainly affects biological matter in two ways: Directly, by transferring energy to a macromolecule such as DNA, and indirectly by causing the generation of reactive oxygen

species (ROS) from water. ROS produced by radiation can amplify the radiation response by damaging other molecules including proteins and lipids. It is estimated that at least 60% of the damage caused by X- and gamma-radiation are due to indirect effects (Barcellos-Hoff et al., 2005). The tumor-killing effects of radiation are largely attributed to the induction of macromolecular damage ultimately leading to cell death. However, there is growing appreciation for the overall tissue response to radiation, which is not simply due to the additive effects of cell death (Barcellos-Hoff, 1998). Radiation initiates tissue-specific patterns of gene expression and activation of stress-response pathways. Key components of the tissue response to radiation include increased production of cytokines, chemokines, growth factors and ROS as well as extracellular matrix remodeling (Barcellos-Hoff et al., 2005). These responses are initiated to heal the tissue and protect it from further damage, but left unchecked can cause deleterious consequences.

The whole tissue response to radiation can lead to effects on cells that weren't directly exposed to radiation. In experiments on co-cultured irradiated and non-irradiated cells, the production of ROS and altered expression of growth factors and adhesion molecules by the irradiated cells led to striking effects on the phenotypes of the non-irradiated cells (Greenberger et al., 1996). Chromosomal instability was also observed in non-irradiated bone marrow cells cultured with irradiated cells (Lorimore et al., 1998). In vivo experiments on mouse mammary gland demonstrated that non-irradiated epithelial cells have increased tumor potential following irradiation of the mammary gland stroma due to changes in the microenvironment (Barcellos-Hoff and Ravani, 2000). Together these studies indicate that the effects of radiation are not solely explained by the sum of individual cell responses but involve complex interactions within the whole tissues.

Investigating consequences of radiation exposure in Drosophila

Drosophila can be used to better understand how tissues respond to radiation and the consequences of radiation-induced inflammation. We have developed a fly model of the neurotoxic side effects of radiation exposure during development and have shown premature death, impaired locomotor behavior, and increased neurodegeneration in adult flies following larval irradiation. We hypothesize that inflammation plays a role in the pathogenesis of these adult consequences of radiation exposure during larval development.

Although clinical radiation is specifically delivered to tumors or the tumor resection bed, normal tissue is often damaged during radiation therapy (Emami et al., 1991). In pediatric brain tumor patients, damage to healthy brain tissue from cranial radiation therapy is associated with long-term neurocognitive deficits (Edelstein et al., 2011; Ellenberg et al., 2009; Mulhern et al., 2005). In order to develop therapeutic strategies to mitigate these side effects, a better understanding of the biological pathways that are activated in irradiated tissues as well as the temporal profile of their activation, the interacting pathways, and the specific effects of their activation will be essential.

Our aim is to dissect the biological pathways underlying radiation-induced tissue damage, specifically in the brain, using the Drosophila model of radiation-induced neurotoxicity described previously. The genetic tools available in Drosophila, which allow temporal and spatial manipulation of gene expression, make this an ideal model for elucidating tissue responses to radiation. The greatest advantage of Drosophila, however, is the ability to perform unbiased forward genetic screens to identify novel pathways underlying radiation-induced damage.

In the experiments presented in the following chapter, we have taken a candidate approach to dissecting the mechanisms underlying the long-term consequences of radiation exposure during development. In the studies that follow, we investigate the role of innate immunity in the acute and long-term response to radiation exposure during development. We hope that these and future studies will aid in the development of therapeutic strategies to protect healthy tissue from damage during radiation therapy.

References

Banerjee, S. and Leptin, M. (2014). Systemic response to ultraviolet radiation involves induction of leukocytic IL-1β and inflammation in zebrafish. *J Immunol* **193**, 1408-15.

Barcellos-Hoff, M. H. (1998). How do tissues respond to damage at the cellular level? The role of cytokines in irradiated tissues. *Radiat Res* **150**, S109-20.

Barcellos-Hoff, M. H., Park, C. and Wright, E. G. (2005). Radiation and the microenvironment - tumorigenesis and therapy. *Nat Rev Cancer* **5**, 867-75.

Barcellos-Hoff, M. H. and Ravani, S. A. (2000). Irradiated mammary gland stroma promotes the expression of tumorigenic potential by unirradiated epithelial cells. *Cancer Res* **60**, 1254-60.

Belvin, M. P. and Anderson, K. V. (1996). A conserved signaling pathway: the Drosophila toll-dorsal pathway. *Annu Rev Cell Dev Biol* **12**, 393-416.

Boman, H. G., Nilsson, I. and Rasmuson, B. (1972). Inducible antibacterial defence system in Drosophila. *Nature* **237**, 232-5.

Boutros, M., Agaisse, H. and Perrimon, N. (2002). Sequential activation of signaling pathways during innate immune responses in Drosophila. *Dev Cell* **3**, 711-22.

Brooks, A. L. and Dauer, L. T. (2014). Advances in radiation biology: effect on nuclear medicine. *Semin Nucl Med* **44**, 179-86.

Buckley, C. D., Pilling, D., Lord, J. M., Akbar, A. N., Scheel-Toellner, D. and Salmon, M. (2001). Fibroblasts regulate the switch from acute resolving to chronic persistent inflammation. *Trends Immunol* **22**, 199-204.

Bulet, P., Stöcklin, R. and Menin, L. (2004). Anti-microbial peptides: from invertebrates to vertebrates. *Immunol Rev* **198**, 169-84.

Cao, Y., Chtarbanova, S., Petersen, A. J. and Ganetzky, B. (2013). Dnr1 mutations cause neurodegeneration in Drosophila by activating the innate immune response in the brain. *Proc Natl Acad Sci U S A* **110**, E1752-60.

Coates, P. J., Robinson, J. I., Lorimore, S. A. and Wright, E. G. (2008). Ongoing activation of p53 pathway responses is a long-term consequence of radiation exposure in vivo and associates with altered macrophage activities. *J Pathol* **214**, 610-6.

De Gregorio, E., Spellman, P. T., Tzou, P., Rubin, G. M. and Lemaitre, B. (2002). The Toll and Imd pathways are the major regulators of the immune response in Drosophila. *EMBO J* **21**, 2568-79.

Edelstein, K., Spiegler, B. J., Fung, S., Panzarella, T., Mabbott, D. J., Jewitt, N., D'Agostino, N. M., Mason, W. P., Bouffet, E., Tabori, U. et al. (2011). Early aging in adult survivors of childhood medulloblastoma: long-term neurocognitive, functional, and physical outcomes. *Neuro-Oncology*. 13, 536-45.

Ellenberg, L., Liu, Q., Gioia, G., Yasui, Y., Packer, R. J., Mertens, A., Donaldson, S. S., Stovall, M., Kadan-Lottick, N., Armstrong, G. et al. (2009). Neurocognitive status in long-term survivors of childhood CNS malignancies: a report from the Childhood Cancer Survivor Study. *Neuropsychology*. 23, 705-717.

Emami, B., Lyman, J., Brown, A., Coia, L., Goitein, M., Munzenrider, J. E., Shank, B., Solin, L. J. and Wesson, M. (1991). Tolerance of normal tissue to therapeutic irradiation. *Int J Radiat Oncol Biol Phys* **21**, 109-22.

Fadok, V. A., Bratton, D. L., Konowal, A., Freed, P. W., Westcott, J. Y. and Henson, P. M. (1998). Macrophages that have ingested apoptotic cells in vitro inhibit proinflammatory cytokine production through autocrine/paracrine mechanisms involving TGF-beta, PGE2, and PAF. *J Clin Invest* **101**, 890-8.

Ferrandon, D., Jung, A. C., Criqui, M., Lemaitre, B., Uttenweiler-Joseph, S., Michaut, L., Reichhart, J. and Hoffmann, J. A. (1998). A drosomycin-GFP reporter transgene reveals a local immune response in Drosophila that is not dependent on the Toll pathway. *EMBO J* **17**, 1217-27.

Georgel, P., Naitza, S., Kappler, C., Ferrandon, D., Zachary, D., Swimmer, C., Kopczynski, C., Duyk, G., Reichhart, J. M. and Hoffmann, J. A. (2001). Drosophila immune deficiency (IMD) is a death domain protein that activates antibacterial defense and can promote apoptosis. *Dev Cell* **1**, 503-14.

Greenberger, J. S., Epperly, M. W., Jahroudi, N., Pogue-Geile, K. L., Berry, L., Bray, J. and Goltry, K. L. (1996). Role of bone marrow stromal cells in irradiation leukemogenesis. *Acta Haematol* **96**, 1-15.

Hayashi, T., Morishita, Y., Kubo, Y., Kusunoki, Y., Hayashi, I., Kasagi, F., Hakoda, M., Kyoizumi, S. and Nakachi, K. (2005). Long-term effects of radiation dose on inflammatory

markers in atomic bomb survivors. *Am J Med* **118**, 83-6.

Hensley, K. (2010). Neuroinflammation in Alzheimer's disease: mechanisms, pathologic consequences, and potential for therapeutic manipulation. *J Alzheimers Dis* **21**, 1-14.

Hoffmann, J. A. (2003). The immune response of Drosophila. *Nature* **426**, 33-8.

Johnson, V. E., Stewart, J. E., Begbie, F. D., Trojanowski, J. Q., Smith, D. H. and Stewart, W. (2013). Inflammation and white matter degeneration persist for years after a single traumatic brain injury. *Brain* **136**, 28-42.

Koedel, U., Merbt, U. M., Schmidt, C., Angele, B., Popp, B., Wagner, H., Pfister, H. W. and Kirschning, C. J. (2007). Acute brain injury triggers MyD88-dependent, TLR2/4-independent inflammatory responses. *Am J Pathol* **171**, 200-13.

Kusunoki, Y., Yamaoka, M., Kubo, Y., Hayashi, T., Kasagi, F., Douple, E. B. and Nakachi, K. (2010). T-cell immunosenescence and inflammatory response in atomic bomb survivors. *Radiat Res* **174**, 870-6.

Lemaitre, B. and Hoffmann, J. (2007). The host defense of Drosophila melanogaster. *Annu Rev Immunol* **25**, 697-743.

Lemaitre, B., Kromer-Metzger, E., Michaut, L., Nicolas, E., Meister, M., Georgel, P., Reichhart, J. M. and Hoffmann, J. A. (1995). A recessive mutation, immune deficiency (imd), defines two distinct control pathways in the Drosophila host defense. *Proc Natl Acad Sci U S A* **92**, 9465-9.

Lemaitre, B., Nicolas, E., Michaut, L., Reichhart, J. M. and Hoffmann, J. A. (1996). The

dorsoventral regulatory gene cassette spätzle/Toll/cactus controls the potent antifungal response in Drosophila adults. *Cell* **86**, 973-83.

Lorimore, S. A., Coates, P. J., Scobie, G. E., Milne, G. and Wright, E. G. (2001). Inflammatory-type responses after exposure to ionizing radiation in vivo: a mechanism for radiation-induced bystander effects? *Oncogene* **20**, 7085-95.

Lorimore, S. A., Kadhim, M. A., Pocock, D. A., Papworth, D., Stevens, D. L., Goodhead, D. T. and Wright, E. G. (1998). Chromosomal instability in the descendants of unirradiated surviving cells after alpha-particle irradiation. *Proc Natl Acad Sci U S A* **95**, 5730-3.

Mothersill, C. E., O'Malley, K. J., Murphy, D. M., Seymour, C. B., Lorimore, S. A. and Wright, E. G. (1999). Identification and characterization of three subtypes of radiation response in normal human urothelial cultures exposed to ionizing radiation. *Carcinogenesis* **20**, 2273-8.

Mukherjee, D., Coates, P. J., Lorimore, S. A. and Wright, E. G. (2012). The in vivo expression of radiation-induced chromosomal instability has an inflammatory mechanism. *Radiat Res* **177**, 18-24.

Mulhern, R. K., Palmer, S. L., Merchant, T. E., Wallace, D., Kocak, M., Brouwers, P., Krull, K., Chintagumpala, M., Stargatt, R., Ashley, D. M., et al. (2005). Neurocognitive consequences of risk-adapted therapy for childhood medulloblastoma. *Journal of Clinical Oncology*. 23, 5511-5519.

Myllymäki, H., Valanne, S. and Rämet, M. (2014). The Drosophila imd signaling pathway. *J Immunol* **192**, 3455-62.

Neriishi, K., Nakashima, E. and Delongchamp, R. R. (2001). Persistent subclinical inflammation among A-bomb survivors. *Int J Radiat Biol* **77**, 475-82.

Nüsslein-Volhard, C. and Wieschaus, E. (1980). Mutations affecting segment number and polarity in Drosophila. *Nature* **287**, 795-801.

Okun, E., Griffioen, K. J., Lathia, J. D., Tang, S. C., Mattson, M. P. and Arumugam, T. V. (2009). Toll-like receptors in neurodegeneration. *Brain Res Rev* **59**, 278-92.

Pálmai-Pallag, T. and Bachrati, C. Z. (2014). Inflammation-induced DNA damage and damage-induced inflammation: a vicious cycle. *Microbes Infect* **16**, 822-32.

Petersen, A. J., Rimkus, S. A. and Wassarman, D. A. (2012). ATM kinase inhibition in glial cells activates the innate immune response and causes neurodegeneration in Drosophila. *Proc Natl Acad Sci U S A* **109**, E656-64.

Ponnaiya, B., Cornforth, M. N. and Ullrich, R. L. (1997). Radiation-induced chromosomal instability in BALB/c and C57BL/6 mice: the difference is as clear as black and white. *Radiat Res* **147**, 121-5.

Rutschmann, S., Kilinc, A. and Ferrandon, D. (2002). Cutting edge: the toll pathway is required for resistance to gram-positive bacterial infections in Drosophila. *J Immunol* **168**, 1542-6.

Savill, J., Dransfield, I., Gregory, C. and Haslett, C. (2002). A blast from the past: clearance

of apoptotic cells regulates immune responses. *Nat Rev Immunol* **2**, 965-75.

Sudmeier, L. J., Howard, S. P., and Ganetzky, B. (2015). A *Drosophila* model to investigate the neurotoxic side effects of radiation exposure. *Disease Models and Mechanisms* **in press**.

Tauszig-Delamasure, S., Bilak, H., Capovilla, M., Hoffmann, J. A. and Imler, J. L. (2002). Drosophila MyD88 is required for the response to fungal and Gram-positive bacterial infections. *Nat Immunol* **3**, 91-7.

Tzou, P., Ohresser, S., Ferrandon, D., Capovilla, M., Reichhart, J. M., Lemaitre, B., Hoffmann, J. A. and Imler, J. L. (2000). Tissue-specific inducible expression of antimicrobial peptide genes in Drosophila surface epithelia. *Immunity* **13**, 737-48.

Valanne, S., Wang, J. H. and Rämet, M. (2011). The Drosophila Toll signaling pathway. *J Immunol* **186**, 649-56.

Watson, G. E., Lorimore, S. A., Clutton, S. M., Kadhim, M. A. and Wright, E. G. (1997). Genetic factors influencing alpha-particle-induced chromosomal instability. *Int J Radiat Biol* **71**, 497-503.

Yamada, M., Wong, F. L., Fujiwara, S., Akahoshi, M. and Suzuki, G. (2004). Noncancer disease incidence in atomic bomb survivors, 1958-1998. *Radiat Res* **161**, 622-32.

CHAPTER 7

Innate immunity is radioprotective during development in Drosophila

The work in this chapter will be submitted for publication in the summer of 2015 by Lisa J. Sudmeier, Suma Samudrala, Steven P. Howard and Barry Ganetzky.

Abstract

Cranial radiation therapy (CRT) is an effective treatment for pediatric central nervous system malignancies, but survivors often suffer from neurological and neurocognitive side effects that persist many years after radiation exposure. The biological mechanisms underlying these outcomes are incompletely understood. Radiation exposure is also associated with an acute inflammatory response that may evolve into chronic inflammation. Recently, we developed a Drosophila model of the neurotoxic side effects of radiation exposure. Here we use this model to investigate the role of the innate immune system in the radiation response. We show that innate immunity is radioprotective during Drosophila larval development. Moreover, this radioprotection seems to be largely attributable to the Toll pathway. Our results indicate that loss of both Toll and Imd signaling, which are responsible for the immune response to fungal and bacterial infections, results in increased mortality following radiation exposure. We also show that activation of the innate immune response is sustained in adult flies weeks after radiation exposure during larval development. NF-κB target gene expression is elevated in adult bodies and heads, including the brain, following irradiation during larval development. Together our data indicate that innate immunity is required for radioresistance during Drosophila development and that chronic inflammation may be contributing to the neurodegenerative phenotypes characterized in our Drosophila model of radiation-induced damage. This work lays the foundation for future studies of radiation-induced activation of the innate immune system in flies. These studies may facilitate the development of therapeutic strategies to reduce the deleterious side effects of radiation therapy.

Introduction

Radiation therapy is an integral component of cancer treatment regimens. Radiation acts by inducing DNA damage and the generation of reactive oxygen species in cancer cells, which together promote cell death. Although radiation is mostly targeted to the tumor or resection bed during therapy, healthy cells are also unavoidably irradiated. Consequently, healthy tissue damage is a side effect of radiation therapy. For example, cognitive deficits resulting from unavoidable injury to healthy brain cells is a common side effect of cranial radiation therapy for brain tumors (Armstrong et al., 2009; Ellenberg et al., 2009; Mulhern et al., 2005; Packer et al., 2003; Redmond et al., 2013). As cancer survival rates increase, there is growing attention on reducing deleterious side effects of therapy. Moreover, developing strategies to protect healthy tissue from radiation damage may allow for the use of higher doses to increase the tumor-killing efficacy of radiation. Developing therapies for protecting healthy tissue from damage will require better understanding of the biological pathways activated by radiation. Some of these pathways may function as endogenous radioprotectors, and others may promote radiation-induced damage. Dissecting the response of healthy tissue to radiation exposure will aid in the development of pharmacologic agents to selectively promote radiation protection or mitigate the side effects of radiation exposure.

Many studies investigating radioprotective compounds have focused on antioxidants and synthetic thiols (Weiss and Landauer, 2003). However, anti-inflammatory drugs may be the most effective agents for reducing damage to healthy tissue from radiation exposure (Moding et al., 2013). A number of mammalian models of radiation-induced damage have demonstrated increased cytokine expression following radiation exposure (Rubin et al., 1995; Hong et al., 1995; Chang et al., 2011). Moreover, increased NF-κB activation is seen in the brain and other

tissues, including liver and intestine, following radiation exposure (Chang et al., 2011; Wang et al., 2004; Zhou et al., 1999; Raju et al., 1998). The level of NF-κB activated by radiation varies between organs and with time since exposure and causes organ-specific changes in gene expression profiles (Chang et al., 2011).

Radiation-induced inflammation can have varied effects. Persistent inflammation in lung tissue after radiation exposure is associated with increased collagen production and pulmonary fibrosis (Rubin et al., 1995). Moreover, sustained activation of astrocytes and microglia months after radiation exposure demonstrate persistent reactive gliosis (Chiang et al., 1993). Despite the negative effects of chronic inflammation, NF-κB is activated by DNA damage (Miyamoto, 2011), and may have an acute radioprotective role. Reduced NF-κB activity in mice increases radiation sensitivity and results in greater lethality from whole-body radiation exposure (Wang et al., 2004), consistent with a radioprotective role for NF-κB. Conversely, promoting NF-κB activation using Toll-like receptor (TLR) agonists increases radioprotection both in mouse and primate models (Burdelya et al., 2008; Hu et al., 2013; Shakhov et al., 2012). Treating mice with the TLR5 agonist bacterial flagellin before total body radiation exposure reduces mortality and promotes maintenance of normal stem cell proliferation levels in the small intestine and reduced apoptosis in hematopoietic and intestinal cells (Burdelya et al., 2008).

The radioprotective benefits of TLR receptor agonists suggest that the immune system may also be a promising target for reducing radiation toxicity following cranial radiation therapy. Studies using mammalian models have demonstrated that inflammatory pathways are activated in the brain following radiation exposure (Chang et al., 2011; Raju et al., 1998; Hong et al., 1995) and that activation of microglia and astrocytes in the brain lead to gliosis months after radiation exposure (Chiang et al., 1993). Nonetheless many questions about the post-radiation

inflammatory response in the brain remain unanswered. Moreover, better understanding of the timecourse of activation of inflammatory pathways, especially in the brain, will be critical for predicting when specific pharmacologic agents could be most beneficial. For example, there is a radioprotective benefit achieved with TLR agonists administered within 24 hours before or 1 hour after irradiation (Burdelya et al., 2008), but another therapeutic strategy could be to target the inflammation that persists after radiation exposure.

Pediatric brain tumor patients in particular would benefit from more effective radioprotective strategies following CRT to treat pediatric central nervous system malignancies. Although cure rates are now over 70%, these patients suffer long-term neurological side effects, including cognitive impairments, motor and coordination deficits and increased susceptibility to seizure disorders (Armstrong et al., 2009; Edelstein et al., 2011b; Ellenberg et al., 2009; Mulhern et al., 2005; Packer et al., 2003; Redmond et al., 2013). This population deserves specific attention in the development of radioprotective agents because pediatric and adult brains differ markedly with the former undergoing dynamic alterations in synaptic density and metabolism throughout development (Huttenlocher, 2002). Consequently, it is not surprising that younger patients undergoing CRT suffer more severe long-term side effects than older patients who receive the same treatment (Edelstein et al., 2011b; Mulhern et al., 2005).

We recently developed a Drosophila model of the long-term neurotoxic side effects of radiation exposure during development (Sudmeier et al., in press). This model demonstrates that in flies, as in human patients who undergo CRT for pediatric malignancies, there are long-term effects in the adult, such as impaired neurological function and cellular changes in the brain. A key advantage of a fly model is that we can use genetic tools to carefully dissect the biological pathways that confer radioprotection or radiosensitivity during development. Moreover, we can

perform interactor screens to identify genes that regulate a pathway of interest such as the signaling pathways of the innate immune system. An additional benefit of using Drosophila to study effects of radiation exposure is that flies are substantially more resistant to radiation than mammals (Parashar et al., 2008). Thus, in screens to identify radioprotective genes, we may identify novel mechanisms that evolved in flies to prevent damage from radiation or more efficiently repair it.

Flies, like other invertebrates have innate immunity but lack an adaptive immune system (Bulet et al., 2004). The Drosophila innate immune system, which is conserved with that of mammals, consists of two pathways to combat fungal and bacterial infections, the Toll pathway and the Imd pathway. The canonical Toll signaling pathway consists of the cytokine Spätzle, the Toll membrane receptor, the adapters MyD88 and Tube, the Pelle kinase, Cactus, which is homologous to IκB, and the transcription factors Dorsal and Dif (Belvin and Anderson, 1996; Tauszig-Delamasure et al., 2002; Valanne et al., 2011). The canonical Imd pathway consists of the transmembrane receptor PCRP-LC, TAK1 (the Mitogen-Activated Protein 3 kinase), an Inhibitor of Apoptosis protein (DIAP2), IKKβ/ird5, IKKγ/Kenny (the Drosophila form of the IKK signalosome), dFADD, the caspase Dredd, and the transcription factor Relish (Myllymäki et al., 2014). Activation of either pathway results in activation of NF-κB transcription factors (Dorsal and Dif in the Toll pathway, Relish in the Imd pathway), which translocate to the nucleus and induce expression of antimicrobial peptides (AMPs). AMPs mediate the humoral component of Drosophila innate immunity (Lemaitre and Hoffmann, 2007). Chronic activation of the innate immune system in neurons and glia of adult flies, via overexpression of AMPs is sufficient to promote neurodegeneration (Cao et al., 2013).

Here we investigate innate immunity and the radiation response during Drosophila development. We show that innate immunity is radioprotective during larval development. Moreover, our data indicate that there is sustained activation of the innate immune system in adult flies that were exposed to radiation during larval development. Together, these data suggest that radiation exposure during development activates the innate immune system to either protect the organism from damage or promote efficient repair of damage. However, this neuroprotective role might also come at a cost: persistent activation of the innate immune system may contribute to the neurodegenerative phenotypes observed in adult flies weeks after radiation exposure.

Results

Innate immunity is radioprotective during development in Drosophila

To examine whether innate immunity is radioprotective during development in Drosophila, we irradiated *Relish, spatzle* (*Rel, spz*) double mutant late third instar larvae and quantified survival to eclosion as described previously (Sudmeier et al., in press). *Rel, spz* mutants are deficient in both the Imd and Toll signaling pathways. Relish is the transcription factor activated by the Imd pathway, and Spatzle is the ligand for the Toll receptor. Although unnirradiated double mutants have nearly normal viability, survival of *Rel,spz* larvae through eclosion is substantially reduced following irradiation. Compared with wild-type controls, eclosion of *Rel, spz* larvae is reduced by 40% and 90% following exposure to radiation doses of 30 Gy and 40 Gy respectively during the late third instar (Figure 1A). This result indicates that innate immunity is required for promoting survival from radiation-induced damage during development.

Rel,spz mutants are deficient in both Imd- and Toll-mediated immunity. Thus, sensitivity to radiation during development of these larvae may be due generally to an impaired immune

response or may be a specific consequence of loss of either the Imd pathway or the Toll pathway. To test these possibilities, we irradiated larvae lacking individual components of the Imd or Toll pathways. Individual loss of Imd, a death domain-containing protein in the Imd pathway for which the pathway was named, or the NF-κB transcription factor in the Imd pathway, Relish, alone did not affect sensitivity to radiation exposure during larval development (Figure 1B). Similarly, loss of the Toll pathway adapter Myd88, or the NF-κB transcription factor Dif did not affect larval radiation sensitivity (Figure 1C). Only loss of the Toll pathway ligand, Spatzle, resulted in radiation sensitivity similar to that observed in the *Rel,spz* double mutant (Figure 1C). Together, these data indicate that the innate immune response, and especially the Toll pathway, promotes survival following radiation during development.

The innate immune response is activated by radiation exposure during development and remains activated weeks afterward

Studies in both mouse and humans demonstrate that radiation exposure can trigger persistent inflammation that is maintained long after the exposure ends (Neriishi et al., 2001; Hayashi et al., 2005; Hayashi et al., 2012; Chiang et al., 1993; Rubin et al., 1995). One of our goals in establishing a Drosophila model of radiation exposure during larval development is to investigate the mechanisms contributing to sustained damage in adults weeks after irradiation because an understanding of these mechanisms could facilitate new approaches for therapeutic intervention following radiation therapy in humans. In particular, we have focused on the neurological consequences in adults following larval irradiation (Sudmeier et al., in press). Consistent with the long-term neurological impairments observed in pediatric CRT patients, including motor deficits, premature aging, and loss of white matter integrity, (Redmond et al., 2013; Edelstein et al., 2011a; Schuitema et al., 2013), we observed impaired motor behavior, shortened lifespan, and

increased neurodegeneration in adult flies exposed to radiation during larval development. Because sustained activation of the innate immune response in the nervous system promotes neurodegeneration in Drosophila (Cao et al., 2013, Peterson et al., 2012), we hypothesized that radiation exposure during larval development leads to persistent inflammation in the brains of adult flies comparable to observations in mice and humans (Neriishi et al., 2001; Hayashi et al., 2005; Chiang et al., 1993).

To measure activation of the innate immune system, we used quantitative real-time PCR (qRT-PCR) to measure AMP transcript levels in heads of adult flies following irradiation during larval development. We observed an increase in AMP expression in heads of 5-day-old adults that were irradiated 10 days earlier, during the late third larval instar, compared with age-matched, non-irradiated controls (Figure 2A). The radiation-induced increase in AMP expression is dose-dependent, as indicated by increased AMP transcript levels at higher doses of radiation. We performed a similar analysis on 15-day old adults and again observed a dose-dependent increase in AMP transcripts compared with age-matched, non-irradiated controls, indicating that the immune response persists at least 3 weeks after radiation exposure (Figure 2B). Furthermore, the overall trend of this late level of increased AMP expression appears greater than that observed 10 days after irradiation (in 5-day-old adults), suggesting that activation of the innate immune system may be continuing to increase following radiation exposure. Together, these results indicate that the innate immune system is activated by radiation exposure during development and remains activated in adulthood, days to weeks after irradiation and may even further increase over time. We propose that this sustained inflammatory response contributes to the neurological deficits we observe in adults following larval irradiation (Sudmeier et al., in press).

To determine whether the radiation-induced activation of the innate immune response is specific for the nervous system or is also present in other adult tissues, we used qRT-PCR to measure AMP transcript levels in bodies of adult flies that were irradiated during larval development. Similar to the trend observed in adult heads following radiation exposure during development, AMP expression is increased in the bodies of both 5-day-old and 15-day-old adult flies that were irradiated during the late third larval instar (Figure 3). Although we did not dissect this response at the level of individual tissues, these results indicate that there is persistent systemic activation of AMP expression in adult flies following radiation exposure during development.

AMP expression is increased in the brain following radiation exposure during development

In response to invading pathogens, AMP expression and secretion is largely induced in the fat body, the fly equivalent of the mammalian liver (Lemaitre and Hoffmann, 2007). Although most of the fat body is located in the abdomen, the Drosophila head also contains fat body tissue. Because our qRT-PCR experiments were performed on whole adult heads, the AMP transcriptional profile we observed could be due to radiation-induced changes in AMP expression in any or all of the tissues in the adult head, including the brain and fat body. To determine whether AMP expression is specifically activated in adult brains following radiation exposure during development, we used AMP-GFP reporter lines to visualize AMP expression. These lines express GFP under the control of AMP promoters (Tzou et al., 2000). In 5-day-old adults that were exposed to radiation during the late third larval instar, we observe increased GFP expression in dissected brains (Figure 4A, E). This result demonstrates that the innate immune system is activated in brains following irradiation during development and remains activated for at least 10 days after exposure. This result is consistent with the increase in AMP transcripts we observe in adult heads following larval irradiation. We suspect that activation of the innate

immune response also occurs in fat body cells in the head, but we do not know the magnitude of this response compared with brain.

Because overexpression of AMPs in Drosophila glia or neurons is sufficient to promote neurodegeneration (Cao et al., 2013), we propose a model in which the innate immune system is activated acutely following radiation exposure during development and remains activated both in brain and in other adult tissues weeks after irradiation. This persistent inflammation likely contributes to the adult neurological deficits and premature aging associated with radiation exposure during development.

Discussion

We have shown that innate immunity is required for radioresistance during Drosophila development. Moreover, our data indicate that the innate immune system is activated in the brain and other adult tissues by radiation exposure during development and that it remains activated up to 3 weeks after exposure. This persistent inflammation likely contributes to the long-term neurotoxic consequences observed in adults following radiation exposure during development.

There has been growing appreciation for the role of radiation-induced inflammation in the deleterious effects in humans following radiation exposure. Decades after radiation exposure, Atomic Bomb survivors still exhibit elevated levels of inflammatory markers (Neriishi et al., 2001; Hayashi et al., 2005; Hayashi et al., 2012). Moreover, these survivors not only have an increased incidence of cancer, but also of inflammatory diseases such as liver cirrhosis and thyroid disease (Yamada et al., 2004). Many studies of neurodegenerative diseases have demonstrated that chronic inflammation contributes to disease pathogenesis. A better

understanding of the inflammatory response to radiation will aid in the development of therapeutic strategies to mitigate the side effects of radiation exposure for treating malignancies.

Work in Drosophila has shown that persistent overexpression of AMPs in neurons and glia causes neurodegeneration (Cao et al., 2013). In our Drosophila model of radiation-induced neurotoxicity, we observe premature aging, impaired locomotor behavior and persistent cell death in the brains of adult flies that were irradiated during larval development (Sudmeier et al., in press). Our recent data demonstrate that the innate immune system in Drosophila is activated by radiation exposure during development and remains activated following metamorphosis for at least three weeks after radiation exposure. We hypothesize that this persistent inflammation contributes to the neurological deficits we observe in adult flies following larval irradiation. To test this hypothesis, future studies will test whether pharmacological or genetic inhibition of the innate immune response in adults can rescue these phenotypes. It will be of interest to determine whether persistent activation of the innate immune system, following its early protective effects immediately after irradiation, is contributing to the early death, impaired locomotion and increased neurodegeneration observed later in adults.

Radiation-induced NF-κB activation has been demonstrated in mammals, and use of TLR5 agonists that lead to NF-κB activation promote radioprotection without interfering with beneficial anti-tumor effects of radiation (Wang et al., 2004; Burdelya et al., 2008; Hu et al., 2013). This is consistent with our data showing a radioprotective role for the innate immune system during development and increased transcription of targets of the Drosophila homologs of NF-κB following irradiation. Our data suggest that loss of the Imd pathway alone does not increase radiosensitivity, but loss of the Toll pathway alone does increase radiosensitivity, as measured by survival to eclosion following larval irradiation. A possibility we did not explore,

however, is that there are long-term consequences on adult radiation-sensitive phenotypes from loss of the Imd pathway. For example, although loss of *Relish* alone does not affect survival to adulthood following irradiation, these mutants may suffer greater damage from radiation and have exacerbated adult consequences including enhanced locomotor impairment and shortened lifespan. Conversely, since *Relish* mutants have decreased innate immunity, inflammation in the *Relish* adults following radiation exposure during development may be decreased and lead to more favorable adult outcomes. The same possibilities exist for the Toll pathway mutants that did not have increased radiosensitivity, as measured by survival to eclosion (e.g. *Myd88* or *Dif* mutants).

It will be of interest to gain a better understanding of how acute inflammation confers radioprotection and what mechanisms are contributing to the long-term elevation in innate immune system activation. An understanding of when and how innate immune responses exert their effect following radiation exposure will be especially important for patients undergoing radiotherapy. To mitigate the deleterious consequences of sustained inflammation, therapeutic interventions to inhibit the innate immune response will need to be applied after the biological benefit of acute activation of the innate immune response has occurred.

Although radiation-induced inflammation has been studied in mammalian models, flies offer a number of advantages to further our understanding of the benefits of acute inflammation following radiation and the long-term consequences of sustained inflammation. Because flies lack an adaptive immune system, innate immunity can be investigated without confounding inputs from the adaptive immune system. However, the most important benefit of a fly model is likely to be application of genetic strategies to dissect the biological pathways that contribute to the effect of innate immunity on radiation-sensitive phenotypes. We have demonstrated that

innate immunity is required for radioresistance during Drosophila development. Our data lay the foundation for future studies of radiation-induced activation of the innate immune system in flies. These studies may facilitate the development of therapeutic strategies to reduce the deleterious side effects of radiation therapy.

Materials and Methods

***Drosophila* strains and culture**: Flies were maintained on standard cornmeal-molasses medium at 25°C. The following stocks were used for eclosion experiments (Figure 1): Rel^{E20}, spz^{4}; $imd^{EY08573}$; Rel^{E20}; $Myd88^{KG03447}$; Dif^{1} (Bloomington Stock Center #s: 55718, 17474, 55714, 14091 and 36559, respectively) and spz^{4} (from L. A. Johnston, Columbia University New York). $y^{1}w*$ and w^{1118} were used as controls for eclosion experiments (Figure 1). *Canton-S* was used for qRT-PCR experiments (Figures 2 & 3). *Metchnikowin::GFP* and *AttacinA::GFP* stocks (David Wassarman, University of Wisconsin-Madison and Ylva Engstrom, Stockholm University, Stockholm, Sweden) were used to visualize AMP expression in the brain (Figure 4).

As described in Sudmeier et al., 2015, "For all experiments involving irradiation of late third instar larvae, adults were allowed to mate and lay eggs in culture bottles on standard medium and cleared from the bottles after 4-5 days to prevent larval crowding. Wandering third instar larvae were collected when they emerged from food. Known numbers of larvae were placed in culture vials with an absorbent tissue at the bottom to reduce excess moisture and prevent newly eclosed flies from getting stuck."

Irradiation of late third instar larvae: As described in Sudmeier et al., 2015, "Vials containing 30-50 late third instar larvae were placed on a rotating plate and exposed to a single dose of

gamma radiation (10, 20, 30, 40 or 50 Gy) using a Cesium-137 irradiator (J. L. Sheppard & Associates San Francisco, California USA; Mark I unit, Model 30, Serial Number 668) with an average dose rate of 6.5 Gy/min. Control larvae were handled identically but without radiation exposure. Irradiated and control larvae were then allowed to complete development at 25°C and all adults that subsequently emerged were collected and counted."

qRT-PCR: Adult flies were allowed to mate for two days following eclosion and then collected, sorted by sex, and transferred to fresh vials (≤ 15 males or females per vial) containing standard medium and aged at 25°C. Flies were transferred to fresh food every three days. On day 5 or 15 of adulthood, flies were anesthetized with CO_2, a razor blade was used to cut heads from bodies, and samples were transferred to microcentrifuge tubes and frozen at -80°C. RNA was extracted from frozen samples using TRI Reagent RT (Molecular Research Center, Cincinnati, OH). The iScript cDNA Synthesis Kit (Bio-Rad, Hercules, CA) was used to generate cDNA. Quantitative real-time PCR was performed using SYBR Green Supermix (Bio-Rad, Hercules, CA). Primer sequences are provided in Table 1. *Rp49* was used as the reference gene. PCR was performed with a Bio-Rad iCycler and the following program: 35 cycles: step1: 95°C for 10 seconds, step 2: 60°C for 30 seconds, step 3: 72°C for 40 seconds each cycle. Males and females both demonstrated a dose-dependent increase in AMP expression at 5 and 15 days in heads and bodies, but only data for males are presented here.

Immunohistochemistry: As described in Sudmeier et al., 2015, "Adult brains were dissected in 1X PBS and fixed at room temperature for 25-30 minutes in 4% formaldehyde in phosphate buffer (4% formaldehyde, 0.1M phosphate buffer (pH 7.2), 0.2% TritonX-100). Samples were

then washed with 1X PBS and placed in blocking buffer (PBS, 0.2% TritonX-100, 0.1% normal goat serum) for 2 hours at room temperature or 4°C overnight. Brains were incubated in primary antibodies diluted with blocking buffer at 4°C overnight then washed 2X with PBST (PBS + 0.1% TritonX-100) and incubated in secondary antibodies diluted with blocking buffer for 4 hours at room temperature, then washed 2X again with PBST. DAPI was added in the final wash for 30 minutes at room temperature. Brains were mounted on slides in Vectashield (Vector Laboratories, Burlingame, California USA).” The antibodies used are as follows: Chicken anti-Green Fluorescent Protein (Life Technologies, Carlsbad, California USA; 1:500), Mouse anti-Repo (Developmental Studies Hybridoma Bank, University of Iowa, Iowa City, Iowa USA; 8D12, 1:50), Rat anti-Elav (Developmental Studies Hybridoma Bank, University of Iowa, Iowa City, Iowa USA; 7E8A10, 1:250), DAPI (Sigma-Aldrich, St. Louis, Missouri, USA; 1mg/L), Goat anti-Chicken Alexa Fluor-488 (Life Technologies, Carlsbad, California USA; 1:200), Goat anti-Mouse Alexa Fluor-568 (Life Technologies, Carlsbad, California USA; 1:200), Goat anti-Rat Alexa Fluor-633 (Invitrogen, Carlsbad, California USA; 1:200).

Microscopy: As described in Sudmeier et al., 2015, “Adult brains were imaged using a Zeiss 510 Confocal Laser Scanning Microscope (Carl Zeiss Microscopy, Jena, Thuringia Germany). ImageJ Software (National Institutes of Health, Bethesda, Maryland USA) and Adobe Photoshop CC (Adobe Systems, San Jose, California USA) were used for adjusting image brightness and contrast.”

Statistical Analyses: GraphPad Prism (GraphPad Software San Diego, California USA) was used for Student’s T-Test analyses of eclosion and AMP transcription levels.

Acknowledgements

We thank members of the Ganetzky Laboratory for comments on the manuscript and helpful discussions, especially Robert Kreber for irradiating all of the larvae used in these experiments. We are especially grateful to Stanislava Chtarbanova for sharing her expertise in Drosophila innate immunity.

References

Armstrong, G. T., Liu, Q., Yasui, Y., Huang, S., Ness, K. K., Leisenring, W., Hudson, M. M., Donaldson, S. S., King, A. A., Stoval, M., et al. (2009). Long-term outcomes among adult survivors of childhood central nervous system malignancies in the Childhood Cancer Survivor Study. *Journal of the National Cancer Institute* **101**, 946-958.

Belvin, M. P. and Anderson, K. V. (1996). A conserved signaling pathway: the Drosophila toll-dorsal pathway. *Annu Rev Cell Dev Biol* **12**, 393-416.

Bulet, P., Stöcklin, R. and Menin, L. (2004). Anti-microbial peptides: from invertebrates to vertebrates. *Immunol Rev* **198**, 169-84.

Burdelya, L. G., Krivokrysenko, V. I., Tallant, T. C., Strom, E., Gleiberman, A. S., Gupta, D., Kurnasov, O. V., Fort, F. L., Osterman, A. L., Didonato, J. A. et al. (2008). An agonist of toll-like receptor 5 has radioprotective activity in mouse and primate models. *Science* **320**, 226-30.

Cao, Y., Chtarbanova, S., Petersen, A. J. and Ganetzky, B. (2013). Dnr1 mutations cause neurodegeneration in Drosophila by activating the innate immune response in the brain. *Proc Natl Acad Sci U S A* **110**, E1752-60.

Chang, C. T., Lin, H., Ho, T. Y., Li, C. C., Lo, H. Y., Wu, S. L., Huang, Y. F., Liang, J. A. and Hsiang, C. Y. (2011). Comprehensive assessment of host responses to ionizing radiation by nuclear factor-κB bioluminescence imaging-guided transcriptomic analysis. *PLoS One* **6**, e23682.

Chiang, C. S., McBride, W. H. and Withers, H. R. (1993). Radiation-induced astrocytic and microglial responses in mouse brain. *Radiother Oncol* **29**, 60-8.

Edelstein, K., Spiegler, B. J., Fung, S., Panzarella, T., Mabbott, D. J., Jewitt, N., D'Agostino, N. M., Mason, W. P., Bouffet, E., Tabori, U. et al. (2011a). Early aging in adult survivors of childhood medulloblastoma: long-term neurocognitive, functional, and physical outcomes. *Neuro-Oncology* **13**, 536-45.

Edelstein, K., D'Agostino, N., Bernstein, L. J., Nathan, P. C., Greenberg, M. L., Hodgson, D. C., Millar, B. A., Laperriere, N. and Spiegler, B. J. (2011b). Long-term neurocognitive outcomes in young adult survivors of childhood acute lymphoblastic leukemia. *Journal of Pediatric Hematology/Oncology* **33**, 450-8.

Ellenberg, L., Liu, Q., Gioia, G., Yasui, Y., Packer, R. J., Mertens, A., Donaldson, S. S., Stovall, M., Kadan-Lottick, N., Armstrong, G. et al. (2009). Neurocognitive status in long-term survivors of childhood CNS malignancies: a report from the Childhood Cancer Survivor Study. *Neuropsychology* **23**, 705-717.

Fernando, M. D., Kounatidis, I. and Ligoxygakis, P. (2014). Loss of Trabid, a new negative regulator of the drosophila immune-deficiency pathway at the level of TAK1, reduces life span. *PLoS Genet* **10**, e1004117.

Hayashi, T., Morishita, Y., Kubo, Y., Kusunoki, Y., Hayashi, I., Kasagi, F., Hakoda, M., Kyoizumi, S. and Nakachi, K. (2005). Long-term effects of radiation dose on inflammatory markers in atomic bomb survivors. *Am J Med* **118**, 83-6.

Hayashi, T., Morishita, Y., Khattree, R., Misumi, M., Sasaki, K., Hayashi, I., Yoshida, K., Kajimura, J., Kyoizumi, S., Imai, K. et al. (2012). Evaluation of systemic markers of inflammation in atomic-bomb survivors with special reference to radiation and age effects. *FASEB J* **26**, 4765-73.

Hong, J. H., Chiang, C. S., Campbell, I. L., Sun, J. R., Withers, H. R. and McBride, W. H. (1995). Induction of acute phase gene expression by brain irradiation. *Int J Radiat Oncol Biol Phys* **33**, 619-26.

Hu, Z., Xing, Y., Qian, Y., Chen, X., Tu, J., Ren, L., Wang, K. and Chen, Z. (2013). Anti-radiation damage effect of polyethylenimine as a toll-like receptor 5 targeted agonist. *J Radiat Res* **54**, 243-50.

Huttenlocher, P. R. (2002). *Neural Plasticity.* Cambridge, Massachusetts: Harvard University Press.

Lemaitre, B. and Hoffmann, J. (2007). The host defense of Drosophila melanogaster. *Annu Rev Immunol* **25**, 697-743.

Miyamoto, S. (2011). Nuclear initiated NF-κB signaling: NEMO and ATM take center stage. *Cell Res* **21**, 116-30.

Moding, E. J., Kastan, M. B. and Kirsch, D. G. (2013). Strategies for optimizing the response of cancer and normal tissues to radiation. *Nat Rev Drug Discov* **12**, 526-42.

Moskalev, A. and Shaposhnikov, M. (2011). Pharmacological inhibition of NF-κB prolongs lifespan of Drosophila melanogaster. *Aging (Albany NY)* **3**, 391-4.

Mulhern, R. K., Palmer, S. L., Merchant, T. E., Wallace, D., Kocak, M., Brouwers, P., Krull, K., Chintagumpala, M., Stargatt, R., Ashley, D. M., et al. (2005). Neurocognitive consequences of risk-adapted therapy for childhood medulloblastoma. *Journal of Clinical Oncology* **23**, 5511-5519.

Myllymäki, H., Valanne, S. and Rämet, M. (2014). The Drosophila imd signaling pathway. *J Immunol* **192**, 3455-62.

Neriishi, K., Nakashima, E. and Delongchamp, R. R. (2001). Persistent subclinical inflammation among A-bomb survivors. *Int J Radiat Biol* **77**, 475-82.

Packer, R. J., Gurney, J. G., Punyko, J. A., Donaldson, S. S., Inskip, P. D., Stovall, M., Yasui, Y., Mertens, A. C., Sklar, C. A., Nicholson, H. S., et al. (2003). Long-term neurologic and neurosensory sequelae in Adult survivors of a childhood brain tumor: Childhood Cancer Survivor Study. *Journal of Clinical Oncology* **21**, 3255-3261.

Parashar, V., Frankel, S., Lurie, A. G. and Rogina, B. (2008). The effects of age on radiation resistance and oxidative stress in adult Drosophila melanogaster. *Radiat Res* **169**, 707-11.

Petersen, A. J., Rimkus, S. A. and Wassarman, D. A. (2012). ATM kinase inhibition in glial cells activates the innate immune response and causes neurodegeneration in Drosophila. *Proc Natl Acad Sci U S A* **109**, E656-64.

Raju, U., Gumin, G. J., Noel, F. and Tofilon, P. J. (1998). IkappaBalpha degradation is not a requirement for the X-ray-induced activation of nuclear factor kappaB in normal rat astrocytes and human brain tumour cells. *Int J Radiat Biol* **74**, 617-24.

Redmond, K. J., Mahone, E. M., Terezakis, S., Ishaq, O., Ford, E., McNutt, T., Kleinberg, L., Cohen, K. J., Wharam, M. and Horska, A. (2013). Association between radiation dose to neuronal progenitor cell niches and temporal lobes and performance on neuropsychological testing in children: a prospective study. *Neuro-Oncology* **15**, 360-9.

Rubin, P., Johnston, C. J., Williams, J. P., McDonald, S. and Finkelstein, J. N. (1995). A perpetual cascade of cytokines postirradiation leads to pulmonary fibrosis. *Int J Radiat Oncol Biol Phys* **33**, 99-109.

Schuitema, I., Deprez, S., Van Hecke, W., Daams, M., Uyttebroeck, A., Sunaert, S., Barkhof, F., van Dulmen-den Broeder, E., van der Pal, H. J., van den Bos, C., et al. (2013). Accelerated aging, decreased white matter integrity, and associated neuropsychological dysfunction 25 years after pediatric lymphoid malignancies. *Journal of Clinical Oncology* **31**, 3378-3388.

Shakhov, A. N., Singh, V. K., Bone, F., Cheney, A., Kononov, Y., Krasnov, P., Bratanova-Toshkova, T. K., Shakhova, V. V., Young, J., Weil, M. M. et al. (2012). Prevention and mitigation of acute radiation syndrome in mice by synthetic lipopeptide agonists of Toll-like receptor 2 (TLR2). *PLoS One* **7**, e33044.

Sudmeier, L. J., Howard, S. P., and Ganetzky, B. (2015). A *Drosophila* model to investigate the neurotoxic side effects of radiation exposure. *Disease Models and Mechanisms* **in press**.

Tauszig-Delamasure, S., Bilak, H., Capovilla, M., Hoffmann, J. A. and Imler, J. L. (2002). Drosophila MyD88 is required for the response to fungal and Gram-positive bacterial infections. *Nat Immunol* **3**, 91-7.

Tran, H., Hamada, F., Schwarz-Romond, T. and Bienz, M. (2008). Trabid, a new positive regulator of Wnt-induced transcription with preference for binding and cleaving K63-linked ubiquitin chains. *Genes Dev* **22**, 528-42.

Tzou, P., Ohresser, S., Ferrandon, D., Capovilla, M., Reichhart, J. M., Lemaitre, B., Hoffmann, J. A. and Imler, J. L. (2000). Tissue-specific inducible expression of antimicrobial peptide genes in Drosophila surface epithelia. *Immunity* **13**, 737-48.

Valanne, S., Wang, J. H. and Rämet, M. (2011). The Drosophila Toll signaling pathway. *J Immunol* **186**, 649-56.

Wang, Y., Meng, A., Lang, H., Brown, S. A., Konopa, J. L., Kindy, M. S., Schmiedt, R. A., Thompson, J. S. and Zhou, D. (2004). Activation of nuclear factor kappaB In vivo selectively protects the murine small intestine against ionizing radiation-induced damage. *Cancer Res* **64**, 6240-6.

Weiss, J. F. and Landauer, M. R. (2003). Protection against ionizing radiation by antioxidant nutrients and phytochemicals. *Toxicology* **189**, 1-20.

Yamada, M., Wong, F. L., Fujiwara, S., Akahoshi, M. and Suzuki, G. (2004). Noncancer disease incidence in atomic bomb survivors, 1958-1998. *Radiat Res* **161**, 622-32.

Zhou, D., Brown, S. A., Yu, T., Chen, G., Barve, S., Kang, B. C. and Thompson, J. S. (1999). A high dose of ionizing radiation induces tissue-specific activation of nuclear factor-kappaB in vivo. *Radiat Res* **151**, 703-9.

Figure 1

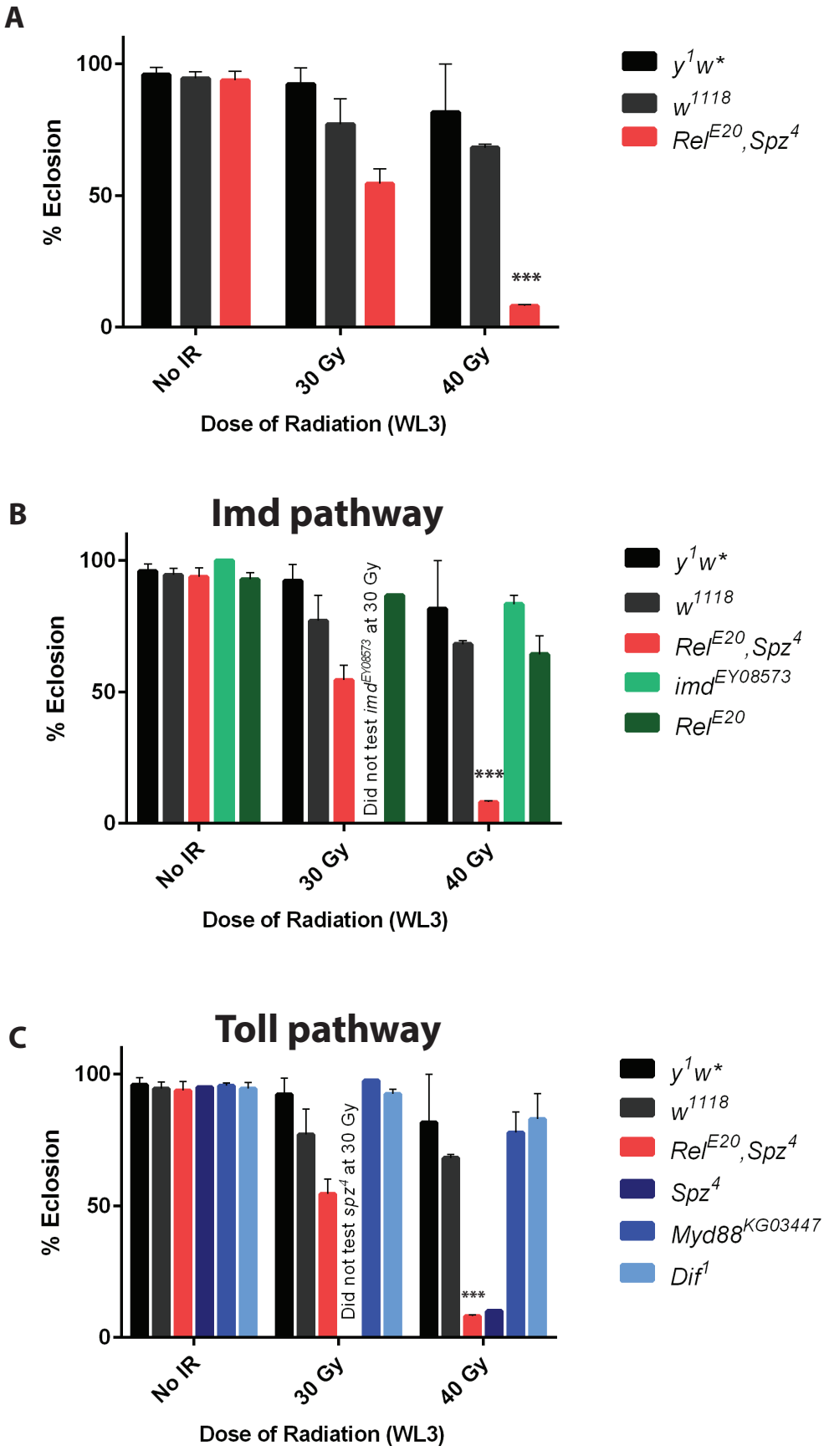
A
100
50
0
% Eclosion
***
No IR
30 Gy
40 Gy
Dose of Radiation (WL3)
y1w*
w1118
RelE20,Spz4
B
Imd pathway
100
50
0
% Eclosion
Did not test imdEY08573 at 30 Gy
***
No IR
30 Gy
40 Gy
Dose of Radiation (WL3)
y1w*
w1118
RelE20,Spz4
imdEY08573
RelE20
C
Toll pathway
100
50
0
% Eclosion
Did not test spz4 at 30 Gy
***
No IR
30 Gy
40 Gy
Dose of Radiation (WL3)
y1w*
w1118
RelE20,Spz4
Spz4
Myd88KG03447
Dif1

Figure 1. Innate immunity is radioprotective during larval development. (A-C) For each dose of radiation, the percentage of irradiated third instar larvae that complete development and eclose as adults is shown for the indicated laboratory background strains (y^1w* and w^{1118}) and mutant strains. (A) Loss of both Toll and Imd signaling (Rel^{E20}, spz^4) results in increased sensitivity to radiation compared to controls during the third larval instar (pink bar). (B) Loss of Imd signaling does not affect radiation sensitivity. *Imd* ($imd^{EY08573}$, light green bar) and *Rel* (Rel^{E20}, dark green bar) mutants have similar eclosion rates to controls (black and gray bars). (C) Loss of Toll signaling results in increased sensitivity to radiation. *Myd88* ($Myd88^{KG03447}$, royal blue bar) and *Dif* (Dif^1, light blue bar) mutants have similar eclosion rates to controls (black and gray bars), but *spz* mutants (spz^4, dark blue bar) are as sensitive to radiation as Rel^{E20}, spz^4 (pink bar). 2-5 trials each with 20-40 larvae per dose per genotype were performed, except for spz^4, which has only been tested once. Each bar represents mean ±SEM. ***$p<0.001$ based on Student's t test comparing Rel^{E20}, spz^4 40Gy to y^1w* or w^{1118} 40 Gy.

Figure 2

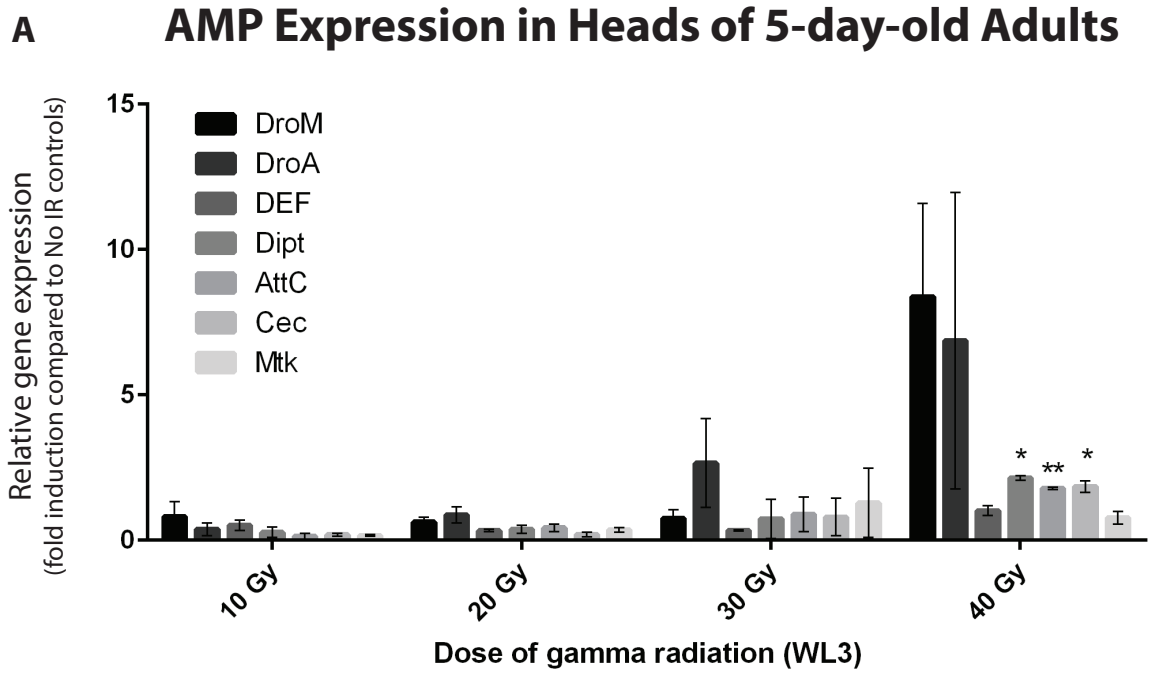
A
AMP Expression in Heads of 5-day-old Adults
Relative gene expression
(fold induction compared to No IR controls)
15
10
5
0
DroM
DroA
DEF
Dipt
AttC
Cec
Mtk
*
**
*
10 Gy
20 Gy
30 Gy
40 Gy
Dose of gamma radiation (WL3)

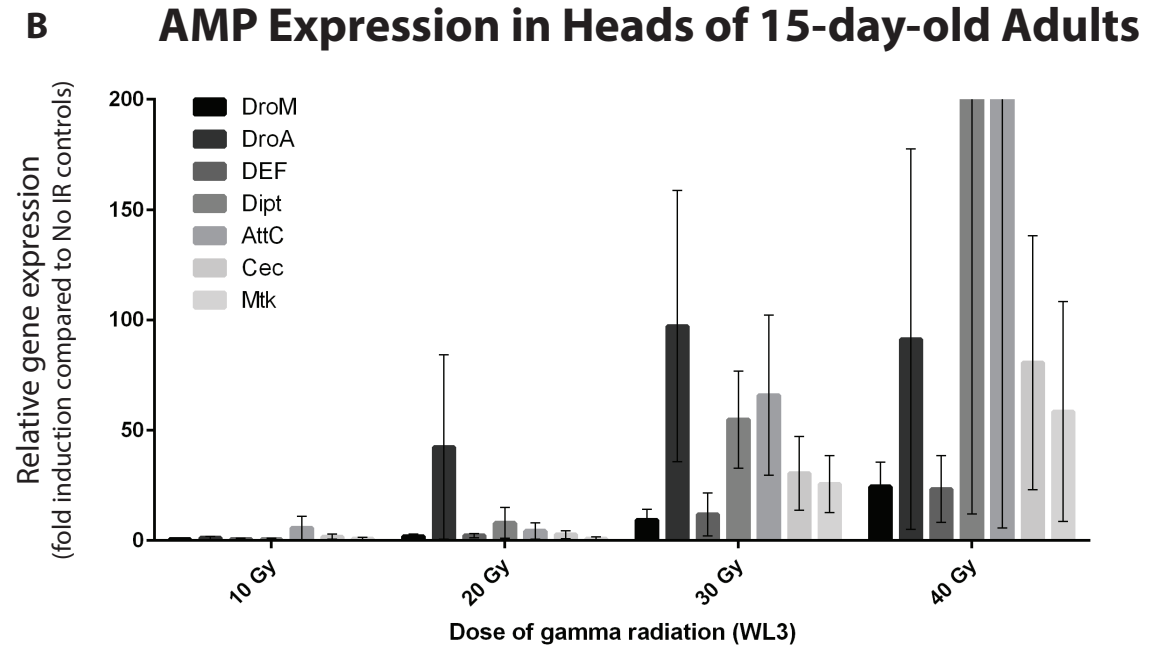
B
AMP Expression in Heads of 15-day-old Adults
Relative gene expression
(fold induction compared to No IR controls)
200
150
100
50
0
DroM
DroA
DEF
Dipt
AttC
Cec
Mtk
10 Gy
20 Gy
30 Gy
40 Gy
Dose of gamma radiation (WL3)

Figure 2. Irradiation during larval development results in increased AMP expression in adult heads. For each dose of radiation during the late third larval instar, expression of seven different AMPs in the heads of 5-day-old (A) and 15-day-old (B) adults was measured with qRT-PCT. The laboratory wild-type *Canton-S* strain was used for these experiments. The bars in each graph represent mean AMP expression normalized to mean AMP expression in non-irradiated age-matched controls. Error bars are SEM. The graph in (A) represents two trials. The graph in (B) represents three trials. The average fold induction for *Dipt* and *AttC* in (B) are 267 and 1628, respectively. *Rp49* was used as the reference gene. Although AMP expression is consistently increased in the heads of flies that were exposed to higher doses of radiation during development (30 Gy and 40 Gy), the large variation in fold induction from one trial to the next results in no statistically significant increases in the 15-day-old experiments (B). *Dipt*, *AttC* and *Cec* expression in heads of 5-day-old adults exposed to a 40 Gy dose of radiation during the late third larval instar is statistically significantly increased (A). *$p<0.05$ and **$p<0.01$ based on Students t test comparing relative expression in 40 Gy and 10 Gy samples.

Figure 3

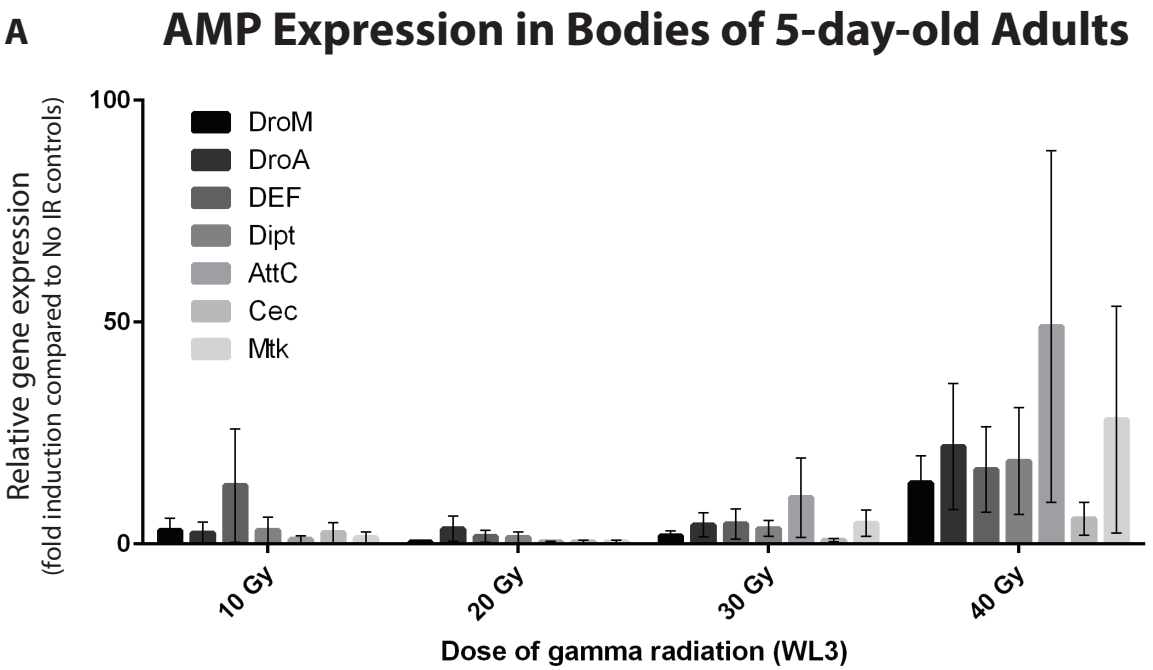
A
AMP Expression in Bodies of 5-day-old Adults
Relative gene expression
(fold induction compared to No IR controls)
100
50
0
DroM
DroA
DEF
Dipt
AttC
Cec
Mtk
10 Gy
20 Gy
30 Gy
40 Gy
Dose of gamma radiation (WL3)

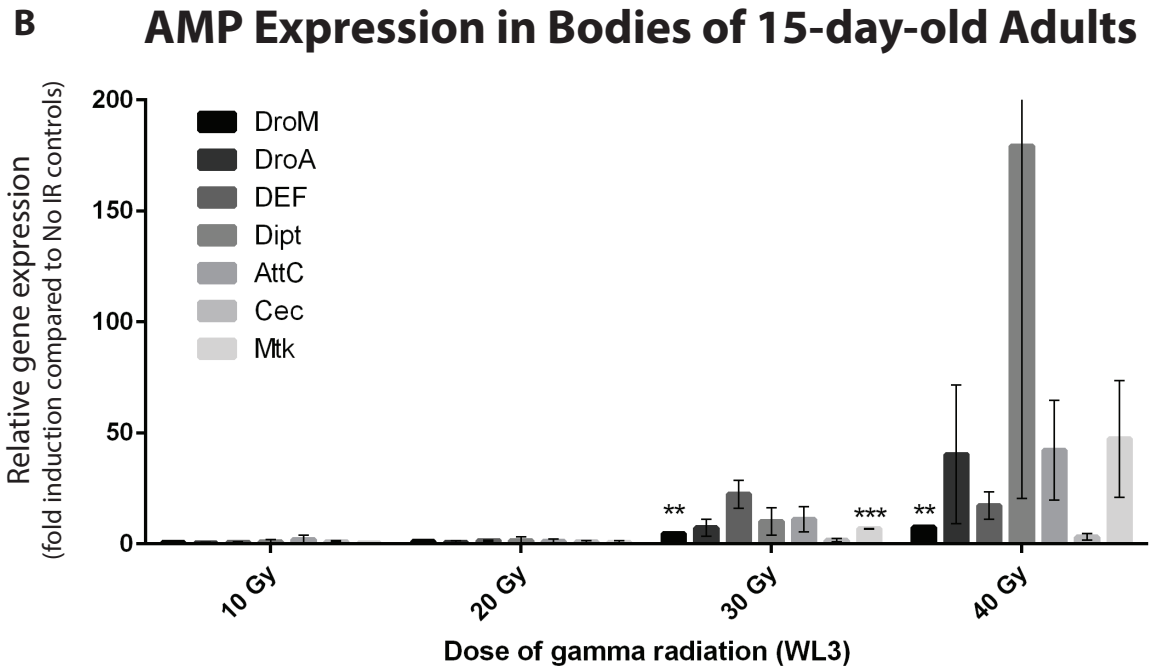
B
AMP Expression in Bodies of 15-day-old Adults
Relative gene expression
(fold induction compared to No IR controls)
200
150
100
50
0
DroM
DroA
DEF
Dipt
AttC
Cec
Mtk
**
***
**
10 Gy
20 Gy
30 Gy
40 Gy
Dose of gamma radiation (WL3)

Figure 3. Irradiation during larval development results in increased AMP expression in adult bodies. For each dose of radiation during the late third larval instar, expression of seven different AMPs in the bodies of 5-day-old (A) and 15-day-old (B) adults was measured with qRT-PCT. The laboratory wild-type *Canton-S* strain was used for these experiments. The bars in each graph represent mean expression normalized to mean expression in non-irradiated age-matched controls. Error bars are SEM. The graph in (A) represents three trials. The graph in (B) represents two trials. Although AMP expression is consistently increased in the bodies of flies that were exposed to higher doses of radiation during development (30 Gy and 40 Gy), the large variation in fold induction from one trial to the next results in no statistically significant increases in the 5-day-old experiments (A). *DroM* and *Mtk* expression in bodies of 15-day-old adults exposed to a 30 Gy dose of radiation (or a 40 Gy dose for *DroM*) during the late third larval instar is statistically significantly increased (B). **$p<0.01$ and ***$p<0.001$ based on Students t test comparing relative expression in 30 Gy or 40 Gy and 10 Gy samples.

Figure 4

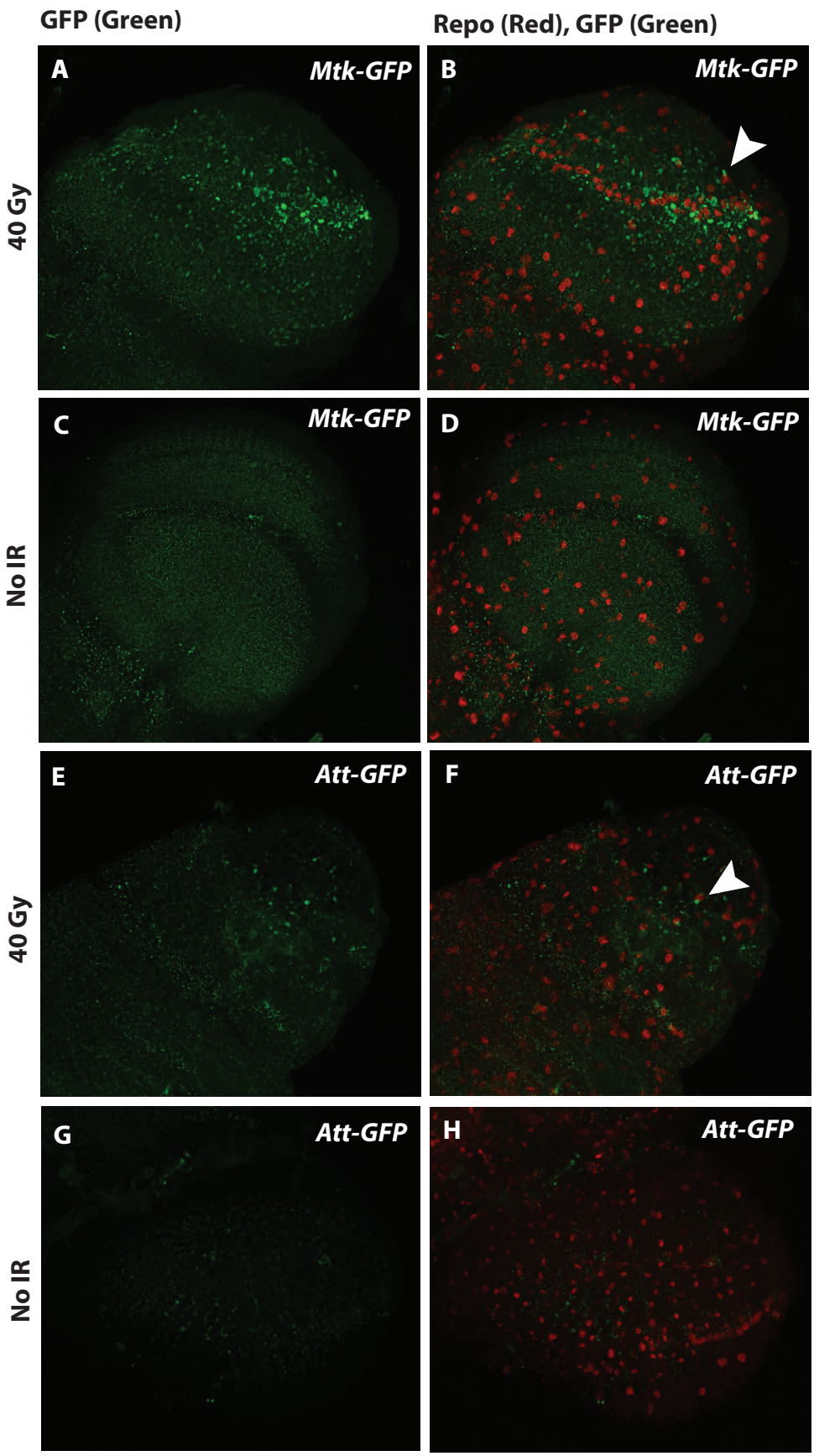
GFP (Green)
Repo (Red), GFP (Green)
A
Mtk-GFP
B
Mtk-GFP
40 Gy
C
Mtk-GFP
D
Mtk-GFP
No IR
E
Att-GFP
F
Att-GFP
40 Gy
G
Att-GFP
H
Att-GFP
No IR

Figure 4. Irradiaton during larval development increases AMP-GFP reporter expression in adult brains. Following exposure of late third instar larvae to a 40 Gy dose of radiation, surviving adults were aged for 5 days after eclosion before brains were dissected for confocal microscopy. (A-D) Confocal stacks of *Metchnikowin-GFP* brains immunostained for GFP (green) and the glial nuclear marker Repo (red). (E-H) Confocal stacks of *Attacin-GFP* brains immunostained for GFP (green) and the glial nuclear marker Repo (red). Brains from adults that were irradiated during larval development have an increased number of GFP+ cells (A,E) compared to brains from adults that were not irradiated (C,G). Some of the GFP+ cells are also Repo+ (arrowheads in B and F). 6 brains of each genotype for each condition were analyzed.

Figure 5

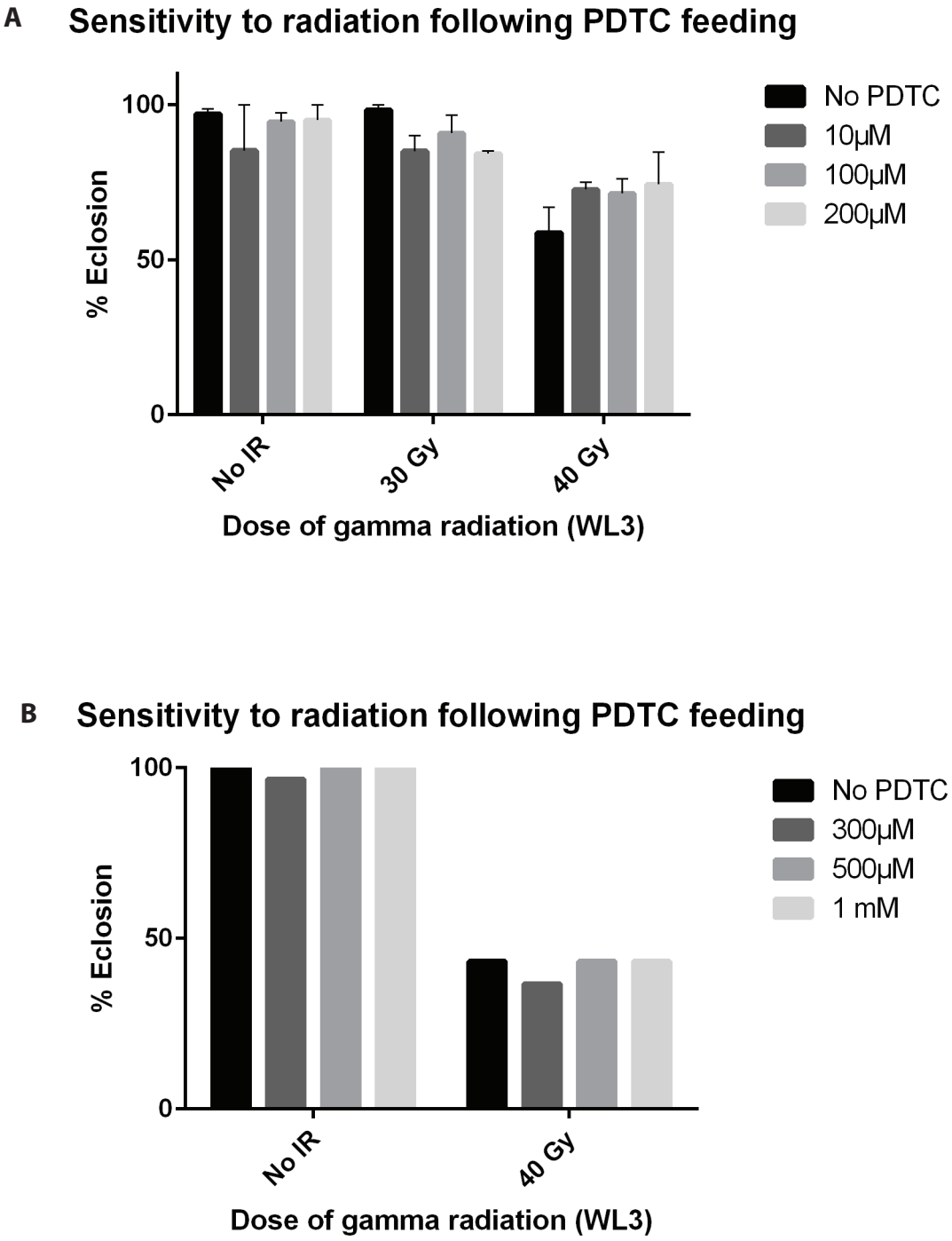
A
Sensitivity to radiation following PDTC feeding
100
50
0
% Eclosion
No IR
30 Gy
40 Gy
Dose of gamma radiation (WL3)
No PDTC
10μM
100μM
200μM
B
Sensitivity to radiation following PDTC feeding
100
50
0
% Eclosion
No IR
40 Gy
Dose of gamma radiation (WL3)
No PDTC
300μM
500μM
1 mM

Figure 5. Pharmacological inhibition of NF-κB does not affect radiation sensitivity during development. (A) The percentage of irradiated late third instar larvae that complete development and eclose as adults is shown for control larvae and larvae raised on food with three different concentrations of the NF-κB inhibitor PDTC (pyrrolidine dithiocarbamate). Successful eclosion following a 30 or 40 Gy dose of radiation in the late third larval instar is not affected by PDTC. Values shown are mean ±SEM for three trials of No IR and 40 Gy and two trials of 30 Gy with 20-30 larvae per trial. (B) Higher doses of PDTC do not affect the percentage of irradiated late third-instar larvae that complete development and eclose as adults. Each bar on the graph represents percent eclosion for a single trial with at least 30 larvae. A w^{1118} strain was used for these experiments.

Figure 6

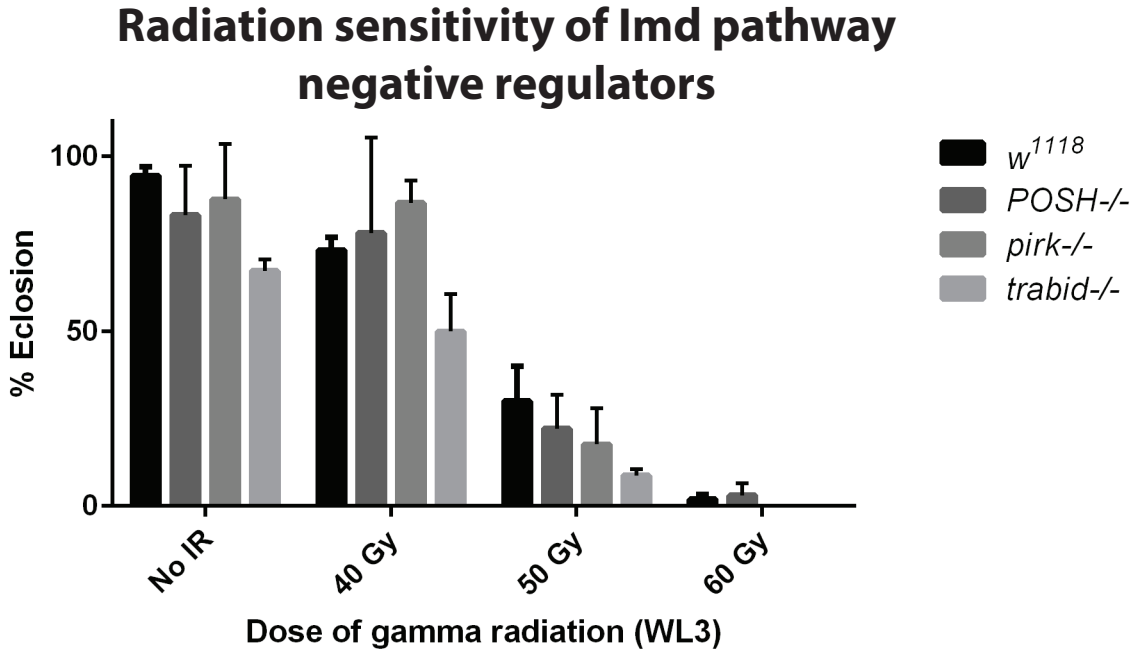
Radiation sensitivity of Imd pathway negative regulators
% Eclosion
100
50
0
No IR
40 Gy
50 Gy
60 Gy
Dose of gamma radiation (WL3)
w1118
POSH-/-
pirk-/-
trabid-/-

Figure 6. Increased activation of the imd pathway does not affect radiation sensitivity during development. For each dose of radiation, the percentage of irradiated third instar larvae that complete development and eclose as adults is shown for the laboratory background strain (w^{1118}) and the indicated mutant strains. POSH, pirk and trabid are each negative regulators of the Imd pathway (Myllymäki et al., 2014; Fernando et al., 2014). Therefore, mutations in these genes should result in increased activity of the Imd pathway. These mutants all have similar eclosion rates to controls. Each bar represents mean ecolosion ±SEM. 3-5 trials of 30-40 larvae each were performed for each genotype at each dose, except *trabid*, which was only tested twice. Alleles used: $POSH^{EY10354}$ (stock#17671), $pirk^{EY00723}$ (stock# 15039), *trabid* (deletion via homologous recombination, Tran et al., 2008).

AMP Expression in Bodies of 5-day-old FEMALE Adults

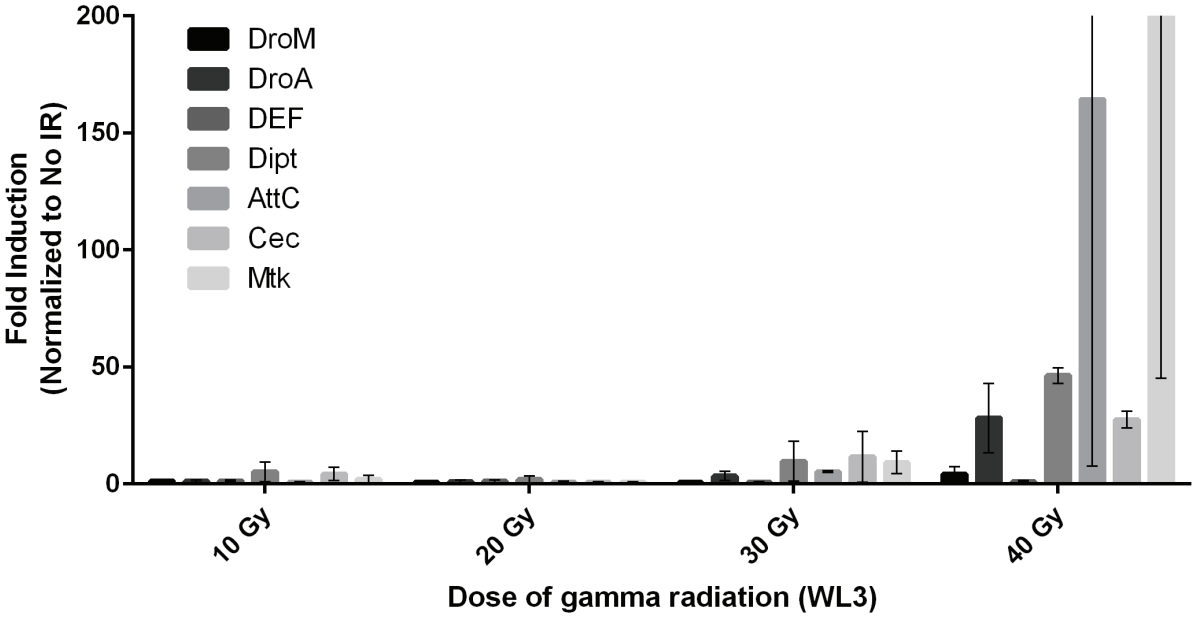

AMP Expression in Bodies of 15-day-old FEMALE Adults

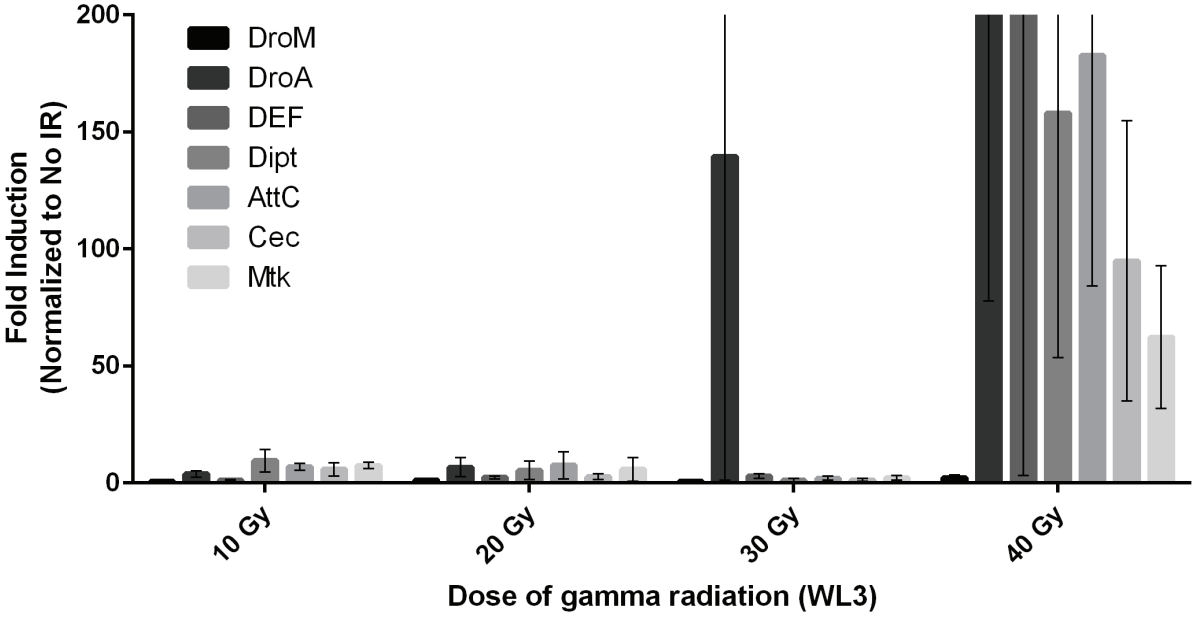

AMP Expression in Heads of 5-day-old FEMALE Adults

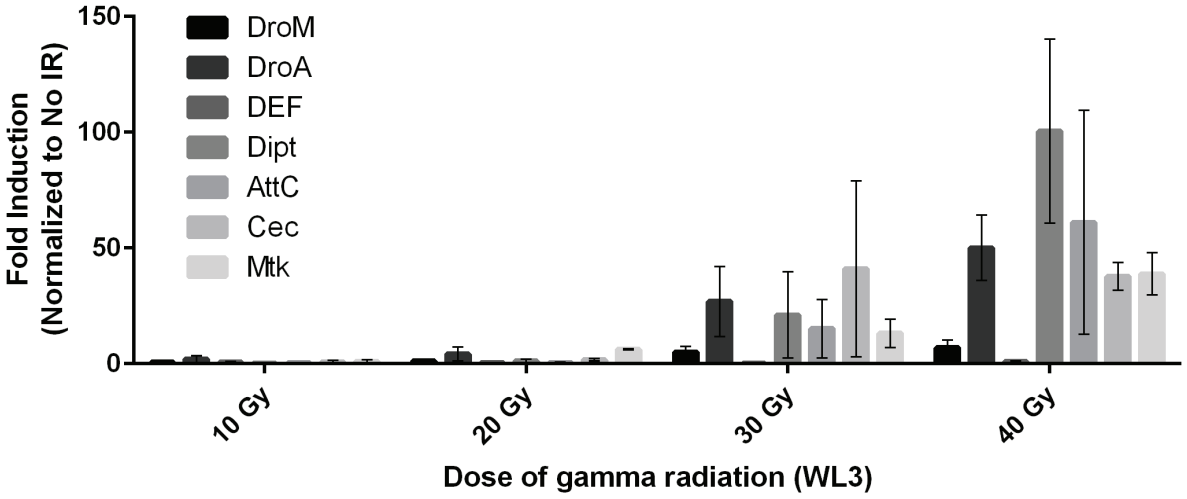

AMP Expression in Heads of 15-day-old FEMALE Adults

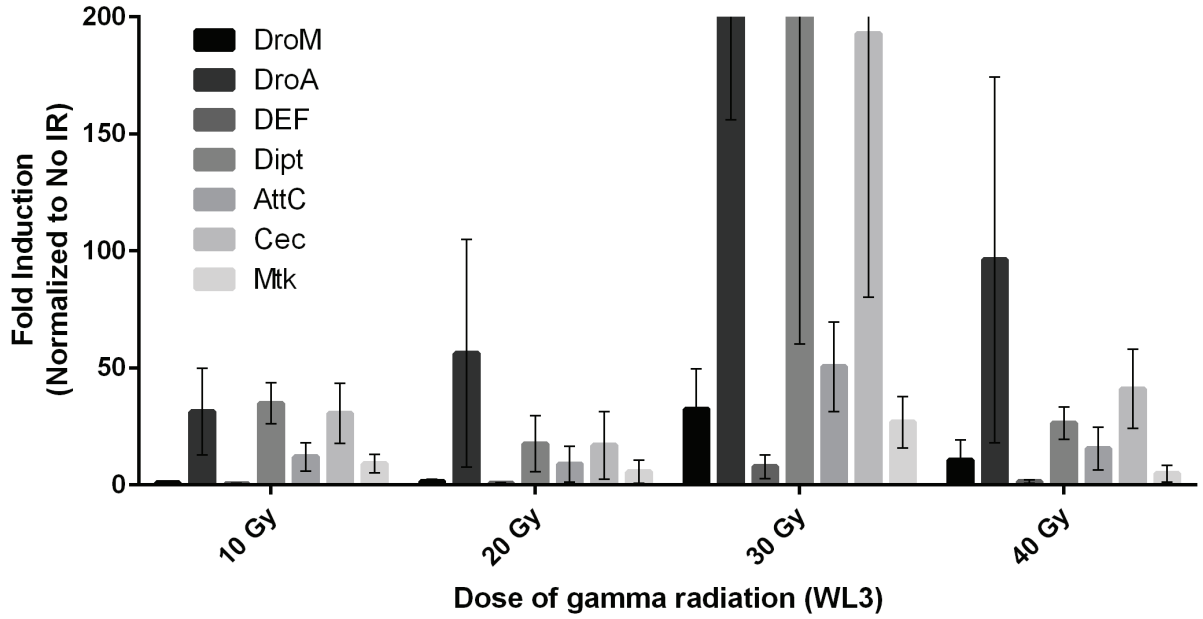

CHAPTER 8

Future Directions

GLaz regulates neuromuscular junction growth by antagonizing postsynaptic insulin signaling in Drosophila

We characterized NMJ morphology in *GLaz* mutants as measured by the number of boutons in the presynaptic terminal. To extend our analysis, it will be of interest to look at individual synapses within the synaptic terminal. Using antibodies to label the presynaptic active zones (anti-bruchpilot) and subunits of the postsynaptic glutamate receptors, we can determine whether GLaz or postsynaptic insulin signaling are required for proper assembly and apposition of the pre- and postsynaptic machinery. Although this was not quantified, the NMJ overgrowth we observed in *GLaz* mutant larvae was qualitatively characterized by an increase in small boutons. We counted all boutons that were stained with FITC-anti-HRP regardless of size when we were quantifying presynaptic terminal morphology. When we are looking at the synaptic machinery in *GLaz* mutants, we will also quantify bouton number as measured by number of varicosities in the presynaptic terminal containing the synaptic release machinery (presence of anti-bruchpilot staining). It is possible that the extra boutons we observe in *GLaz* mutants are not fully functional boutons and may not contain the synaptic vesicle release machinery.

We demonstrated that postsynaptic insulin signaling promotes presynaptic terminal growth and, as has been previously described, that manipulation of postsynaptic insulin signaling affects muscle size (Demontis and Perrimon, 2009). Although there were no obvious changes in overall body size in *GLaz* larvae, it will be important to measure muscle size in these animals. We propose that the NMJ overgrowth observed in *GLaz* mutants is caused by increased insulin signaling in muscle. When we increase insulin signaling in muscle by overexpressing an activated insulin receptor (*UAS-InR-Act*) we observe both an increase in bouton number and muscle size. If insulin signaling is sufficiently increased in muscle in *GLaz* larvae, we predict

that they should be larger than controls. Similarly, according to our model, insulin signaling in muscle should be reduced when GLaz or hApoD are overexpressed in glia. Therefore, we will also measure muscle size in *Repo>>GLaz* and *Repo>>hApoD* larvae to test the prediction that muscle size should be reduced in these larvae.

Although glial expression of GLaz in *GLaz* mutant larvae fully rescues the NMJ overgrowth phenotype associated with loss of GLaz, expression of RNAi against GLaz in glia does not result in substantial NMJ overgrowth. Moreover, expression of *GLaz-RNAi* using the ubiquitous promoter Tubulin (*Tubulin-Gal4*) causes greater NMJ overgrowth than that observed with glial expression of *GLaz-RNAi*. These results suggest that there are other sources of GLaz besides glia contributing to the pool of GLaz acting at the NMJ. The Drosophila gene expression resource FlyAtlas indicates that there is substantial GLaz expression in the larval hindgut. Future experiments should determine whether expression of *GLaz-RNAi* specifically in the larval hindgut causes NMJ overgrowth. If NMJ overgrowth is observed in larvae with reduced GLaz expression in the hindgut, it would suggest that GLaz does not need to be locally secreted from glia at the NMJ to restrict NMJ growth.

One of the most puzzling results we observe is the variation in NMJ overgrowth among different *GLaz* mutants. Although we see consistent overgrowth in homozygous *GLaz* mutants ($GLaz^{MB01748}$, $GLaz^{MI02243}$, and $GLaz^{1}$), NMJ overgrowth is less impressive in $GLaz^{MI02243}$*/Deficiency* and $GLaz^{1}$*/Deficiency* larvae. This is especially confusing because part of the *GLaz* gene is deleted in the $GLaz^{1}$ allele, and no GLaz RNA transcripts are expressed from this allele (Sanchez et al., 2006). In contrast, the two other alleles we analyzed, $GLaz^{MI02243}$ and $GLaz^{MB01748}$ contain p-elements in intronic regions of the *GLaz* gene. Therefore, we predict that the allelic combination with the lowest expression of GLaz is $GLaz^{1}$*/Deficiency*. If this is true, it

is confusing that the larvae with the lowest GLaz expression should have the weakest phenotype. One explanation for this could be that there is a suppressor of the *GLaz* mutant phenotype in the genetic background of the deficiency line. We will be measuring GLaz transcript levels in these mutants with quantitative RT-PCR.

Finally, one of the most intriguing questions we hope to address is how GLaz secretion and action at the NMJ are regulated. The NMJ undergrowth phenotype we observe in *Repo>>GLaz* larvae is stronger than the overgrowth phenotype we observe in *GLaz* mutants. This suggests that GLaz may play a greater role in regulating NMJ development when there is a trigger that increases its expression rather than acting constitutively to restrict NMJ growth. GLaz is expressed in response to stress (Muffat et al., 2008). It will be of interest to expose developing larvae to different types of stress as was done with adult flies (for example paraquat or hyperoxia) to determine whether GLaz expression changes and how this affects NMJ growth. It will be especially interesting to analyze stress-induced effects on NMJ growth in *GLaz* mutant larvae.

Together our data support a model in which GLaz is secreted from glia and antagonizes postsynaptic insulin signaling to restrict NMJ growth. However, unanswered questions remain, some of which are addressed above. Future experiments will clarify some of these uncertainties and help us refine our model of how GLaz functions to restrict NMJ growth.

A Drosophila model to investigate the neurotoxic side effects of radiation exposure

In developing a Drosophila model of the side effects of radiation exposure our goal was to use this model to dissect the mechanisms underlying radiation-induced tissue damage. This involves studying previously identified radioprotective or radiosensitive pathways and discovering novel pathways underlying the tissue response to radiation. We have begun studying the innate immune response following radiation exposure and are gaining an understanding of the spatial and temporal patterns of radiation-induced activation of innate immunity. We will continue these studies, as discussed below, but we also aim to identify pathways that have yet to be implicated in radioprotection.

The results of the GWAS (Chapter 5) provided us with candidate genes that may be involved in the tissue response to radiation. We will continue to screen the genes from these studies that contained genetic variations associated with radioprotection or radioresistance. We hope that additional genes from these studies will prove to be involved in the tissue response to radiation. However, we will not restrict our analysis to GWAS. Forward mutagenesis screens have been invaluable in the discovery of pathways underlying processes from embryonic patterning to neurodegeneration. We hope to use our model to screen a Drosophila mutagenesis collection for radioprotective or radiosensitive phenotypes. Drosophila collections containing ENU- (N-ethyl-N-nitrosourea) or EMS- (ethyl methanesulfonate) induced mutations contain point mutations randomly throughout the genome. If a particular strain has a phenotype of interest, the causative mutation can be identified by deletion mapping. We will first use this approach to screen for mutations that alter sensitivity to radiation as measured by survival to eclosion following radiation exposure during larval development. This approach will facilitate the discovery of additional radioresponsive pathways with a substantially lower false positive rate compared to GWAS.

Innate immunity is radioprotective during development in Drosophila

We demonstrate that loss of both the Imd and Toll pathways results in increased sensitivity to radiation as measured by decreased survival to adulthood following radiation exposure during development in *Rel, spz* double mutant larvae. Moreover, since loss of the Toll ligand Spz results in similar radiosensitivity compared to *Rel, spz* double mutants, we suggest that the radiosensitivity in the double mutant is largely due to loss of Toll signaling. However, mutations in other signaling components of the Toll pathway did not affect radiation sensitivity.

For example, loss of the adapter MyD88 does not affect sensitivity to radiation as measured by survival to adulthood following radiation exposure during larval development. However, it is known that MyD88 is essential for normal Toll signaling. Loss of MyD88 results in reduced activation of *Drosomycin* expression upon infection with fungal or gram-positive bacteria, and *MyD88* mutant flies are more susceptible to infection by fungi or gram positive bacteria (Tauszig-Delamasure et al., 2002). The allele tested in the studies presented here, $MyD88^{KG03447}$ has a p-element in the genomic region of the *MyD88* gene, but it is located upstream of the coding region, and therefore may have little effect on overall gene expression or protein levels. To confirm that loss of MyD88 does not affect sensitivity to radiation, additional mutant alleles should be tested. MyD88 transcript levels should also be measured in the $MyD88^{KG03447}$ strain.

Loss of Dif, a NF-κB transcription factor activated by the Toll pathway also doesn't affect sensitivity to radiation as measured by survival to adulthood following radiation exposure during the late third instar larval stage. This result could be due to the functional redundancy of Dorsal, the other NF-κB transcription factor activated by the Toll pathway (Lemaitre and Hoffmann, 2007; Manfruelli et al., 1999). It would be of interest to test the effect of loss of both Dorsal and

Dif. A fly strain with a deletion of both the *Dif* and *Dorsal* genes does exist, but more than 99% of these flies do not survive to adulthood in the absence of radiation (Meng et al., 1999), so it would be very difficult to test the radiosensitivity of this strain. The activity of Dif and Dorsal could also be inhibited by overexpressing Cactus, the Drosophila IκB homolog.

Another possibility is that the Spz ligand is activating a noncannonical signaling cascade to achieve its radioprotective effects. Recently, it was shown that Spz activates noncannonical Toll-related receptors (TRRs) and signals through distinct components of the Imd and Toll pathways to promote elimination of unfit cells (Meyer et al., 2014). It will be imperative in future studies to dissect the radioprotective pathway activated by Spz. Thus, Drosophila strains with mutations in additional downstream components of the Toll and Imd pathways as well as noncannonical TRR mutants should be tested for sensitivity to radiation.

The Imd pathways mutants we tested did not demonstrate increased radiosensitivity as measured by survival to eclosion following radiation exposure during larval development. A possibility we have not explored, however, is that mutations in the Imd pathway may affect radiosensitivity of different phenotypes. For example, loss of Imd signaling may cause inefficient repair of radiation-induced damage during development and lead to more severe adult neurodegeneration and early death. To test this possibility, we will quantify adult phenotypes such as climbing behavior, neuronal cell death and mortality in Imd pathway mutants that were exposed to radiation during larval development.

A confounding variable that we have not addressed in studying the role of innate immunity in radioprotection is that our experiments were not performed under aseptic conditions. Thus, there is a possibility that the increase in AMP expression we observe is due to increased rates of

infection in irradiated flies rather than an effect of the radiation itself. We attempted to control for variations in naturally-present microbes from one vial of flies to the next by irradiating, aging and extracting the RNA from all of the flies being tested for each dose in a given biological replicate at the same time. Furthermore, we are measuring the fold increase in AMP transcripts compared to non-irradiated controls that were handled identically to groups that were irradiated throughout each biological replicate. The fact that we see a dose-response suggests that radiation affects the innate immune response independent of variable culture conditions. However, radiation exposure may increase susceptibility to infection, and therefore the dose-dependent increase in AMP expression we observe could be due to increased rates of infection in the flies that received a higher dose of radiation. If this is the cause of the sustained increase in inflammation, antimicrobial agents would have great therapeutic potential for reducing the long-term negative side effects of radiation exposure during development. Future experiments will focus on determining whether radiation exposure confers an increased susceptibility to infection in flies, and if it does, separating this effect from radiation-induced inflammation alone. For example, adult flies that complete development after larval irradiation could be maintained on medium containing a broad spectrum antibiotic until tissue processing for qRT-PCR. Similarly, an increased susceptibility to infection may be responsible for enhanced sensitivity to radiation in *Rel, spz* double mutants as measured by survival to eclosion following radiation exposure during the late third larval instar. To test this possibility, *Rel, spz* larvae will be raised on food containing a broad spectrum antibiotic before irradiation.

We demonstrate that *Attacin* (*Att*) and *Metchnikowin* (*Mtk*) expression are increased in the brains of 5-day-old adult flies following radiation exposure during larval development using the AMP-GFP transgenic reporter lines, *Att-GFP* and *Mtk-GFP*. It will be of interest to determine whether

other AMP-GFP reporter lines such as *Drosocin-GFP* and *Cecropin-GFP* also show increased expression in adult brains following radiation exposure during development. Moreover, an important question is whether elevated AMP expression in the brain is sustained in older adults (e.g. 15-day-old adults, which have increased AMP transcripts in heads) following radiation exposure during development. Future studies will also more carefully characterize the cells in which AMP expression is elevated by co-staining with neuronal and glial markers and taking high-magnification images. Moreover, to determine whether cells with elevated AMP expression are more likely to undergo cell death, dissected AMP-GFP brains will also be stained with an antibody to cleaved Death caspase-1.

Finally, we aim to specifically study the effects of chronic inflammation on the neurological outcomes in adults following radiation exposure during development. Since the innate immune response is radioprotective early, we will use methods to inhibit inflammation later in adults and allow activation of the innate immune pathway during development when irradiation occurs. In one experiment we will feed adult flies anti-inflammatory agents to pharmacologically inhibit inflammation in adults that were exposed to radiation during larval development. We can also use Heatshock-Gal4 and RNAi against specific components of the innate immune pathways to inhibit expression of innate immunity genes in adults that were exposed to radiation during larval development. After suppressing the innate immune response, either pharmacologically or genetically, we will measure the effect on locomotor behavior, lifespan and neuronal cell death. Together these experiments will help us better understand innate immunity and the tissue response to radiation exposure.

References

Demontis, F. and Perrimon, N. (2009). Integration of Insulin receptor/Foxo signaling and dMyc activity during muscle growth regulates body size in Drosophila. *Development* **136**, 983-93.

Lemaitre, B. and Hoffmann, J. (2007). The host defense of Drosophila melanogaster. *Annu Rev Immunol* **25**, 697-743.

Manfruelli, P., Reichhart, J. M., Steward, R., Hoffmann, J. A. and Lemaitre, B. (1999). A mosaic analysis in Drosophila fat body cells of the control of antimicrobial peptide genes by the Rel proteins Dorsal and DIF. *EMBO J* **18**, 3380-91.

Meng, X., Khanuja, B. S. and Ip, Y. T. (1999). Toll receptor-mediated Drosophila immune response requires Dif, an NF-kappaB factor. *Genes Dev* **13**, 792-7.

Meyer, S. N., Amoyel, M., Bergantiños, C., de la Cova, C., Schertel, C., Basler, K. and Johnston, L. A. (2014). An ancient defense system eliminates unfit cells from developing tissues during cell competition. *Science* **346**, 1258236.

Muffat, J., Walker, D. W. and Benzer, S. (2008). Human ApoD, an apolipoprotein up-regulated in neurodegenerative diseases, extends lifespan and increases stress resistance in Drosophila. *Proc Natl Acad Sci U S A* **105**, 7088-93.

Sanchez, D., López-Arias, B., Torroja, L., Canal, I., Wang, X., Bastiani, M. J. and Ganfornina, M. D. (2006). Loss of glial lazarillo, a homolog of apolipoprotein D, reduces lifespan and stress resistance in Drosophila. *Curr Biol* **16**, 680-6.

Tauszig-Delamasure, S., Bilak, H., Capovilla, M., Hoffmann, J. A. and Imler, J. L. (2002). Drosophila MyD88 is required for the response to fungal and Gram-positive bacterial infections. *Nat Immunol* **3**, 91-7.